**TECHNISCHE UNIVERSITÄT MÜNCHEN**
Fakultät für Medizin

# Deciphering mechanisms of postnatal β-cell heterogeneity and maturation

## Ciro Salinno

Vollständiger Abdruck der von der Fakultät für Medizin der Technischen Universität München zur Erlangung des akademischen Grades eines

**Doktors der Naturwissenschaften (Dr. rer. nat.)**

genehmigten Dissertation.

Vorsitzender: Prof. Dr. Radu Roland Rad

Prüfer der Dissertation: 1. Prof. Dr. Heiko Lickert

2. apl. Prof. Dr. Johannes Beckers

Die Dissertation wurde am 21.04.2021 bei der Technischen Universität München eingereicht und durch die Fakultät für Medizin am 12.10.2021 angenommen.

All β-cells are equal.

But some β-cells are more equal than others.

# Table of Contents

# Index of Figures

# Index of Tables

# 1 Abstract

Pancreatic beta (β) cells produce insulin, which is a fundamental hormone responsible for the maintenance of the physiological glucose levels. Loss or dysfunction of the β-cell mass are the root causes of diabetes mellitus (DM), a complex metabolic disease characterized by hyperglycemia and peripheral insulin resistance. Despite having the same function, secreting insulin in response to glucose, β-cells are heterogeneous in terms of morphology and functionality. Pioneer studies in the 60s and 70s described differences in cell size, nuclear size, granularity, and later about glucose responsiveness, insulin secretion, electrical activity and proliferative capacity. Nevertheless, the mechanisms underlying the establishment and maintenance of β-cell heterogeneity are not well understood.

The primary aim of this thesis was to investigate the molecular mechanisms governing the acquisition of the mature β-cell phenotype. Secondly, we screened for novel heterogeneity markers, in particular aiming at surface molecules, with high targetability potential, on immature or diseased cells. To achieve these aims, we combined the Fltp lineage tracing mouse model with the innovative technology of the single cell RNA sequencing. Fltp (*Cfap126*) was previously described as Wnt - Planar Cell Polarity (PCP) effector and reporter gene. Subsequently identified as heterogeneously expressed in β-cells, its expression was correlated with a functionally mature phenotype, while cells not expressing it were observed to retain a higher proliferative capacity and an immature metabolism. Hence, we analyzed nine postnatal stages and demonstrated a progressive increase in Fltp lineage-positive populations and an inverse reduction of the lineage-negative population, directly linking PCP acquisition with endocrine maturation. To decipher the molecular mechanisms behind Fltp transition and β-cell maturation process, we profiled 18716 endocrine cells of postnatal islets from Fltp lineage tracing mice. Through computational and immunofluorescence analysis, we demonstrate that Fltp lineage positive β-cells possessed an overall more mature phenotype. In addition, we hypothesized that upon PCP acquisition changes in cytoskeleton might prompt β-cell maturation. Finally, we also discovered an inverse relationship between Fltp lineage-positive cells and mTORC1 activity, which led to the hypothesis that PCP might play a role in the metabolic maturation of β-cells. We further exploited the postnatal scRNA-seq dataset to screen for novel markers heterogeneously expressed in β-cells. We identified CD81, a member of the tetraspanins protein family, never before characterized in the islets of Langerhans. Deeper analysis revealed that CD81 labels immature and dedifferentiated murine β-cells. In human, we showed that CD81 is differentially expressed, possibly upon stress exposure. Altogether, we characterized the postnatal β-cell maturation landscape and proposed PCP as critical player for the acquisition of the mature phenotype. Additionally, we identified and characterized CD81 as a novel immature and dedifferentiated β-cell marker, a possible target to ameliorate diabetes.

# 2 Introduction

## 2.1 Diabetes Mellitus

Diabetes mellitus (DM) is an endemic disease. Recent data showed that 463 million people live with diabetes, 0.2% are children, 72% are adults and 28% are elderly (9th IDF Atlas). The projections for the near future depict an even worse scenario, with estimated 700 million patients by 2045 (Nam Han Cho., 2019) (Figure 1a). The United Nations has declared DM a global threat, a socioeconomic burden afflicting modern society. Thus, actions need to be taken to arrest this dangerous trend and find solutions to halt the disease.

### 2.1.1 Diabetes types

We can distinguish different forms of DM based on the pathogenesis. However, the clinical manifestation of the disease remains the same, hyperglycemia. Type 1 diabetes (T1D) is the autoimmune form of diabetes. The root causes of the disease, both genetic and environmental, determine the attack of the islets of Langerhans from the immune system, generating a slow but progressive loss of pancreatic β-cell mass and therefore hyperglycemia. The onset of T1D usually occurs in young children and teenagers, causing a life-lasting dependency from exogenous insulin. It accounts for less than 10% of all DM cases (Katsarou et al., 2017). Type 2 diabetes (T2D) is the most common form of DM (90%) and it is determined by a genetic susceptibility and by dietary factors. Here, prior the clinical onset, hyperglycemia builds up for several years; pancreatic β-cells respond by over-producing insulin to compensate the high glucose levels. Slowly, the systemic insulin sensitivity decreases, thus despite the hyperinsulinemia it is observed an increase of the glycaemia levels. Lastly, β-cells under metabolic stress, fail, undergoing dedifferentiation and apoptosis, resulting in β-cell mass loss (DeFronzo et al., 2015). Another form of diabetes is gestational diabetes (GDM), which occurs during pregnancy. This form is characterized by a transient hyperglycemia that disappears after the pregnancy. However, this is not a harmless event, since both the mother and the child have higher risk of developing obesity and T2D during their lives (McIntyre et al., 2019). Other rare forms of DM exist, usually determined by genetic mutations (usually autosomal dominant) in a gene important for the development of the pancreas or the maturation process of β-cells (*HNF1a*, *HNF1b*, *HNF4a*, *PDX1*, etc.). These are named MODY (maturity onset diabetes of the young) and eleven different MODY types have been reported in literature (Urakami, 2019).

### 2.1.2 Diabetes treatments

Up-to-date, no curative treatment has been developed for diabetes. Several treatments are available (Tan et al., 2019), among which drugs designed to reduce the hepatic glucose production (metformin) or glucose

reuptake in the kidneys (SGLT2 inhibitors), to improve the insulin secretion (sulfonylureas) and the peripheral sensitivity (metformin and thiazolidinedione). In early stages of T2D, these drugs are effective and help to manage the disease. However, in late T2D stages and in T1D, exogenous insulin remains the only life-saving treatment, administrated either by subcutaneous injections or via insulin pumps. Alternatives to the pharmacological treatments are the transplantation of pancreas/islets of Langerhans and the bariatric surgery. The first approach, despite its effectiveness, cannot be available to all patients due to the limited availability of pancreas or islets donors, in addition to the necessity of using immunosuppressive drugs (Shapiro et al., 2017). The second approach has been proved to resolve T2D, but it is an invasive approach, with the rescission of a major portion of the stomach, not recommended if not in cases of severe obesity (Madadi et al., 2019).

### 2.1.3 Diabetes a worldwide - present and future - burden

The costs to treat DM and its complications are estimated to be 760 billion US dollars per year, approximately 10% of the global health expenditure. Furthermore, DM incidence is higher in counties with low-average income, which is also connected to limited access to treatments (Figure 1a and 1b) (Nam Han Cho., 2019).

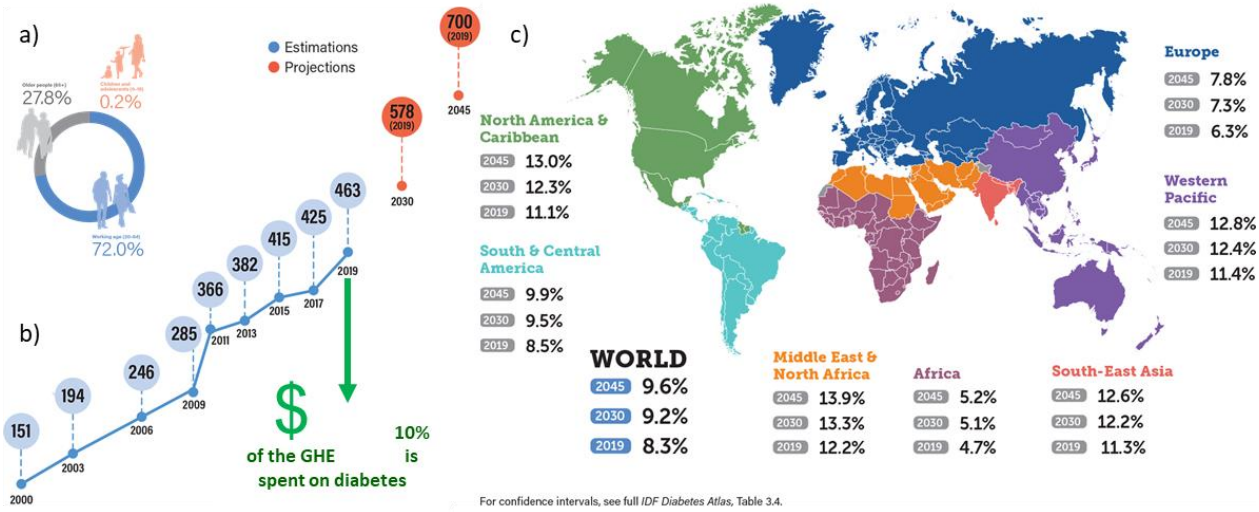


**Figure 1: Present and future data of diabetes cases worldwide**.

a) Demographic distribution of diabetes patients; b) in blue number of adults (millions) affected with diabetes in the past 20 years and in red projections for the near future; c) geographical distribution and future projections of diabetic patients. GHE = Global Health Expenditure. All data are retrieved from *IDF Diabetes Atlas 2019*

### 2.1.4 Future perspectives

It is clear that DM is a social, ethical and economic burden. Worldwide, national and international organizations are working for a common goal, to slow down the exponential growth rate of diabetes in the population, by providing information regarding the importance of a healthy lifestyle and universal access to treatments. Currently, only bariatric surgery and islets transplantation are able to resolve diabetes. All other available treatments target the symptoms but do not cure the root causes of the disease. Great investments are being made on diabetes research in order to find, as soon as possible, treatments to protect or regenerate β-cells. One possibility is to discover novel pharmacological targets to ameliorate the diabetic conditions (i.e. GLP-1 agonists) (Karakose et al., 2018; Sachs et al., 2020; Villalba et al., 2020). Alternatively, replacement therapy approaches aim at generating *in vitro* functional β-cells, ready to be transplanted in diabetic patients (Bourgeois et al., 2021).

## 2.2 Pancreas and islets of Langerhans

The pancreas is an organ situated in the abdominal cavity. It has an exocrine and an endocrine compartment. 98% of the organ is composed of the exocrine compartment (acinar and ductal cells) and has a fundamental role in the digestive system. It produces the so-called "pancreatic juice", made of a series of enzymes, necessary to break down the macromolecules, and chemicals, like the bicarbonate, to neutralize stomach´s acids. This mixture is released via the pancreatic duct in the duodenum (Islam, 2015). The endocrine compartment of the pancreas is made of the islets of Langerhans, which represents barely the 2% of the adult pancreas weight (Islam, 2015). They function as blood glucose levels regulators by secreting hormones via the dense microvasculature, which act on the peripheral organs. Different cell types exist within the islets, the two most abundant are the insulin-producing β cells and the glucagon-producing *alpha* (α) cells. Less abundant in the islets are the somatostatin-producing *delta* (δ) cells, pancreatic polypeptide-producing *gamma* (γ) or PP cells and the ghrelin-producing *epsilon* (ε) cells (Figure 2). These hormones are important to regulate blood glucose levels and they usually antagonize each other (Brissova et al., 2005; Islam, 2015). Insulin is the main hormone released in response to high glucose levels (hyperglycemia). Once circulating in the bloodstream, it acts on the organs expressing the insulin receptor, in particular liver, adipose tissues and muscles, inducing an uptake of glucose that is stored in these organs as glycogen. Glucagon is the antagonist of insulin and it is released in response to low blood glucose levels (hypoglycemia). Thus, once circulating, glucagon acts on the same organs as insulin, this time inhibiting the glucose uptake and inducing mechanism to deplete the glycogen storages and to generate glucose from lipids in the liver (Da Silva Xavier, 2018). Somatostatin is a negative regulator of the other islets' hormones, thus fine tuning the islets' function in response to the other hormones secretion (Hauge-Evans et al., 2009).

PP is another hormone inhibiting glucagon secretion at low glucose concentrations, thus fine tuning α-cells function, avoiding the dangerous state of hypoglycemia. Ghrelin is more abundant in embryonic and postnatal stages and might regulate the secretion of the other hormones (Melissa F. Brereton et al., 2015; Da Silva Xavier, 2018).

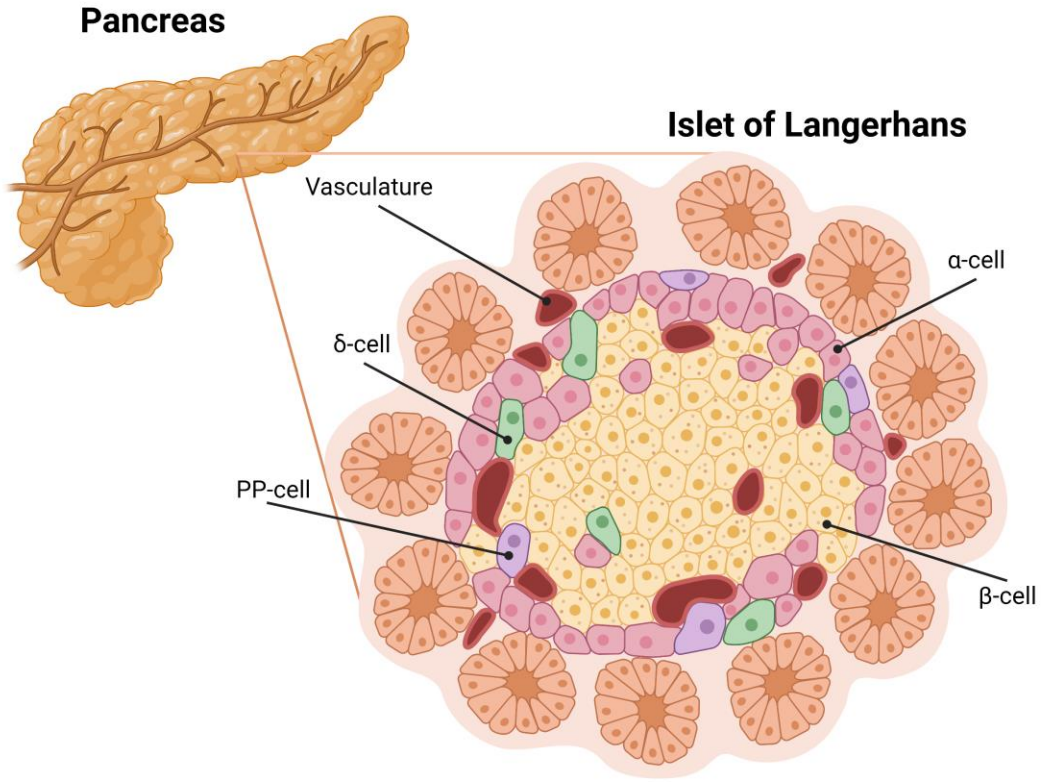


**Figure 2: Schematic representation of the pancreas and the islet of Langerhans**

Cartoon of the pancreas (left) and a mouse islet of Langerhans (right), with the typical distribution of the α-cells as outer shell and β-cells in the core. The islets are surrounded by the acinar structures and intermingled by the rich microvasculature. Figure was created with BioRender.com.

The islets of Langerhans are heterogeneous mini organs. Their composition is extremely variable. In mouse, the islets of Langerhans have a recurrent structure with a core of insulin-producing β-cells (65-90%, average 77%) and an external shell of α-cells (5-20%, average 18%). The rest of the cells are in minority and they are localized in the periphery. In human, the islet composition and architecture differ from the mouse ones. β-cells (32-77%, average 55%) and α-cells (15-50%, average 38%) are intermingled and do not segregate to form an external shell and an internal core. The other endocrine types are the minority and they also distribute without a typical localization within the islets (Brissova et al., 2005; Cabrera et al., 2006; Da Silva Xavier, 2018; Islam, 2015; Steiner et al., 2010).

## 2.3 Pancreas embryonic development

Mouse pancreas development has been broadly described in the past decades (Bastidas-Ponce et al., 2017; Pan & Wright, 2011). The process starts around embryonic day 8.5 (E8.5), within the foregut endoderm, with the expression of two fundamental transcription factors (TFs), Pdx1 (pancreatic and duodenal homeobox 1) and Ptf1a (pancreas-specific transcription factor 1a). Several studies have confirmed the necessity of these two TFs in order to induce the formation of the pancreatic buds (Ahlgren et al., 1996; Jonsson et al., 1994; Marty-Santos & Cleaver, 2015; Offield et al., 1996; Stoffers et al., 1997; Wu et al., 1997). In mouse, there are two main stages, called transitions, in which endocrine cells arise. The primary transition occurs between E8.5 and E12.5, when the epithelium shapes up into tubular structures and the multipotent pancreatic progenitor cells (MPC) proliferate (Burlison et al., 2008; Villasenor et al., 2010). These cells are the building blocks of the entire organ, since they can give rise to all pancreatic lineages (Pan & Wright, 2011). During this phase, it is possible to observe the presence of few endocrine cells, mostly α-cells. The secondary transition occurs between E12.5 and E15.5 and it is characterized by the formation of tip and trunk domains. The MPCs in the tip will originate acinar cells (Solar et al., 2009), while the ones in the trunk will generate bipotent (BP) and ductal progenitors (Zhou et al., 2008), underlying the importance of the surrounding environment in fate determination. The process that leads to the formation of all endocrine lineages is named endocrinogenesis. The master regulator of this process is the TF neurogenin 3 (Neurog3, Ngn3), which controls the genetic program behind the differentiation of the bipotent progenitors in the trunk towards endocrine progenitors (EPro) and precursors (EPre) (Johansson et al., 2007), followed by another TF, known as Fev (E26 transformation-specific transcriptional factor) (Byrnes et al., 2018). These cells are committed towards the endocrine fate but not hormone producing, yet. Thus, another differentiation program is initiated and determines the acquisition of the molecular mechanisms necessary for the synthesis and secretion of hormones (Bastidas-Ponce et al., 2017, 2019; Byrnes et al., 2018) (Figure 3). These cells are located in proximity to the ductal structures and are considered immature endocrine cells. One of the most intriguing process, and yet not well understood, is the endocrine fate determination. Recent studies suggest that the endocrine precursors are transcriptionally heterogeneous, thus it is likely that these heterogeneity might skew the fate determination process towards one cell type over the others (Bastidas-Ponce et al., 2019; Jennings et al., 2017). As today, what is well known is that the differentiation process requires the expression of certain TFs. In particular, Arx determines the α-cell fate (Wilcox et al., 2013), while Pax4 (Collombat et al., 2003), followed by Nkx2-2, Neurod1, Nkx6-1, among others, are essential for the β-cell phenotype acquisition (Arda et al., 2013). The endocrinogenesis process in human has not been fully understood, yet. One important difference concerns the single transition phase, different from the two observed in rodents, during which the endocrine

population arises (Jennings et al., 2013). Therefore, additional studies in human need to be done in order to uncover the endocrinogenesis mechanisms.

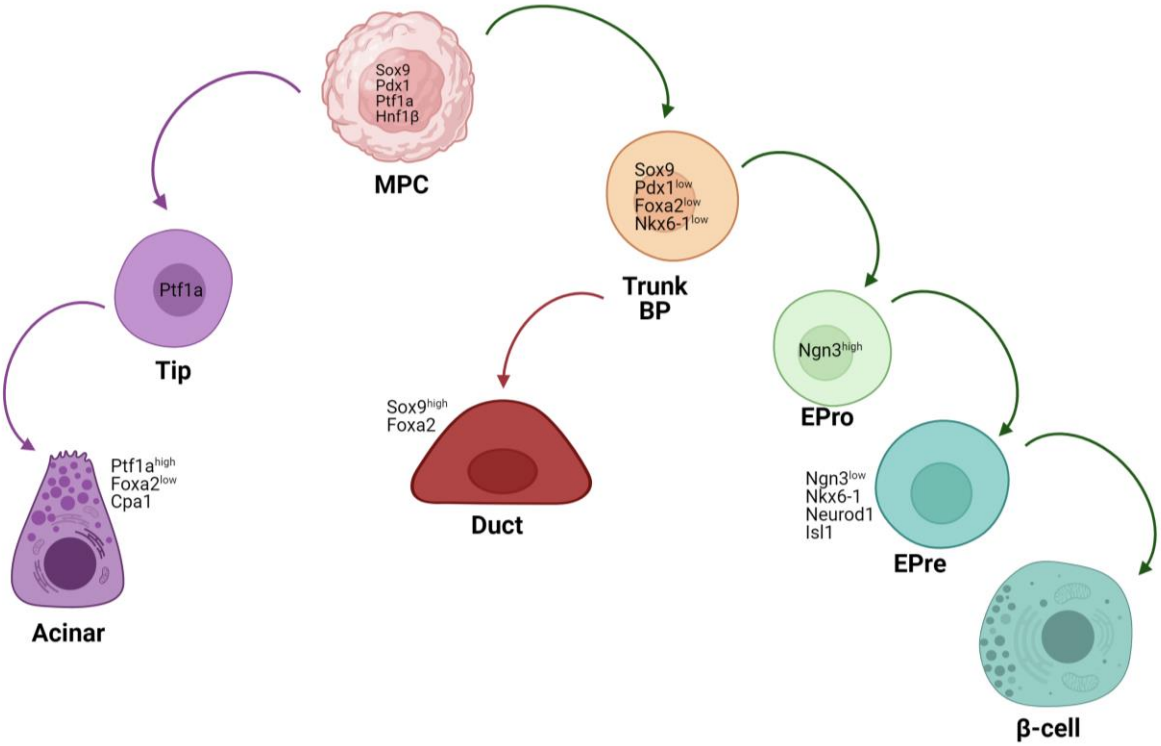


**Figure 3: Schematic representation of pancreas progenitor differentiation**

Representation of the main cell types appearing during pancreas development. From the common multipotent pancreas progenitor (MPC), two intermediates arise: the tip cells which give rise to the acinar cells and the trunk bipotent progenitors (BP). The latter can originate both ductal and endocrine cells (EPro: Endocrine Progenitors; EPre: Endocrine Precursors) (Bastidas-Ponce et al., 2017). Figure was created with BioRender.com.

## 2.4 Timeline of postnatal development

In mice, the postnatal period is defined as the time window from birth to the days following the weaning from the mother, which account for roughly 30 days (Bonner-Weir et al., 2016). Here we schematically separate, for the sake of description, this month in three equal fractions (Figure 4).

At birth, the pancreas undergoes important changes. To begin, the organism has to deal with the disconnection to the mother's system, thus achieving an independent systemic state. Among the most important changes compared to the embryonic stages, there is the initiation of the oral feeding. The entire

digestive system is involved in the process of digestion and absorption of nutrients from the breast milk of the mother (Dore et al., 1981). Once the nutrients are absorbed, the system is challenged, for the first time, with a wave of glucose, amino acids and lipids. At birth, the pancreas is disseminated with a high number of endocrine cells, scattered all over the area of the organ, organized in proto-islets, clusters of cells with low compaction (Bastidas-Ponce et al., 2017). At this point, β-cells are in an immature state and respond to glucose and amino acid stimuli, differently to what is happening in adults. In fact, low glucose and high amino acid concentrations trigger a high insulin release (Martens et al., 2013). During the first ten days after birth, the new nutritional environment determines changes in the β-cell compartment. It is still possible to observe an intense proliferative activity, residual from the embryonic development, gradually decreasing after birth (Garofano et al., 1998). The second ten days after birth are as eventful. The pups start eating crumbs and solid food, richer in carbohydrates (Abbott, 1996). Thus, the mixture between high fat milk and high carbohydrate solid food triggers changes within β-cells, initiating a second wave of maturation that strikingly reduce the proliferation rate (Bonner-Weir, 2000a), in favor of a more accurate insulin release in response to glucose stimuli. The last third of the first month of the life is marked by the full switch to the carbohydrates diet, in preparation to the most significant event of the postnatal development, the weaning, which usually occurs after the third week of life of the mouse. This event seems to trigger the final phase of maturation, where β-cells acquire the mature phenotype, with a more compact islet structure and an insulin release strictly controlled by the circulating glucose levels (Stolovich-Rain et al., 2015).

In the next paragraphs, the events occurring during the postnatal development will be described according to different parameters: markers, functionality and signaling pathways.

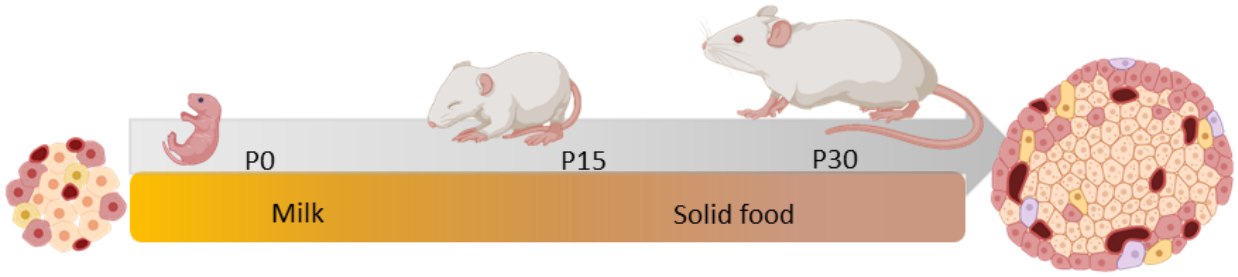


**Figure 4: Representation of the postnatal stage in mice**

Graphical summary of the postnatal stage in mice, starting from birth, up to the first month of life. The orange bar represents the important change of diet during this period, driving the metabolic maturation of the islets. Two islets are placed at the beginning and at the end of the timeline, differing in cell number, size, compaction and architecture. Figure was created with BioRender.com

### 2.4.1 Maturation Markers

#### 2.4.1.1 Transcription Factors

At birth, β-cells are committed cells, with TFs as Pdx1, Nkx6-1, Isl1, Nkx2-2 and Neurod1 already in place and defining a transcriptional landscape which specify the identity of these cells. During the postnatal development, other TFs determine the final steps of maturation. Here we want to focus on two Maf transcription factor family members, MafA and MafB (Hang & Stein, 2011) (Figure 5a). MafB is first expressed at E10.5 in the pancreatic epithelium, while MafA is expressed later at E13.5, only in insulin-positive cells. During the gestation period, almost all β-cells are MafB positive. Just after birth, this percentage falls and very few cells remain MafB positive by the second week after birth and the TF will remain exclusive for α-cells. On the contrary, MafA is gradually more expressed from embryonic until birth and even more importantly, the expression levels of the gene are incremented from neonatal to adulthood (Nishimura et al., 2015). Knock-Out (KO) studies have demonstrated that these two TFs are not essential for the lineage specification or differentiation process. MafB is required for α- and β-cell development (I. Artner et al., 2007), considering its role in promoting the glucagon and insulin transcription and the maintenance of other key β-cell genes. In early stages, MafA is dispensable due to the compensatory effect of MafB, thus only enhancing the *Ins1* gene transcription. The importance of MafA is significant only after birth. Several studies have shown that MafA is a potent glucose-responsive insulin transcriptional activator and is the determinant of the β-cell maturation (Nishimura et al., 2015). MafB regulates many genes involved in glucose sensing, insulin secretion, vesicle maturation and calcium signaling (i.e., Slc2a2, Nnat, Slc30a8, Camk2b). After birth, MafA takes over the role of controlling the transcription of these genes important for the β-cell functionality (Gck, Slc2a2, Pdx1, Nkx6.1, Glp1r, Pcsk1, Pcx, GLP1R) (Nishimura et al., 2015).

#### 2.4.1.2 Cytoplasmic molecules

In the past years, a panel of markers was identified in order to follow β-cell maturation (Figure 5b). In this paragraph, we will describe the most commonly used. Neuropeptide Y (NPY) is a neuropeptide expressed in the terminations of the sympathetic nerve of the pancreas and in endocrine cells. NPY is expressed in embryonic and early postnatal β-cells and its physiological function has been associated with inhibition of the insulin secretion and increased proliferation. Thus, NPY is a marker for an immature, more proliferative group of neonatal β-cells (Rodnoi et al., 2017). Urocortin 3 (Ucn3) is a secreted peptide, used as molecular marker that, opposite to NPY, is upregulated during the first two weeks postnatal and has been extensively used to follow the functional maturation process of β-cells (Blum et al., 2012). Recent studies have shown that Ucn3 has no role in the differentiation and maturation processes (J. L. Huang et al., 2020a), and its action might mediate a somatostatin-dependent negative feedback control of insulin secretion (Van Der

Meulen et al., 2015). Synaptotagmin 4 (Syt4) is an atypical member of the synaptotagmin family, due to the lack of the calcium-binding domain. It is a synaptic vesicle protein, which has been shown to be upregulated during β-cell postnatal development. In contrast to Ucn3, Syt4 has a functional role in the maturation process, inducing a reduction of β-cell calcium sensitivity, which determines the basal insulin secretion level, fundamental step to acquire a fine-tuning insulin secretion (C. Huang et al., 2018). Transferrin receptor protein 1 (TfR1 or CD71) has been recently identified as another marker which also increases during the postnatal stage on β-cells. Its expression is upregulated during the first weeks of life and correlates with an increased iron metabolism of β-cells (Berthault et al., 2020). Flattop (Cfap126, Fltp) is another molecular maturation marker recently identified in our laboratory (Gegg et al., 2014; Lange et al., 2012). Interestingly, Fltp distinguishes two β-cell populations. A positive one, with mature physiological features and a negative one, with a less mature phenotype and a higher proliferation rate. In addition, Fltp reports for the activation of Wnt/PCP, which has been identified as one of the pathways necessary to acquire the mature phenotype (Bader et al., 2016).

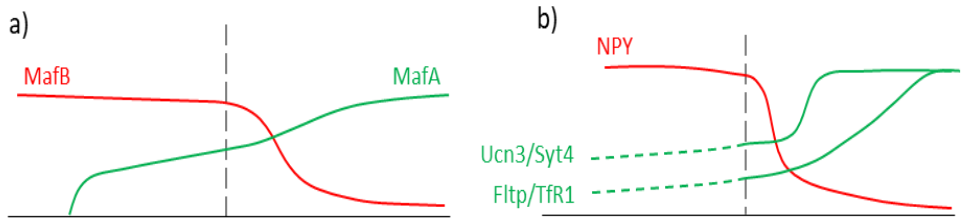


**Figure 5: Dynamic of expression of commonly used β-cell markers**

a) Dynamic of expression of two transcription factors, MafB indicating the immature β-cells and MafA indicating the mature ones; b) similarly, dynamic of expression of other proteins used to define the acquisition of the mature phenotype, NPY rapidly downregulated and Ucn3, Syt4, Fltp and TfT1 gradually expressed after birth. Grey dashed line indicates the birth date.

### 2.4.2 Functionality

Two major functional characteristics define the β-cell postnatal maturation process are the proliferative capacity and the insulin secretion in response to glucose.

#### 2.4.2.1 Proliferation

The proliferative capacity is usually possessed by cells for a short time period, during the early stages of development. In adulthood, this capacity is restricted to a minor pool of cells, resident stem cells that have the function to fuel the tissues with new cells, allowing the cellular turnover. The islets of Langerhans are mini organs with an extremely low turnover rate in adulthood (Arrojo e Drigo et al., 2019; Teta et al., 2005). The proliferative capacity in β-cells is kept under control and restricted to immature cells at the latest stages of embryonic and early stages of postnatal development (Bonner-Weir, 2000b) (Figure 6) or in high

metabolic demanding situations like pregnancy (Baeyens et al., 2016). The final aim of the proliferation is to maintain an adequate β-cell mass to fulfill the insulin needs (Bonner-Weir, 2000). During the embryonic development, the β-cell mass relays on the endocrinogenesis, process that determines the formation of β-cells from the MPCs, while the proliferation of the newly formed endocrine cells is minimal (Bastidas-Ponce et al., 2017). The significant expansion of the β-cell mass occurs during the perinatal period, where β-cells become more proliferative, together with a negative regulation of the apoptosis process (Scaglia et al., 1997). Studies have shown that the mechanisms regulating the proliferation in embryonic and postnatal are different. If the loss of cyclin D2 (Ccnd2) (Georgia & Bhushan, 2004a) or cyclin-dependent kinase 4 (Cdk4) (Martín et al., 2003) have little or no effect on the embryonic β-cell mass, in postnatal it determines a massive reduction. Similarly, forkhead box M1 (FoxM1), a TF important for the cell cycle progression, has no impact on the embryonic β-cell proliferation (H. Zhang et al., 2006). The postnatal and adult cycling cells are different from the embryonic ones and they have an immature phenotype, probably because their main function, in that specific moment, is not to respond to glucose challenges, but to divide and increase the mass (Gunasekaran et al., 2012). One of the main driver of this proliferation wave is glucose (Moullé et al., 2017). As mentioned, after birth the body is independent from the glycaemia regulation of the mother, thus glucose waves arrive to β-cells. The glucose signaling serves to expand the β-cell mass. Together, the expansion of the mass and the acquisition of a better control of the insulin secretion lead to the exit of the cell cycle after the first week of life. Another proliferation wave arises at weaning age; however the β-cell mass is not substantially changed due to the increased apoptosis rate (Stolovich-Rain et al., 2015). Recent studies have shown that if cells are forced to reenter the cell cycle, these adapt transcriptional programs resembling postnatal β-cells. Therefore, the proliferation is strictly associated with an immature β-cell phenotype (Puri et al., 2018).

#### 2.4.2.2 Insulin secretion

The glucose-stimulated insulin secretion (GSIS) is a characterizing feature of β-cells in their final differentiation stage (Blum et al., 2012). This capacity is established at the moment of their commitment to the β-cell lineage. However, secreting an appropriate amount of insulin in response to the blood glucose levels is not developed until later in life (Figure 6). These cells are naïve and they have not been primed yet in the embryonic stages, since the system is still depending from the mother. The priming occurs once the oral feeding begins, when the system is autonomous and needs to control its own blood glucose levels. Furthermore, these cells need to be "trained" according to a recent study describing circadian feeding/fasting cycles as necessary triggers for the metabolic maturation (Alvarez-Dominguez et al., 2020), followed by changes in diet type to complete the process (Stolovich-Rain et al., 2015). Thus, the fine-tuned insulin secretion requires several weeks and a cascade of stimuli to achieve a perfect GSIS. The insulin

secretion is a harmonized process, result of a complex number of events. First, β-cells need to sense glucose, thus they have to express an adequate number of glucose transporters (Glut2/Slc2a2) on the plasma membrane. Another essential player, the enzyme glucokinase (GCK), converts the monosaccharides in glucose-6-phosphate (G6P) molecules, which are now spendable cellular currencies and can enter one of the two metabolic pathways: glycolysis and oxidative phosphorylation. End-goal of the glucose metabolism is the generation of ATP molecules and oxidation of the glucose-derived carbons in the mitochondria. The increased ATP concentrations determine the inhibition of the potassium ATP-dependent channels ($K_{ATP}$ channels), generating a depolarization event on the plasma membrane, resulting in the opening of the calcium voltage dependent channels (VDCC), which restores the membrane potential. The calcium influx induces the fusion of the insulin granules to the plasma membrane, in the complex mechanism called exocytosis (Alcazar & Buchwald, 2019; Kang et al., 2018; Komatsu et al., 2013). The process of sensing and secreting is already functional at the moment of the specification towards the β-cell lineage, but not fine-tuned. A number of studies have shown that neonatal β-cells are "leaky", thus missing the control of the insulin secretion at low glucose concentrations. This phenomenon indicates the immaturity of the cells at birth. To begin, the glucose sensing relays on the presence of Glut2 on the cell membranes and its expression has to be maintained at high levels. Due to its high glucose affinity and fast transport capacity, Glut2 allows a quick entrance of the glucose in the cells, substrate of the GK that catalyzes the rate-controlling step in the GSIS (Thorens, 2015). Examples of the importance of this protein come from both KO studies and physiological conditions observations. Mice lacking Glu2 specifically in β-cells develop an early form of diabetes (Guillam et al., 1997). Furthermore it has been shown that in pregnancy, before the β-cell mass expansion, these cells downregulate Glut2 expression, acquiring an immature phenotype (Beamish et al., 2017). As mentioned before, glucose enters the cellular metabolism to generate ATP. Several studies have shown that postnatal β-cells have lower expression of several metabolic genes as mitochondrial shuttles (Mdh1, Gpd1 and Got1), pyruvate carboxylase (PC) and Cpt2, indicating a lack of specialized metabolic pathways. These are slowly acquired until after weaning, when the metabolism of β-cells is fully mature (Jermendy et al., 2011). The increase in ATP concentrations determine one of the signature characteristic of β-cells, the excitability of their plasma membranes (Richards et al., 2020; Patrik Rorsman & Ashcroft, 2018). The ATP-dependent potassium channels determine the depolarization process, while the voltage dependent calcium channels induce the repolarization as a consequence of a calcium influx. Studies have shown that during postnatal development an array of excitability genes is upregulated (García-Delgado et al., 2018). The final step of the process is the release of insulin in the bloodstream. It should be noted that two pools of insulin granules exist, named "releasable" and "reserve" pools. A fraction of the total insulin granules (<5%) is always ready to be immediately released, thus it is in close proximity to the plasma membrane. The rest, and majority, of the

granules exist as reserve pool and are mobilized only after the first line of granules have been secreted (P. Rorsman & Renström, 2003). Both pools have strong dependency to calcium signaling. However, the releasable granules depend on the extracellular calcium influx, while the reserve pool relies on the ER-calcium efflux for their mobilization (Hao et al., 2005). The molecular mechanisms guiding the exocytosis have been vastly studied. The SNARE proteins are expressed on the granules membranes and form structures that interact with other complexes on the plasma membrane (VAMPs with syntaxis and SNAP-25), forming a "zip" type of connection, responsible to bring in proximity the granules to the membranes and favor the membrane fusion (Thurmond, 2007). The role of calcium sensing is took over by the synaptotagmin (SYT) protein family which through conformational changes after binding with calcium, determine the fusion of the granules to the plasma membrane and the final insulin release (Gilbert & Blum, 2018). The SYT proteins have different roles, the best characterized in β-cells are Syt7 and Syt4, the first mediating calcium sensing, the second reducing the calcium sensitivity during postnatal development and fundamental in increasing the basal insulin secretion (Dolai et al., 2016; C. Huang et al., 2018). Of note, a healthy and mature insulin secretion has a biphasic modality (Patrik Rorsman et al., 2000). The first phase is the consequence of the sudden high calcium influx and determines the secretion of the pre-docked insulin granules (short duration, high concentration) for a fast action. The second phase is the result of the mobilization of the reserve granules. It is more sustained over time but its magnitude, usually reduced compared to the first phase, is determined by amplifying signals, coming from the glucose metabolism or external factors (Henquin et al., 2002).

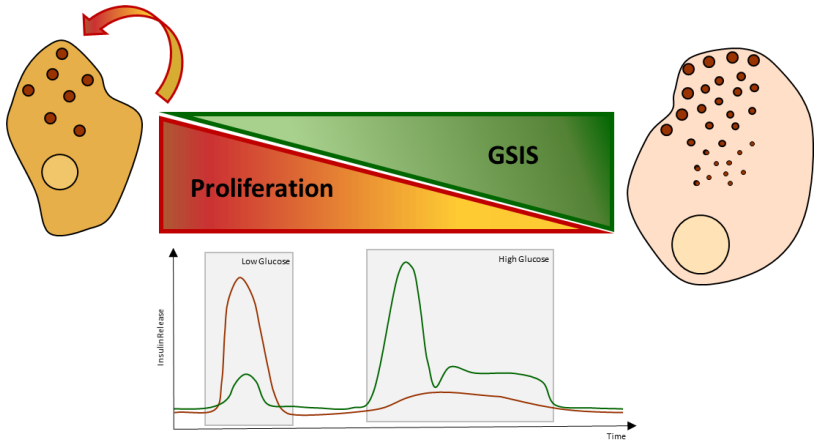


**Figure 6: Functional characteristics of mature and immature β-cells**

Graphical representation of the two signature characteristics of mature and immature β-cells: proliferative capacity typical of immature cells and adequate insulin secretion to glucose challenges for mature cells. On the bottom, GSIS profiles of immature cells (red line, high insulin secretion with low glucose levels and lack of second phase of insulin secretion) and mature cells (green line, low insulin secretion at low glucose concentrations and two phases of high insulin secretion at high glucose levels).

### 2.4.3 Signaling Pathways

Behind the changes happening during the postnatal period we can observe a complex network of signaling pathways, often connected one another, and responsible for the complex phenotypes described in the previous paragraphs.

#### 2.4.3.1 mTOR and AMPK

Considering that the endocrine pancreas is involved in the regulation of the glucose homeostasis, it is not surprising to find two of the most important nutrient-sensing pathways involved in the process of β-cell maturation.

Mechanistic target of rapamycin (motor) is the scaffold protein of two serine-threonine kinase complexes, known as mTORC1 and mTORC2. They are involved in several different cellular functions as proliferation, survival, transcription and translation, among others, in connection to nutrients and growth factors availability (Kim & Guan, 2019; Laplante & Sabatini, 2009). In the mTORC1 complex, we find the adaptor protein Raptor, which directly phosphorylates S6 kinase (S6K) and Eif4ebp1, enhancing protein translation (Condon & Sabatini, 2019). In the mTORC2 complex, we find a different adaptor protein, Rictor, involved mostly in cytoskeletal reorganization and maintenance of the cell size (Jacinto et al., 2004). Several studies have investigated the role of mTOR in islets. In particular, dysregulation of the pathway in β-cells leads to obesity and diabetes, while rapamycin-inhibition leads to improved blood glucose levels in hyperglycemic patients. However, the exact role and mechanisms of mTOR in healthy β-cells is yet to be clarified, due to the plethora of factors that can affect the function of mTOR within a specific environment, in particular due to its role of modulating mitochondrial oxidative stress and ER stress (J. Wang et al., 2016). During the embryonic development, mTOR has a dispensable role in endocrine specification and differentiation but assumes a fundamental role after birth. Both mTOR complexes are required for the morphogenesis process and the establishment and maintenance of the β-cell mass. However, mTORC1 leads more specifically the maturation process, partially via Pax6 regulation (Sinagoga et al., 2017).

5′ AMP-activated protein kinase (AMPK) is a serine/threonine protein kinase complex, made of three subunits, α- (catalytic), β- (scaffold), and γ- (regulatory), sensing the nutritional environment through the intracellular ATP/ADP ratio levels. Thus it is responsible for the maintenance of the energy homeostasis and function as stress sensor (Herzig & Shaw, 2018). In β-cells, AMPK activity is detectable under basal glucose conditions and it is downregulated upon high glucose stimulations. AMPK activity is reported to influence the insulin secretion via inhibition of glucose oxidation, insulin vesicle mobilization to the plasma membrane and calcium influx (Rourke et al., 2018). Finally, it has not been clarified yet whether AMPK might also influence the maintenance of a physiological β-cell mass, by regulating the apoptotic processes (Szkudelski & Szkudelska, 2019). Recent studies have identified a critical functional switch between

mTOR and AMPK during the β-cell postnatal maturation process. The weaning process was previously identified as trigger for the final maturation step (Stolovich-Rain et al., 2015). Changes in diet, moving from high fat to high carb food, activates more strongly AMPK, which in turn inhibits mTORC1, predominantly activated during the first two weeks after birth and responsible for the functional immaturity of β-cells (Jaafar et al., 2019). Another study dissected this phenomenon, explaining the shift in nutrient sensitivity of mTORC1-dependant insulin secretion, from amino acids to glucose. Thus, immature β-cells respond to amino acid, highly abundant in the early postnatal plasma, determining a constitutive activation of mTORC1. On the contrary, mature β-cells respond to a mixture of high glucose and amino acids and mTORC1 activity becomes intermittent and glucose-dependent (Helman et al., 2020a).

In conclusion, the nutrients availability directly determines the type of metabolism necessary in β-cells. The metabolic plasticity of these cells at the postnatal stage allows a phenotypical adaptation that is reflected on the changes in GSIS.

#### 2.4.3.2 Wnt signaling

The Wnt signaling pathway is famously known for its involvement in organogenesis, development and cancer (Jung & Park, 2020; Steinhart & Angers, 2018). This pathway acts via specific Wnt proteins that can bind a set of two family of receptors, the Frizzled (Fzd) and the LDL-receptor-related protein (LRP). The complexity of this pathway resides on the multiplicity of modulators and interactions that can activate/inhibit several intracellular responses (H. C. Huang & Klein, 2004; Jennings et al., 2017b; Mikels & Nusse, 2006; Tamai et al., 2000; Willert & Nusse, 2012). Classically, Wnt is divided in two branches, known as “canonical” Wnt/β-catenin and two “non-canonical” pathways, the 'Wnt/Planar Cell Polarity (PCP) and the Wnt/Ca2+ (Komiya & Habas, 2008). Wnt/β-catenin is the most studied among the three. As the name suggests, the pathway relays β-catenin proteins´ levels. In absence of Wnt stimulation, a destruction complex (Axin, APC, and Gsk3β) targets β-catenin, preventing its accumulation. Wnt stimulation, in contrast, prevents the formation of the destruction complex, thus favoring the cytoplasmic accumulation of β-catenin and its subsequent nuclear translocation, where it will promote (as co-activator with the transcription factor Tcf/Lef) the transcription of a series of target genes (MacDonald et al., 2009). Wnt/PCP is important for the establishment and maintenance of the cell polarity. Its role has been shown in processes like gastrulation, neurulation, cilium orientation and asymmetric cell division, by inducing transcriptional changes or acting on the cytoskeleton. The mechanism of action remains more elusive, but it is known that it might act by asymmetrically distributing core PCP components (i.e., Van Gogh/Vangl, Frizzled, Disheveled, Prickle/Spiny-Legs, and Fmi/Celsr and Diego) in different regions of the cell (Y. Yang & Mlodzik, 2015). Wnt/$Ca^{2+}$ acts via intracellular calcium release, which in turn will activate two

calcium sensitive enzymes, $Ca^{2+}$/calmodulin-dependent protein kinase II (CamKII) and protein kinase C (PKC) (Kühl et al., 2000).

Wnt signaling is actively involved in developmental processes and the pancreas does not make an exception. Both Wnt branches contribute, in a spatial-temporal manner, to the pancreatic induction process, endocrine and exocrine lineage segregation and endocrine functional maturation (Scheibner et al., 2019). It has been broadly described that canonical Wnt is essential for endoderm (germ layer, which will generate tissues belonging to the gastrointestinal and respiratory tracts and endocrine organs) induction and posterior endoderm patterning (McLin et al., 2007; Rodríguez-Seguel et al., 2013). Wnt/β-catenin is essential to maintain the proliferative capacity of the pancreatic progenitors and inhibits Notch signaling in order to favor the formation of tip cells instead of truck cells (Baumgartner et al., 2014; Rulifson et al., 2007). In contrast, Wnt/β-catenin inhibition is crucial for the endocrinogenesis process and the differentiation process appears to be dependent on Wnt/PCP, as shown from the presence of active PCP in pancreatic progenitors (Cortijo et al., 2012). Wnt signaling has also a role during the final steps of maturation of endocrine cells, although not yet fully understood. As expected, it has been proved that canonical Wnt signaling is essential for the neonatal β-cell expansion mediated by proliferation. Furthermore, in the same study, it was shown that inhibition of Gsk3β, a β-catenin negative regulator, stimulates β-cell proliferation by stabilizing β-catenin and re-expression of cyclin D (Figeac et al., 2010). Another study underlined an intriguing hypothesis involving Wnt/PCP. Fltp has been identified as Wnt/PCP downstream effector, interacting with the PCP core and cytoskeleton components (Gegg et al., 2014). In a recent study from our lab, Fltp was discovered to be heterogeneously expressed in pancreatic islets. Characterization of the two β-cell populations, linked the positive cells to a mature phenotype and the negative cells to an immature and more proliferative phenotype (Bader et al., 2016). From this study, it has been concluded that PCP is required for the reorganization of the cytoskeleton and the establishment of the islets architecture, thus the acquisition of the mature phenotype (Roscioni et al., 2016). An additional proof that Wnt is essential for the pancreatic endocrine formation and maturation comes from the differentiation protocols used to derive β-cells from human induced pluripotent stem cells (iPSC). In fact, in these protocols several Wnt modulators are used to prompt endoderm induction, endocrinogenesis and endocrine maturation (Wesolowska-Andersen et al., 2020). Several recent studies have unlighted our understanding of these processes. One linked the inhibition of ROCKII with a more mature β-cell phenotype (Ghazizadeh et al., 2017) while another showed how by chemically manipulating the cytoskeleton it was possible to obtain better stem cell derived β-cells (Hogrebe et al., 2020a). Both studies put an accent on the cytoskeletal modifications in order to obtain cells capable of recapitulating human β-cells. The last proof came from a study in which it was demonstrated that non canonical Wnt signaling is needed to achieve the metabolic maturation of stem-cell derived β-cells, with a focus on the acquisition of an appropriate GSIS (Yoshihara et al., 2020). Last, Wnt has been associated

with diabetes. TCF7L2 has been identified as a major risk component for T2D, since mutations in the gene lead to a dysfunctional β-cell phenotype with impaired insulin secretion (Welters & Kulkarni, 2008).

#### 2.4.3.3 Others pathways

Other important pathways are involved in the complex process of β-cell maturation. The Hippo signaling pathway is broadly known for its role in controlling tissue and organ sizes by regulating proliferation and apoptosis (Zhao et al., 2010). When the pathway is inactive, Yes-associated protein 1 (YAP) and the transcriptional coactivator PDZ-binding motif (TAZ) bind a series of genomic elements using a co-transcription factor named transcriptional enhanced associate domain (TEAD), which regulate genes involved in proliferation and survival. When the Hippo signaling is active, it controls the fate of these proteins by retaining them in the cytoplasm or sending them to the proteasome, thus promoting the cell cycle exit (R. Johnson & Halder, 2014). YAP is broadly expressed in the early stages of pancreas development (Gao et al., 2013; N. M. George et al., 2012), but becomes restricted to the exocrine compartment and completely silenced in endocrine progenitors once Ngn3 is active (Cebola et al., 2015; Nicholas M. George et al., 2015). Studies have shown that YAP inhibition is therefore necessary to make β-cells during the differentiation and maturation process. At postnatal, Yap expression is completely lost and this coincides with the loss of proliferative capacity and the acquisition of the mature phenotype. Thus, Hippo might play an essential role in the maturation process. Estrogen-related receptor γ (Err) has been identified to be expressed in adult but not pre- and postnatal islets. Once abundant in β-cells, ERRγ activates a transcriptional profile which leads to a metabolic maturation. In particular, a series of changes were observed in mitochondrial oxidative phosphorylation, the electron transport chain, and ATP production, responsible for the improvement of the insulin secretion at different glucose concentrations. Similarly, ERRγ expression in iPSC-derived β-cells determined a functional switch with subsequent improvement of GSIS (Yoshihara et al., 2016). However, the main question regarding how this signal is transduced to the nucleus remains unanswered. Future studies should focus on connecting the knowledge accumulated.

### 2.4.4 External influences on islets maturation

The previous paragraphs have summarized our understanding of the β-cell maturation process in transcriptional and functional terms. However, this is an oversimplified view of what really occurs *in vivo*. In fact, the so-called islet niche contains many players, among which vessels, nerves, immune cells and extracellular matrix (Alessandra et al., 2020). The role of the blood vessels is undeniable in the context of the pancreas and islet function. At the base of this relationship there is a functional interconnection. The capillaries deliver glucose to the islets and β-cells secrete an appropriate amount of insulin in response to the blood glucose levels to maintain the systemic euglycemia. β-cells control the intra-islet vasculature by secreting VEGF-A, which recruits endothelial cells and has a trophic function in the maintenance of the

vasculature survival. The endothelial cells and the capillaries contribute to the pancreas development, the insulin secretion and β-cell proliferation by providing nutrients, oxygen, growth factors and a structural support (Staels et al., 2019). Thus, it is not surprising to see many studies confirming the importance of endothelial cells in the context of the human islets transplantation or to improve the current β-cell differentiation protocols (Arrojo e Drigo et al., 2019; Narayanan et al., 2017). Another less known player in the islet maturation process is the nervous system. Studies have shown the importance of the sympathetic innervation during pancreas development and islet maturation (Borden et al., 2013; Burris & Hebrok, 2007) and that the autonomic nervous system may play a role in controlling β-cell proliferation via vagus nerve stimulation (Moullé et al., 2019). The immune system is no stranger in the islets. T1D is the outcome of the association between islets and immune cells, due to the autoimmune attack of β-cells. However, the immune system has important role during development and in islets. Myeloid cells, with an accent on macrophages, seem to acquire a specific phenotype and become resident in the exocrine or endocrine pancreas (Guo & Fu, 2021). In a less understood fashion, macrophages are involved in the regulation of insulin secretion (Jensen et al., 2020; Ying et al., 2019). Finally, we need to acknowledge the importance of the extracellular matrix (ECM) component for the islet functions. The ECM strongly contributes to the generation of a three-dimensional structure, in which islets are submerged. In addition, the ECM provides also cytokine and growth factors which sustain the islet survival and functionality (Townsend & Gannon, 2019a). Several reports have linked ECM components with the establishment of β-cell polarity towards the vessels (Cottle et al., 2021; Wan J. Gan et al., 2017) and its role in the maintenance of a mature type of functionality (Arous & Wehrle-Haller, 2017). Other regulators of β –cell functionality and proliferation are the integrins (Wan Jun Gan et al., 2018). The best characterized are the $\alpha_v\beta_3$ and $\alpha_v\beta_5$ during pancreas development (Cirulli et al., 2000) and β1-integrin for β-cell expansion (Diaferia et al., 2013).

### 2.4.5 β-cell heterogeneity: an evolving concept

All β-cells are characterized by the expression of insulin and by the release of this hormone upon glucose stimulation. However, not all β-cells are the same (Roscioni et al., 2016). This notion was already known in the 60s, when differences in nuclear size among insulin producing cells were observed within the islets (HELLERSTROM et al., 1960). A few years later it was also observed that the electrical activity differed from β-cells in the core and in the periphery of the islets (Dean & Matthews, 1968). In the 80s, the concept of a functional heterogeneity was strengthen by demonstrating that not all β-cells were capable of secreting the same amount of insulin upon same glucose stimulation (Stefan et al., 1987). Thus, it became common knowledge that β-cells were heterogeneous but remained an unexplored concept until the last decade, when thanks to several technological advances (lineage tracing systems, scRNA-seq, *in situ* calcium imaging, proteomics, etc.), it was possible to characterize transcriptionally and functionally the different β-cell

populations (Liu & Hebrok, 2017). For simplicity, we describe the β-cell heterogeneity according to three features: space, time and disease (Figure 7).

#### 2.4.5.1 Spatial heterogeneity

The spatial heterogeneity (a.k.a. inter-islet) characterizes the entire pancreas. This organ can be divided in four regions: head, neck, body and tail (Ellis, 2007). Several studies have pinpointed that islets' composition and size differ depending on their physical localization in the pancreas (Steiner et al., 2010; X. Wang et al., 2013). This spatial heterogeneity may derive from the embryonic development. It is known that the pancreas arises from two distinct buds (dorsal and ventral) which merge during the early stages of development (Aimeé Bastidas-Ponce et al., 2017). It is likely that the two pancreatic buds possess different flavors of progenitors that likely determine the differentiation towards α- and γ- or β- and δ- cells. In addition, this spatial heterogeneity may be influenced by differences in vascularization and innervation, thus environmental cues (Chien et al., 2019; Kulenović & Sarač-Hadžihalilović, 2010; Muratore et al., 2021; Saricaoglu et al., 2020). What is also interesting is the observation that in diabetic conditions, not all islets are affected in the same way. It appears that certain pancreas lobes are less affected than others (Rodriguez-Calvo et al., 2015; X. Wang et al., 2013). One unsolved question regards the distribution of the different β-cell subpopulations according to the pancreas regions. It is not yet understood if the localization determines different β-cell phenotypes.

#### 2.4.5.2 Temporal heterogeneity

A second level of heterogeneity, here referred as temporal heterogeneity, indicates the presence of different β-cell populations according to the stage of life. This is probably the best characterized type of heterogeneity, related to the concepts of β-cell maturity and immaturity. In early stages of development, the majority of β-cells have an immature phenotypical (high basal insulin secretion, proliferative and glycolytic metabolism). These cells can be recognized by the presence of markers like MafB, NPY, Rbp4 and CD81 (which we will describe in detail in the Results section). After birth, the maturation process induces the acquisition of a mature phenotype (appropriate GSIS, abundant mature insulin granules, high mitochondrial activity and oxphos metabolism) (Salinno et al., 2019). Surprisingly, even after the postnatal maturation stage, β-cells remain extremely heterogeneous also in adulthood, mixing cells with more or less mature features (Liu & Hebrok, 2017). The discovery of the numerous markers to classify β-cells also revealed the complexity of this cell type. Often, similar markers can have different pattern of expression, leading to another open question, what factors determine a specific β-cell phenotype?

### 2.4.5.3 Pathological heterogeneity

The last layer of heterogeneity is what here we call pathological heterogeneity. With this term, we indicate dysfunctional β-cells arising in response to the establishment of metabolic stress. Dedifferentiation, the process leading to the loss of mature phenotype, reversing it to an embryonic/neonatal state (Talchai et al., 2012). Transdifferentiation, in which a cell type, by losing key transcription factors, undergoes a change in cell fate program, thus leading to polyhormonal cells expressing insulin but together with other hormones as glucagon, somatostatin and PP (M. F. Brereton et al., 2016; Hunter & Stein, 2017). Last, senescence, a process normally occurring during aging; however, diabetes is known to accelerate stress-induced senescence, producing damaging conditions via senescence-associated secretory phenotype (SASP) (Aguayo-Mazzucato et al., 2019; Thompson et al., 2019). Therefore, in diabetes, we might find β-cells that are usually not present in adult healthy islets. Interestingly, the ratio of the different β-cell subpopulations is skewed, allowing the possibility to target the unhealthy subpopulations in order to restore the healthy mature one (Bader et al., 2016; Dorrell et al., 2016a; Rui et al., 2017; Sachs et al., 2020).

In conclusion, our current understanding points at a dynamic cellular heterogeneity of β-cells which changes depending of several factors, including age and diseases. Therefore, understanding the molecular mechanisms determining and controlling β-cell heterogeneity might unveil pharmacological targets for regenerative therapy and to improve the current stem cell differentiation protocols. Some questions remain unsolved: how do islets control this heterogeneity? What signaling pathways are associated to a less mature β-cell phenotype? How do we target a specific subgroup of β-cell for regenerative and therapeutic targets?

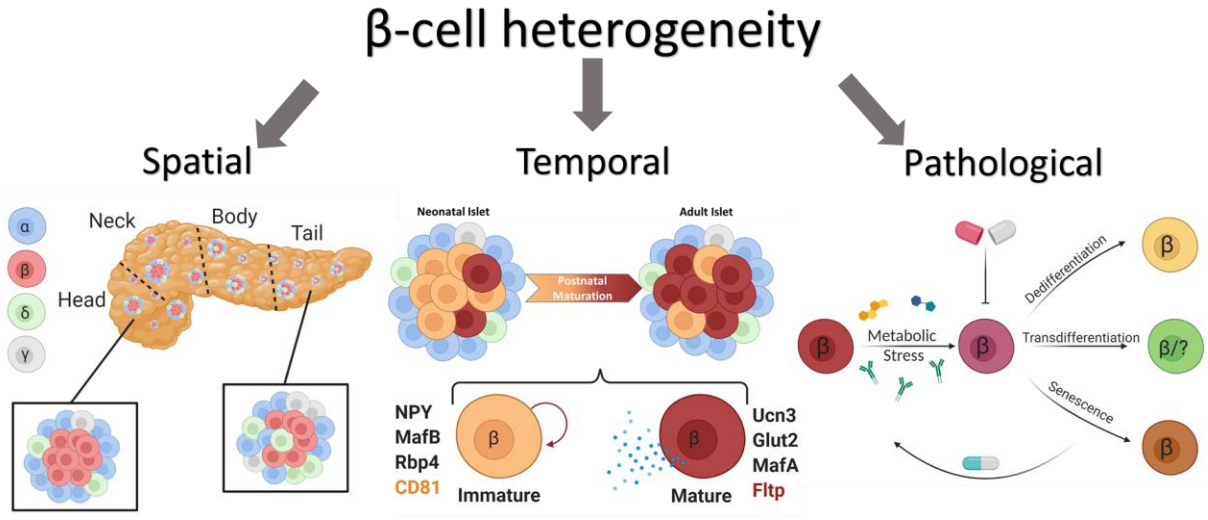


**Figure 7: Snapshot of β-cell heterogeneity**

Graphical representation of the three types of heterogeneity. Spatial, regarding the islet composition based on their pancreas localization. Temporal, referring the changes of β-cell subpopulations throughout life. Pathological, indicating the unhealthy β-cells appearing under diseased conditions. Figure was created with BioRender.com

# 3 Aims of the thesis

Pancreatic β-cell heterogeneity has been first described in the 1960s but its relevance, in the context of development and disease, has recently reemerged. Today it is known that mature and immature β-cells coexist in the islet of Langerhans. The ratio between these two subpopulations is determined by the specific stage of life (embryonic vs postnatal vs adult), systemic metabolic demands (pregnancy and obesity) or pathological conditions (hyperglycemia, hyperlipidemia and autoimmunity). A number of markers, in combination with innovative approaches, among which transgenic animals, transcriptomic, computational biology and functional assays, greatly improved the understanding of β-cell heterogeneity. The overarching goal is to distinguish the different subpopulation and decipher the mechanisms behind the establishment of the heterogeneity to have entry points for β-cell protection and regeneration for improved diabetes therapy. Therefore, in this thesis we were interested to address the two following objectives:

Aim 1: Deciphering the molecular mechanisms behind Wnt/PCP acquisition

Previous research from our lab demonstrated the role of Wnt - planar cell polarity (PCP) in the context of β-cell mature phenotype acquisition. Nevertheless, several open questions remain to be answered. First and most importantly, it is still unknown the mechanism through which PCP regulates β-cell maturation. Several hypotheses have been formulated involving the establishment of islets' architecture via cell-cell adhesions and cytoskeleton rearrangements, which would affect, in unknown ways, the gene expression of these cells. Thus, we aimed to decipher these mechanisms using Fltp lineage-tracing mice in combination with single cell RNA sequencing (scRNA-seq) analysis.

Aim 2: Discovery and characterization of novel β-cell immaturity markers

The existence of immature β-cells has been demonstrated multiple times in previous years. This β-cell population has attracted attentions due to its intrinsic proliferative capacity, thus the possibility to understand what mechanisms are behind the maintenance of an immature phenotype. However, most of the markers employed to study β-cell heterogeneity are either targeting mature cells or are cytoplasmic, thus requiring genetically modified reporter animals and cell lines. To this end, we aimed at discovering novel β-cell immaturity surface markers by screening scRNA-seq dataset and confirming the candidates via flow cytometry, histology, confocal imaging, protein biochemistry and *in vitro* assays.

# 4 Results

## 4.1 Part 1: Deciphering the postnatal β-cell heterogeneity

### 4.1.1 Tracing Fltp transition state in islets using the FltpiCre$^{mTmG}$ mouse line

Flattop (Fltp) has been previously described as a Wnt/PCP reporter gene (Böttcher et al., 2021; Gegg et al., 2014; Lange et al., 2012) and heterogeneously expressed in islets of Langerhans. Its expression, thus PCP acquisition, has been associated with a mature β-cell phenotype (Bader et al., 2016). Here we tackled the unanswered questions regarding the mechanisms promoted upon PCP acquisition in endocrine cells.

The mouse line Fltp iCre$^{mTmG}$ was an important tool for our research. This lineage tracing mouse line was previously used in our laboratory (Lange et al., 2012; Muzumdar et al., 2007) to irreversibly mark cells receiving Wnt/PCP signals (Figure 8a). In brief, every cell was labelled on the plasma membrane by the TdTomato fluorescent protein (red), which indicated Fltp negative cells (Fltp$^{-}$). Upon receipt of the Wnt/PCP signals, the Fltp gene and the downstream knocked-in T2A-iCre sequence were expressed. The Cre enzyme would excide the TdTomato sequence, due to the two adjacent LoxP sequences, and lead to the constitutive expression of another gene, the mGFP (green), marking the so called Fltp positive cells (Fltp$^{+}$). Interestingly, this mechanism generated a short time window during which we could observe the cells that recently received the Wnt/PCP signaling. These cells (Fltp transient or Fltp$^{\pm}$) appeared to be yellow, due to the coexistence of both the red (slowly degraded) and green (beginning to be expressed) proteins on the plasma membrane (Figure 8a, c, d). We decided to quantify the transition time during which we can detect the Fltp$^{\pm}$ cells by live imaging, using dispersed islets of Langerhans. The results showed an estimated transition period of 48 hours, when the red fluorescence was almost undetectable (Figure 8b).

In conclusion, the lineage tracing mouse model chosen allows following and separating a rare β-cell population, which can help to elucidate the mechanisms behind β-cell maturation.

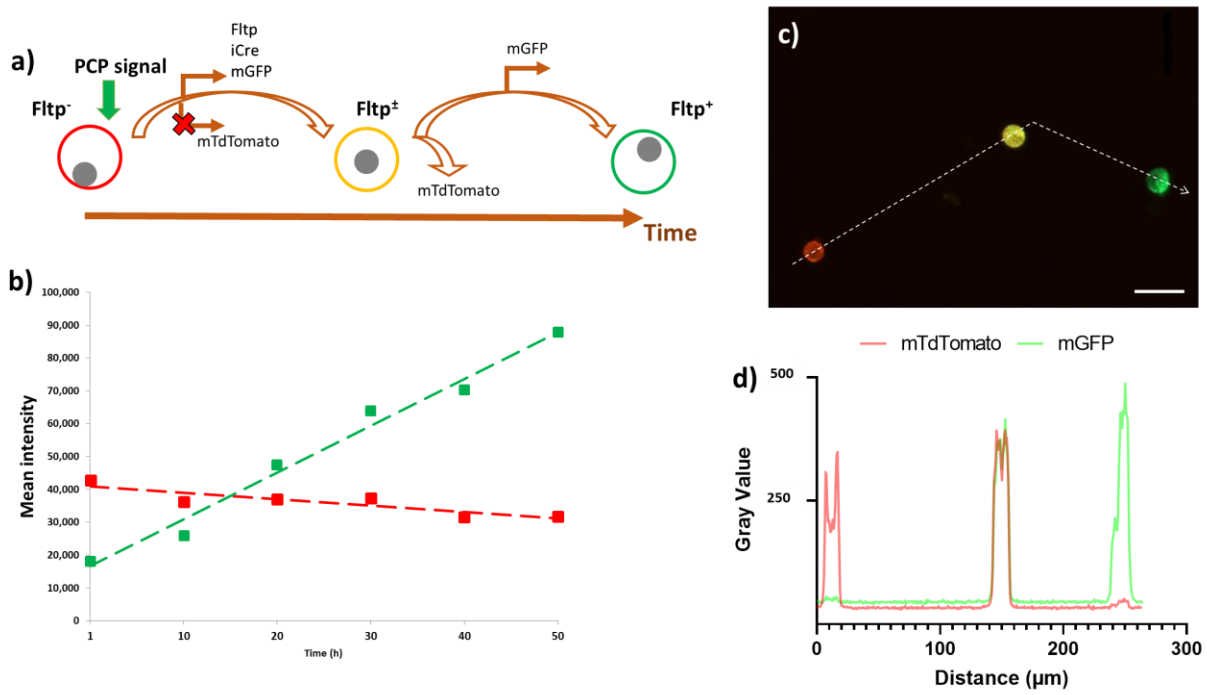


**Figure 8: Fltp iCre$^{mTmG}$ allows the isolation of the Fltp transient population**

**a)** Schematic representation of the mechanism of action of the mouse line FltpiCre$^{mTmG}$; **b)** representative quantification, from a time-lapse experiment, of the red and green fluorescence intensity of one cell undergoing the Fltp transition; **c)** representative confocal image and **d)** quantification of the fluorescence intensity of three cells with either one or both the fluorescent proteins; scale bar 20µm.

### 4.1.2 Fltp expression in endocrine cells occurs throughout the postnatal period

The link between Fltp expression and the mature β-cell phenotype has been previously demonstrated. In particular, evidences revealed that the cells positive for the Fltp reporter (FVR$^{+}$) expressed higher levels of maturation markers (Pdx1, Nkx6-1, Ucn3, Glut2 and MafA), possessed higher number of mature insulin granules and had improved glucose sensing and insulin secretion. In contrast, cells negative for the Fltp reporter (FVR$^{-}$) had higher proliferative rate, typical sign of a less mature phenotype (Bader et al., 2016). Considering the previous research, we decided to investigate whether Fltp onset could mark a specific time window during the postnatal maturation process that would allow us to pinpoint the events determining the acquisition of the terminal mature state.

We performed a longitudinal analysis to define the proportion of distinct endocrine Fltp subpopulations based on Fltp expression, using the linage tracing mouse line FltpiCre$^{mTmG}$. We isolated islets from mice at 7 different developmental stages, from right after birth to adulthood (P0, P9, P14, P16, P21, P30 and P45)

(Figure 10b and Table 1). Via flow cytometry (Figure 9a), we separated the three Fltp populations and quantified the percentages of each group in every stage. We found that the percentage of positive cells was gradually increasing, in a linear fashion, starting from 1.42 ± 0.6649 % afterbirth (P1) to arrive at 62.48 ± 15.94% at 45 postnatally (Figure 9f, Table 1). When we focused on the transient populations, we observed higher percentages of these cells from P9 to P30 (Figure 9e). To determine the "speed" of transition, we divided the percentage of Fltp$^{\pm}$ to the percentage of Fltp$^{-}$ cells. The conversion rate (Figure 9c) displayed two peaks, at P9 and P30.

In conclusion, the lineage tracing system revealed a steady increase in Fltp$^{+}$ and decrease in Fltp$^{-}$ cells. Furthermore, we observed a continuous conversion process from immature to mature (Fltp$^{\pm}$) throughout the postnatal development, likely reflecting β-cell maturation process. Finally, we observed an interesting overlap between the Fltp induction peaks at P9 and P30 and two pivotal periods of endocrine maturation, after the first week of life and after weaning.

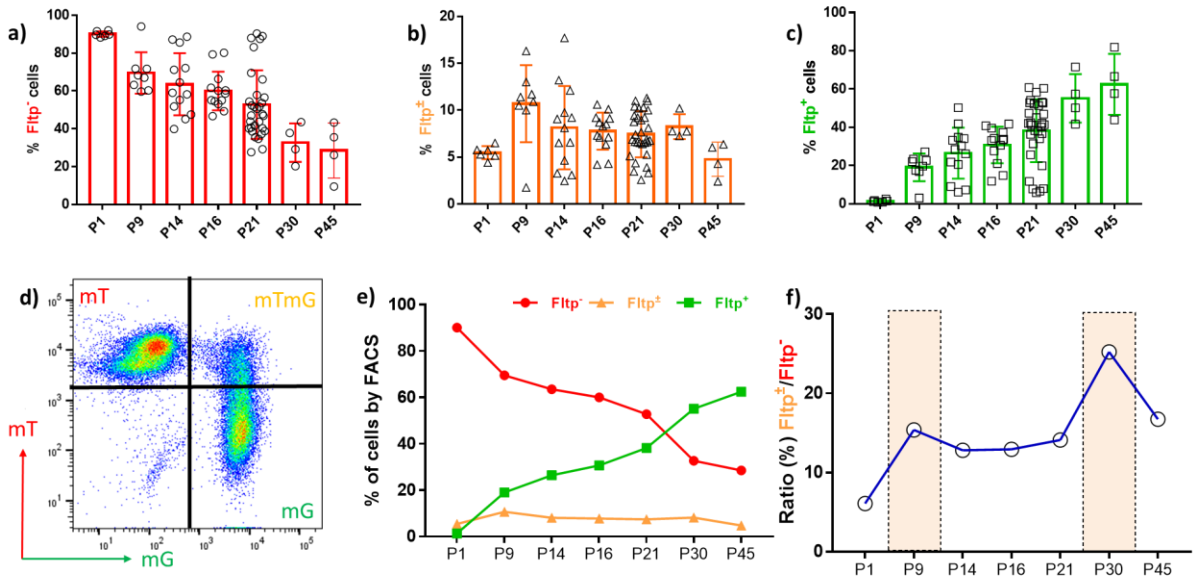


**Figure 9: Time-course analysis of Fltp expression during postnatal development**

**a)**, **b)** and **c)** bar plots representing the mean with standard deviation (SD) of the percentages of Fltp negative, transient and positive populations for each time point; symbols represents the number of replicates (statistical details in Table 1); **d)** representative FACS plot with the separation scheme used to analyze islets; **e)** plot with the overview of the mean percentage for all three Fltp populations by flow cytometry, in all stages; **f)** plot representing the ratio of the average Fltp$^{\pm}$ over the average Fltp$^{-}$ percentage, to estimate the speed of transition at each stage; respectively for each stage: 6.1%, 15.4%, 12.8%, 12.9%, 14.1%, 25.2%, and 16.7%.

| | Postnatal day | 1 | 9 | 14 | 16 | 21 | 30 | 45 |
|---|---|---|---|---|---|---|---|---|
| | Replicates | 6 | 8 | 13 | 13 | 31 | 4 | 4 |
| Fltp$^{-}$ | Mean | 90.1 | 69.51 | 63.55 | 60.03 | 52.77 | 32.68 | 28.58 |
| | SD | 1.435 | 10.98 | 16.39 | 10.2 | 18.16 | 10.18 | 14.58 |
| | SEM | 0.5859 | 3.881 | 4.545 | 2.829 | 3.262 | 5.092 | 7.291 |
| Fltp $^{\pm}$ | Mean | 5.482 | 10.7 | 8.138 | 7.768 | 7.448 | 8.248 | 4.783 |
| | SD | 0.6972 | 4.111 | 4.434 | 1.975 | 2.45 | 1.323 | 1.818 |
| | SEM | 0.2846 | 1.453 | 1.23 | 0.5477 | 0.44 | 0.6617 | 0.909 |
| Fltp$^{+}$ | Mean | 1.415 | 19.06 | 26.44 | 30.75 | 38.21 | 55.15 | 62.48 |
| | SD | 0.6649 | 7.269 | 13.34 | 9.539 | 16.45 | 12.67 | 15.94 |
| | SEM | 0.2714 | 2.57 | 3.699 | 2.646 | 2.955 | 6.334 | 7.97 |

**Table 1: Quantification of the time-course analysis of Fltp expression**

Table with the details of the analysis showed in Figure 10, showing number of replicates, mean, standard deviation (SD) and standard error of the mean (SEM) for each population at each stage analyzed.

### 4.1.3 Dissecting Fltp β-cell postnatal heterogeneity by scRNA-seq

Understanding β-cell heterogeneity is pivotal not only to characterize the different type of subpopulations within the islets but also to uncover the mechanisms that determine the adult functional phenotype. Considering that, Fltp is not restricted to β-cells and to understand the molecular mechanisms underlining the postnatal maturation, we combined the Fltp lineage labeling and tracing system (FltpiCre$^{mTmG}$) with scRNA-seq. The tracing system allowed separating cells that recently acquired PCP from the PCP negative and long-standing positive populations, meanwhile the scRNA-seq enabled to characterize each endocrine population separately. Therefore, the experimental design integrated Wnt/PCP readout with single cell transcriptional readout (Figure 10).

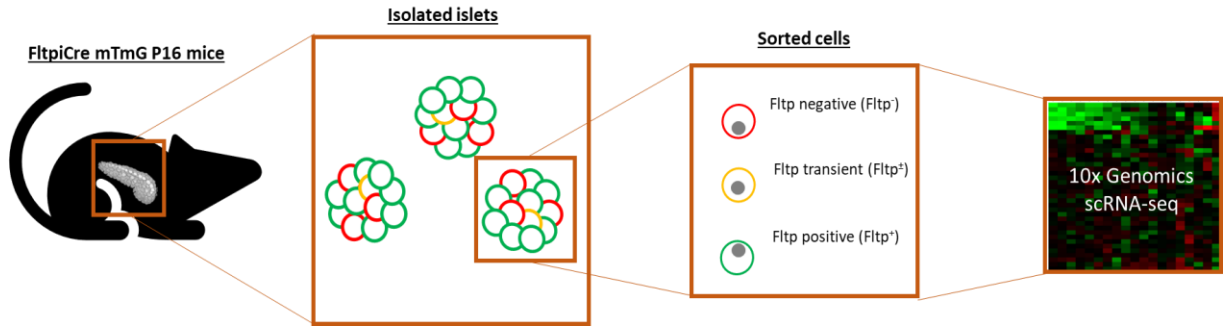


**Figure 10: Schematic representation of the procedure followed to generate the scRNAseq dataset**

Mice at the age of 16 days were used to isolate islets of Langerhans. These were then dissociated into single cells and FAC sorted according to their fluorescence signature. Each population has been used to generate independent libraries using the 10x Genomics® technology.

Islets of Langerhans were isolated from 16 days old pups. After dissociation, cells were sorted according to their fluorescence signature and processed according to the 10x Genomics® protocol to obtain genomic libraries for each Fltp population. After sequencing, raw data was processed from our bioinformatics partner (Dr. Maren Büttner, ICB) and the final annotation successfully displayed an output of 18716 endocrine cells (after quality control) in which we could distinguish each endocrine population: α-cells [7604], β-cells [7275], δ-cells [1687], γ-cells [684], ε-cells [16] and Poly hormonal [1450] (Figure 11a, b and d) (Salinno et al., 2021). These were then annotated according to the Fltp-sorting strategy ($Fltp^+$ 9168, $Fltp^-$ 6217, and $Fltp^\pm$ 3331) and their spatial distribution is shown in the density UMAPs in Figure 11c. From the multidimensional space of the UMAPs, we observed no evident cluster separation based on the Fltp sorting strategy. Interestingly, the majority of cells in the $Fltp^\pm$ population were β-cells, indicating that at this stage, β-cells were the ones undergoing the transition (Figure 11d). In conclusion, we successfully generated a postnatal scRNA-seq dataset, observing a significant number of β-cells undergoing the Fltp transition. Here we could speculate that as α-cells are formed before β-cells, they might acquire PCP before. Alternatively, the localization of α-cells at edge of the islets and their proliferative potential might also contribute to the less abundant transient population at this stage.

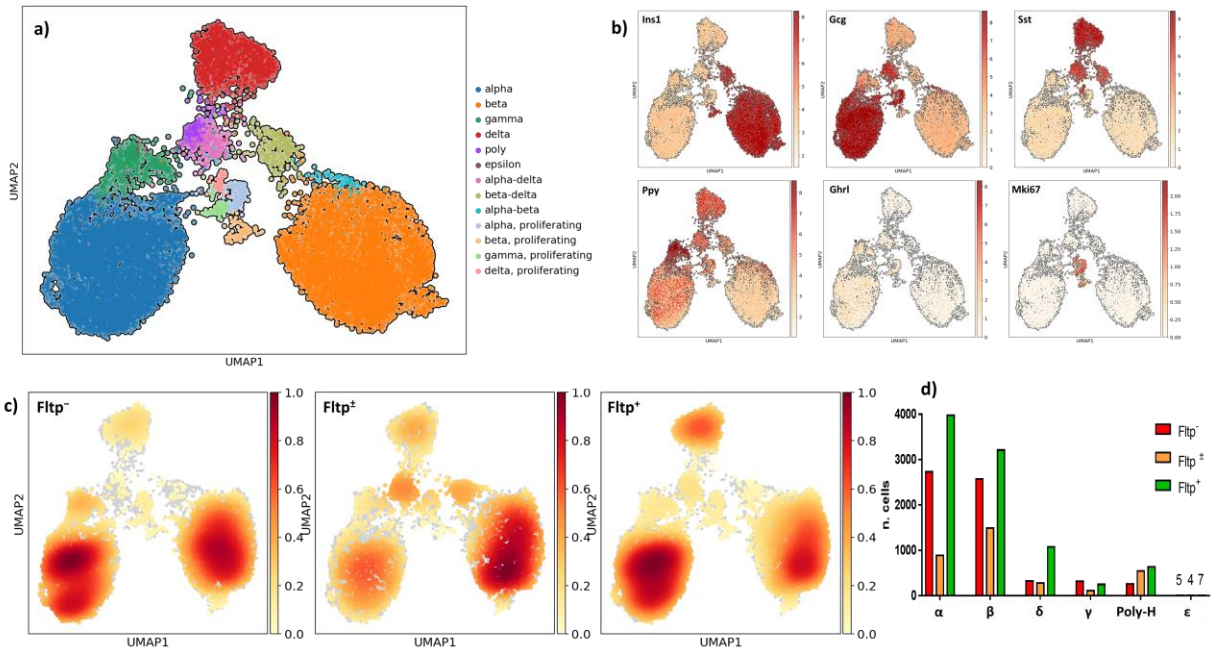


**Figure 11: scRNA-seq analysis of postnatal islets of Langerhans**

**a)** UMAP representing the annotation of the refined endocrine clusters according to known signature markers; **b)** UMAPs with the expression levels of the islets' hormones genes (*Ins1*, *Gcg*, *Sst*, *Ppy*, *Ghrl*) and *Mki67* to define the proliferative cells; **c)** UMAPs showing the approximate accumulation (density) of the three sorted Fltp populations in the endocrine UMAP; **d)** Bar plot indicating the number of cells analyzed per Fltp-population for each endocrine cell type. Poly-H: polyhormonal. UMAP: Uniform Manifold Approximation and Projection.

### 4.1.4 Fltp marks the acquisition of a mature β-cell transcriptional profile

We next focused our analysis only on the β-cell population (Figure 12a). With our sorting strategy we obtained 44.14% Fltp$^{+}$, 20.52% Fltp$^{\pm}$ and 35.44% Fltp$^{-}$ β-cells. As explained before, no significant clustering based on Fltp sorting strategy was observed on the UMAP. However, the three subgroups accumulated (density) in different spatial localizations of the UMAP, indicating that the three populations, despite their similar transcriptome, possessed underlying differences. Next, we explored the most common β-cell identity genes in the three subpopulation (Figure 12b). We observed that all the known maturation markers were upregulated in the two Fltp lineage-positive populations. Conversely, *Mafb* and *Rbp4*, two of the best characterized markers for immature β-cells, were upregulated in the Fltp negative population. RT-qPCR on sorted cells further confirmed higher expression levels of *Fltp* and *Ucn3* genes in the Fltp lineage-positive populations (Figure 12c). Furthermore, E-cadherin (*Cdh1*) and β-catenin (*Ctnnb1*), important elements in cell adhesion processes, were higher expressed in the transient population. To confirm the in silico data, we performed immunofluorescence (IF) staining of two maturation markers (Ucn3 and MafA)

on pancreatic sections at different stages (P2, P9, P16) of postnatal development (Figure 12d and e). We counted the number of β-cells (Nkx6-1$^+$) positive for Fltp only (Fltp$^+$) (Figure 12f) and afterwards the ones double positive for Fltp and Ucn3 (Figure 12g) or Fltp and MafA (Figure 12h). The results showed that Fltp followed the same dynamic of expression of the other two maturation markers. However, we did not observe a complete overlap between them, since we could detect Fltp$^+$ cells negative for Ucn3 or MafA and *vice versa* (Figure 12g and h).

In conclusion, these data present Fltp as maturation marker in postnatal development, in line with other common markers as Ucn3, MafA and Glut2. In addition, Nkx6-1 is expressed higher in the transient population, in accordance to previous data showing Fltp and Nkx6-1 upregulation upon islet formation from cord-like structures (Bader et al., 2016).

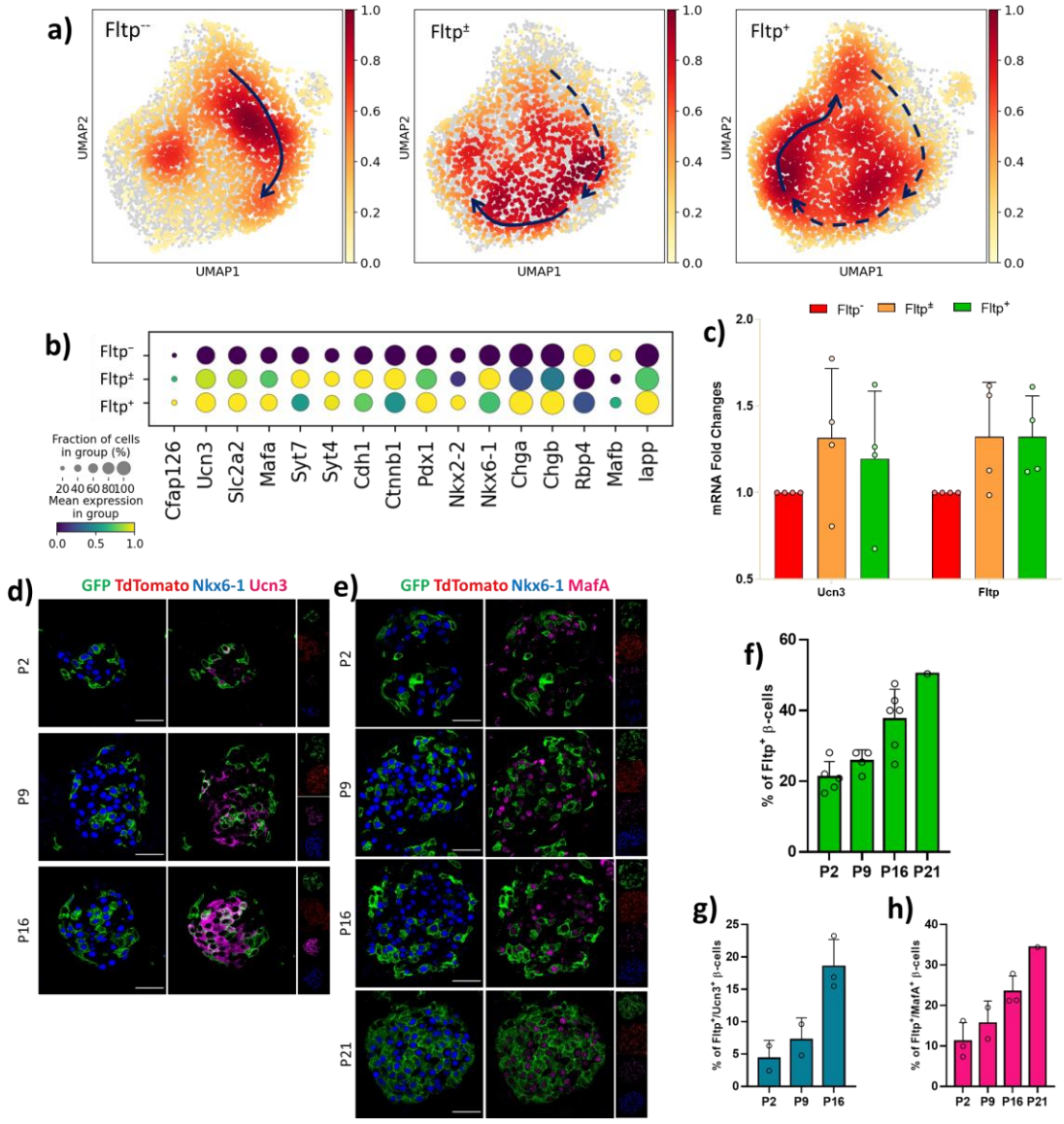


**Figure 12: Relationship between Fltp and other known maturation markers in β-cells**

**a)** Density UMAPs for the three Fltp-sorted population within the β-cell cluster; black arrows (hand drawn) indicate a possible dynamic of maturation; **b)** dot plot representing the expression levels (color shades) and percentage of cells expressing the gene (size) of the indicated genes on the x-axis; **c)** bar plot indicating the mean + SD of the mRNA fold changes in the three Fltp populations of *Ucn3* (respectively 1, 1.315 ± 0.4, 1.195 ± 0.39, ns) and *Fltp* (1, 1.32 ± 0.31, 1.32 ± 0.24, ns) expression, (data normalized on the $Fltp^-$ population, n=4, P21); **d)** representative confocal pictures of IF staining on pancreatic sections with Nkx6-1 (blue), Ucn3 (magenta), $Fltp^-$ (TdTomato, red) and $Fltp^+$ (GFP, green); **e)** Representative confocal pictures of IF staining on pancreatic sections with Nkx6-1 (blue), MafA (magenta), $Fltp^-$ (TdTomato, red) and $Fltp^+$ (GFP, green); Scale bars: 30μm; **f)**, **g)** and **h)** Bar plots representing, respectively, mean + SD of the counting of $Fltp^+$ only (P2, n=5, 21.17 ± 4.39; P9, n=4, 25.71 ± 3.15; P16, n=6, 37.58 ± 8.45; P21, n=1, 50.35), $Fltp^+/Ucn3^+$ (P2, n=2, 4.36 ± 2.73; P9, n=2, 7.21 ± 3.394 P16, n=3, 18.54 ± 4.14) and $Fltp^+/MafA^+$ (P2, n=3, 11.18 ± 4.56; P9, n=2, 15.62 ± 5.49; P16, n=3, 23.46 ± 3.81; P21, n=1, 34.4) β-cells at different postnatal stages.

### 4.1.5 Fltp β-cell populations differ in pathways and cellular components

The previous paragraphs showed that the three Fltp subpopulations differ for transcriptional profiles and maturation markers. Thus, we performed in depth computational analysis of the three β-cell subpopulations to uncover the characteristics of these cells. Thus, we computed the differential gene expression analysis (DGEA) by comparing Fltp-β-cell populations among each others ($Fltp^+$ vs $Fltp^-$ / $Fltp^\pm$ vs $Fltp^+$ / $Fltp^-$ vs $Fltp^\pm$). We observed 140 and 298 genes upregulated, respectively, in the $Fltp^+$ and in the $Fltp^-$ populations, 56 and 173 genes for the $Fltp^+$ compared to the $Fltp^\pm$ and finally 336 and 311 genes differentially regulated between $Fltp^-$ and $Fltp^\pm$ (Figure 13b, d). These genes where then used as input to perform the pathway enrichment analysis, via Metascape, to uncover differences in signaling pathways within each subpopulation. Figure 13a shows the most significant differences in terms of pathways. The $Fltp^+$ subpopulation was enriched with terms related to insulin pathway, response to unfolded proteins, autophagy, estrogen signaling, iron metabolism and cell-cell contact (GAP junctions, cell adhesion) (Figure 13a). The $Fltp^\pm$ subpopulation presented upregulation of non-canonical Wnt signaling, MAPK kinase signaling, PTEN pathway, unfolded protein response, cell growth, cell cycle arrest, VEGF signaling, mTOR pathway, regulation of actin cytoskeleton and cell adhesion (Figure 13e). To conclude, the $Fltp^-$ subpopulation showed terms related to ROS detox processes, cell cycle, MAPK, Wnt and ephrin signaling (Figure 13f). This data is in line with the current literature. $Fltp^-$ cells possess a higher proliferative capacity, likely to support the β-cell mass expansion in response to the organism´s growth. The $Fltp^+$ cells appeared transcriptionally more mature, with terms pointing out at the acquisition of metabolic sensing and insulin secretion. Last, the $Fltp^\pm$ population presented terms related to cell cycle inhibition and non-canonical Wnt signaling, possible the latter as proliferation break. In addition, we found regulators of cytoskeleton

dynamics and vasculature signaling, possibly hinting at processes related to the acquisition of a 3D architecture.

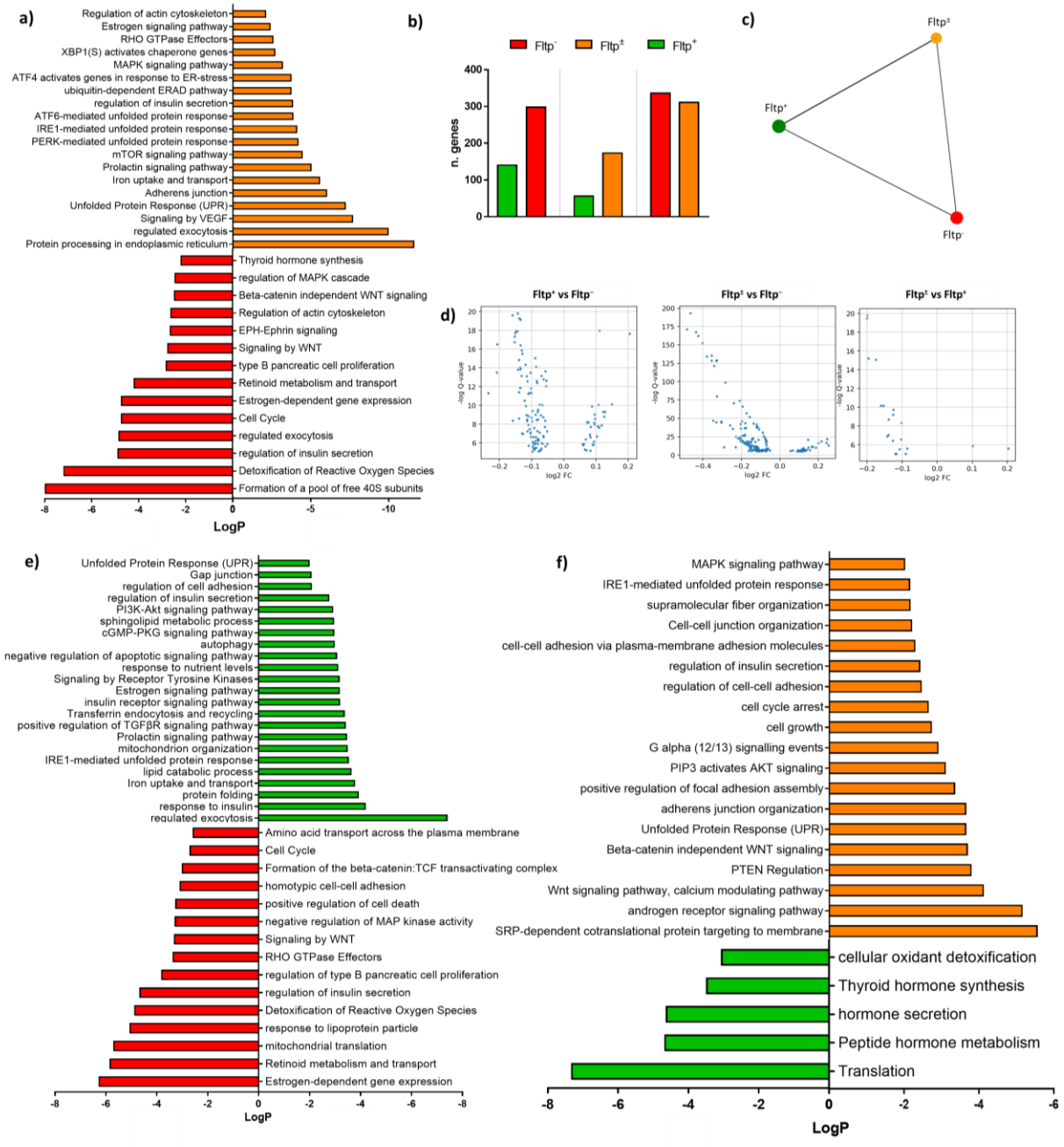


**Figure 13: Pathway analysis reveals differences between Fltp populations**

**a)**, **e)** and **f)** Bar plots representing enriched pathways in each Fltp population after pair-wise comparison (color coded); **b)** bar plot with the number of genes differentially expressed in each pair-wise comparison Fltp-β-cell population; **c)** PAGA (partition-based graph abstraction) plot, estimating the connectivity between Fltp population; **d)**

volcano plot for each pair of Fltp-populations compared; each dot represent a differentially regulated gene according to statistical significance (Q value) and magnitude of change (fold change).

To gain a better insight into the molecular changes of postnatal changes, we clustered the genes obtained from the DGEA into protein classes (PC via Panther). This clustering informed us about cellular components upregulated in each Fltp-based β-cell subpopulation (Figure 14a). Among the most interesting results, we noticed that the Fltp$^{-}$ β-cells were enriched for calcium-binding proteins, intracellular signal molecules, nucleic acid binding proteins, transfer/carrier proteins and above all translational proteins. The Fltp$^{\pm}$ β-cells had higher number of gene-specific transcriptional regulators, membrane traffic proteins, protein binding activity modulators, scaffold and adaptor proteins and transporters. Finally, the Fltp$^{+}$ β-cells were enriched for cell junction proteins, storage and structural proteins, chaperons and membrane traffic proteins. We further showed some of these differentially regulated genes in dot plots, from the P16 scRNAseq dataset (Figure 14b, c, d). These results presented a specific molecular profile for each subpopulation, hinting at functional differences among them. Of notice, Fltp$^{-}$ cells were enriched in translational proteins, characteristics of immature cells still in a growing phase. The Fltp lineage-positive cells, instead, were enriched for specific transcription factors and transporters, suggesting how, upon PCP acquisition, these cells modified transcriptional profile and metabolism.

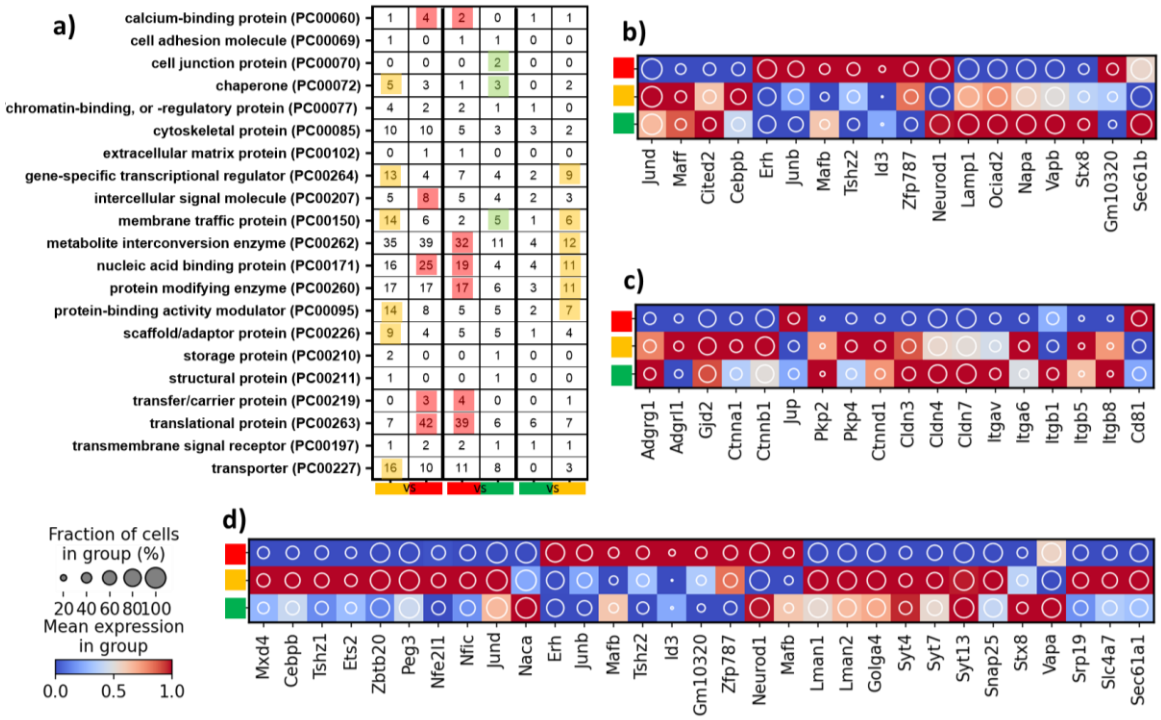


**Figure 14: Protein families' enrichment among Fltp-β-cell-populations**

**a)** Schematic representation of the protein classes (PC) enrichment, in a pair-wise comparison fashion; **b), c)** and **d)** dot plots of some of the most significant genes obtained from the PC enrichment, c) surface molecules, d) and e); expression levels (color shades) and percentage of cells expressing the gene (size) of the indicated genes. Colored squares next to the dot plot represent the associated Fltp population, red ($Fltp^-$), yellow ($Fltp^\pm$) and green ($Fltp^+$).

### 4.1.6 $Fltp^\pm$ β-cells are transcriptionally enriched for Wnt components

Fltp has been described as Wnt/PCP effector and reporter protein (Bader et al., 2016; Gegg et al., 2014). Thus, we explored the expression of several different Wnt components (ligands, receptors and downstream targets), in our scRNA-seq dataset. In Figure 15a we have a schematic representation of a generic Wnt signaling pathway, color-coded according to the Fltp population(s) in which the gene was expressed the highest. In Figure 15b-g we show several genes of the Wnt signaling, PCP core components and other non-canonical Wnt effectors. What was clearly visible is that the majority of the genes plotted are upregulated in the $Fltp^\pm$ β-cells. Canonical Wnt target genes (*Tcf7l2, Gja1, Myc, Axin2, Tek*) had higher expression in $Fltp^-$ cells. Non-canonical Wnt components (*Gsk3b*, several Mapk components, Rho and Rac family members) had higher expression either in the $Fltp^\pm$ or in the $Fltp^+$ populations. We speculate that canonical Wnt signaling could promote β-cell proliferation (Migliorini & Lickert, 2015; Shirakawa & Kulkarni, 2016). In the gut, the inhibition of canonical Wnt in favor to non-canonical Wnt signaling pathway determined endocrine fate determination in the resident stem cells (Böttcher et al., 2021). Similarly, the transition might explain the loss of proliferative capacity and the acquisition of the mature phenotype in β-cells.

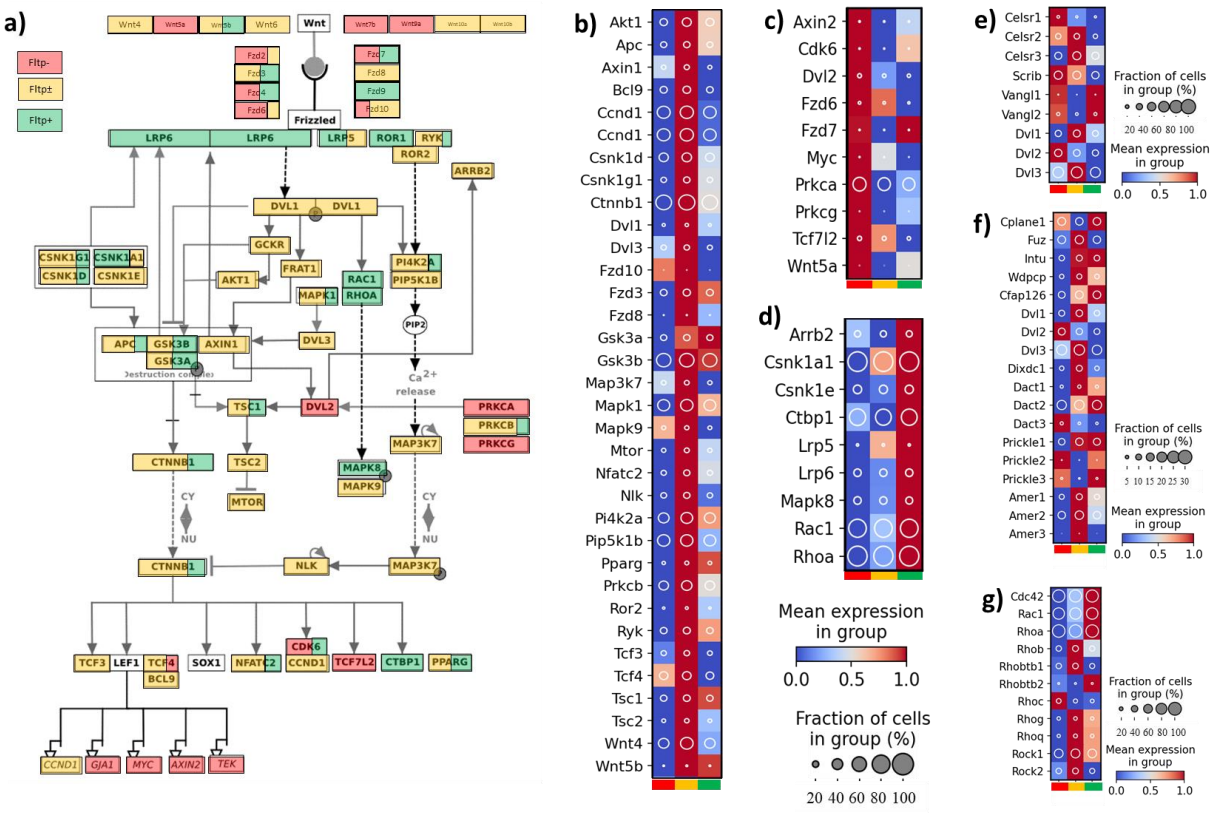


**Figure 15: Analysis of Wnt components via scRNA-seq**

**a)** Iconographic summary of Wnt signaling pathway, color-coded according to the population(s) in which the gene is expressed the highest; **b) - g)** dot plots of Wnt signaling pathway's genes, with the normalized expression levels (color shades) and percentage of cells expressing the gene (size) of the indicated genes; **b)**, **c)** and **d)** dot plots with Wnt genes upregulated in each Fltp population, respectively Fltp$^{\pm}$, Fltp$^{-}$ and Fltp$^{+}$; **e)** group of genes representing the PCP core components; **f)** and **g)** genes directly or indirectly (Rho family) related to non-canonical Wnt signaling pathway.

To understand if Fltp$^{-}$ cells received canonical Wnt while the Fltp lineage-positive non-canonical Wnt, we performed IF staining, on dispersed islets from adult mice for two common Wnt readouts, phosphor Jnk (pJnk) and β-catenin (Figure 16a - h). We quantified the intensity of the signal coming from the two different cell types (Fltp$^{+}$ and the Fltp$^{-}$) and plotted them as shown in Figure 16i and 16j. No significant differences were detected between these populations. B-catenin seemed relatively homogeneous in all cells, while pJnk was heterogeneous but not directly connected to Fltp subpopulations. Of note, this result might be influenced by technical difficulties, since we dispersed and left cells overnight to attach on the dish, or by the age (3 months old) of the mice used for the experiment. We also performed WB analysis on sorted

cells to check other components of Wnt signaling. Of relevance, we observed a strong Dvl2 signal in the Fltp$^{\pm}$ population (Figure 16k). No differences were observed for pJnk or pGSK3/GSK3 signals (Figure 16l).

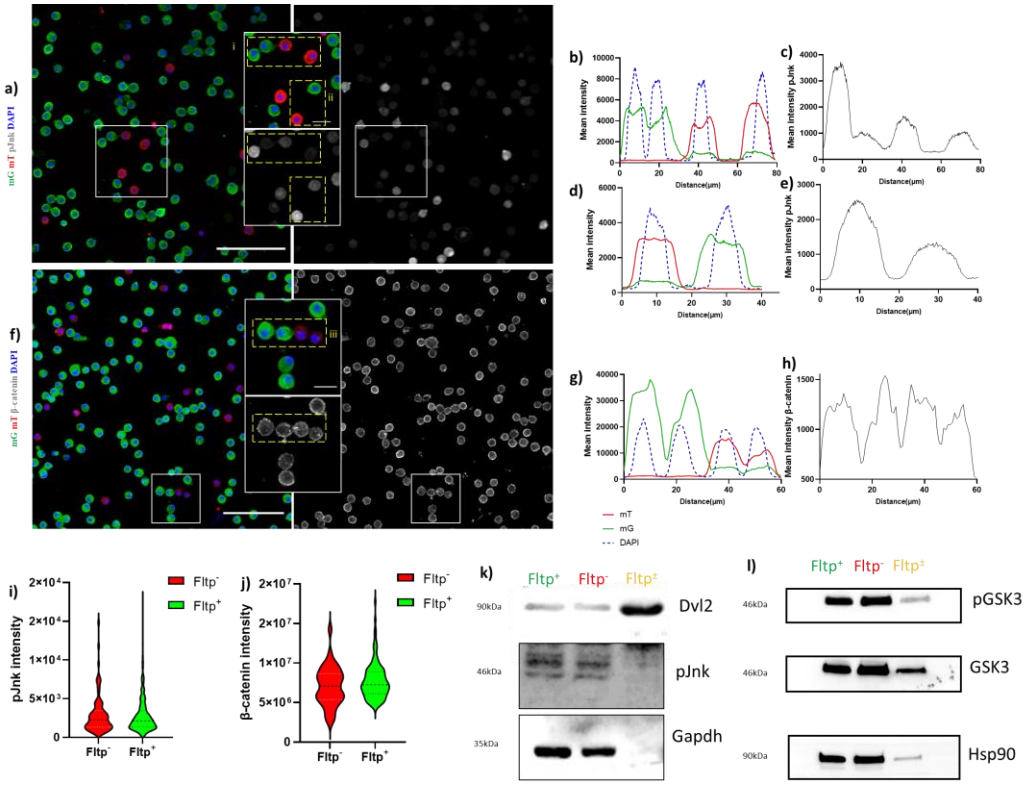


**Figure 16: Wnt signaling in the islets of Langerhans**

**a)** and **f)** Representative pictures of IF staining, on dispersed islets, respectively for pJnk and β-catenin. In green (Fltp$^{+}$) and red (Fltp$^{-}$), blue (DAPI) and in grey pJnk and β-catenin; scale bars 100µm and 20µm for the zoom-in; **b)**, **d)** and **g)** representative plots with the quantification of the red, green and blue fluorescence intensity respectively in the dashed yellow boxes i), ii) and iii); **c)**, **e)** and **h)** representative plots with the quantification of the grey fluorescence intensity respectively in the dashed yellow boxes i), ii) for pJnk and iii) for β-catenin; **i)** and **j)** violin plots with the quantification of the signal intensity for the staining of pJnk and β-catenin respectively, in the Fltp$^{+}$ (green bar) and Fltp$^{-}$ (red bar) cells (n=1, 3 animals pulled together; β-catenin: Fltp$^{-}$ 34 cells, 7083334 ± 2475840 and Fltp$^{+}$ 121 cells 7744671 ± 2302286; pJnk: Fltp$^{-}$ 82 cells, 7083334 ± 2475840 and Fltp$^{+}$ 542 cells 7744671 ± 2302286 ); **e)** and **f)** WB pictures of Dvl2, pJnk, pGSK3, GSK3, Gapdh and Hsp90 (n=1, 5 animals pooled together).

Wnt/PCP activation often leads to cytoskeletal reorganization via small GTPases activation (Schlessinger et al., 2009). Thus, we assessed whether differences in cytoskeleton could be indirectly observed via cell biological behaviors of dispersed islets in culture. Therefore, we isolated islets from adult mice, dispersed them into single cells and seeded them on Ibidi® chambers. We performed time-lapse imaging for 48 hours with a confocal microscope. Here, we observed that cells belonging to different Fltp populations possessed different motility properties. In particular, the Fltp$^{-}$ population was the most static one, while the Fltp$^{\pm}$ and

Fltp$^+$ cells were travelling longer distances on average (Figure 17a and 17b). Furthermore, observations of the initial (T$^i$ – time 0h) and final (T$^f$ – time 48h) time points displayed differences in protrusions extensions, in favor of the Fltp lineage positive cells (Figure 17c). To support our observations, we evaluated the expression levels of several genes member of the actin (Figure 17e) or tubulin (Figure 17f) associated gene families, in the postnatal scRNA-seq. We found that most of the genes probed were upregulated in the Fltp lineage-positive populations, if compared to the negative one. Furthermore, also the three Elmo (Engulfment and cell motility proteins) genes were upregulated in the lineage-positive populations (Figure 17d). From this data, we concluded that the Fltp subpopulations differ in cytoskeleton properties and dynamics, in accordance with what we observed from the scRNAseq data. We hypothesized that these differences are the result of the PCP acquisition.

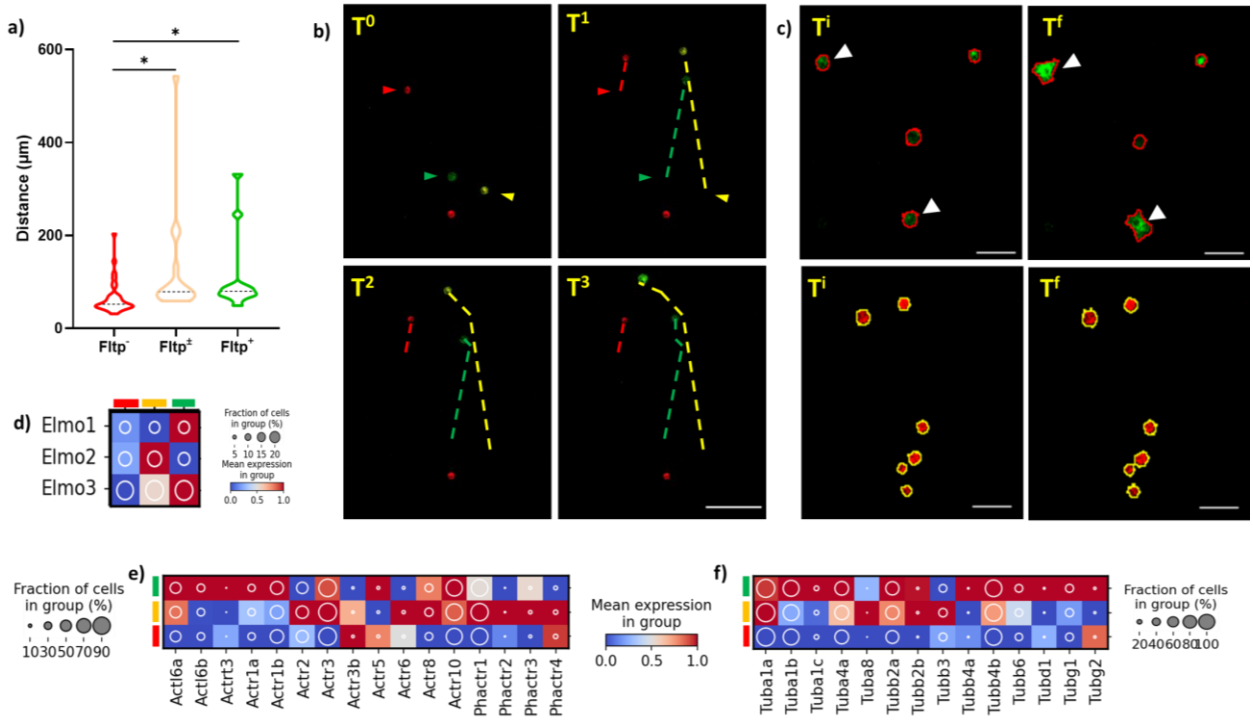


**Figure 17: Differences in cytoskeleton properties among Fltp populations**

**a)** Violin plot representing the mean ± SD of the distance (µm) travelled by the different Fltp cells (n=1; 33,16 and 13 cells respectively analyzed for each population; 64.99 ± 35.25, 123.4 ± 121.6, 108.2 ± 82.81; *P < 0.05; t-test); **b)** representative pictures of a group of cells observed moving in time-laps; dashed lines represent the distance travelled by the cells; **c)** representative confocal pictures showing the different capacity of the Fltp$^+$ and Fltp$^-$ cells in extending protrusions after 48 hours; scale bar: 50 µm; **d)**, **e)** and **f)** dot plots representing group of genes (ELMOs, actin and tubulin components) playing a role in the cytoskeleton rearrangements; normalized expression levels (color shades) and percentage of cells expressing the gene (size) of the indicated genes.

### 4.1.7 Fltp interactome reveals possible connections with metabolic pathways

Previous work from our laboratory described Fltp interacting with a PCP core component (Dlg3) and cortical actin (Gegg et al., 2014). We further explored Fltp interaction partners in order to gain insights into the mechanisms behind PCP acquisition. Dr. Anika Böttcher generated Fltp interactome in HEK293 cell line. Here, we clustered the unfiltered results of the mass spectrometry in cellular component families (Figure 18a) and found that Fltp interacts with microtubule organizing center proteins, contractile fibers, focal adhesions, in addition to members of the Wnt/RTK signaling (Tsc2, Erk2, Grb2, Gsk3β) and mTOR related proteins (Raptor and Rheb) (Figure 18b).

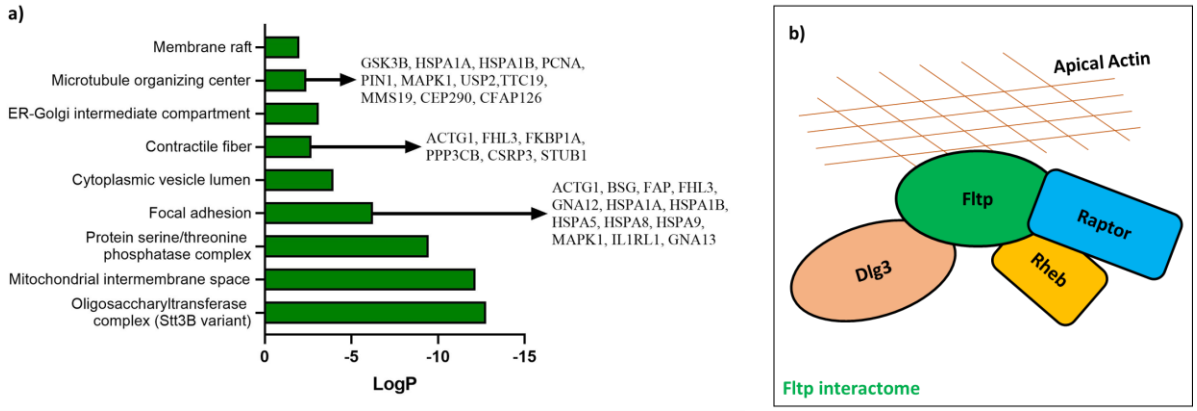


**Figure 18: Fltp interacts with cytoskeleton and mTOR components**

**a)** Bar plot representing potential Fltp interaction partners, clustered based on their cellular components (GOCC); LogP on the X-axis represents the confidence with whom those proteins belong to the protein class displayed; **b)** Cartoon representing known (apical actin, Dlg3) and unknown (Raptor and Rheb) interaction partners of Fltp.

To explore the possible connection between Fltp (Wnt/PCP) and Raptor/Rheb (mTOR), we used mTORC1 most common readout, the phosphorylation of the serines 235 and 236 on the ribosomal protein s6 ($pS6^{Ser235/236}$). This protein is phosphorylated when the mTORC1 complex (mTOR with a several other proteins among which Raptor) is formed and phosphorylate the S6 kinase which subsequently phosphorylates S6 protein. IF staining of pS6 on pancreatic sections of mice at weaning age showed a heterogeneous pattern within the islets. However, it was possible to observe higher signal intensity in the $Fltp^-$ population (Figure 19a). To reinforce this observation, we performed IF staining on sorted endocrine cells and confirmed that the $Fltp^-$ cells were abundantly positive for pS6 compared to the $Fltp^+$ ones (Figure 19b). Finally, we quantified the percentages of pS6 positive cells in the three Fltp populations, both in low and high glucose, and observed higher phosphorylation levels in in the $Fltp^-$ and $Fltp^{\pm}$ populations (Figure 19c). These results confirmed that Wnt/PCP and the mTORC1 complex are connected and might be involved in the β-cell maturation process. In addition, the fact that mTORC1 was downregulated in the

Fltp$^{+}$ population supports our idea that these cells are metabolically more mature, compared to the others two groups.

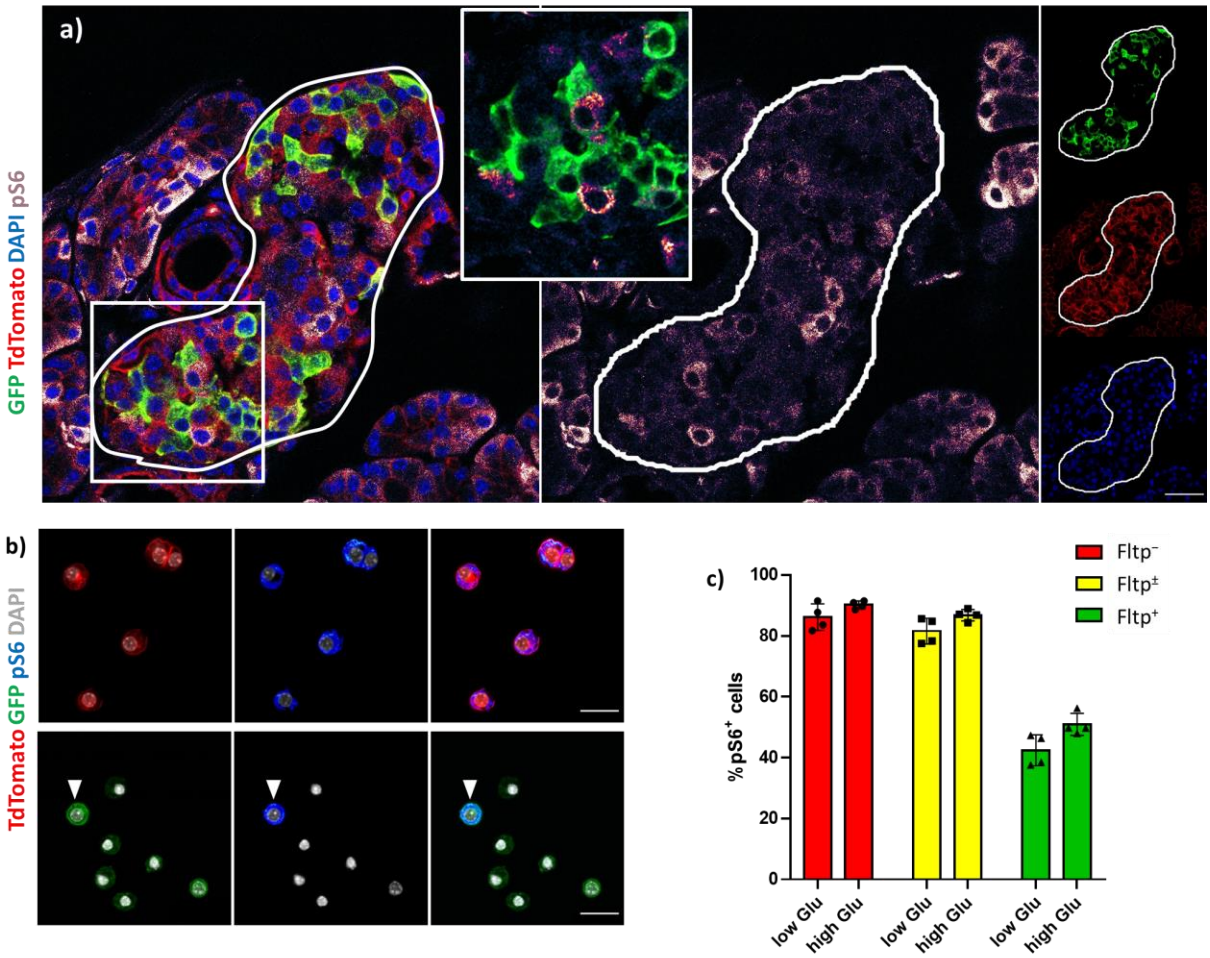


**Figure 19: Different activity of mTORC1 among Fltp populations**

**a)** Representative IF staining of pancreatic section of 21 days old mice, showing Fltp$^{-}$ (red), Fltp$^{+}$ (green), DAPI (blue) and pS6 (purple - LUT gem); scale bar: 50µm; **b)** representative IF staining of pS6 (blue) on sorted Fltp endocrine cells, according to their membrane fluorescent signal; scale bar: 20 µm; **c)** bar plot (mean ± SD) representing the quantification of the percentages of pS6 positive cells for the three Fltp subpopulations, in two different metabolic conditions (n=4, low glucose 86.12 ± 4.37, 81.55 ± 4.23, 42.425 ± 5.08; high glucose: 90.175 ± 1.28; 86.77 ± 1.89, 50.9± 3.63).

### 4.1.8 Islet architectural changes during postnatal stages

mTORC1 is involved in several cellular functions. For instance, it is involved in the growth and proliferation processes of the endocrine cells (Sinagoga et al., 2017). We hypothesized that changes in cell dimensions might induce a compaction phenomenon, thus contributing to the islet architecture

establishment (Roscioni et al., 2016). To test our hypothesis we quantified the area of the cells within the islets at two different postnatal stages: day 9 and 25. We performed IF staining on pancreatic sections for TdTomato and GFP to detect the cell membranes (Figure 20a). After picture acquisition, we applied a custom-made algorithm (Dr. Tihomir Georgiev, HPC) that detected the cell membranes and quantified the area of each cell (Figure 20b-d). We demonstrated that at P25 cells were significantly larger compared to the counterparts at P9 (Figure 20e, f). In addition to the well described postnatal β-cell replication phenomenon (Georgia & Bhushan, 2004), and considering that islet size does not differ substantially at this stage (Jo et al., 2007), we can hypothesize that changes in endocrine cell size affect the islet architecture by inducing a compaction phenomenon.

Considering the data shown up to this point, one could speculate that upon PCP acquisition, Fltp might play a role in dragging Raptor away from the lysosomes (Rogala et al., 2019) and towards the apical membrane, inactivating it (Benjamin & Hall, 2014) and consequently promoting cell cycle exit. The hypothesis would fit with the current literature, in which only immature β-cells, as the Fltp$^-$ cells, possess high basal mTORC1 activity (Helman et al., 2020b; Jaafar et al., 2019). Additionally, changes in cellular polarity might regulate mTORC1 activity (Zhu et al., 2015), possibly regulating by Tsc1/2 complex (Choo et al., 2006), in pancreatic endocrine cells.

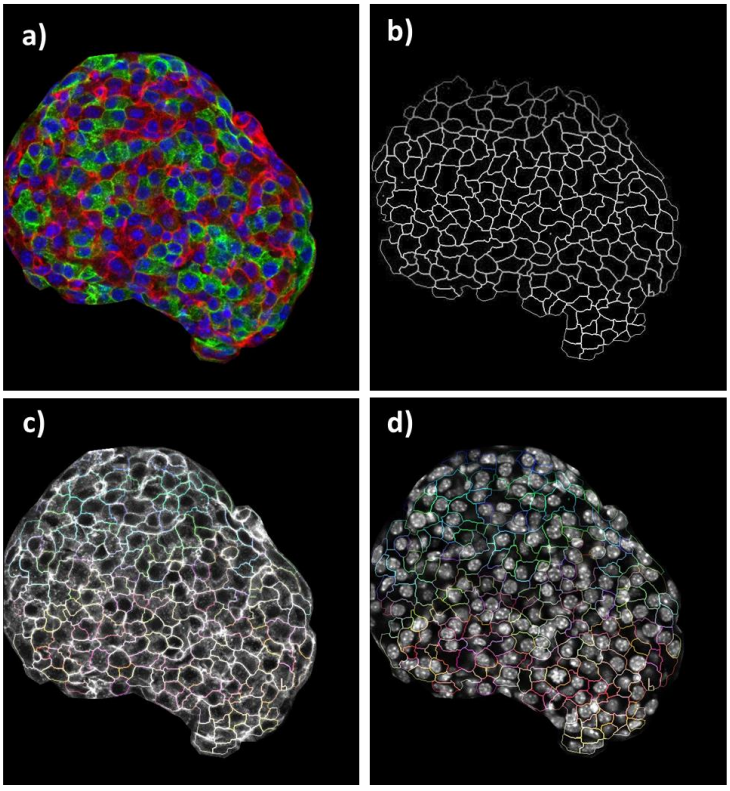


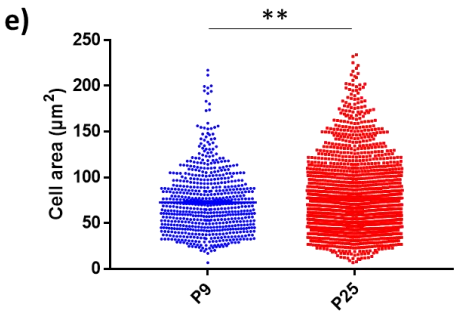


f)

| | P9 | P25 |
|---|---|---|
| Cell evaluated | 653 | 1678 |
| Mean | 72.63 | 77.491 |
| Std. Deviation | 34.38 | 40.48 |
| Std. Error of Mean | 1.34 | 0.98 |

**Figure 20: Cell size increases during postnatal development**

**a)** Representative IF staining of an islet used for the analysis, red and green show, respectively, the Fltp$^{+}$ and Fltp$^{-}$ cells; islets were manually cleared from the surrounding exocrine component; **b)** mask representing the result of the computational analysis used to define the perimeter of each cell; **c)** representative picture of the overlap between the IF staining and the digital cell mask; **d)** representative picture of the overlap between the nuclei and the cell masks, used as quality control to exclude cell areas without nuclei; **e)** scatter plot representing the quantified area of cells at P9 (blue) and P25 (red) (10 islet per group, 72.63 ± 34.38 77.49 ± 40.48; **P < 0.01; t-test); **f)** table with detailed analysis of the quantification.

### 4.1.9 Role of non-endocrine cells in the process of PCP acquisition

The vasculature has an important role during the development and functionality of the islets of Langerhans (Mazier & Cota, 2017). The endothelial cells provide the ECM structure within the islets (Akhmanova et al., 2015; Zaret, 2006) and it was proved to be essential for the islet function (Townsend & Gannon, 2019b) and to improve the islet transplantation outcome (Llacua et al., 2018; Saunders et al., 2020). Furthermore, recent studies demonstrated that β-cells are polarized towards the vasculature (Cottle et al., 2021; Wan J. Gan et al., 2017) and that the ECM might play a role in modulating Wnt signaling (Du et al., 2016). Thus, we wondered whether the vasculature might have directly influenced the acquisition of Wnt/PCP. To this end, we assessed the islet vasculature structure and abundance at distinct maturation stages (P0, P9, P14 and P25). No major changes in vasculature abundance were observed (Figure 21). Not surprisingly, it appeared that the islet growth was accompanied by the vasculature growth. Therefore, we concluded that the simple presence of vessels might not be enough to determine the acquisition of Wnt/PCP.

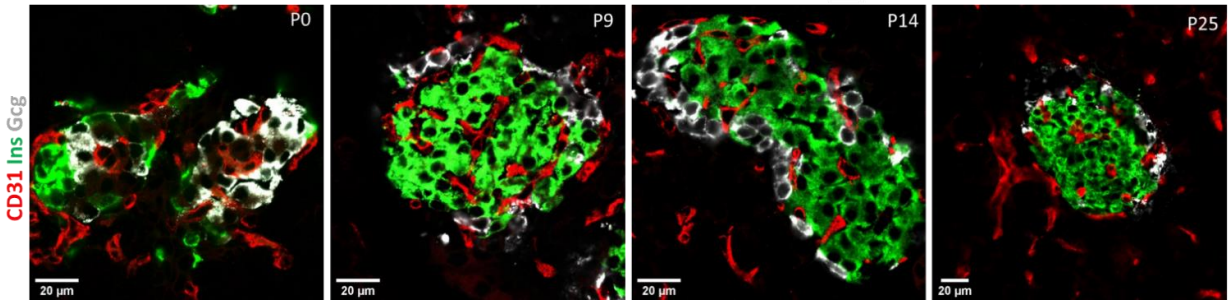


**Figure 21: Islet vascularization in postnatal islets**

Representative IF staining of insulin (green), glucagon (grey) and CD31 (endothelial cells - red) of islets at four different postnatal development stages. Scale bar 20µm.

We next used our genetic linage tracer mouse line to determine if the cells undergoing the transition would have a specific localization in the islets. Here we gathered two evidences. First, during the early postnatal development (P14) we observed the new Fltp$^{+}$ cells in close proximity to the vasculature (Figure 22a). Second, in adult, we localized some Fltp$^{\pm}$ cells attached to endothelial cells (Figure 22b). These data suggest

that the vasculature might contribute to the polarity establishment in the islets by providing ECM structure, thus polarity cues.

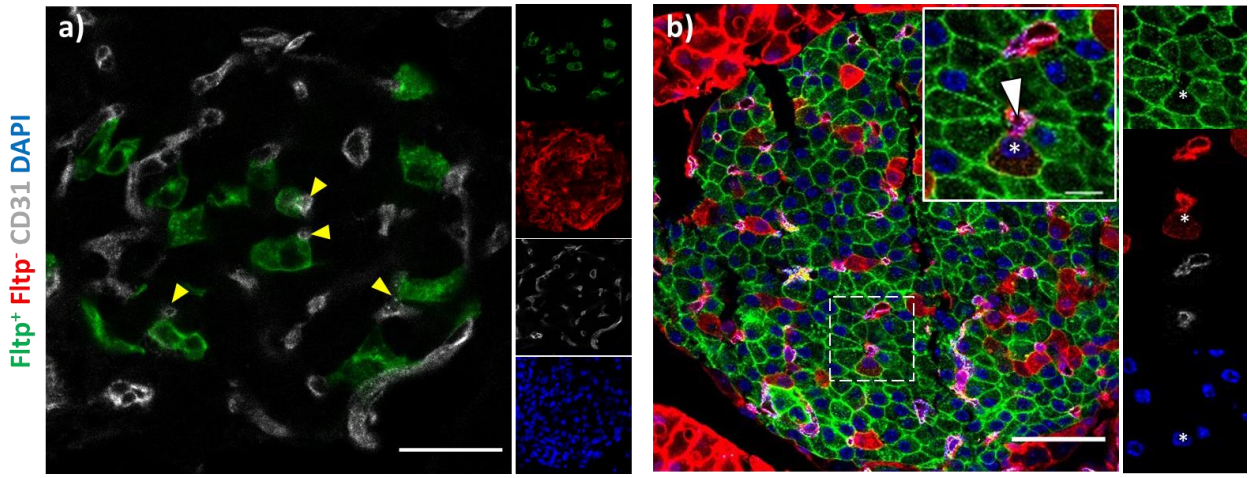


**Figure 22: Relationship between Fltp and vasculature**

**a)** Representative IF staining of an islets at P14 with CD31 (white), $Fltp^+$ (green), $Fltp^-$ (red) cells and DAPI in blue for nuclei; yellow arrows indicate the connection between $Fltp^+$ cells and endothelial cells; **b)** IF staining of an adult islet; the white triangle indicates the vessel at the center of the rosette structure-like, while the asterisk indicates the $Fltp^{\pm}$ cell. Scale bar 20 and 50 µm respectively.

### 4.1.10 Islet heterogeneity and age mosaicism

Up to this point, we have described work made mostly on postnatal islets, intriguing age due to our lack of knowledge about the precise mechanisms leading to the mature β-cell phenotype. In the next paragraphs, we introduce the work done in the latest part of my PhD, by generating an adult and aged islet scRNA-seq dataset. The aim of this work is to elucidate the mechanisms regulating the ageing of β-cell, focusing on possible dysregulated pathways in older mice. In addition, thanks to the Fltp reporter and linage tracing, we add another layer to the analysis, which might reveal differential Wnt signaling activation among ages.

#### 4.1.10.1 Deciphering heterogeneity in adult islets

The first dataset was generated using the $Fltp^{ZV}$ mouse line. This mouse line has been extensively described before (Bader et al., 2016; Gegg et al., 2014). In brief, the entire Fltp genomic sequence was removed and substituted by a NLS-LacZ-H2B-Venus construct. Differently to the previously described mouse model ($FltpiCre^{mTmG}$), this is a reporter line (Fltp Venus Reporter – FVR). For our experiment, we used 3-month-old heterozygous mice, in order to avoid the possible effect of Fltp knockout on the transcriptome of the islets. Six mice were used and pulled together after separating the pancreas regions in head (H) and tail (T) and then the two FVR populations (FVR+ and FVR-) were sorted via FACS, for a total of 4 samples: $FVR^{H+}$, $FVR^{T+}$, $FVR^{H-}$ and $FVR^{T-}$ (Figure 23a). The clustering of the four samples revealed interesting features. α-cells were mostly distributed (79%) in the tail portion of the pancreas and only 21% in the head portion, while β-cells were equally distributed (55% head and 45% tail) between the two regions. Almost all γ-cells were coming from the head region (98% head vs 2% tail), while δ-cells were more abundant in the tail (33% head vs 67% tail) (Figure 23c, e). We collected respectively 63.3% $FVR^-$ and 36.7% $FVR^+$ α-cells, 37.8% $FVR^-$ and 62.2% $FVR^+$ β-cells, 68.8% $FVR^-$ and 31.2% $FVR^+$ cells γ-cells and 45.7% $FVR^-$ and 54.3% $FVR^+$ δ-cells (Figure 23c, e). The stratified results according to pancreas region and FVR sorting strategy are shown in Figure 23c. Density UMAPs for $FVR^+$ and $FVR^-$ (Figure 23d) and FVR in relation to the pancreatic region (Figure 23f), graphically displayed what described by the previous statistics. In particular it was visible that the majority of α-cells are $FVR^-$ and localized in the tail region of the pancreas.

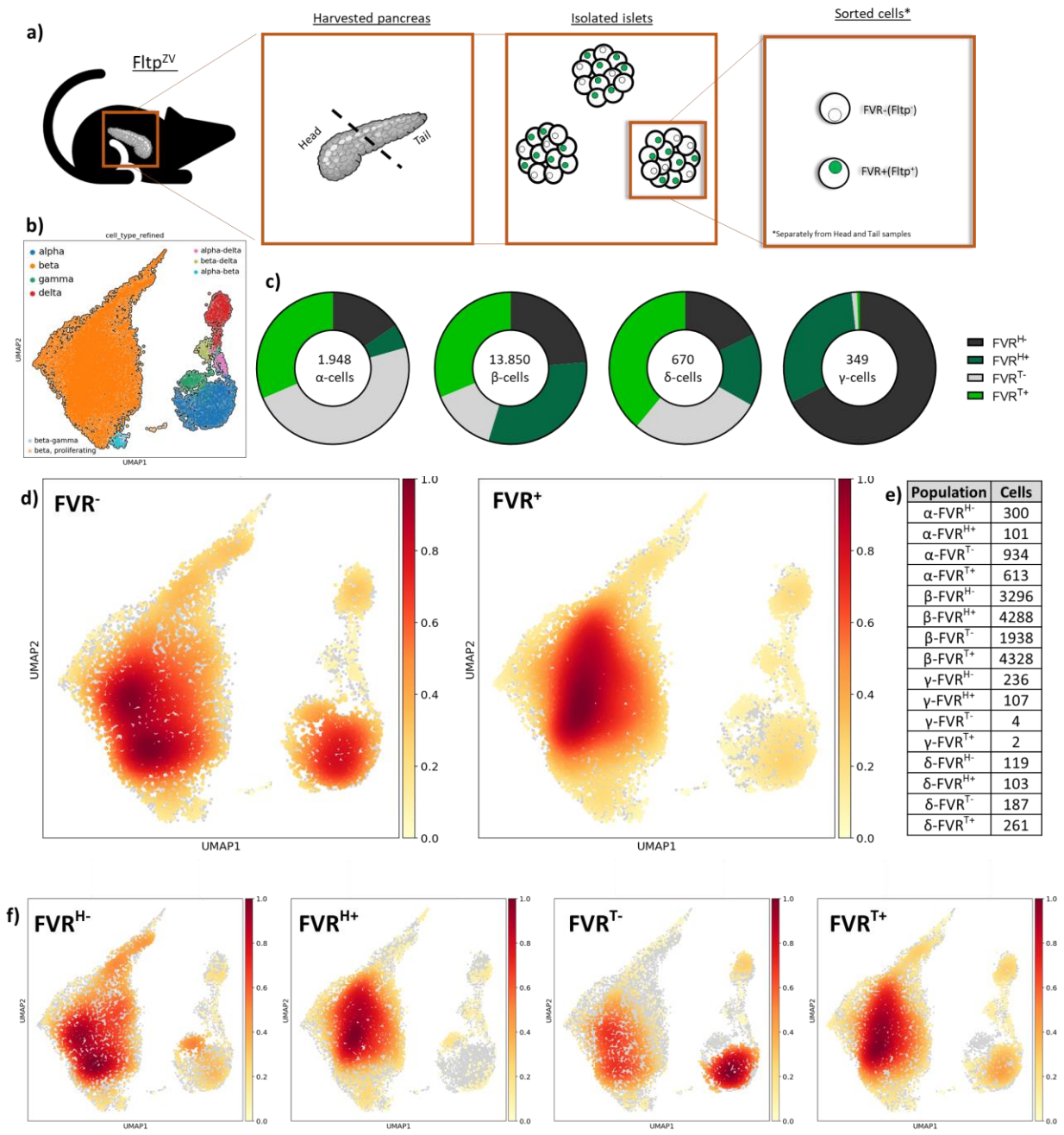


| Population | Cells |
|---|---|
| α-FVR$^{H-}$ | 300 |
| α-FVR$^{H+}$ | 101 |
| α-FVR$^{T-}$ | 934 |
| α-FVR$^{T+}$ | 613 |
| β-FVR$^{H-}$ | 3296 |
| β-FVR$^{H+}$ | 4288 |
| β-FVR$^{T-}$ | 1938 |
| β-FVR$^{T+}$ | 4328 |
| γ-FVR$^{H-}$ | 236 |
| γ-FVR$^{H+}$ | 107 |
| γ-FVR$^{T-}$ | 4 |
| γ-FVR$^{T+}$ | 2 |
| δ-FVR$^{H-}$ | 119 |
| δ-FVR$^{H+}$ | 103 |
| δ-FVR$^{T-}$ | 187 |
| δ-FVR$^{T+}$ | 261 |

**Figure 23: Characterization of the adult islets scRNA-seq**

**a)** Cartoon depicting the strategy used to generate the scRNAseq dataset (N=1, 6 mice); **b)** UMAP describing the clustering of the adult endocrine populations, annotated according to commonly used markers; c) Donut plots showing the stratified results according to endocrine cell-type, FVR and pancreas localization of the analyzed cells; **d)** and **f)** Density UMAPs showing the accumulation of the indicated populations in the multidimensional space; **e)** Table with the number of cells analyzed per cell type.

Next, we focused on the β-cell population. Here, as already seen from the previous plots, we could observe a higher density of cells in the $FVR^+$ cells but no visible differences between head and tail (Figure 24a). Next, we computed the differential gene expression analysis (DGEA) between $FVR^+$ and $FVR^-$ cells (using Limma). The results showed the majority of the genes were differentially regulated in the $FVR^+$ cells (1449 vs 192 genes). Pathway enrichment analysis (Figure 24b) outlined the following results. $FVR^+$ β-cells were significantly enriched for terms related to maturity, as FoxO, insulin signaling, estrogen signaling, insulin secretion, AMPK and terms related to GLP1 response. In addition, we detected terms related to non-canonical Wnt signaling (Degradation of Axin, Degradation of DVL, Auto-degradation of Cdh1, PCP/CE pathway) (Figure 24c). $FVR^-$ β-cells showed terms related to response to cAMP, purines, vitamins and ions, and upregulated lipid metabolism. Furthermore, we observed terms of negative regulation of proliferation (Figure 24d). Taken together, also in adult β-cells we observed a mature transcriptional profile. While the negative population presented terms related to cell cycle, hinting at the capacity of these cells of replicating.

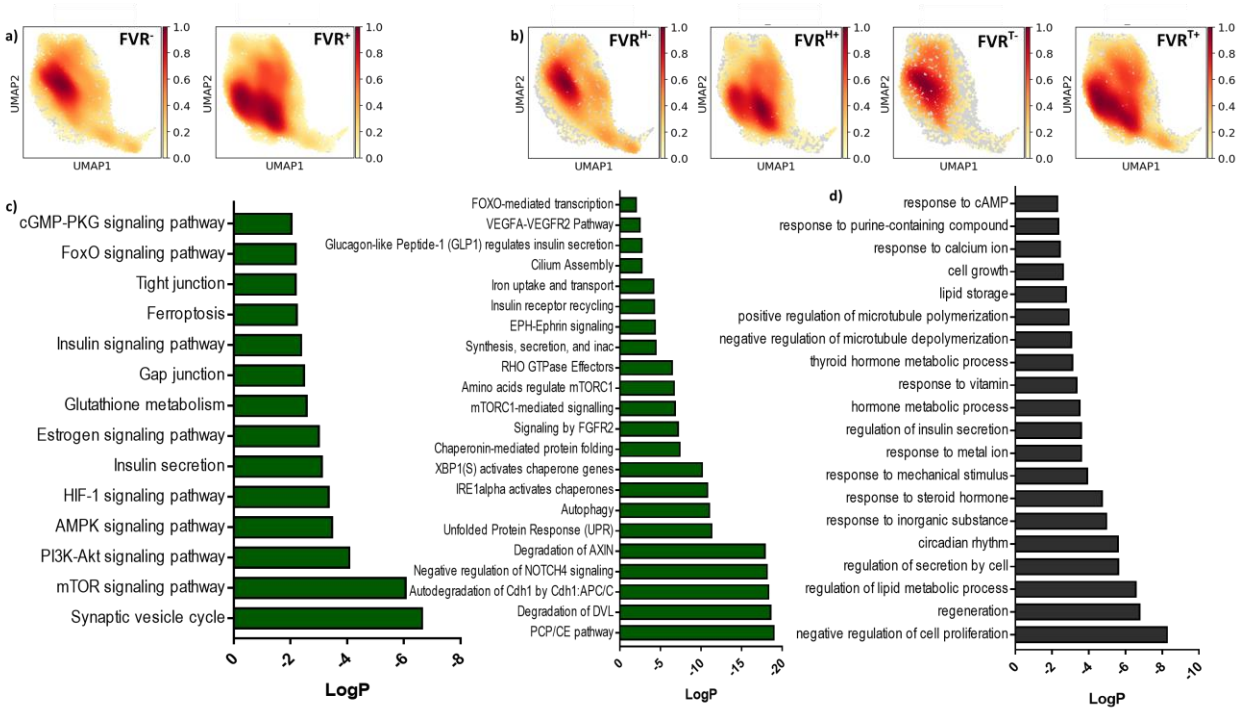


**Figure 24: DGEA and pathway enrichment analysis of FVR-β-cells**

**a)** and **b)** Density UMAPs of FVR only and FVR together with pancreas localization of β-cells; **c)** and **d)** Pathway enrichment analysis generated using the differentially regulated genes from the two FVR- β-cell clusters; LogP indicates the significance of the displayed term in relation to the genes upregulated in the cluster.

We further explored β-cell heterogeneity, without considering Fltp as separating marker. Thus, we computed Louvain clustering (resolution at 0.5), which grouped cells based on their transcriptional profiles, and observed 5 different β-cell subclusters (Figure 25a). We computed the top 20 highest ranked genes per cluster (Figure 25b) and explored the relationship among clusters via PAGA (Figure 25c). Together with gene ontology analysis, clusters 0 and 1 seemd more similar and probably more mature cells (*Ucn3*, *Cpe*, *Pccsk1* and *2*). Clusters 2 and 4 also shared common features, resembleing immature and immunereactive cells (*Cd81*, *Ifit1*, *Ifit3*, *Stat2*). Cluster 3 appeared different from the others and no enriched pathway was found there, thus it could represent dying cells. In conclusion, this analysis depicted a complex degree of heterogeneity in adulthood. Further studies need to address several questions regarding adult β-cell, possibly characterizing these clusters using novel markers.

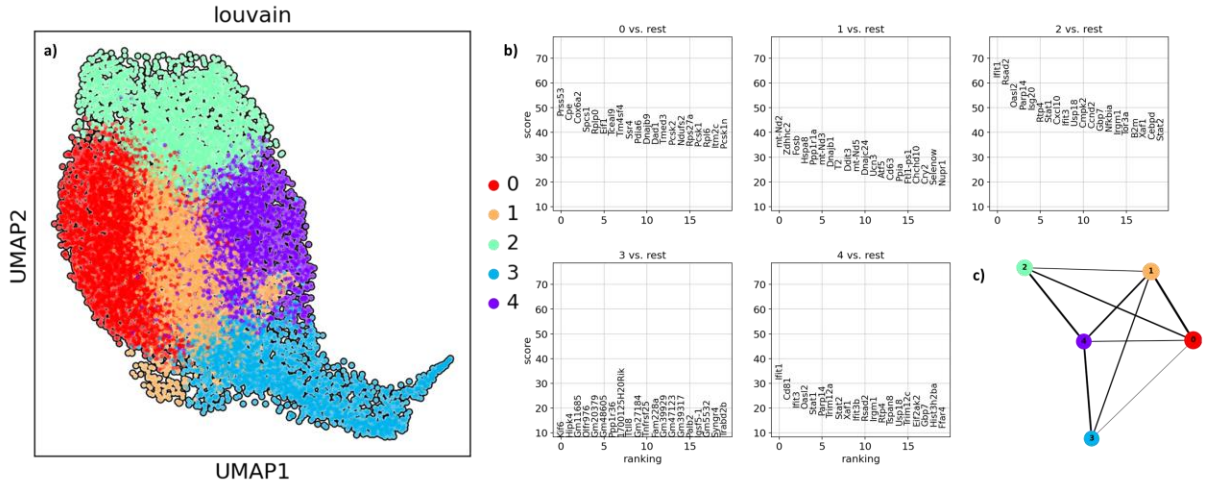


**Figure 25: Unbiased clustering reveals complex heterogeneity in adult β-cells**

**a)** UMAP of β-cells, color-coded based on the Louvain clustering; **b)** Summary of the 20 highest ranked genes per cluster compared to the rest of the β-cells; **c)** PAGA plot representing the connections among Louvain clusters; the thicker the line, the higher the similarity between clusters.

### 4.1.10.2 Deciphering heterogeneity in aged islets

The second dataset was generated from a cohort of 2-year-old mice. Like the postnatal dataset, we used the lineage tracing FltpiCre$^{mTmG}$ mouse model for the experiment. Four mice were used to isolate islets and sort the three Fltp subpopulations according to the same scheme described in the previous paragraphs. The dataset has not been fully analyzed yet, thus here we present a brief overview of what obtained so far (Figure 26). From the first clustering, we observed that the most abundant population in aged islets were β-cells, followed by a reduced portion of α- and δ-cells (Figure 26a-c). Whether this data is affected by our sorting

or it is a feature of rodent islets need to be investigated. The sorting scheme used resulted in the profiling of valid numbers for each Fltp population. We obtained 31% (Fltp$^{-}$), 29% (Fltp$^{\pm}$) and 40% (Fltp$^{+}$) α-cells; 45% (Fltp$^{-}$), 17% (Fltp$^{\pm}$) and 38% (Fltp$^{+}$) β-cells; 38% (Fltp$^{-}$), 37% (Fltp$^{\pm}$) and 25% (Fltp$^{+}$) δ-cells (Figure 26b, d). Of note, these percentages are only informative about the abundance of each Fltp subpopulation per endocrine cluster, but do not reflect the real numbers we might find in islets. In conclusion, the presence of an abundant number of cells from Fltp$^{-}$ and Fltp$^{\pm}$ populations indicate that endocrine cells undergo, through the life, a continuous process of renewal.

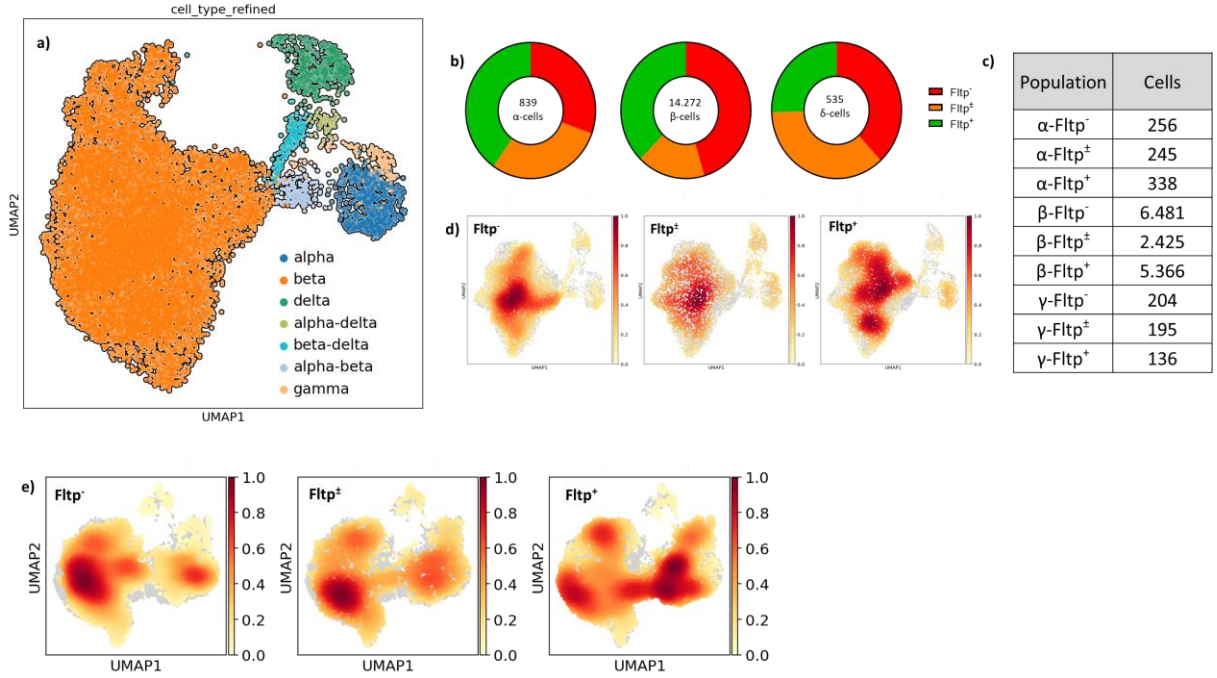


| Population | Cells |
|---|---|
| α-Fltp$^{-}$ | 256 |
| α-Fltp$^{\pm}$ | 245 |
| α-Fltp$^{+}$ | 338 |
| β-Fltp$^{-}$ | 6.481 |
| β-Fltp$^{\pm}$ | 2.425 |
| β-Fltp$^{+}$ | 5.366 |
| γ-Fltp$^{-}$ | 204 |
| γ-Fltp$^{\pm}$ | 195 |
| γ-Fltp$^{+}$ | 136 |

**Figure 26: Characterization of the ageing islets scRNA-seq**

**a)** UMAP describing the clustering of the ageing endocrine populations, annotated according to commonly used markers; **b)** Donut plots showing the stratified results according to endocrine cell-type and split according to the three Fltp subpopulations; **c)** Table with the number of cells analyzed per cell type and Fltp subpopulation; **d)** and **e)** Density UMAPs showing the accumulation of the indicated Fltp populations in the multidimensional space, respectively for all endocrine or just β-cells.

## 4.2 Part 2: CD81 as novel β-cell immaturity marker

### 4.2.1 CD81 is differentially expressed among pancreatic endocrine cells

The postnatal endocrine environment revealed interesting insights in connection with Fltp and Wnt/PCP. We observed a significant degree of heterogeneity within the β-cell population (Figure 27a). The two most common maturation markers, *Ucn3* and *Mafa*, were present in the vast majority of β-cells, clustering on the center and right sides of the UMAP (Figure 27b and c). The transcription factor *Mafb* is known to be downregulated after birth, and here we confirmed its presence, during postnatal, in a restricted group of cells clustering on the left side of the UMAP (Figure 27e). These data confirmed the quality of our dataset, overlapping with what is described in literature. Next, we dissected the β-cell heterogeneity and as shown in Figure 27a, the Louvain clustering determined the presence of 5 different β-cell clusters coexisting at this stage. Among these, one subgroup presented an interesting transcriptional profile. Within cluster number 2 we found a gene, known as *Cd81* or TAPA-1 that, similarly to *Mafb*, was differentially expressed if compared to all other subgroups (Figure 27f). We also evaluated the expression levels in the other endocrine cell types, observing high levels of the transcripts in almost all the other endocrine cells (Figure 27d) (Salinno et al., 2021).

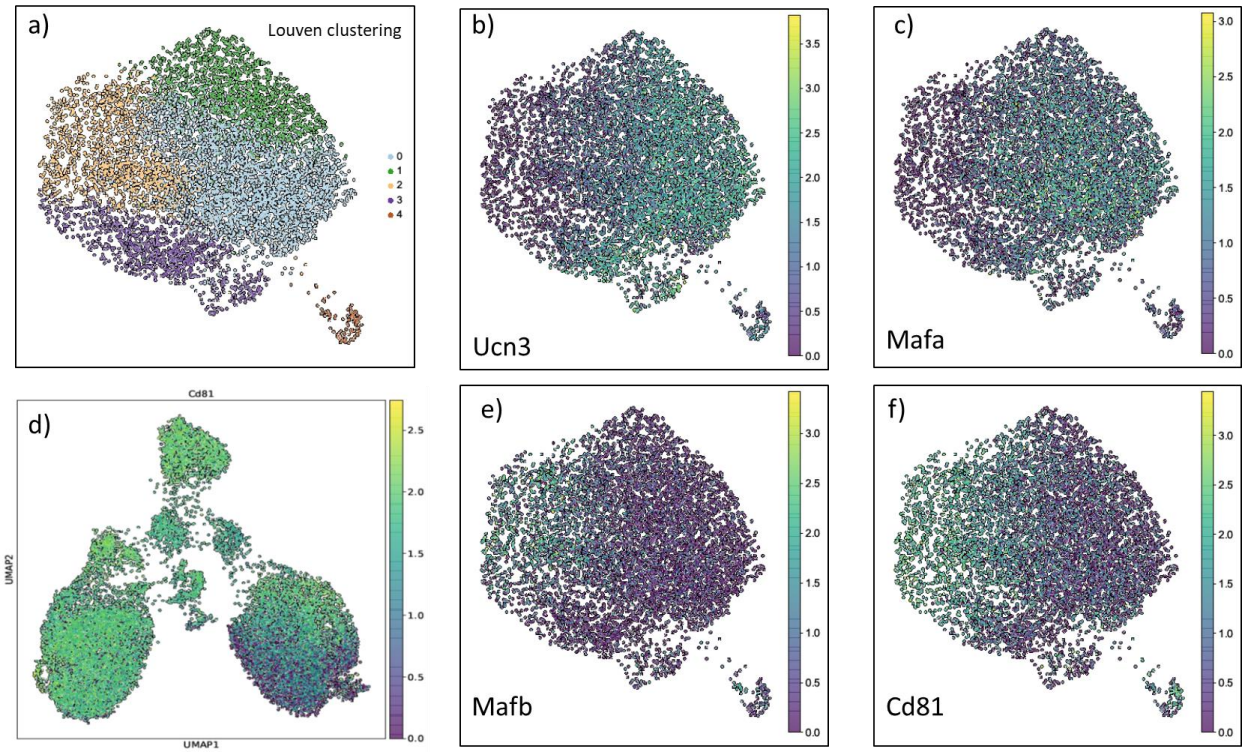


**Figure 27: Cd81 is heterogeneous in postnatal β-cells**

**a)** Color-coded UMAP with Louvain clustering representing distinct β-cell populations; UMAPs representing the level of expression (LogCPM; Log Counts Per Million) in β-cells of the following genes: **b)** *Ucn3*, **c)** *Mafa*, **e)** *Mafb*, **d)** and **f)** *Cd81* in β-cells and in all endocrine compartments, respectively; (Salinno et al., 2021).

Next, we evaluated whether we could detect the protein associated to the transcript. We tested a commercial monoclonal antibody with different methods. First, we isolated islets of Langerhans from adult mice, dissociated them and incubated with the antibody. The cells were then analyzed and sorted by flow cytometry. In Figure 28a, we could observe two distinct populations according to the fluorescence intensity. The sorted cells were sampled and analyzed under the microscope to evaluate the quality of the antibody binding, observing a clean membrane staining, as expected (Figure 28b). The rest of the sorted cells were used for WB analysis (Figure 28c), once again confirming the quality of the sorting, or RT-qPCR (Figure 28d). With the latter, we confirmed the scRNAseq data, the CD81 negative (called low/-) population was enriched for the *Ins1* transcript, while the CD81 positive (called high) for *Gcg* and *Cd81* transcripts. Finally, we performed IF staining on dispersed islets (Figure 28e) and pancreas paraffin sections (Figure 28f) to strengthen the concept that CD81 is enriched in non-β endocrine cells. In conclusion, we present a novel marker differentially expressed in β-cells but not exclusive for them.

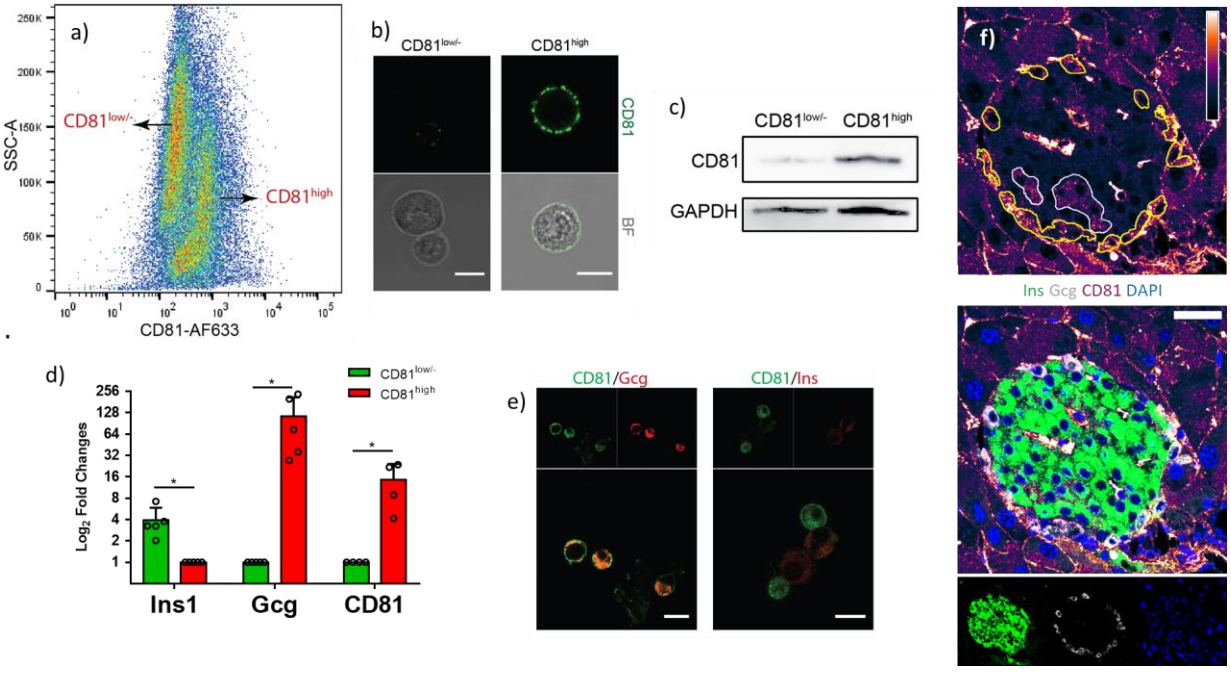


**Figure 28: Characterization of CD81 is adult islets of Langerhans**

**a)** FACS analysis of dispersed islets of Langerhans stained for CD81 and Alexa Fluor 633 displayed as scatter plot; **b)** representative confocal picture of single endocrine cells right after sorting for CD81; scale bar: 10 µm; **c)** western blot image from sorted $CD81^{high}$ and $CD81^{low/-}$ endocrine cells, showing CD81 levels and GAPDH as loading control (n=1, 4 mice pulled together); **d)** RT-qPCR analysis of CD81-based sorted cells (n=5 and n=4 respectively, *P < 0.05;

t-test); **e)** Immunostaining on dispersed adult islets for insulin (Ins - red), glucagon (Gcg - red) and CD81 (green), scale bar: 10 µm; **f)** IF staining of paraffin sections from adult mouse pancreas showing one islet of Langerhans; insulin (green), glucagon (white) and CD81 in GEM (calibration bar indicates the intensity of the signal); white lines surround the β-cells positive for CD81, yellow lines surround all α-cells ; scale bar: 50 µm; (Salinno et al., 2021).

We further wanted to understand the subcellular localization of CD81 in β-cells. In literature, it is reported that CD81 localizes on the plasma membrane and marks vesicles and exosomes. To confirm this data, we performed IF staining of CD81, on Min6 K8 insulinoma cell line, in combination with Pro-Insulin for immature granules, C-Peptide for mature granules, GM130 for the Golgi apparatus and Lamp1 for lysosomes. We observed a partial colocalization of CD81 with both mature and immature insulin granules but minimal colocalization with the Golgi or with the lysosomes (Figure 29).

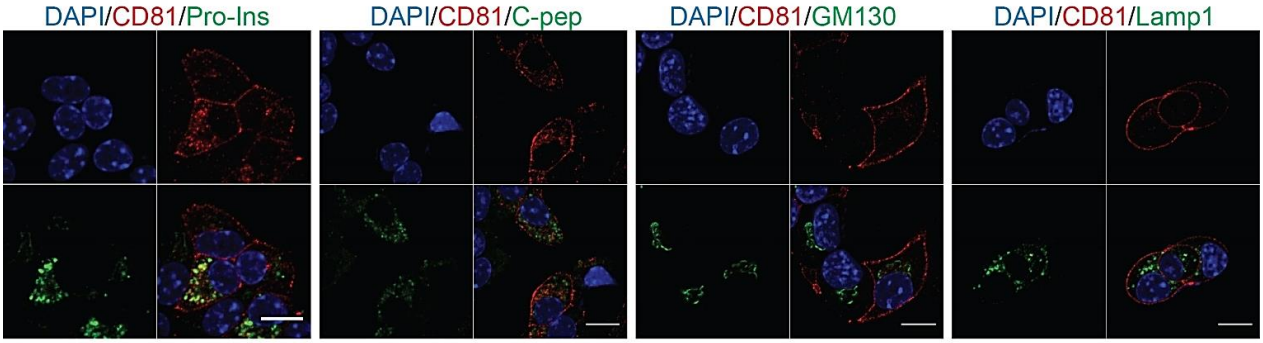


**Figure 29: CD81 subcellular localization in β-cells**

IF staining on Min6 K8 insulinoma cell line for CD81 (red) and **a)** Pro-Insulin; **b)** C-peptide; **c)** GM130; **d)** Lamp1; scale bar: 10 µm

### 4.2.2 Longitudinal analysis of CD81 in mouse islets

Considering the restricted expression of CD81 to a limited fraction of β-cells, we wondered about its dynamic of expression at different stages of life. We analyzed the pattern of expression of *Cd81* from embryonic to adulthood using the scRNA-seq data from the P16 dataset, together with other published dataset from embryonic pancreas (Aimée Bastidas-Ponce et al., 2019) and adult islets (Sachs et al., 2020). As visible in the violin plots, *Cd81* was highly expressed in endocrine and exocrine embryonic cells from the developing pancreas (Figure 30a). More in detail, once we dissected the endocrine population in the four main populations, we observed a similar level of expression among all the endocrine cell types (Figure 30b). At P16, we observed a significant decline of Cd81-expressing β-cells (Figure 30c), further reduced in the adult stage (Figure 30d).

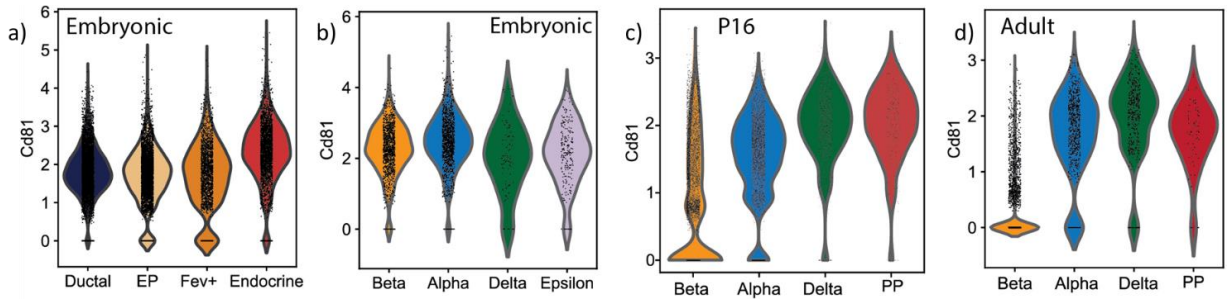


**Figure 30: Longitudinal analysis of Cd81 expression via scRNAseq**

Violin plots depicting the expression levels of Cd81 in scRNAseq in**: a)** embryonic ductal, Fev$^{+}$, endocrine precursors (EP) and endocrine cells; **b)** embryonic endocrine cells; **c)** postnatal endocrine cells; **d)** adult endocrine cells; (Salinno et al., 2021).

We experimentally confirmed the scRNA-seq results by using a novel β-cell reporter mouse model generated in our lab. In brief, a Venus sequence has been inserted, in frame, after the endogenous sequence of the Nkx6-1 gene. In this way, there would be the co-expression of both the genes in the nucleus (Figure 31a). Therefore, the line has been named Nkx6-1 Venus Fusion (Nkx6-1VF) (Burtscher et al., 2021). In Figure 31b, IF staining of two islets of Langerhans stained for insulin, glucagon, Venus and DAPI, showing the specific expression of the fusion protein in β-cell. Thanks to this mouse line, it was possible to distinguish β-cells without any additional staining (Figure 31c), to perform flow cytometry time course analysis of CD81 expression in β-cells (Figure 31d). The analysis confirmed a striking decline of CD81$^{high}$ cells in postnatal and a subsequent decrease until adulthood (Figure 32e). We further stained dispersed islets for Venus and CD81, to confirm the presence of both CD81 positive and negative β-cells (Figure 31f). Finally, we performed an RT-qPCR on sorted cells for the different populations that confirmed the quality of our sorting strategy (Figure 31g). Our data confirmed that CD81 is downregulated throughout the β-cell maturation process and is restricted to a subpopulation of β-cell in adulthood.

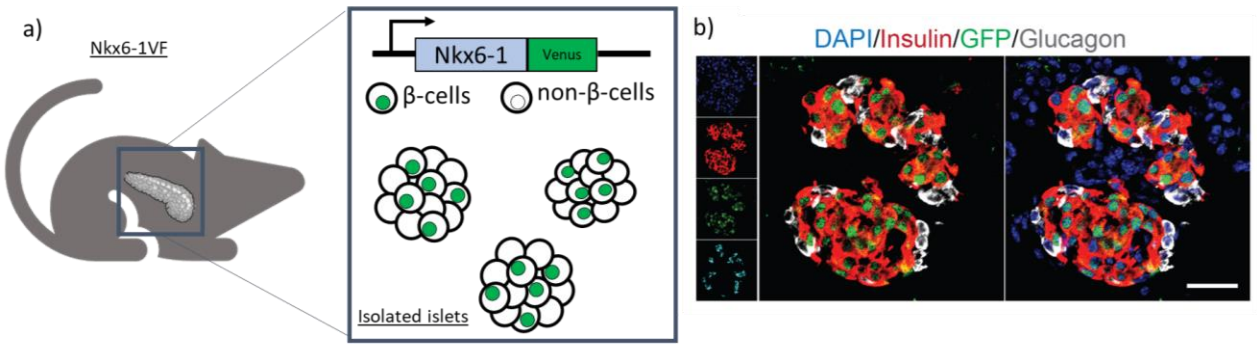

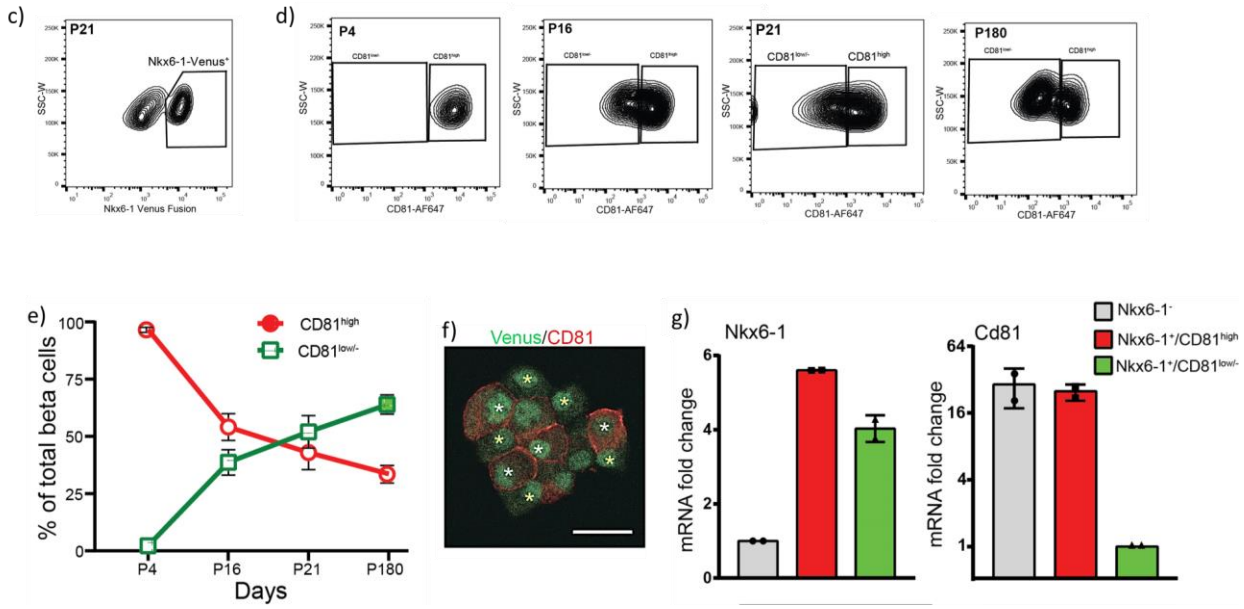


**Figure 31: CD81 is downregulated during β-cells postnatal development**

**a)** Schematic representation of the Nkx6-1VF mouse model (Burtscher et al., 2021) used for the experiments; **b)** IF staining of pancreatic sections from Nkx6-1VF mouse, showing the specificity of the reporter for β-cells; insulin (red), glucagon (grey), GFP (green) and DAPI (blue), scale bar: 30µm; **c)** FACS counter plot showing the analysis of dispersed islets from Nkx6-VF mouse; visible two distinct populations, the right one in the box represents β-cells, (Venus positive); **d)** representative FACS counter plots showing CD81 staining on β-cells at different time-points; **e)** quantification of the FACS analysis of the percentages of $CD81^{low/-}$ and $CD81^{high}$ for the different time points analyzed (n=3 for P4 and n=4 for the others); **f)** IF staining of dispersed islets from Nkx6-1VF mice, Venus (green) reporting for Nkx6-1 and CD81 (red); yellow asterisks mark $CD81^{low/-}$ β-cells, while white asterisks label $CD81^{high}$ β-cells, scale: bar 20 µm; **g)** bar plots showing the results of the RT-qPCR (n=2) for the Nkx6-1 and Cd81 genes in the three sorted populations indicated; (Salinno et al., 2021)

### 4.2.3 CD81 marks immature β-cells

CD81 marked the majority of β-cells during the early stages of development, while only a minor fraction retained this marker in adult β-cells. We hypnotized that CD81 could label immature β-cells within the islets of Langerhans. We used the scRNA-seq from P16 mice and decided to split β-cells in two groups: $CD81^{low/-}$ (threshold<1) and $CD81^{high}$ (threshold>1) and observed that 59.11% of β-cells were already low or negative for *Cd81* (Figure 32a). These groups of cells were then used to perform a differential gene expression analysis (DGEA by limma test), showing 322 and 331 upregulated genes respectively (Figure 32b, c). In the heatmap are represented the highest differentially regulated genes, in which we observed

genes as *Ucn3*, *Mafa*, *Sytl4* and *Ero1lb* for the CD81$^{low/-}$ population, *Mafb* and *Rbp4* for the CD81$^{high}$ population. In Figure 32f we showed violin plots with the expression levels of the above-mentioned genes and other important markers for mature or immature β-cells (*Slc2a2* and *Chga*), pointing out at the fact that the CD81$^{high}$ cells expressed lower levels of maturity markers. We confirmed the scRNA-seq observations in RT-qPCR (Figure 32d); *Ucn3* and *Mafa* were significantly upregulated in the CD81$^{low/-}$ population, while *Rbp4* was upregulated in the CD81$^{high}$ β-cells. We further proved in IF that MafA is upregulated in β-cells lacking CD81 expression (Figure 32e).

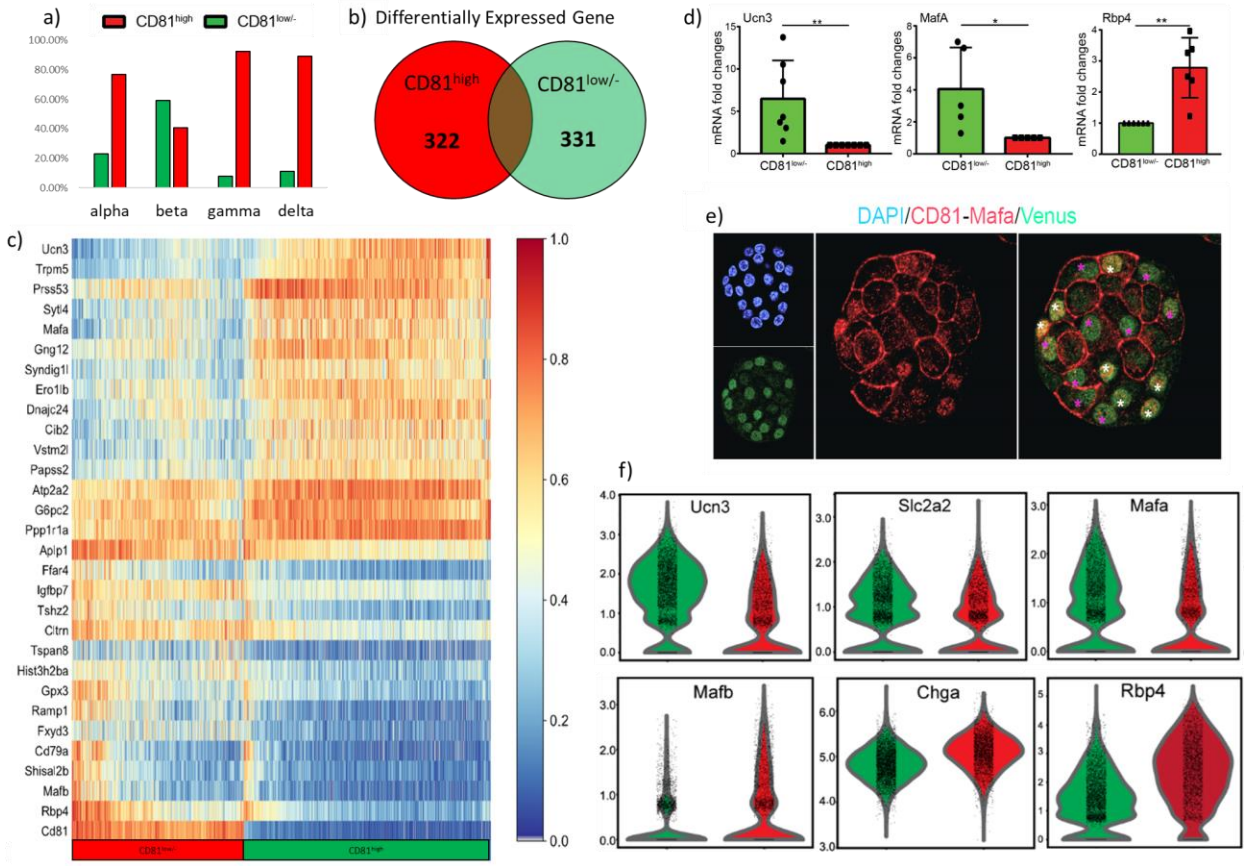


**Figure 32: CD81 labels an immature cluster of β-cells**

**a)** Histogram representing the percentages of endocrine cells high or negative/low for CD81; **b)** Schematic representation of the number of genes differentially regulated in the two CD81 clusters, coming from the DGEA; **c)** ) Heatmap representing the top 30 differentially regulated genes in P16 CD81$^{high}$ and CD81$^{low/-}$ β-cells; **d)** qPCR analysis on sorted CD81$^{high}$ and CD81$^{low/-}$ β-cells (Nkx6-1VF$^{+}$) of two maturation markers, *Ucn3* (n=7) and *Mafa* (n=5), and one immature marker *Rbp4* (n=6) (*P < 0.05; **P < 0.01; t-test); **e)** IF staining on dispersed islet from weaning age Nkx6-1VF mice. Pink asterisks indicate MafA$^{-}$ β-cells and white asterisks show MafA$^{+}$ β-cells. CD81 and MafA have been imaged with the same confocal channel; scale bar 20 µm; **f)** Violin plots from the P16 scRNA-seq representing

the expression levels of three maturation markers (*Ucn3*, *Slc2a2* and *Mafa*) and three immaturity markers (*Chga*, *Rbp4* and *Mafb*). (Salinno et al., 2021)

The differentially regulated genes were used as input for Metascape, a gene ontology enrichment tool. The CD81$^{low/-}$ β-cells presented terms related to regulation of mTORC1 by amino acids or by the LKB1-AMPK complex (i.e. genes as *Rheb*, *Rragd*, *Fnip 1* and *2*, *Flcn*, *Prkab2* and many members of the *Atp6v* family), Wnt signaling pathway (*Gng12*, *Gng4*, *H3f3b*, *Ywhaz*, *Vps35*, *Ctnnbip1*, *H2bc4*, *H4c8*, *Daam1*, *H2aj* and *H4c9*), glucose metabolism (*G6pc2*, *Gapdh*, *Mdh1*, *Pkm*, *Pfkp* and *Nup93*), FoxO signaling pathway (*Setd7*, *Gabarap*, *Plk3*, *Prkab2*, *Ccnd2* and *G6pc2*), insulin signaling (*Rheb*, *Shc1*, *Rhoq*, *Prkab2* and *G6pc2*) and ERAD pathway (*Dnajb9*, *Sec61b*, *Derl1*, *Svip*, *Derl2* and *Edem1*) (Figure 33a, b). These terms pointed out at a mature type of phenotype. On the contrary, the GO-terms of the *CD81*$^{high}$ β-cells were related to lipid metabolism (i.e., *Tspo*, *Cpt2*, *Gpd1*, *Gm2a*, *Pla2g2d*, *Pla2g2f*, *Ormdl3*, *Mid1ip1*, *Ddhd2*, *Dhcr24*, *Abcc3*, *Aacs*, *Acat2*, *Stard5*, *Sumo2*, *Mvd* , *Plaat3* and *Pon2*), membrane potential and sodium channels (*Kcnk1*, *Kcnk3*, *Kcnk16* and *Atp1a1*, *Fgf12*, *Kcnk1*, *Fxyd3*, *Scn3a*, *Chp1*, *Fxyd6*, *Wnk4*) and PPAR signaling (*Lpl*, *Fabp5*, *Cpt2*, *Ubc*) (Figure 33a, b). Thus, we hypothesized that these cells possess an immature phenotype. To test our hypothesis, we benchmarked the transcriptional profiles of CD81$^{low/-}$ and CD81$^{high}$ postnatal β-cells with those of the Fev$^{+}$, embryonic endocrine cells, β1 and β2 populations, described in literature (Aimée Bastidas-Ponce et al., 2019; Sachs et al., 2020). As predicted, the Fev$^{+}$, embryonic and the β2 (immature cells) populations had higher number of genes in common with the P16 CD81$^{high}$ β-cells, while the more mature β1 population overlapped more with the CD81$^{low/-}$ β-cells (Figure 33d). Finally, we clustered the differentially regulated genes in protein families. The CD81$^{low/-}$ β-cells possessed more signal molecules, modulators of protein binding activity, scaffold and adaptor proteins, structural proteins, translational proteins and transporters. While the CD81$^{high}$ β-cells were enriched in calcium-binding proteins, cell adhesion and junction proteins, cytoskeletal proteins, gene specific transcriptional regulators, protein modifying enzymes, transfer and carrier proteins and transmembrane receptors (Figure 33c).

Fltp has been described before as a maturation marker for β-cells. Here we explored the relationship between Fltp and CD81. We used the P16 scRNAseq and clustered together the Fltp$^{+}$ and Flrp$^{\pm}$ populations (now only Fltp$^{+}$). The violin plot in Figure 33e showed that *Cd81* was more abundantly expressed in the Fltp$^{-}$ population if compared to the Fltp$^{+}$. To confirm this data, we used the Flattop Venus Reporter (FVR) mouse model. Islets were isolated from adult mice and cells were stained with CD81 antibody (Figure 33f). Analysis by flow cytometry revealed that the FVR$^{-}$ cells were equally positive and negative for CD81 (46.4% vs 53.6%), while the FVR$^{+}$ cells had more CD81 $^{low/-}$ cells (37.2% vs 62.8%) (Figure 33g).

Considering that adult mice had low number of CD81$^{high}$ cells, it did not surprise to see that in both FVR populations we had an abundance of CD81$^{low/-}$. Although it was relevant that in the FVR$^{-}$ β-cells we had more CD81$^{high}$ compared to the FVR$^{+}$. Therefore, CD81 followed an inverse dynamic of expression compared to Fltp. In conclusion, we confirm that using the surface marker CD81 we can distinguish two transcriptionally distinct groups of β-cells, one more mature (CD81$^{low/-}$) and one immature (CD81$^{high}$).

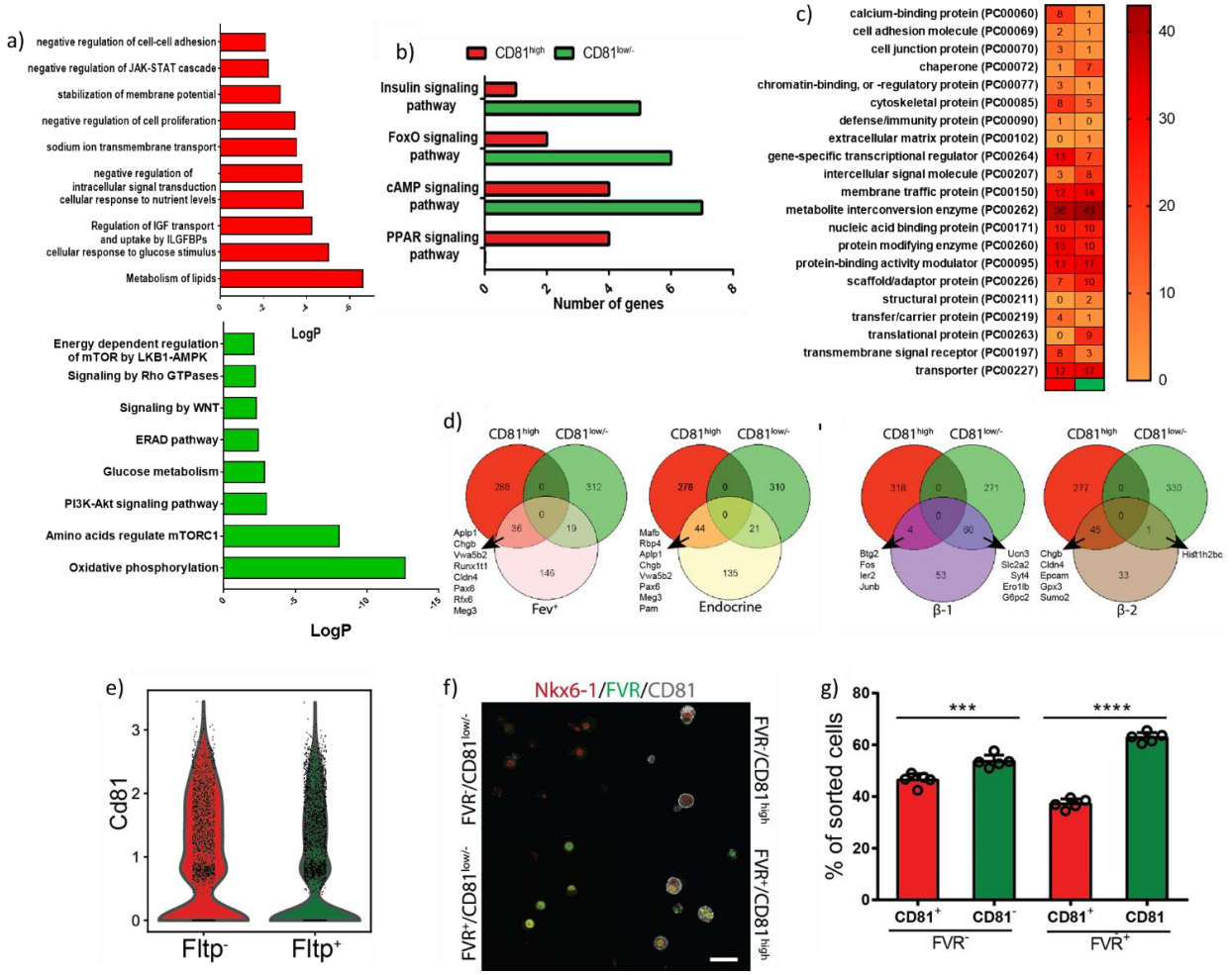


**Figure 33: CD81 is downregulated during postnatal development of β-cells**

**a)** Bar plot representing the pathway enrichment analysis obtained from the differentially regulated genes of P16 Cd81$^{high}$ and Cd81$^{low/-}$ β-cells.; **b)** Targeted analysis of specific signaling pathways differentially regulated between; the two Cd81-β-cell populations; **c)** Map representing the enrichment of each protein class (rows) for the two CD81 populations (columns); each cell contains the number of genes, also depicted with a color code; **d**) Venn diagrams representing the comparison between the differentially regulated genes of the postnatal Cd81-splitted β-cells and the profiling of the Fev, embryonic endocrine, adult β1 and β2 populations; **e**) Violin plots depicting the expression levels of Cd81 in the Fltp$^{+}$ and Fltp$^{-}$ β-cells; f) IF staining of dispersed islets of Langerhans from FVR mice; Nkx6-1 (red), CD81(grey), FVR (green), DAPI (blue), scale bar: 50 µm; **g**) Flow cytometry quantification representing the

percentages of CD81$^{high}$ and CD81$^{low/-}$ in FVR$^{-}$ (left) and FVR$^{+}$ (right) β-cell populations, (n=5, ***P < 0.001; t-test). (Salinno et al., 2021)

### 4.2.4 CD81 is upregulated in diabetic conditions

The data showed so far clearly indicate that CD81 marks immature β-cells. A small pool of these CD81$^{high}$ β-cells remain also within the adult islets. Considering that in many diabetic conditions β-cells dedifferentiate and acquire an immature/embryonic phenotype, we wondered whether CD81 labelled dedifferentiated β-cells in diabetic conditions.

To test our hypothesis, we re-analyzed the scRNA-seq dataset from Sachs and colleagues. In their experiments, mice had been treated with multiple low doses of streptozotocin (STZ) and afterwards treated with different compounds (here we took in consideration only PEG-Insulin "PEG-Ins" and PEG-Insulin with GLP-1-Estrogen "PEG-Ins/GLP-1-Oe"), in order to restore their functional phenotype. In Figure 34a and 34b we showed the UMAPs of the endocrine clusters colored by treatment and with the expression levels of *Cd81*. In the next two UMAPs (Figure 34c and d) we focused only on β-cells. From these data it was evident that *Cd81* had low expression levels in the control sample, while it was higher in all other treatments. Additionally, we observed that *Cd81* was unchanged in all non-β-cells for all conditions (Figure 34e). In addition, we compared the differentially expressed genes from the P16 CD81-grouped β-cells with the profiles of the abovementioned groups of treated β-cells (Figure 34f). Interestingly, the STZ-treated β-cells transcriptional profile had higher overlap with the CD81$^{high}$ postnatal β-cells. Conversely, the two restorative treatments shifted the STZ-treated β-cells transcriptional profiles to overlap more with the CD81$^{low/-}$ β-cells (Figure 34f). To confirm our observations, we performed IF staining on pancreatic sections of control and STZ treated mice (Figure 34h). The images showed higher number of positive β-cells in the STZ-sample, while the control sample has barely detectable CD81 positive β-cells.

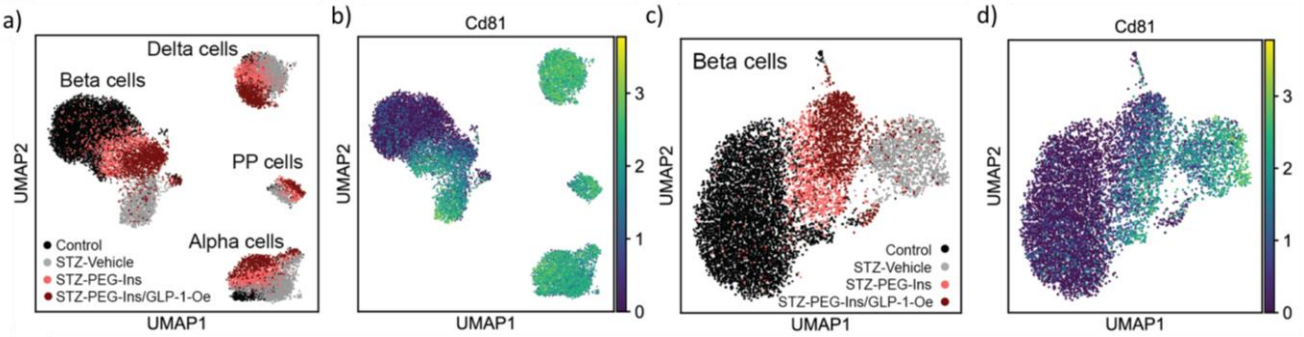

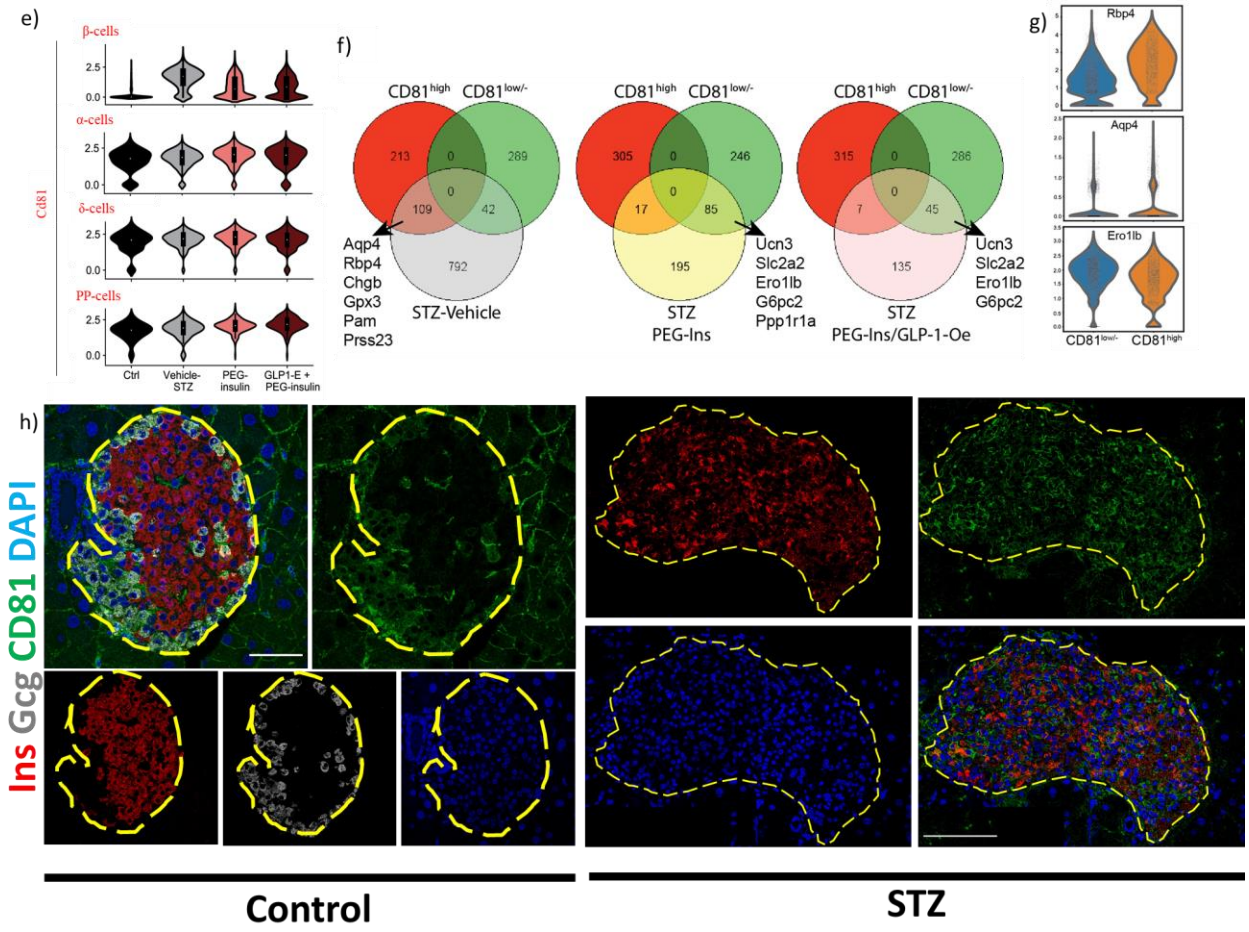


**Figure 34: CD81 is upregulated in STZ-treated β-cells**

**a**) and **b**) UMAPs representing different endocrine populations in control and treated animals and indicating the expression levels of *Cd81* in different endocrine cell types; **c**) and **d**) UMAPs representing only β-cells; on the left, color coded for the different treatments, on the right, *Cd81* expression levels; **e**) Stacked violin plots showing the expression levels of *Cd81* in all endocrine cell types and for each treatment condition; **f**) Venn diagrams representing the comparison between the differentially regulated genes of the postnatal Cd81-splitted β-cells and the profiling of the drug treated- β-cells; **g**) Violin plots representing the expression levels in Cd81-splitted β-cells of some key genes upregulated (*Rbp4* and *Aqp4*) or downregulated (*Ero1lb*) in STZ- treated β-cells; **h**) IF staining of paraffin sections from adult healthy (left) and STZ treated (right) mouse pancreas, showing the expression of CD81 (green), insulin (red), glucagon (green) and DAPI (blue); scale bar: 50μm. (Salinno et al., 2021)

We hypothesized that Cd81 is upregulated in glucotoxic or lipotoxic conditions. We further investigated whether CD81 was also upregulated in other two mouse models, the non-obese diabetic (NOD) and the leptin receptor-deficient (db/db) mice where, respectively, T1D and T2D are emulated. In Figure 35a, we showed UMAPs representing the endocrine clusters from the NOD scRNA-seq dataset at 8 and 14 weeks

of age and on the right side the expression levels of *Cd81*. When we analyzed the data based on the age of the mice and compared to control β-cells (Sachs et al., 2020) we observed a clear increase of *Cd81* in NOD β-cells together with a downregulation of other markers as *Ucn3*, *Slc2a2* and *Nkx6-1* (Figure 35b). For the db/db mouse model, we performed a whole mount IF staining on isolated islets and compared with the WT counterpart (Figure 35c). As hypothesized, the majority of the β-cells (Nkx6-1 positive) were expressing CD81. In conclusion, we can state that CD81 is upregulated in diabetic conditions and is dynamically downregulated upon restorative treatments.

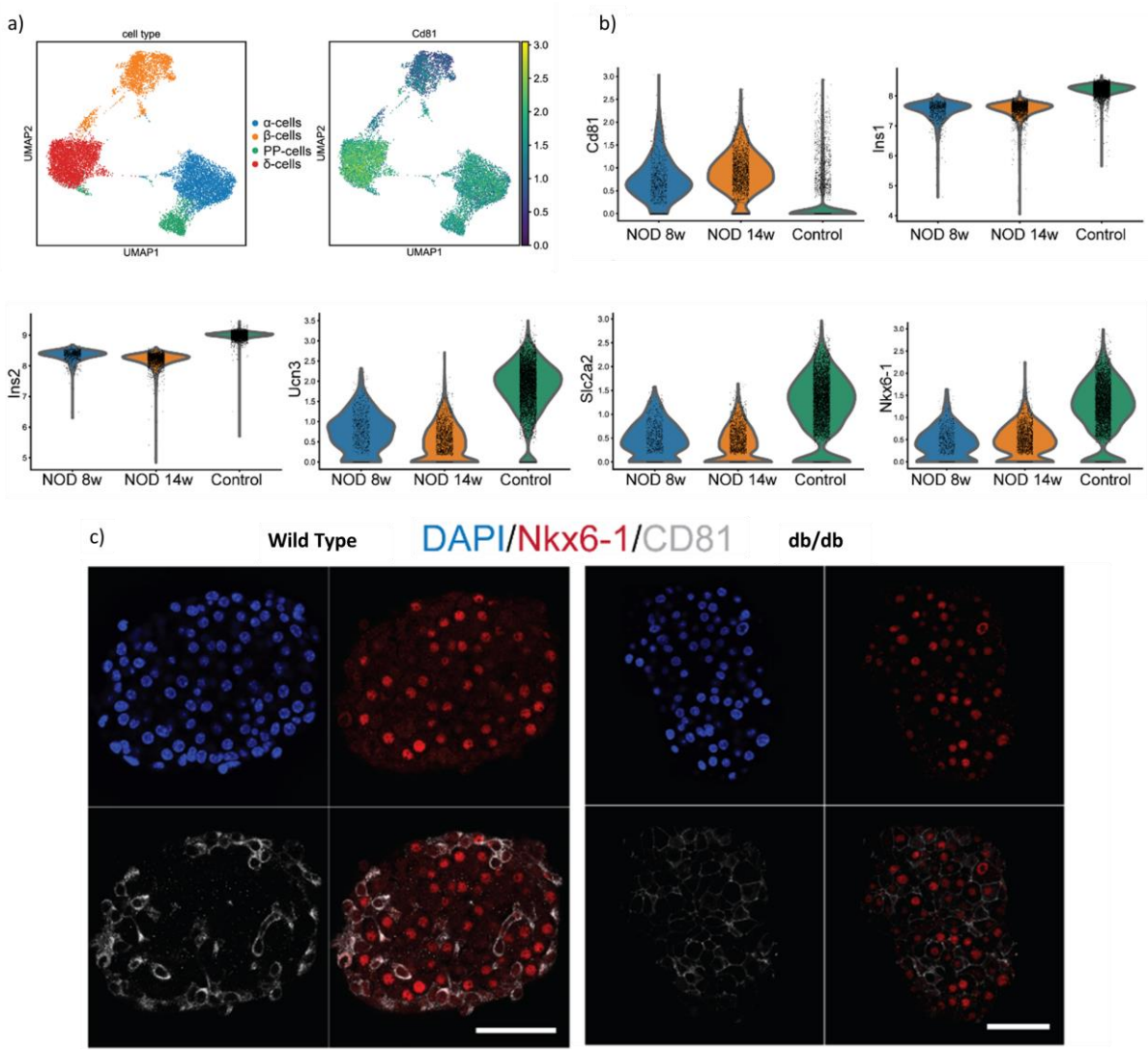


**Figure 35: CD81 is upregulated in β-cells of NOD and db/db mice**

**a**) UMAPs representing, respectively, endocrine clusters and Cd81 expression in NOD scRNA-seq data; **b**) Violin plots showing the expression levels of key β-cell genes in control vs NOD at 8 and 14 weeks, in order: *Cd81*, *Ins1*, *Ins2*, *Ucn3*, *Slc2a2* and *Nkx6-1*; **c**) Whole mount IF staining of WT and db/db islet of Langerhans; nuclei in blue, Nkx6-1 in red, CD81 in grey; scale bar: 50µm. (Salinno et al., 2021)

Dysfunctional β-cells are the result of a functional overload and/or a toxic environment. Therefore, to confirm our observations from the scRNA-seq data, we reproduced, *in vitro*, stressful conditions to determine whether CD81 would be upregulated or not. First, we assessed, by flow cytometry and by WB on sorted cells, that CD81 is heterogeneously expressed also in a Min6 insulinoma cells (Figure 36a and b). Next, we performed flow cytometry time-response experiment by treating Min6 with the designated doses of glucose and palmitate (to reproduce a gluco-lipotoxic environment, Glu-Pal) or tunicamycin (potent inducer of ER-stress, Tun). With glucose and palmitate, we observed a time dependent increase of CD81 positive cells. With tunicamycin treatment after only one day, we observed a reduction of the CD81 positive cells, due to the massive death induced by the drug (Figure 36c). We performed a stress assay on both Min6 cells (4 days Glu-Pal and 2 days for Tun) and on primary material (islets of Langerhans) (2 days for both treatments). In this experiment, we treated cells with a combination of high glucose (additional 10mM) and fatty acid (0.4mM Palmitate) and analyzed by flow cytometry if the expression of CD81 on the plasma membrane was increased after the treatment. In both Min6 and primary β-cells, we observed a significant increase of CD81 positive cells after Glucose and Palmitate treatment. On the other hand, we did not observe any significant difference in number of CD81 positive cells after Tunicamycin (5µg/ml) treatment (Figure 36d, e and f). However, as it is possible to observe on the histogram and on the counter plots (Figure 36d and f) the surviving cells after Tunicamycin treatment had higher intensity levels of CD81 staining. We speculated that these cells expressed higher number of CD81 on the plasma membrane due to the ER-stress generated from the compound. In conclusion, we report CD81 as dedifferentiation and stress marker for pancreatic β-cells due to its upregulation both *in vivo* and *in vitro*, following the establishment of diabetic conditions.

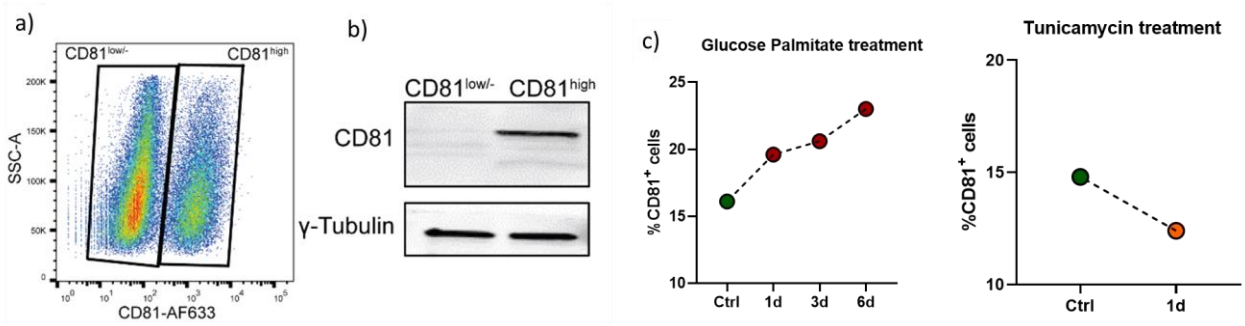

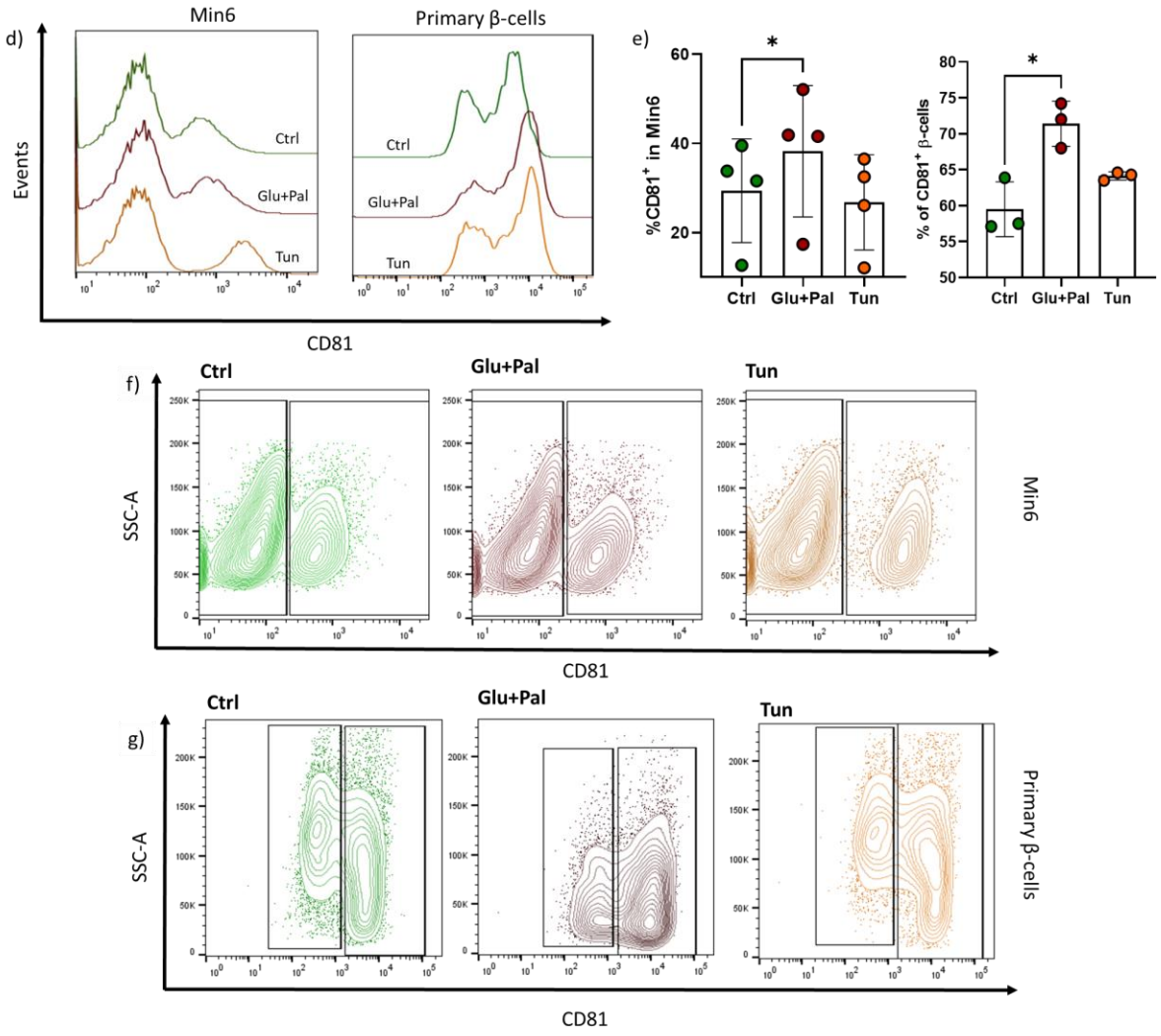


**Figure 36:** ***In vitro*** **stress assay induces CD81 upregulation in β-cells**

**a**) FACS dot plot representing two clear and distinct Min6 populations after CD81 staining; **b**) Western blot image from sorted $CD81^{high}$ and $CD81^{low/-}$ Min6 cells, showing CD81 levels and γ-tubulin as loading control (15µg protein/lane); **c**) and **d**) Plot representing flow cytometry analysis of Min6 stained for CD81 in a time-response experiment after treatment with glucose and palmitate or tunicamycin (n=1); **e**) Representative stacked histograms from stress assay on Min6 or primary β-cells; Y-axis represents the counts of cells normalized to the mode; X-axis is the intensity levels of CD81; **e**) Bar plot with the quantification of the %of CD81 positive cells in the experiments on Min6 or primary β-cells (n=4 and n=3, *P < 0.05, **P < 0.01; t test); **f**) and **g**) Representative counter plots from flow cytometry analysis of Min6 and primary β-cells stained for CD81 and in different treatment conditions. (Salinno et al., 2021)

### 4.2.5 CD81 expression in healthy and stressed human β-cells

We translated our findings from rodents to human. We tested if the pattern of expression in development and in stress conditions was similar also in human endocrine cells.

To begin, we evaluated the expression levels of CD81 in human iPSCs differentiation thus we re-analyzed the scRNAseq from Veres and colleagues (Veres et al., 2019). We observed that CD81 was expressed in all the subgroups, from the early progenitors to the late endocrine cells (Figure 37a). Interestingly, we noticed that CD81 mRNA levels were higher in the endocrine cells compared to the progenitors, pattern resembling what we observed also in mouse embryonic development. IF of *in vitro* differentiated endocrine cells indicated the expression of CD81 protein in SC-β- and SC-α cells (Figure 37b). We further investigated CD81 expression in adult, healthy, human islets, by reanalyzing the scRNA-seq from Baron and colleagues (Baron et al., 2016). In contrast to what we observed in mouse, in human islets all endocrine populations were heterogeneous for CD81 and adult β-cells retained a great percentage of $CD81^{high}$ cells (Figure 37c). This major difference between mouse and human led us to focus on β-cells only. Thus, we performed the DGEA between $CD81^{high}$ and $CD81^{low/-}$ and used the differentially regulated genes to compute the GO-enrichment pathway analysis. Interestingly, we discovered that $CD81^{high}$ β-cells exhibited terms related to exocytosis, insulin secretion and glucose homeostasis. In contrast, the $CD81^{low/-}$ population presented terms related to metabolism, ribosome biogenesis, positive regulation of gene expression and regulation of primary metabolic processes (Figure 37d). Very surprisingly, both β-cell populations were associated to ER-stress terms. If the $CD81^{high}$ group was enriched with genes related to ATF6, IRE1 and ERAD pathways, the $CD81^{low/-}$ group instead was defined by PERK signaling pathway. Furthermore, we discovered that the $CD81^{low/-}$ population was enriched in genes related to proteasomal protein catabolic process, mitochondrial respiratory chain complex assembly and cell redox homeostasis. These data resembled the recently reported discovery of different β-cell status in physiological conditions, based on insulin secretion and unfolded protein response (UPR). Xin and colleagues (Xin et al., 2018) performed a pseudo-time ordering of β-cell transcriptional profiles which revealed that these cells undergo, at different times, phases of low and high insulin biosynthesis. These phases are associated with different levels of unfolded protein response (UPR). On one hand, they observed a state of high insulin biogenesis and low UPR activity ($INS^{high}/UPR^{low}$), on the other hand they found a state of low insulin biogenesis and high UPR activity ($INS^{low}/UPR^{high}$). We compared the expression profiles of our $CD81^{high}$ and $CD81^{low/-}$ β-cells with the profile of the differentially expressed genes between $INS^{low}/UPR^{high}$ and $INS^{high}/UPR^{low}$ β-cells and observed a higher similarity with the $CD81^{low/-}$ group (342 vs 106 genes), pointing out that these cells possessed reduced insulin biosynthesis and enhanced UPR, contrarily to the $CD81^{high}$ (Figure 37e).

To test if we could reproduce this phenotype, we performed *in vitro* stress assay on human β-cell line, (EndoC-βH1) by supplementing the culture medium with either tunicamycin or glucose and palmitate. IF staining for CD81, on control and treated EndoCs, showed a significant increase of the CD81 fluorescent intensity levels, in treated conditions (Figure 37f and 37g), confirming our hypothesis that CD81 is upregulated also in human β-cells under stress conditions.

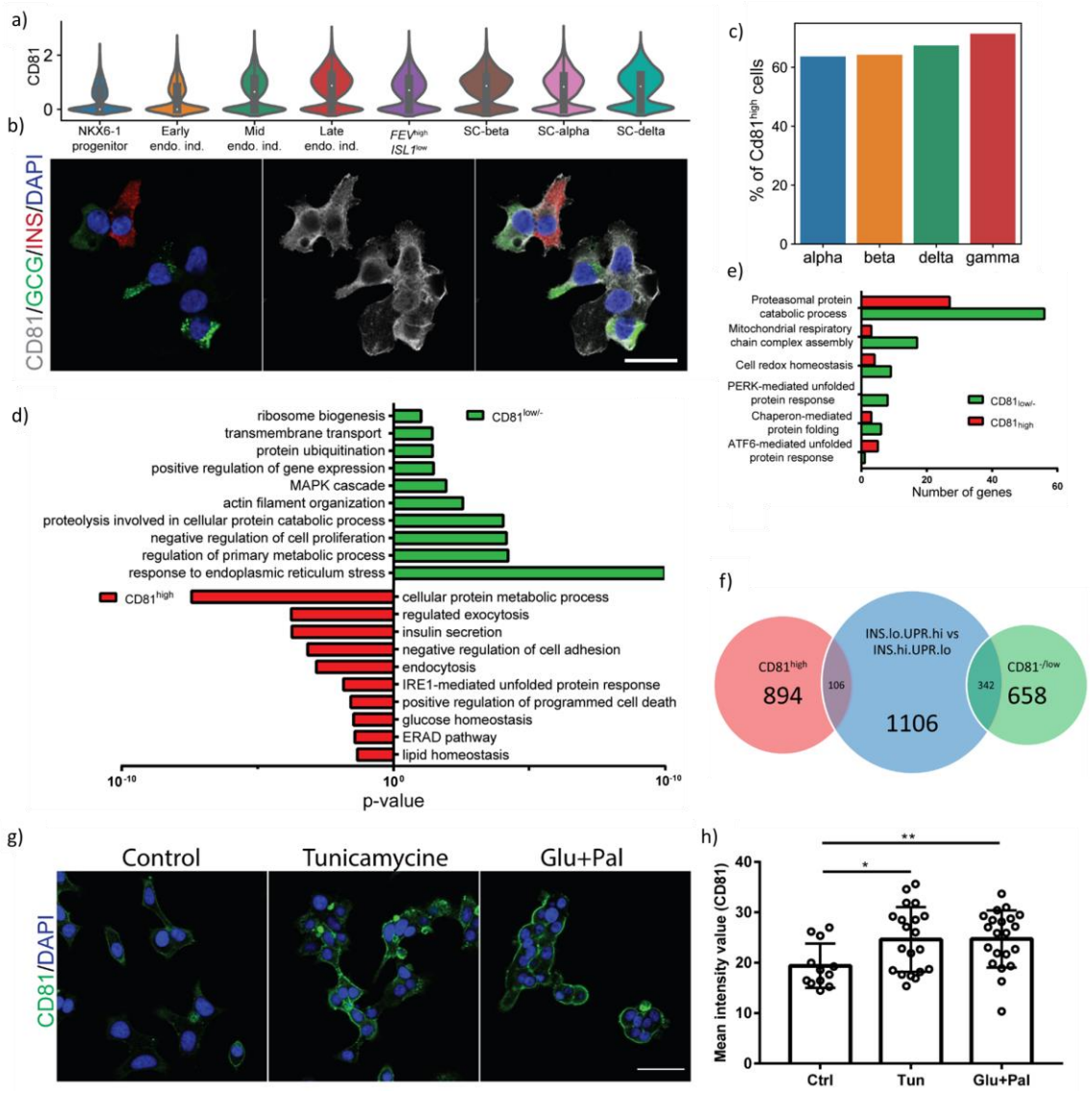


**Figure 37: CD81 in SC-β-cells and human β-cells**

**a**) Violin plots showing CD81 expression during *in vitro* differentiation of iPSCs into endocrine lineages; **b**) IF staining of stage (S) 6 of human iPSCs differentiation; CD81 (white), GCG (green), INS (red) and DAPI (blue), scale bar 20 µm; **c**) Bar plot from human healthy adult scRNA-seq, indicating the percentage of $CD81^{high}$ cells in the four main endocrine populations; **d**) Human $CD81^{high}$ and $CD81^{low/-}$ β-cells differentially regulated genes were used to

compute the GO-terms enrichment analysis shown in this figure; **e**) Targeted pathway analysis differentially regulated between the two CD81-β-cell populations; **f**) Venn diagram indicating the comparison between DE gene from human $CD81^{high}$ and $CD81^{low/-}$ β-cells with differentially expressed genes from the β-cell cluster with low insulin levels and high UPR signaling pathway (INSlow/UPRhigh) vs high insulin levels and low UPR signaling pathway (INShigh/UPRlow), as described in Xin et al 2018; **g**) IF staining for CD81 (green) and DAPI (blue) in control and Tunicamycin (5µg/µl) or Glucose and Palmitate (30mM + 10mM) treated EndoC-βH1 cells, scale bar 40 µm; **h**) Quantification of the intensity signal of CD81 staining in EndoC-βH1 cells (2 independent experiments, *P < 0.05, **P < 0.01; t test). (Salinno et al., 2021)

Therefore, we hypothesized that high levels of CD81, in human β-cells, mark the physiological state in which β-cells are undergoing an intense metabolic state of insulin biosynthesis thus increasing the endogenous ER-stress.

### 4.2.6 CD81 inversely correlated with E-cad in Min6 cells

The next step will be to assess which pathways are associated with CD81 expression. We have collected evidences of an inverse correlation between CD81 and E-cad. We proved in IF staining on 2D Min6 culture (Figure 38a, b), CD81-sorted and re-aggregated 3D Min6 (Figure 38c, d), on WB (Figure 38e) and in adult scRNA-seq (Figure 38f) that E-cad has low expression levels in the CD81 positive cells. Considering that E-cad is involved in several different signaling pathway and CD81 is known to be involved in the transduction of extracellular signaling, it is necessary to generate a CD81 conditional knock out mouse line, to investigate the functionality of this tetraspanin in β-cells.

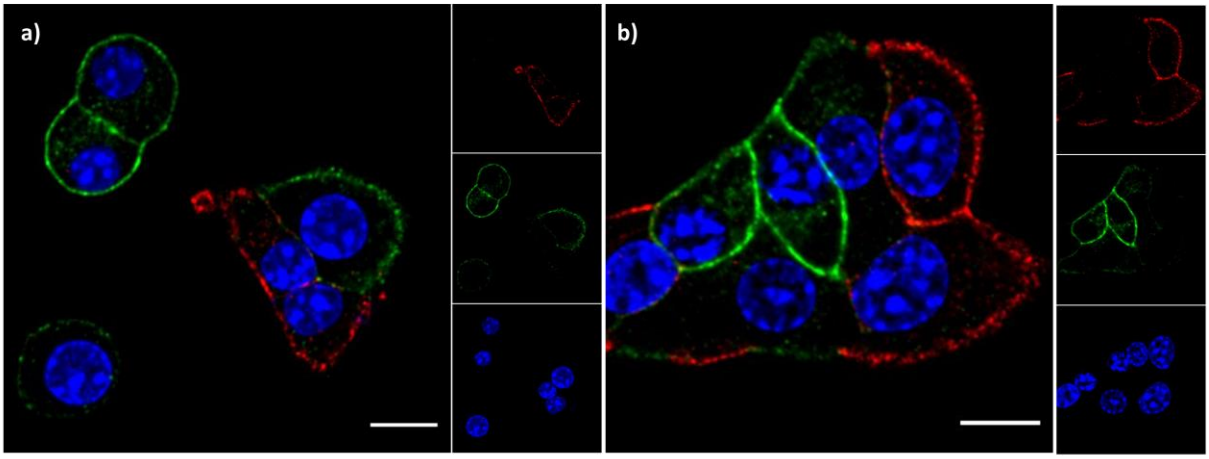

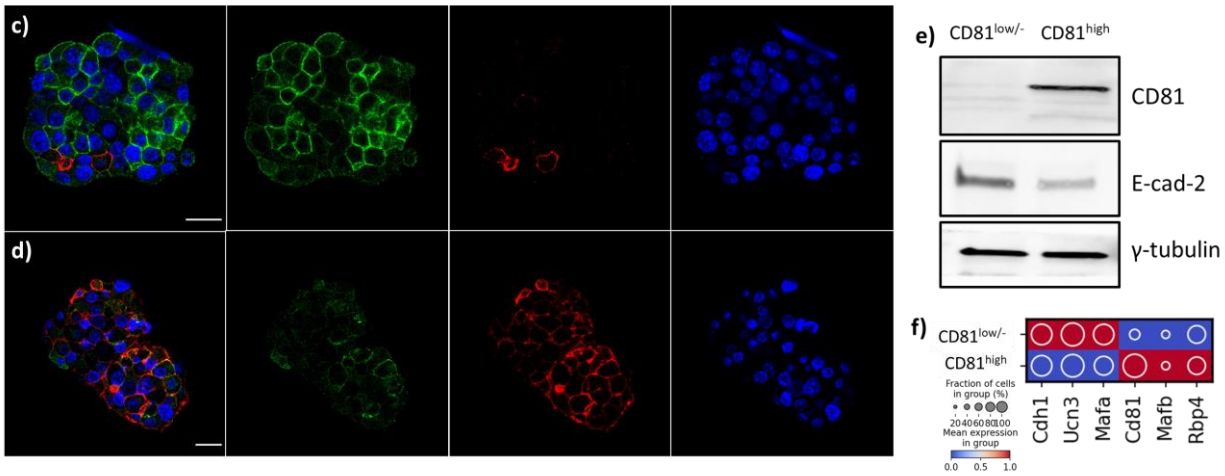


**Figure 38: CD81 is inversely correlated with E-cad in Min6 cells**

IF staining for CD81 (red), E-cad (green) and nuclei (DAPI- blue) of Min6 in **a-b)** 2D and **c-d**) on CD81-scorted and aggregated pseudo-islets; scale bars 10 and 20µm respectively; c) representative WB pictures of Min6 lysate after CD81-sorting, showing CD81 and E-cad, and gamma tubulin as loading control; **f)** Dot plot with normalized expression of several markers on CD81 split adult β-cells.

# 5 Discussion

DM is a worldwide spread disease. Projections for the next 25 years are estimating that by 2045 more than 700 million people will suffer from the disease (Nam Han Cho., 2019). Diabetes is caused by dysfunctional or lost β-cells, which determine low insulin secretion and high blood glucose levels. As of today, diabetes treatments are limited. Pharmacological treatments for insulin resistance and hyperglycemia, transplantation of pancreatic islets from cadaveric donors, gastric bypass and exogenous insulin injection are the available options on the market (Barnes, 2011; Khan et al., 2019). Unfortunately, these are only treating the symptoms and do not prevent the long-term secondary consequences of diabetes, thus urgent new treatment options are needed. One key feature of β-cells is their extensive heterogeneity both in healthy and diabetic conditions. Understanding the mechanisms of establishment of β-cell heterogeneity, in addition to clarify the root causes that alter the equilibrium among populations, could provide novel entry points to protect and regenerate β-cells.

In order to understand the mechanisms behind β-cell maturation and responsible for the establishment of the heterogeneity, we combined the Fltp lineage tracing mouse model with the scRNA-seq technology. While Fltp allowed to discriminate cells before, during and after Wnt/PCP acquisition, the scRNA-seq technology allowed to separate the different endocrine clusters and to profile rare populations at the transcriptional level. Fltp is increasingly expressed in all endocrine lineages throughout the postnatal stage but β-cells are the predominant population to acquire PCP during this period. Furthermore, β-cells belonging to different Fltp-subpopulations presented differences in movement capabilities and protrusion extension, hinting at changes in cytoskeleton dynamics after PCP acquisition. Lastly, Fltp lineage-positive β-cells displayed downregulated mTORC1 activity, hallmark of a mature β-cell phenotype. Altogether, we identified Wnt/PCP as pivotal signaling pathway for the establishment of the mature β-cell phenotype and we hypothesized that PCP acquisition could be the trigger for the metabolic changes observed during postnatal development.

Additionally, we identified and described CD81 as novel surface marker for immature and dedifferentiated β-cells. CD81 is highly expressed in all embryonic and the majority of postnatal β-cells and it becomes restricted to a subpopulation of β-cells in adulthood. Transcriptional analysis of postnatal β-cells with high ($CD81^{high}$) and low or negative expression levels ($CD81^{low/-}$) for *Cd81* revealed a global immature profile of the latter subpopulation. Furthermore, CD81 was re-expressed in dedifferentiated β-cells *in vivo* (STZ, db/db and NOD diabetic mouse models) and *in vitro* stress conditions. Lastly, CD81 was differentially expressed in human β-cells and upregulated *in vitro* stress conditions. Altogether, we proposed CD81 as a

novel surface marker to identify, follow and target immature and dedifferentiated β-cells in mouse and human islets.

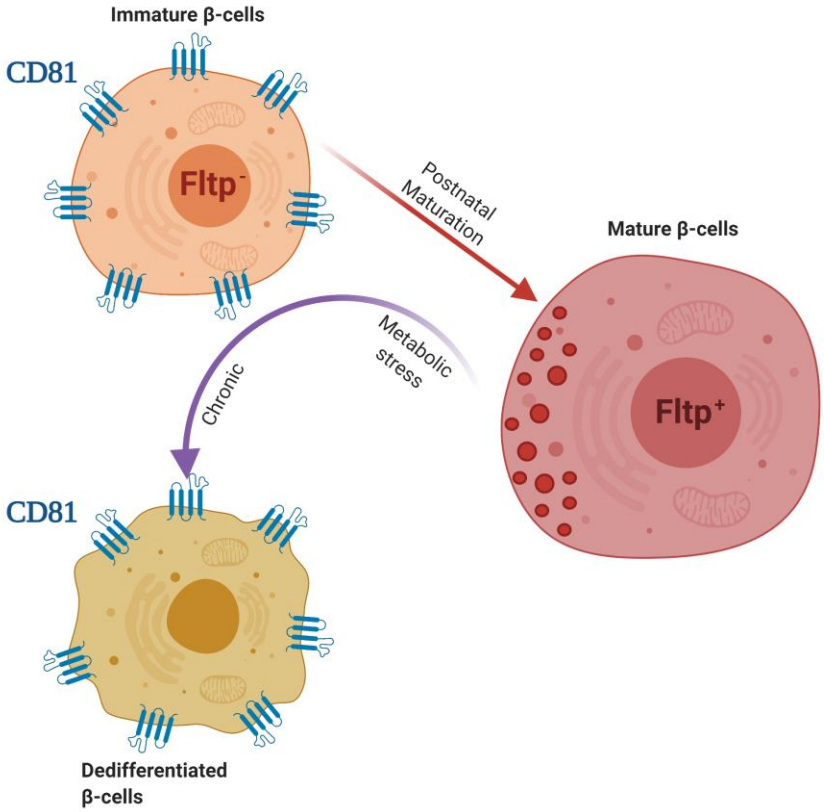


**Figure 39: β-cell maturation and dedifferentiation processes**

Simplified representation of the maturation and dedifferentiation processes according to Fltp and CD81. Immature β-cells ($CD81^+$ $Fltp^-$) undergo the postnatal maturation process, which leads to the mature phenotype ($CD81^-$ $Fltp^+$). Upon metabolic stress, mature β-cells undergo a reverse differentiation process, leading to an immature phenotype ($CD81^+$) and later dedifferentiation. Figure was created with BioRender.com.

## 5.1 CD81 as target for regenerative therapy

Prolonged periods of hyperglycemia determine changes in β-cell phenotype, slowly driving cells into dysfunction and lastly dedifferentiation. Similarly, the immunological attack of β-cells defines the loss of the majority of the β-cell mass. Specific markers for dysfunctional β-cells are essential to understand the mechanisms driving the disease progression and more importantly the possibility to pharmacologically target these cells, in order to either protect or regenerate β-cells.

To the best of our knowledge, no specific surface marker was described in the context of diseased β-cells. In this dissertation, we presented CD81 as a novel immaturity marker for pancreatic β-cells. CD81 (cluster of differentiation 81, also known as Tspan-28/TAPA1) belongs to the tetraspanins family, it is a transmembrane protein of typical structure, with four transmembrane domains, a small (SED) and a large (LED) extracellular loop and short carboxyl and amino cytoplasmic termini (Termini & Gillette, 2017). The biological role of tetraspanins is complex to summarize since the specific cell type of interest heavily affects it. In brief, several studies have described these proteins as important for the functionality of the immune system (Jones et al., 2011), viral pathogenesis (Hantak et al., 2018) and cancer, particularly involved in promoting or inhibiting the metastatic process by regulating the motility of these cells (Hemler, 2014). Tetraspanins have been also described as signal transductors from the outside to the inside of cells. Thus, the C-terminus of these proteins interacts with several kinases, among which PKC, PI4K and GTPases, which amplify the signal received at the surface (Termini & Gillette, 2017).

### 5.1.1 Relevance of CD81 for β-cell biology

CD81 was never described in the context of the islet of Langerhans, thus we reported CD81 expression in all pancreatic endocrine lineages and differentially expressed in a subpopulation of adult β-cells (Salinno et al., 2021). The identification of CD81 added another element to the broad set of markers used to dissect β-cell heterogeneity. However, our marker differed from many others for two important reasons, the localization on the plasma membrane and the specificity for immature cells. In fact, the majority of the markers routinely used are either cytoplasmic or nuclear (Salinno et al., 2019) and only a handful are surface markers, as CD9 and ST8SIA1, which together distinguished four β-cell subpopulations but only in humans (Dorrell et al., 2016b). Surface markers for immature and dedifferentiated β-cells are essential to develop novel pharmacological treatments to target these cells. In addition, the most common markers are usually related to mature β-cells. In example, MafA (C. Zhang et al., 2005), Ucn3 (Blum et al., 2012), Syt4 (C. Huang et al., 2018) and Fltp (Bader et al., 2016) are upregulated during the postnatal stage and their onset correlates with the acquisition of an adult and mature phenotype. The other known immaturity markers are MafB (Isabella Artner et al., 2007) and Rbp4 (Segerstolpe et al., 2016) which follow the same dynamic of downregulation of CD81, but are more difficult to use due to their intracellular localization. A fraction of immature β-cells remains in adult islets. The concept of immaturity is often related to higher proliferative capacity (Puri et al., 2018). One important consideration comes from the observation that in adult mouse islets around 30% of β-cells retained CD81, while it is broadly accepted that only 2% of β-cells are actively entering the cell cycle (Brennand & Melton, 2009). Therefore, we can speculate that not every immature β-cells are proliferating, but they might retain the capacity to re-enter the cell cycle, which could possibly

become a pharmacological target to prompt this specific subpopulation of cells to proliferate to restore the β-cell mass lost in diabetic conditions.

### 5.1.2 CD81 possible mechanism of action

As mentioned before, CD81 is expressed in several tissues. A recent study has identified a CD81 positive population as adipocyte progenitors. Surprisingly, CD81 plays a crucial role in the process of *de novo* biogenesis of beige fat upon cold exposure. In addition, it was found to be interacting with $\alpha_V/\beta_1$ and $\alpha_V/\beta_5$ integrins, mediating focal adhesion kinase (FAK) signaling necessary for the proliferation of these adipocytes subpopulation (Oguri et al., 2020). Interestingly, we observed *Cd81* expression levels increased during endocrinogenesis, suggesting a potential role during lineage allocation and fate decision. A similar connection was observed between pancreatic progenitors and extracellular matrix, via integrin α5-F-actin-YAP1-Notch axis, which promotes the formation of ductal cells (Mamidi et al., 2018). Other studies in liver have shown a possible mechanism of action. Once CD81 is engaged, SYK kinase phosphorylates several substrate, most prominently ezrin (Ezr), which undergoes a cytoplasmic redistribution, forming a cap-structure together with F-actin, which is stabilized under the plasma membrane (Coffey et al., 2009). Additionally, on T cells and NK cells, CD81 was connected with similar cytoskeleton rearrangements (Crotta et al., 2006). Subsequent studies have identified that the specific phosphorylation of ezrin on the threonine 567 (p-Ezrin$^{Thr567}$) mediates the downregulation of Hippo pathways and enhancing YAP and β-catenin signaling pathways in hepatocytes (Xue et al., 2020). These studies, despite not being on islets, could be translated to the endocrine setting. The role of the cytoskeleton dynamic has been under the spotlight in recent works. As previously discussed, by supplementing actin depolymerization compounds, it is possible to improve the SC-β-cells functionality (Hogrebe et al., 2020b). Similarly, inhibition of ROCKII in SC-β-cells, likely by inhibiting the actin polymerization mechanisms, improves the mature phenotype of these cells (Ghazizadeh et al., 2017). Here we could hypothesize that immature β-cells, by expressing CD81, have more stabilized actin filaments, which leads to a less secretory phenotype. Contrary, once β-cells downregulate CD81, actin filaments might depolymerize, with the consequence of the acquisition of a mature phenotype. In addition, we have also presented the inverse correlation, in Min6, between CD81 and E-cad, other fundamental player in the actin cytoskeleton dynamics. It was reported that E-cad is heterogeneously expressed in β-cells, and actin depolymerization can induce an increase of E-cad on the plasma membrane (Bosco et al., 2007). In conclusion, *adherent* junctions (cadherin and catenin complex) are crucial components for establishing cell-cell adhesion and tissue architecture, by establishing a direct connection with actin filaments (Mège & Ishiyama, 2017). Our data suggests a potential role of CD81 in modulating β-cell cytoskeleton dynamics (Figure 39) and future studies should aim to elucidate this hypothesis by interfering with CD81 expression in cell lines and animal models and test the effect on cell-cell adhesion and its interconnected actin cytoskeleton.

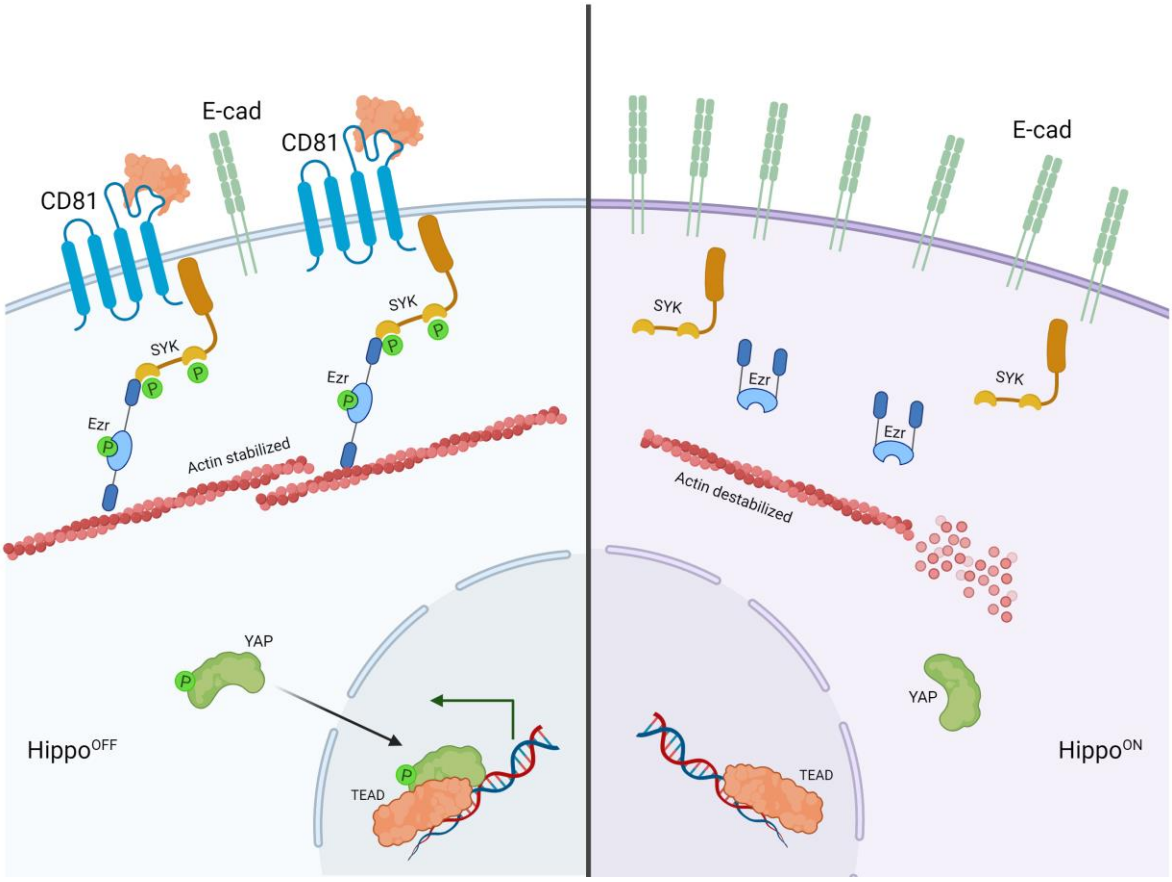


**Figure 40: Possible mechanism of action of CD81 in endocrine cells**

Schematic representation of CD81 possible mechanism of action. Once abundant on the plasma membrane, it might activate the SYK-Ezr axis, promoting acting stabilization. In absence of CD81, we speculate the possibility of destabilized actin filaments with subsequent E-cad expression upregulation. Figure was created with BioRender.com.

### 5.1.3 The islets of Langerhans require immature β-cells

In rodents, only a small subpopulation of adult β-cells expresses CD81. Our finding is in line with what has been described in literature using different approaches and methodologies. For example, according to Fltp separation scheme, in adult islets around 20% of β-cells remain negative for the reporter and present immature phenotypical features (Bader et al., 2016). Similarly, Ucn3 lineage negative β-cells were identified at the edge of the islets and have been renamed as "virgin" β-cells, following the hypothesis that these do not derive from cycling β-cells (van der Meulen et al., 2017). Therefore, the existence of immature β-cells has been confirmed multiple times and a recent study has shown that these cells are maintained in an immature state via regulation of two transcription factors, MafA and Pdx1, and that their presence is necessary for the physiological functionality of the islets (Nasteska et al., 2021). Future studies need to

address the question of whether CD81 is involved in the maintenance of the immature phenotype, and if that is the case how it contributes to it and eventually whether CD81 could be used to manipulate the state of these immature population.

Contrary to what described in rodents, CD81 is heterogeneously expressed in all adult human endocrine cells. We can hypothesize that one of the reasons for this major difference is determined by the islet architecture (Roscioni et al., 2016). Human islets have α and β cells intermingled, without the typical shell-core structure observed in mice (Cabrera et al., 2006). Here we speculate that the topographical localization of β-cells might determine CD81 expression. In fact, in mouse islets we noticed that CD81-expressing β-cells often localized at the periphery of the islet, suggesting that the interaction with other endocrine cell types, endothelial cells or ECM might lead to the expression of the protein. Similarly, in human islets, it is possible that the more frequent contacts with non-β-cells can influence CD81 expression. Nevertheless, whether the neighbors of these cells are the cause or the effect of the immature phenotype need to be further investigated.

### 5.1.4 Immaturity vs Dedifferentiation

In our work, we showed that CD81 is re-expressed upon metabolic stress. It is likely that these cells are undergoing a reverse developmental trajectory, which leads to the expression of immature and embryonic markers. However, CD81 is not a disallowed gene but an immaturity marker expressed in diabetic conditions. With our marker, we elucidated the differences between immature and dedifferentiated β-cells (Figure 41). With the term immature β-cells, we indicate insulin-producing cells, at the embryonic and neonatal stages and less frequently in adulthood. These cells are fully committed to the β-cell fate but have high basal insulin secretion due to the lack of fine-tuned mechanisms of insulin granules fusion and release, and have a glycolytic type of metabolism due to the high fat (milk-based) diet. These cells are usually recognizable by the lack of maturity markers, as Ucn3, MafA, Flattop or Glut2. Few markers can be directly attributed to these cells, like the residues of embryonic hormones as gastrin and cholecystokinin, the transcription marker MafB, downregulated after birth and the retinol binding protein Rbp4. Our work demonstrated that the tetraspanin CD81 is highly expressed in immature pancreatic β-cells. Its expression is downregulated in the postnatal stage and in adulthood, only a small subpopulation retained this protein. Dedifferentiated β-cells are cells that underwent a revers trajectory of development, thus, adult β-cells under stress conditions derived from chronic gluco- and lipo- toxicity, excessive ER-stress, or by the immunological attack towards the islets. Under these conditions, β-cells become dysfunctional from a metabolic and, consequently, functional perspective, followed by dysregulation of the transcriptional β-cell program, which determines the re-expression of embryonic/neonatal markers and later genes, usually not

present in β-cells, known as disallowed genes (Lemaire et al., 2016). Several studies have explored dedifferentiated β-cells and the most prominent marker for these cells is the aldehyde dehydrogenase 1 family member A3 (Aldh1a3) (Kim-Muller et al., 2016). Other known markers are AldoB (Gerst et al., 2018) and Ldha (Ainscow et al., 2000), enzymes reflecting the metabolic dysfunction of these cells, with impaired mitochondrial function and oxidative phosphorylation. Therefore, dedifferentiated β-cells share several characteristics with immature β-cells. The overlap ends when disallowed genes and dysfunctional metabolic processes appear in these cells. However, as demonstrated in a recent work from our lab, these cells can be forced to undergo a new "differentiation" trajectory, via pharmacological treatment, in order to reestablish a mature and healthy phenotype (Sachs et al., 2020). This leaves hope for future diabetes treatments, once the source of metabolic stress is removed, β-cells functionality and/or mass can be restored. In addition, a recent study has developed a sorting strategy to identify β-cells with two surface markers (low CD24 and high CD71) (Berthault et al., 2020). We can speculate that by using panel of antibodies against surface markers, it could be possible to isolate different β-cells subpopulations without the need of fluorescent reporters. In conclusion, the discovery of novel surface markers targeting immature and dedifferentiated β-cells is crucial to prevent, protect and treat the islets in diabetic conditions.

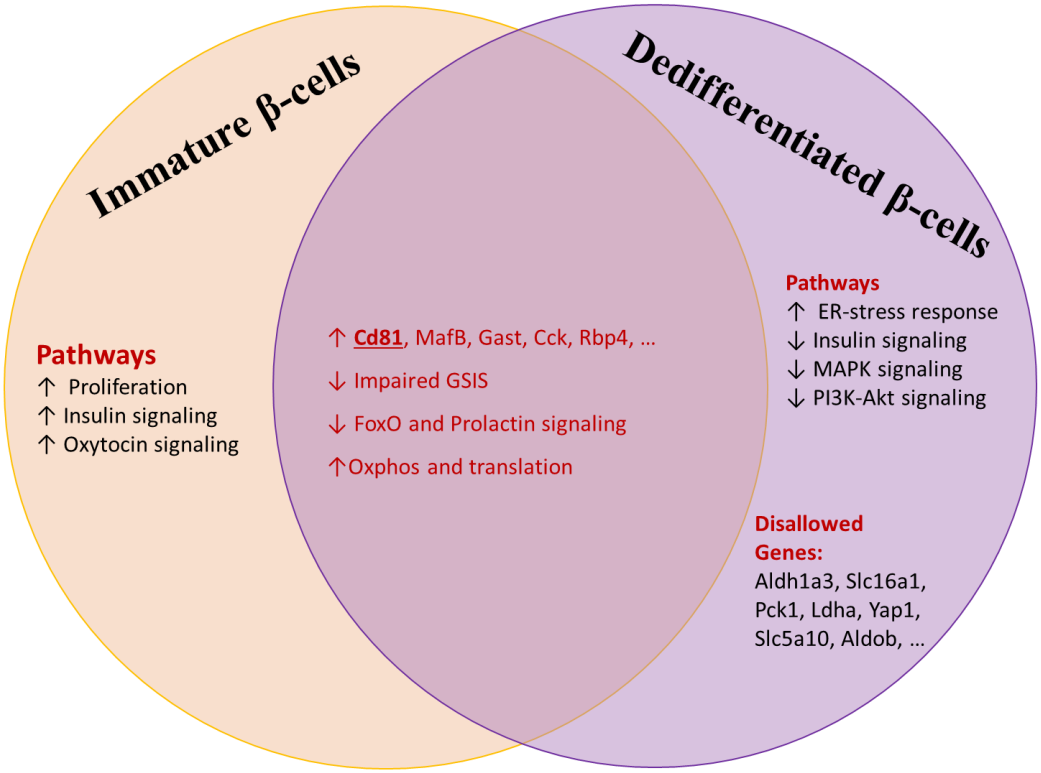


**Figure 41: Comparison between immature and dedifferentiated β-cells**

Venn diagram representing unique and shared feature between immature (orange) and dedifferentiated (purple) β-cells.

### 5.1.5 CD81 as possible entry point for regenerative therapies

In rodents CD81 is directly connected with an immature β-cell transcriptional profile and correlates with the establishment of diabetic conditions. However, in human islets the situation is different starting with the presence of a higher degree of heterogeneity in all endocrine lineages of the islets. In addition, our data in adult human β-cells does not directly correlate with an immature profile but with higher levels of ER-stress. A recent study on human β-cells have identified transient states of ER-stress and insulin biogenesis in adult healthy islets. Briefly, β-cells can be found in one of these three states: 1) low UPR and high insulin gene expression, 2) high UPR and low insulin gene expression or 3) low UPR and low insulin gene expression. The first state relates to cells that upon higher demands upregulate insulin production. Consequently, these cells have higher rate of unfolded proteins, which in time determines high levels of ER-stress. In response to this status, cells undergo a transition to the second state, in which insulin gene expression is suppressed and mechanisms of ER-stress compensation (UPR) are put in place. Once the intracellular stress is resolved (3), β-cells downregulate the stress-response mechanisms and enter a quiescent phase with low insulin expression (Xin et al., 2018). Our data suggests that CD81 might be related to these transition states. β-cells with high levels of CD81 have a closer transcriptional profile with those under stress due to high insulin biogenesis and compensatory ER-stress mechanisms. Contrary, β-cells low or negative for CD81 are in an anabolic phase, recovering. We proved that upon exposure to stressors in EndoC cells expressed higher levels of CD81. Further studies need to address whether this relationship is maintained also in islets from diabetic donors and whether CD81 could be used to target these metabolically overloaded cells, restoring a healthy functional phenotype.

In conclusion, we hypothesized that CD81 could be a possible entry point for novel therapeutic approaches. By specifically targeting the cells re-expressing CD81, we speculate the possibility to force a re-differentiation process in β-cells, generating an improvement of the metabolic conditions.

## 5.2 Wnt/PCP connects metabolism and cytoskeleton dynamics

Diabetes is a heterogeneous disease, pathogenesis, symptoms, therapies and long-term consequences (Redondo et al., 2020). Nevertheless, all patients have one thing in common, dysfunctional or lost β-cells. The ideal therapeutic approach would need to either replace or replenish β-cells. Replacement therapies could be achieved by using stem cell (iPSCs or hESC) derived β-cells (de Klerk & Hebrok, 2021). Alternatively, pharmacological treatments could aim at replenishing the β-cell mass by boosting the proliferation (Oakie & Nostro, 2021; Rathwa et al., 2020), followed by drugs inducing a phenotypical maturation of these cells (Sachs et al., 2020). In both cases, our knowledge of the β-cell maturation phenomenon remains incomplete and further studies are necessary to elucidate the mechanisms driving the maturation process.

### 5.2.1 Wnt/PCP role in endocrine maturation

Part of this dissertation focused on exploring mechanisms behind the postnatal β-cell maturation process, with an accent on the role of Wnt/PCP in mouse islets. Non-canonical Wnt signaling remains elusive in the context of the islets of Langerhans. The first evidence of a possible role of PCP arised from loss-of-function studies on Celsr2 and Celsr3, two PCP core components. It was reported that PCP is required during the embryonic development for the endocrine differentiation process, with a particular impact on β-cells (Cortijo et al., 2012). Afterwards, in our laboratory, a FoxA2 target gene, Flattop, was discovered to be transcriptionally activated in mono- and multi-ciliated tissues during PCP acquisition and acted by modulating cytoskeleton dynamics (Gegg et al., 2014). Last, it was demonstrated that Fltp is heterogeneously expressed in pancreatic islets. Comparison of β-cells positive and negative for the Flattop reporter indicated that those which acquired PCP and are positive for Flattop, possessed a mature phenotype, characterized by higher expression of MafA and Glut2, improved GSIS and oxphos-based metabolism. The cells that are negative for the marker appeared less mature and with a more pronounced proliferative capacity. Therefore, for the first time, the acquisition of PCP was directly connected with the mature β-cell phenotype (Bader et al., 2016). We continued the work previously conducted in our laboratory using the Fltp lineage tracing mouse line (FltpiCre$^{mTmG}$), and quantified Fltp expressing cells via flow cytometry, revealing that PCP, in the majority of endocrine cells, is acquired after birth. In addition, we observed that during the postnatal stage, β-cells are the major cell population undergoing the transition, which could explain the reason why in adult islets 80% of β-cells are Flattop positive, while the other endocrine cell types are barely 50% positive (Bader et al., 2016). To decipher the molecular mechanisms behind the PCP acquisition, we performed scRNA-seq of postnatal islets from the Fltp lineage tracing mouse line. The transcriptional profiles of the three Fltp-sorted β-cell populations revealed differences in

pathways enrichment and cellular components. Of relevance, we showed that the Fltp lineage negative population was enriched in terms related to Wnt, cell cycle, amino acids transport, translation and ROS detoxification. The Fltp lineage positive population, instead, presented terms related to the UPR, regulation of insulin secretion, several cell adhesion components, PI3K-Akt signaling pathway, autophagy, iron metabolism and mitochondria organization. Finally, the population in transition for Fltp was enriched for ER-stress response pathways, VEGF signaling, non-canonical Wnt signaling pathway and a vast array of cell adhesion molecules and fiber organization components. Our data are of relevance in the understanding of the transition from an immature to a mature phenotype. In example, the immature Fltp lineage-negative population possessed proliferative capacity, amino acid metabolism and high translation activity. Thus, we speculated that driven by canonical Wnt signaling, these cells are still capable of entering the cell cycle (Puri et al., 2018) thus maintained in an immature state. In addition, the enrichment for the amino acid metabolism terms supports the recent evidences that immature β-cells possess high mTORC1 activity due to a high amino acids nutritional environment (Helman et al., 2020b). And lastly, these cells are intensively engaged in translational activities, thus engaged in an immature anabolic state (Brouwers et al., 2021). The two Fltp-positive lineages instead presented terms related insulin secretion to ER-stress coping mechanism. This is not a surprise, considering that mature β-cells are producing great amounts of insulin, which need to be processed in the ER. This is a high-risk misfolding process, thus mature β-cells activate mechanisms to degrade misfolded proteins and avoid accumulation of toxic intermediates (M. K. Kim et al., 2012; Volchuk & Ron, 2010). Another interesting term associated with the Fltp-lineage positive β-cells was the iron metabolism term. A recent studied has proved that CD71, the transferrin receptor, is expressed at high levels during the first weeks postnatal thus playing an important role in the adult β-cell metabolism (Berthault et al., 2020). Finally, we also observed several different types of adhesion molecules being differentially regulated in the three Fltp subpopulation. In-depth analysis of these molecular differences could offer insights to understand the polarization of β-cells within the islets and revel possible pharmacological targets for regenerative purposes.

These summarized data here are in line with the current literature that broadly described the postnatal period as central for the acquisition of the mature β-cell phenotype (Helman et al., 2020b; Jaafar et al., 2019; Salinno et al., 2019). However, understanding the role of PCP is further complicated by the lack of dependency from Wnt ligands (Ewen-Campen et al., 2020) and by the redundancy of this pathway (van Amerongen & Berns, 2006). For example, there are three Dishevelled paralogues (Dvl1, 2 and 3) (Mlodzik, 2016), three flamingo-related mouse Celsr paralogues (Celsr1, 2 and 3) (Formstone & Little, 2001) and two VANGL Planar Cell Polarity Protein paralogues (Vangl1 and 2) (Katoh, 2002). Considering the fundamental role of Wnt/PCP in several developmental processes (Dale et al., 2009), the system evolved to compensate the loss of one these genes. Therefore, future studies should address this topic by knocking

out multiple core PCP components in β-cells and at specific developmental stages. One possibility is to use stem cell differentiation, in combination with CRISPR-Cas9 (Ishibashi et al., 2020) and scRNA-seq (L. Yang et al., 2020). CRISPR technology would allow to knockout different non-canonical Wnt genes by using multiple guiding RNAs, while scRNA-seq would allow profiling cells with several different genotypes. This strategy could be applied at specific time-points, for example during endocrine induction or during the β-cell maturation phase, in order to understand the impact of this pathway on the processes.

### 5.2.2 Heterogeneity during β-cell postnatal maturation

Fltp association with the mature β-cell phenotype (Bader et al., 2016) resembled two known markers, Ucn3 (Blum et al., 2012) and MafA (Nishimura et al., 2015). Here we demonstrated that Fltp, Ucn3 and MafA followed the same dynamic of expression in postnatal β-cells. In addition, by analyzing the postnatal scRNA-seq we showed that at P16, the Fltp lineage negative β-cells possessed a transcriptional profile less mature compared to the two Fltp lineage positive populations. Thus, our data underlined the importance of PCP in the maturation process. Additionally, we observed an interesting phenomenon related to heterogeneity. It is well known and characterized that β-cells are a heterogeneous population, mixing mature and immature cells, and capable of dynamic changes based on the metabolic requirements of the body (Liu & Hebrok, 2017). However, up to date, no study has explored the heterogeneity in postnatal β-cells. Our data showed that in this period not all β-cells expressed Ucn3, MafA and Fltp at the same time. Why is that? We could speculate that despite sharing the same final destination, β-cells might follow different patterns to reach maturity. One hypothesis could be that external factors influence this process, in example, vasculature (In't Veld & Lammert, 2015), innervation (Ahrén, 2012; Alvarsson et al., 2020) or contact with other endocrine cells (Jain & Lammert, 2009; Meda, 2013). Furthermore, the three markers mentioned have different functions and this could be an additional explanation for non-synchronous expression. In fact, MafA is a transcription factor and its expression is crucial for the expression of β-cell function-related genes, as demonstrated by knockout studies (Nishimura et al., 2015). Deletion of Ucn3 (J. L. Huang et al., 2020b) and Fltp (Bader et al., 2016), contrary, did not lead to severe β-cell dysfunction, nor is maturation affected. Ucn3 might be upregulated when insulin secretion needs to be fine-tuned (Van Der Meulen et al., 2015), while Fltp, upon PCP acquisition, reports for changes in cytoskeleton dynamics, necessary to promote a mature phenotype (Bader et al., 2016). Therefore, understanding the dynamic of expression of these markers and translating these studies in humans is crucial to recapitulate the β-cell maturation process *in vitro*.

### 5.2.3 PCP regulates cytoskeleton dynamics in postnatal β-cells

Wnt/PCP signaling pathway is in charge of several developmental processes like gastrulation or the neural tube formation, by determining the tissue polarity and acting on cell movement (Davey & Moens, 2017; Gray et al., 2011). Therefore, most of the studies regarding PCP have been conducted during embryogenesis or in aberrant situations like in cancer, by promoting cell metastasis and malignancy (VanderVorst et al., 2018). In the context of the islets, little is known about PCP mechanism of action. In this dissertation, we reported two biological processes that potentially reflected PCP acquisition in the Fltp-lineage positive population: movement capability and ability of extending membrane protrusions, supported by differentially regulated genes in actin and tubulin components. Both observations can be directly linked to differences in cytoskeleton dynamics. In cancer, Wnt/PCP determines an asymmetric distribution of the PCP components, which impairs actin cytoskeletal dynamics, promoting oriented migration by generating cellular protrusions (VanderVorst et al., 2018). The similarities between the cancerous cells and our observations in endocrine cells are striking. In addition, two recent works support the hypothesis that in endocrine cells, PCP acts on cytoskeleton. The first reported the use of a non-canonical Wnt ligand (Wnt4) to prompt SC-β-cells developing a human-islet-like GSIS (Yoshihara et al., 2020). The second instead reported an improvement of the functionality of SC-β-cells after using latrunculin A, a compound inducing F-actin network depolymerization (Hogrebe et al., 2020a). Therefore, our data in combination with recent studies from other groups might dictate a novel idea that upon PCP acquisition, immature β-cells undergo a cytoskeleton rearrangement that promotes the acquisition of a mature phenotype. More questions need to be answered. How does PCP determine phenotypical changes by acting on the cytoskeleton? What are the transcriptional and post-translational changes occurring during PCP acquisition?

### 5.2.4 Wnt promotes changes in β-cell metabolic pathways

In the past years, several studies have demonstrated the importance of deciphering the metabolic pathways behind β-cell function and dysfunction (Da Silva Xavier & Rutter, 2020). On this line, β-cells are heterogeneous and adapt the metabolic processes based on the available nutrients, both during development and in diabetic conditions.

We performed experiments to discover possible interaction partners of Fltp and among the most interesting hits, we found members of the mTOR family (Raptor and Rheb). We further investigated this potential interaction and we unveiled a difference in mTORC1 activity, downregulated in the Fltp positive population. Our data fits well with the recent literature, which explored the metabolic maturation of β-cells. A first study reported important metabolic changes, improving insulin secretion, upon weaning upon transition from fat rich milk to high carbohydrates chow (Stolovich-Rain et al., 2015). A second study

explored the mechanisms associated with changes in diet composition. In particular, it was revealed that β-cells underwent a transition from mTORC1 to AMPK basal activity, in response to nutritional changes (Jaafar et al., 2019). Finally, another study connected *in utero* high availability of amino acids with the constitutive activation of mTORC1 at birth. The subsequent changes in nutritional environment triggered an intermittent mTORC1 activity in response to glucose and amino acids, coinciding with the acquisition of a fine-tuned insulin secretion (Helman et al., 2020a). Therefore, our data is in line with the state of the art, since the Fltp negative and transient populations possessed a higher mTORC1 activity, due to the lack of a fully mature type of metabolism. However, how does Wnt signaling connect with metabolism?

An elegant study reported the molecular interconnection between Wnt signaling and the metabolic pathways mTOR and AMPK (Inoki et al., 2006). The central player in this mechanism is the tumor suppressor protein TSC2, capable of inhibiting mTOR activity via negative regulation of Rheb (otherwise Wnt directly stimulates mTORC1 activity via TSC1/2 complex and GSK3 inhibition). TSC2 is phosphorylated, among others, by two crucial kinases, AMPK and GSK3. Reduced nutrients availability enhances AMPK activity, while canonical Wnt signaling negatively regulates GSK3. Thus, low energy conditions and inactive canonical Wnt signaling pathway are required to phosphorylate and promote TSC2 inhibitory action on Rheb, leading to mTORC1 activity downregulation (Inoki et al., 2006). One possible TSC2 mechanism of action concerns its cellular localization. TSC2, in association with TSC1 and the β-catenin destruction complex (APC/Axin/GSK3) (Mak et al., 2005) is localized near the endomembrane, in case of nutritional deprivation and GSK3 activation, where it acts as Rheb inhibitor, thus mTOR negative regulator. Once the nutritional environment changes and GSK3 is inactivated, TSC2 is phosphorylated on other sites, leading to the dissociation from TSC1 and the endomembrane. Once in the cytoplasm, TSC2 is often found bound to Dsh (Dishevelled), important transducer of the Wnt signaling and negative regulator of GSK3 (Wilkinson et al., 2011). Some of these data are in resonance with data shown in this dissertation and with the recent discoveries regarding the metabolic transition in β-cells. Our data reported Fltp lineage positive cells, thus after PCP acquisition, with lower mTORC1 activity. In addition, we observed Dvl2 highly expressed in the Fltp transient population and a recent paper in gut confirmed the downregulation of canonical Wnt, in favor of Wnt/PCP, after Fltp expression (Böttcher et al., 2021). Altogether, our data might reveal a crucial role of Wnt in regulating the metabolic transition. Thus, in immature β-cells canonical Wnt promotes basal mTORC1 activity. Inhibition of canonical Wnt potentially induces loss of basal mTORC1 activity in favor of AMPK, which contributes to the negative regulation of mTORC1 under starvation conditions. In Figure 42, we depicted our hypothesis of how Wnt might prompt the metabolic switch as explained in this paragraph. Additionally, TSC2, GSK3 and Rheb are Fltp possible interaction partners, key players in the work presented before. Here we want to propose a provoking hypothesis: upon PCP acquisition, canonical Wnt is inhibited and changes in cytoskeleton dynamics (possibly via Rho GTPases)

promote the delocalization of the FLTP-TSC2-Rheb complex away from the endomembrane (lysosomes), downregulating mTORC1 basal activity and prompting a mature insulin secretory behavior.

These hypotheses need further studies to be confirmed. In addition, we strengthen the need to identify the PCP triggers in the context of the islets of Langerhans. Once clarified the potential targets that modulate PCP in β-cells, these could be used as novel drugs to be delivered in dedifferentiated β-cells in diabetic patients or to improve stem cell differentiation protocols, to produce mature SC-β-cells for transplantation purposes.

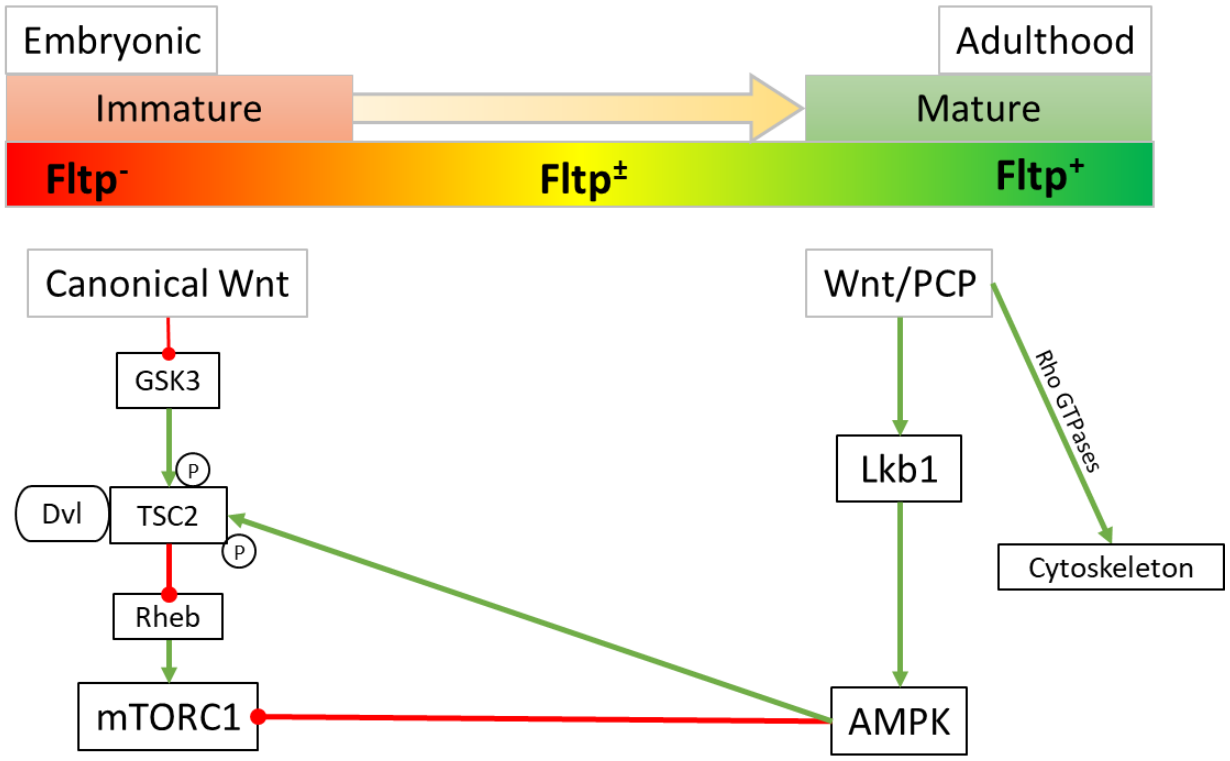


**Figure 42: Wnt transition precedes metabolic changes in β-cells**

Schematic representation of our working hypothesis. Immature β-cells are maintained in this state by canonical Wnt signaling, which promotes mTORC1 activity. Upon transition from canonical to non-canonical Wnt, direct or indirect factors promote the downregulation of basal mTORC1 in favor of AMPK activity. PCP acts on cytoskeleton by regulating Rho GTPases.

## 5.3 Conclusions

Diabetes remains a burden affecting millions of people worldwide. Understanding β-cell heterogeneity could provide novel entry points for β-cell protection and regeneration.

In this dissertation, we focused on two distinct heterogeneity markers. First, Fltp, previously associated with β-cell mature phenotype (Bader et al., 2016). Here, we aimed at elucidating the molecular mechanisms driving the acquisition of the mature β-cell phenotype. Combining single cell transcriptomic with Fltp lineage tracing mouse line, we showed how Wnt signaling pathway promotes the maturation process, possibly acting, during the postnatal development, upstream metabolic pathways (mTORC1-AMPK axis). Understanding the mechanisms of maturation is pivotal to develop pharmacological treatments to restore the molecular mechanisms disrupted in diabetes. Thus, targeting Wnt signaling in diabetes might offer alternative pharmacological approaches to restore β-cell functionality. Additionally, modulating Wnt signaling might allow generating SC-β-cells for transplantation purposes, with a metabolic and functional profile similar to those of human β-cells.

Second, we characterized CD81 in the context of the islets of Langerhans, providing a novel surface marker that labels immature and dedifferentiated β-cells (Salinno et al., 2021). Here, we demonstrated that CD81 expression, high in embryonic and postnatal stages β-cells, is progressively restricted to a minor population of β-cells in adult islets, which retains an immature transcriptional profile. Additionally, CD81 is re-expressed upon diabetic conditions, labelling dysfunctional β-cells. Surface markers for dedifferentiated β-cells, as CD81, are crucial to develop regenerative therapies. In fact, identifying specific targets expressed on dysfunctional β-cells would allow discriminating healthy cells from diseased cells. Ideally, CD81 could be an entry point for regenerative therapies, by using antibodies against CD81 and conjugated with other compounds to ameliorate and restore a healthy β-cell phenotype.

Altogether, this dissertation provides insights into β-cell maturation process and a potential target on dysfunctional β-cells for regenerative therapies.

# 6 Material and Methods

## 6.1 Materials

### 6.1.1 Equipment

| | |
|---|---|
| Agarose gel chamber | Midi 450 (Neolab) |
| Balances | ABS, EWB (Kern & Sohn GmbH) |
| Bioanalyzer | Agilent 2100 Bioanalyzer (Agilent) |
| Centrifuges | 5417R, 5430C, 5804 R (Eppendorf), Microcentrifuge (Roth), Micro 220 (Hettich), Universal 320R (Hettich), 6767 (Corning) |
| Cryostat | Ag Protect (Leica) |
| Developing machine | AGFA Curix 60 developing machine (AGFA HealthCare GmbH), ChemStudio SA2 Darkroom (Analytik Jena AG) |
| FACS | BD FACSAria III (Becton and Dickinson and Company) |
| Film cassettes | Hypercassette (Amersham) |
| Gel documentation system | UVsolo TS Imaging System (Biometra) |
| Incubation systems/ovens | Thermomixer comfort, Thermomixer 5436 (Eppendorf), Oven (Thermo Scientific) |
| Incubator | BBD6220 (Thermo Scientific), C16 (Labortect) |
| Microscopes | TCS SP5 (Leica) and Cube (heating), Brick ($CO_2$), M80 (Leica), Dissection light (Leica), LSM 800 with Airyscan (Zeiss) |
| Microwave | 700W (Severin) |
| $N_2$ tank | Biostore systems (Cryo Anlagenbau GmbH) |
| PCR machines | Personal Thermocycler, Professional Trio Thermocycler (Biometra) |
| pH meter | Mettler Toledo (Hanna Instruments) |
| Photometer | NanoDrop 2000c (Thermo Fisher Scientific) |
| Pipettes | 1000 µL / 100 µL / 10 µL Gilson (Gilson) |
| Pipettboy | Accu-jet® pro (Brand GmbH) |
| Polyacrylamid gel chamber | Mini Trans-Blot® Cell (Biorad) |
| Power supply (agarose gel) | Power Source 300V (VWR) |
| qPCR cycler | ViiA7 Real-time PCR system (Life Technologies) |

| | |
|---|---|
| Roller/Mixer | VSR 23 (VWR international), Shaker DOS-10L (Neolab), RMS (Assistent), Rocker 247 (Everlast) |
| Sterile hoods | MSC Advantage (Thermo Scientific) |
| Stirrer | D-6011 (Neolab) |
| Timer | Roth |
| Tissue Homogenizer | Ultra Turrax T25 (IKA) |
| Ultrasonic bath | Ultrasonic cleaner (VWR) |
| Vortexer | LSE Vortex Mixer (Corning), IKA Vortex |
| Water bath | Memmert |
| Western Blot semi-dry | Trans-Blot® SD, Semi-Dry Transfer cell (Biorad) |
| scRNA-seq machine | 10x Genomics' Chromium (10x Genomics) |

### 6.1.2 Consumables, ladder and serum

| | |
|---|---|
| 50mL/ 15mL tubes | Falkon, Fisher Scientific (Thermo Fisher Scientific) |
| 2mL/ 1.5mL / 0.2mL tubes | Safe-lock reaction tubes (Eppendorf) |
| 15cm/ 10cm/ 6cm dishes | Thermo Scientific Fisher |
| 6-well/ 12-well/ 48-well/ 96-well plates | Straight/conical (Thermo Fisher Scientific) |
| 10cm bacterial plates | BD Falcon™ Becton (Dickinson GmbH) |
| Embedding molds | Peel-a-way embedding molds (Leica) |
| Pasteur pipettes, plastic | Carl Roth GmbH & Co. KG |
| Blotting paper | Whatman paper (GE Healthcare Buchler GmbH & Co) |
| Cell strainer | Nylon cell stainer 70 µm (Falcon) |
| FACS tubes | 5 mL polystyrene round bottom tube with cell strainer cap (Falcon) |
| Films | Sigma-Aldrich |
| Glass slides | Thermo Scientific |
| Midori Green Direct | NIPPON Genetics Europe |
| Needles | Sterican 27G ½, Sterican 30G ½ |
| Parafilm | Pechiney Plastic Packaging |
| PVDF membrane | Biorad |

| | |
|---|---|
| Scalpels | Aesculap AG & Co |
| Spacer | Secure-Sela, 9mm 0.12 mm deep (Life Technologies) |
| Syringes | Omnifix 30 mL/3 mL (Braun) |
| Syringe filter | Filter unit fast flow and low binding 0.22 µm (Millex-GP) |
| TEM tubes | BEEM® capsules (Ted Pella, Inc.) |
| qPCR 96-well plates | MicroAmp Fast optcal 96-well reaction plate (Life Technologies) |
| Adhesive covers | Optical adhesive covers (Life Technologies) |
| Protein ladder | PageRuler Plus Pre-Stained (Life Technologies) |
| DNA ladder | DNA ladder 100 bp (NEB) |
| Donkey serum | Millipore |

### 6.1.3 Kits and Mixes

| | |
|---|---|
| Agilent RNA 6000 Pico kit | Agilent Technologies |
| Dynamo Color Flash SYBR Green qPCR kit | Life Technologies |
| Pierce ™ ECL Western Blotting Substrate<br>SuperSignal™ West Femto Chemiluminescent-Substrate | Thermo Fisher Scientific |
| Primers | Eurofins |
| miRNA Micro Kit | Qiagen |
| SuperScript Vilo cDNA synthesis kit | Life Technologies |
| TaqMan Fast Advanced Master Mix | Life Technologies |

### 6.1.4 Chemicals

| | |
|---|---|
| Acrylamide/bisacrylamide | eBioscience |
| Agarose | Rotiphorese |
| APS | Biozym Scientific |
| L-Arginine | Sigma |

| | |
|---|---|
| BCA | |
| Bromophenol blue | |
| BSA | |
| Calcium chloride | |
| Chloroform, 99+% | |
| DAPI | |
| Developer G135 A/B | |
| 1,4-Diazabicyclo[2.2.2]octane | AGFA |
| Dimethylsulfoxide (DMSO), >99,9% | Dapco |
| Dithiothreitol (DTT) | |
| Dithizone | |
| DNAZap | Thermo Fisher Scientific |
| dNTPs | Fermentas |
| EDTA | |
| Ethanol, 96% | |
| L-Glutamine | |
| D-Glucose | |
| Glutaraldehyde | |
| Glycerol | |
| Glycin | |
| 10N HCl | |
| HEPES (powder) | |
| Isopropanol, 100% | |
| Magnesium chloride | |
| Methanol, 100% | |
| Milk powder | Becton Dickinson |
| Mounting medium; Jung Tissue Freezing medium | Leica |
| Nitrogen (l) | Linde AG |
| NP40 | Life Technologies |
| Paraformaldehyde | |
| Polyacrylamide | |
| Polyvinyl-alcohol | |

| | |
|---|---|
| Potassium chloride (KCl) | |
| Potassium hydrogenphosphate ($KH_2PO_4$) | |
| Rapid fixer G356 | AGFA |
| RNaseZAP | |
| Sodium chloride | |
| Sodium desoxycholate | |
| Sodium dodecylsulphate (SDS) | |
| Sodium hydrogenic phosphate ($Na_2HPO_4$) | |
| Sodium hydroxide | |
| Sodium tetraborate ($Na_2B_2O_7$) | |
| TEMED | |
| Tris | |
| Triton X-100 | |
| Tween-20 | |

### 6.1.5 Buffers and solutions

#### 6.1.5.1 Western blot

RIPA buffer: 75 mM NaCl, 6.37 mM Natriumdesoxycholat
0.005% NP40, 0.05% SDS, 25 mM Tris pH8

APS: 10% APS (in $dH_2O$)

4x Tris/SDS: 1.5 M Tris, 0.4% SDS (adjust to pH8.8)

4x Tris/SDS: 0.5 M Tris, 0.4% SDS (adjust to pH6.8)

10x Tris-Glycine: 1.0% SDS, 0.25 M Tris, 1.92 M Glycine

4x SDS-loading buffer: 200 mM Tris/HCl, pH6.8, 8% SDS, 40% Glycerol 0.4% bromine phenol blue (add freshly 400 mM DTT)

Buffer cathode (KP): 25 mM Tris/HCl, 40 mM Glycine, 10% Methanol (adjust to pH9.4)

Buffer anode I (API): 300 mM Tris/HCl, 10% Methanol (adjust to pH10.4)

Buffer anode II (APII): 25 mM Tris/HCl, 10% Methanol (adjust to pH10.4)

10x TBST: 100 mM Tris/HCl, 1.5 M NaCl, 2.0% Tween20 (adjust to pH7.4)

| | |
|---|---|
| Blocking solution: | 5% milk powder or BSA in 1x TBST |

(Femto-) ECL-solution: Solution A and B mix: 1:1 (mix shortly before usage)

### 6.1.5.2 Immunostainings

| | |
|---|---|
| 10X PBS | 1.37 M NaCl, 26.8 mM KCl, 0,101 M $Na_2HPO_4$, 13.8 mM $KH_2PO_4$ |
| PBST: | 1X PBS + 0.1% Tween20 (adjust to pH7.4) |
| 4% PFA: | 1.3 M PFA in 1X PBS (adjust to pH7.2-7.4) |
| Permeabilization (sections): | 0.2% TritonX-100, 100 mM Glycin in $dH_2O$ |
| Permeabilization (islets): | 0.5% TritonX-100, 100 mM Glycin in $dH_2O$ |
| Blocking solution: | 5% FCS, 1% serum (goat or donkey) in PBST |
| DAPI: | 5 mg DAPI in 25 mL PBS |
| Elvanol (embedding): | 0.015 mM Polyvinyl-alcohol, 24 mM Tris pH 6.0, 2 g DABCO in 90 mL $H_2O$ and 37.8 mL Glycerol |
| Antigen retrieval: | Antigen Unmasking Solution, Citrate-Based H-3300 (Vector Laboratories) |

10X Tris-Borat-Buffer: 10 mM $Na_2B_2O_7$ in $dH_2O$

### 6.1.5.3 Enzymes and inhibitors

| | |
|---|---|
| DNA-Polymerases | Thermo Fisher Scientific (Taq DNA Polymerase, recombinant) |
| DNase I | Qiagen |
| RNase-free DNase I | Qiagen |
| Phosphatase & Proteinase inhibitors | Sigma-Aldrich |

### 6.1.5.4 Antibodies

| Protein Name | Host | Dilution | Company |
|---|---|---|---|
| CD31 | rat | IF 1:500 | BD |
| CD81 | rabbit | IF 1:300 FACS 1:50 WB 1:1000 | Cell Signaling |
| CD81 | mouse | IF 1:300 | Novus Bio |
| C-peptide | guinea pig | IF 1:500 | Abcam |
| Dvl2 | rabbit | WB 1:1000 | Cell Signaling |
| Gapdh | mouse | WB 1:5000 | Abbexa |
| GFP | chicken | IF 1:1000 | Aves Labs |
| Glucagon | goat | IF 1:500 | Bio-Rad |
| Glucagon | rabbit | IF 1:400 | Covalab |
| Glucagon | guinea pig | IF 1:3500 | Takara |
| GM130 | mouse | IF 1:300 | BD |
| Gsk3 | rabbit | IF 1:500 WB 1:5000 | Cell Signaling |
| Gsk3-phospho | rabbit | IF 1:500 WB 1:5000 | Cell Signaling |
| Hsp90 | rabbit | WB 1:5000 | Cell Signaling |
| Insulin | guinea pig | IF 1:100 | Thermo Scientific |
| Insulin | mouse | IF 1:300 | Abcam |
| Insulin | rabbit | IF 1:300 | Cell Signaling |
| Lamp1 | rat | IF 1:1000 | BD |
| MafA | rabbit | IF 1:200 | Novus Bio |
| Nkx6.1 | goat | IF 1:200 | R&D systems |
| pJnk | rabbit | IF 1:300 WB 1:1000 | Cell Signaling |
| Pro-Insulin | mouse | IF 1:300 | R&D Systems |
| pS6 | rabbit | IF 1:300 | Cell Signaling |
| RFP (5F8) | rat | IF 1:1000 | Chromotek |
| Urocortin 3 | rabbit | IF 1:300 | Phoenix Pharmaceuticals |
| β-Catenin | mouse | IF 1:1000 WB 1:5000 | BD |
| γ-tubulin | mouse | WB 1:10000 | Sigma |
| Secondary Antibodies (Invitrogen, Dianova) were used 1:800 for IF, 1:500 for FACS and 1:10000 for WB | | | |

### 6.1.5.5 TaqMan primers

| Gene | Reference |
|---|---|
| 18S | Mm03928990_g1 |
| Cd81 | Mm00504870_m1 |
| Cfap126 | Mm01290541_m1 |
| Gapdh | Mm99999915_g1 |
| Gcg | Mm01269055_m1 |
| Ins1 | Mm01950294_s1 |

| | |
|---|---|
| Mafa | Mm00845206_s1 |
| Nkx6-1 | Mm00454961_m1 |
| Rbp4 | Mm00803264_g1 |
| Slc2a2 | Mm00446229_m1 |
| Ucn3 | Mm00453206_s1 |

### 6.1.5.6 Culture Medium

G-Solution: HBSS (Lonza) supplemented with 1x P/S (Gibco) and 1% BSA

Collagenase: 1 mg/mL Collagenase P (Roche) in G-solution

Gradient medium: 5 mL G-solution, 30 µL 1M HEPES (Life Technologies), 970 µL DPBS (Lonza Verviers), 2 mL Optiprep Density Gradient medium (Sigma)

Islet culture medium: RPMI1640 (Lonza) supplemented with 1X P/S and 10% FCS (PAA)

Min6 medium: DMEM high glucose, 10% FBS, 1% Penicillin/Streptomycin and β-mercaptoethanol

EndoC medium: Cells were grown according to the official "EndoC-βH1® cells User's Manual Guide"

### 6.1.5.7 Mouse lines and Genotyping primers

| Mouse Line | Primers | Wt (bp) | Target (bp) |
|---|---|---|---|
| Fltp iCre (Protocol #021) | EP 565 CAGCATGGCATAGATCTGGAC<br>EP 566 GAGGCTGACTGGGAACAATC<br>EP 568 GCTGGTGGCTGGACCAATGTG | 317 | 229 |
| Rosa26 mTmG (Protocol #051) | EP 1302 CTCTGCTGCCTCCTGGCTTCT<br>EP 1303 CGAGGCGGATCACAAGCAATA<br>EP 1304 TCAATGGGCGGGGGTCGTT | 330 | 250 |
| Fltp NLS LacZ (Protocol #022) | EP 418 AGCCATACCACATTTGTAGAGG<br>EP 565 CAGCATGGCATAGATCTGGAC<br>EP 566 GAGGCTGACTGGGAACAATC | 317 | 387 |

## 6.2 Methods

### 6.2.1 General mouse handling

The animal experiments were conducted in accordance with the German Animal Protection Act, the guidelines of the Society of Laboratory Animals (GV-SOLAS) and Federation of Laboratory Animal Science Associations (FELASA).

### 6.2.2 Genotyping

DNA isolation. The genomic DNA was isolated from ear punches of mice at weaning age (older than 3 weeks). Samples were lysed in 500µL of homemade lysis buffer and freshly added proteinase K (100 µg/mL), then incubated at 55°C in shaking overnight. Isopropanol (500 µL) and centrifugation (14.000 rpm, 10 min, 4 °C) were used to precipitate the DNA, then washed with 70% EtOH and pelleted again (14 000 rpm, 10 min). After drying, the DNA pellet was resuspended in 100 µL nuclease-free $H_2O$.

PCR Genotyping. The isolated DNA was stored at 4°C until usage. Polymerase chain reaction (PCR) was applied to amplify a specific portion of genomic DNA necessary to verify the presence/absence of the specific sequence. Specific forward and reverse primers (see section above "Mouse lines and Genotyping primers") were added to the PCR mixture to amply the sequence.

Electrophoresis. Agarose gels were prepared by dissolving agarose (1 or 2%) in TAE (Tris-acetate, EDTA) buffer and heated up in the microwave for 2 minutes. The solution was cooled down under running water and Midori Green Direct (5 µL/100ml) was added to the solution. This was then poured into a gel tray with combs of appropriate size. The solidified gel was transferred into a gel chamber filled with TAE buffer. The PCR products generated before were mixed with Orange G (Ratio 1:4) and loaded into the wells of the gel. A current (80-120V) was applied to the gel to separate the DNA fragments based on their size. A UV-chamber was used to detect and acquire images of the PCR products bands.

### 6.2.3 Tissue dissection and islet isolation

Islet isolation. Islets of Langerhans were isolated from mice according to the standard protocol (Szot et al., 2007). Mice were sacrificed by cervical dislocation or decapitation, depending on the age of the animal. The abdominal cavity was then opened to expose pancreas, common bile duct and gallbladder. The ampulla, connecting the common bile duct to the duodenum, was sealed with a bulldog clamp. Finally, under a stereoscope, Collagenase P (Roche) (1 mg/mL in G-solution) was injected in the bile duct with a syringe and a 30G needle. Once the organ was perfused with 3ml of the abovementioned solution, it was dissected

and incubated in 3ml of Collagenase P solution and placed on ice. Afterwards, the pancreas was digested at 37°C for a variable amount of time (15 minutes for adult pancreata, 10 minutes for postnatal pancreata) and shacked vigorously at least once at half the time of incubation. The digestion was stopped on ice and adding 10ml G-solution plus 10% FBS. The mixture was centrifugated (1620rpm, 3 min, 4°C) in order to pellet the digested organ and remove the solution containing the collagenase. The pellet was then resuspended in 5.5ml of gradient solution (40% Optiprep). This was then centrifugated at 1700rpm, 10 min, RT, acceleration 3 and deceleration 0. Islets were sedimented at the interface between the first and second phase. They were collected and washed on a 70µm cell strainer with G-solution, then placed in a 10cm dish in islets medium. Considering that the obtained solution is still rich in exocrine cells, islets were handpicked and placed in a new dish with fresh medium. Islets are cultured at 37°C and 5%$CO_2$.

### 6.2.4 Single cell suspension.

Islets were picked in a 1.5 mL Eppendorf tube, pelleted (800 rpm, 2 min) washed with PBS (-Mg/Ca) and digested with TrypLE™ Express Enzyme (1X) (Thermo Fisher Scientific) at 37 °C for 10 min, gently pipetting every 2 minutes. After this, the tube was placed in ice and FACS buffer was added to the cells and finally centrifuged at 900rpm for 5 min. The supernatant was discarded and an appropriate amount of FACS buffer or islet medium was added to resuspend the single cells.

### 6.2.5 Flow Cytometry.

Flow cytometry analysis and sorting was done via FACS-Aria III (BD). The endocrine population was gated using forward and side scatter area (FSC-A vs SSC-A). Doublets (two or more cells attached together) were excluded, visualizing them via front scatter width and front scatter height (FSC-W vs FSC-H). Next, dead cells were excluded if positive to DAPI staining. The residual population was then separated according to the specific fluorescent signals associated. To obtain nucleic acids from sorted cells, these were sorted directly in Quiazol (Qiagen), otherwise cells were always sorted in FACS buffer to preserve viability.

For immunofluorescence of surface markers on living cells, after generating single cell suspensions, cells were incubated with conjugated or unconjugated primary antibody for 30 minutes, on ice. After three rounds of washings, a step of incubation with fluorophore conjugated secondary antibodies (20 minutes on ice and in the dark) was necessary to label primary unconjugated antibodies. Cells were then washed again, filtered on a cell strainer and collected in a low attachment flow cytometry tube.

### 6.2.6 RNA biochemistry

#### 6.2.6.1 RNA isolation

To preserve the integrity of RNA, all work involving RNA was performed under a sterile hood, previously cleaned with RNase inhibitor (RNAZap, Thermo Fisher Scientific). RNA extraction was performed using columns and reagents from the miRNA micro kit (Qiagen), according to the manufacturer instructions. Once isolated, RNA was eluted in nuclease free water and quantified at the NanoDrop, evaluating the wavelengths 230nm, 260nm and 280nm and evaluating the overall quality and presence of contaminants with the ratio 260/230 and 260/280. At this point RNA was either stored at -80°C or processed into cDNA.

#### 6.2.6.2 Reverse transcription

The isolated RNA was converted (reverse transcription) in cDNA. The chosen kit to generate first strand cDNA was the SuperScript Vilo cDNA synthesis kit (Thermo Fisher Scientific), according to the manufacturer instructions. This was then saved at -20°C, for long term storage or +4°C, for short term storage.

#### 6.2.6.3 Quantitative PCR (qPCR)

This method allowed to quantify the number of copies of a specific mRNA in a sample. The experiments used the TaqMan™ probes (Thermo Fisher Scientific) for the detection of the specific target transcripts. The mixture used for the experiment contained four components: cDNA in nuclease free water (4.5 µl, equal to 5 to 15ng RNA depending on the experiment), TaqMan™ Fast Advanced Master Mix (5 µL) and TaqMan probe™ (0.5 µL). The amplification and detection were performed in the ViiA 7 Real-Time PCR System (Thermo Fisher Scientific). The ΔΔCt method was the chosen one for the analysis of the results. In brief, the Ct (cycle threshold) value of each gene corresponds to the number of cycles necessary for the fluorescent signal of the probe to cross the signal value of the background (the so-called threshold). The equation below shows the method used to obtain the results:

$$\Delta\text{Ct} = Ct_{(gene\ of\ interest)} - Ct_{(housekeeping\ gene)}$$

$$\Delta\Delta\text{Ct} = \Delta Ct_{(treated\ sample)} - \Delta Ct_{(control\ sample)}$$

$$\text{Fold changes} = 2^{-\Delta\Delta\text{Ct}}$$

Normalized gene expression was shown as mean ± Standard Deviation. Significance was tested by two-tailed t-test.

#### 6.2.6.4 Single cell RNA Sequencing.

Sorted cells were separated by flow cytometry and sorted in FACS buffer with low EDTA. These were counted and cell death evaluated by trypan blue staining. Libraries for single-cell were prepared using ChromiumTM Single cell 3' library and gel bead kit v2 (10x Genomics) according to the manufacturer's instructions. At least 15.000 cells were loaded onto a channel of the 10x chip to generate Gel Bead-in-Emulsions (GEMs), in order to hit the maximum number of cell coverage of the chip (10.000). Next, reverse transcription, clean-up and cDNA amplification were performed. cDNA was enzymatically fragmented and attached to 5' adaptor and sample indexing performed. Libraries were sequenced on the HiSeq4000 (Illumina) with 150 bp paired-end sequencing of read. CellRanger analysis pipeline by 10X Genomics was used for demultiplexing of raw base call (BCL) files, alignment to the mm10-reference genome, filtering, barcode and UMI counting. Scanpy API (Wolf et al., 2018), a python based application was used to analyze the data. Cells with high mitochondrial genes fraction (>10%) and genes present in less than 20 cells were excluded from the analysis. Finally, ComBat application was used to perform batch correction (W. E. Johnson et al., 2007). Visualization of multidimensional plots was done via UMAP (Uniform Manifold Approximation and Projection) algorithm. Louvain-based clustering was applied in order to discriminate cell subtypes, which were then annotated based on an array of known marker genes. Differential expression analysis was performed using limma-trend (Law et al., 2014) via an rpy2 (2.9.1) interface.

### 6.2.7 Protein biochemistry

#### 6.2.7.1 Protein extraction.

Isolated islets or cultured cells were washed with ice cold DPBS (-$Ca^{+2}Mg^{+2}$) and lysed with an appropriate amount of homemade RIPA buffer. For cells in culture, these were scraped from the bottom of the dish with a sterile mono-use cell scraper. The lysate was collected in Eppendorf tubes and placed on ice for 30 minutes, vortexing for 30 second every 10 minutes. Afterwards, samples were placed for 1 minutes in a water bath sonicator and finally centrifuged for 20 minutes at 14.000rpm at 4°C. The supernatant was collected in a new tube and stored at -80°C or immediately processed for quantification.

#### 6.2.7.2 Protein quantification.

Proteins were quantified using the Pierce™ BCA Protein Assay Kit (Thermo Fisher Scientific). In brief, the reagents were prepared according to the manufacturer instructions and 3 µl of standards (bovine albumin) or samples were added to it. Proteins and reagents were incubated at 37°C for 30 minutes, after which the absorbance at 562nm was detected at the plate reader. Finally, the standard curve was prepared and interpolation of the absorbance of the unknown samples to the standard curve allowed the determination of the protein concentration.

#### 6.2.7.3 Western Blot.

Protein loading buffer (sodium dodecyl sulfate (SDS) and dithiothreitol (DTT)) was added to the lysate and the mixture boiled at 95°C for 10 minutes. The process denatures the proteins and coat them with a uniform negatively charged layer. SDS gels were prepared according to the standard protocol: stacking gel (1.3 mL acrylamide/bisacrylamide-mixture, 2.5 mL 4x Tris/SDS buffer, pH6.8, 6.2 mL H2O, 20 µL TEMED, 100 µL APS) and a 10% separating gel (10.0 mL acrylamide/bisacrylamide-mixture, 7.5 mL 4x Tris/SDS buffer, pH8.8, 12.5 mL H2O, 40 µL TEMED, 300 µL APS). Proteins and ladder were loaded onto the gel and an electric charge was applied to the gel to separate proteins according to their molecular weight. After gel separation, proteins needed to be transferred on a membrane. The blotting is prepared as followed: two blotting papers equilibrated with API buffer and one blotting paper equilibrated with APII buffer. On top, the PVFD membrane (previously activated with 100% methanol and equilibrated in APII) and the gel. Finally, three blotting papers equilibrated with KP buffer were added to the pile. The semi-dry system applied a constant current to the pile from top to bottom (cathode to anode), which moves the proteins from the gel to the membrane, where they will be trapped in the net structure of the membrane. Once transferred, the membrane was washed with TBS-T and blocked with a solution of TBS-T plus 5% milk powder or BSA for two hours at room temperature. This step is pivotal to block unspecific binding of antibodies to the membrane and on other proteins. Primary antibodies were diluted in blocking solution and incubated with the membrane at 4°C overnight. Subsequently, 3 washes of 10 minutes were performed before adding the secondary antibodies (always in blocking solution) for 2 hours at room temperature. Finally, after three more washings in TBS-T, membranes were developed using ECL or super-ECL solutions, which provided the substrates to the HRP enzyme (conjugated to the secondary antibodies) that generated the chemiluminescent signal, detected with a developing machine (Analytik Jena).

### 6.2.8 Histology

#### 6.2.8.1 Cryosections.

Harvested organs (pancreas and spleen) were fixed in 4% paraformaldehyde (PFA) for 2-24 hours at 4 °C. Then, organs underwent dehydration process using 10% and 30% sucrose solutions for 2 hours each. Finally, organs were incubated overnight at 4°C in a solution of 30% sucrose and OCT (1:1). The following day, organs were OCT-embedded in plastic cassettes of appropriate size, slow frozen on dry ice and saved at -80°C. The cryosections were obtained using a Leica cryostat. Three sections of 10-20 µm were placed on a glass slide (Thermo Fisher Scientific), dried at room temperature and stored at -20°C until usage.

#### 6.2.8.2 Paraffin section.

Organs were fixed in formalin, then incubated sequentially in ethanol, xylol and wax solutions and finally embedded in wax. Using a vibratome, blocks were sectioned in 3µm thickness and placed on a glass slide and saved at 4°C. Prior the immunofluorescence, sections were rehydrated in xylol and ethanol, and processed with citrate buffer to retrieve antigens. The rest of the protocol is the same as described above.

#### 6.2.8.3 Attached cells.

Dispersed islets, Min6 cells and EndoC cells were fixed in 4% PFA (10 minutes 37°C) or 100% methanol (15 min on ice) before staining. Cells fixed with PFA were permeabilized with 0.2% Triton X-100, 0.1 M glycine solution for 10 minutes at room temperature. For both methods, cells were then incubated for 1 hour in blocking solution and then with primary antibodies for 2-3 hours RT. After PBS washings, cells were incubated with secondary antibodies for 1 hour at room temperature and stained with DAPI for 15min at room temperature. After three washing, cells were embedded in self-made Elvanol.

#### 6.2.8.4 Immunofluorescence.

Cryosections were processed as followed: rehydration in PBS for 30 minutes at RT, permeabilization with 0.2% Triton X-100 and 0.1M Glycine in $H_2O$ for 15 min and blocked in blocking solution (PBS, 0.1% Tween-20, 1% donkey serum, 5% FCS) for 2 hours at room temperature. Primary antibodies were diluted in blocking solution and incubated overnight at 4°C in a humid chamber. The next day, slides were washed (3 times) in PBS and then incubated with secondary antibodies, diluted in blocking solution, for at least 2 hours at room temperature. Finally, nuclei were stained with DAPI diluted in PBS (1:500) by incubation for 30 minutes. To conclude, slides were washed again (3 times) and coverslips were mounted on them using self-made mounting solution.

#### 6.2.8.5 Whole mount islets.

After isolation, islets are placed in a V-shape 96-well plate, washed with DPBS and fixed with 100% ice cold Methanol (15 min on ice) or 4% PFA (15min, 37°C). The ones fixed with PFA required an additional permeabilization step (30 min, 0.5% Triton X-100 and 0.1mM Glycine in $H_2O$) before being blocked with blocking solution (as below) for 2 hours. Primary antibodies were diluted in blocking solution and islets incubated at 4°C overnight or longer. Next, isles were washed (3 times/10 minutes each), incubated with secondary antibodies diluted in blocking solution, for 4 hours at room temperature and with DAPI for 30 minutes. After other 3 rounds of washings, islets were mounted in self-made Elvanol on 96-well plate glass bottom or Ibidi chambers.

#### 6.2.8.6 Microscopy & Analysis.

Images were acquired with a ZEISS LSM 880 Airyscan and Leica SP5 confocal microscopes. Image processing was performed on Fiji - ImageJ software program and related plug-ins.

### 6.2.9 Stress Assay

Min6 cells were seeded in 6-well plates with a density of 250.000 cells per well and left to recover for one day. Next day, control medium or medium containing respectively tunicamycin (5µg/ml) or glucose (additional 10mM) and Palmitate (0.4mM) were added to the culture. Treatment lasted 2 days for tunicamycin and for 4 days for glucose and palmitate. Medium was changed every 48 hours.

EndoC human cells were seeded in 6-welll plates with a density of 250.000 cells per well and left to recover for one day. Next, normal growth medium or containing cytokines (IL-1β 2ng/ml, TNF-α 10ng/ml and IFN-γ 10ng/ml), tunicamycin (5µg/ml) or glucose (additional 30mM) and palmitate (1mM) was added to the culture for 4 days and changed every 48 hours.

Adult islets were isolated and left to recover overnight. 60 islets per conditions were then treated with glucose (additional 25mM) and palmitate (0.4mM) for 2 days or tunicamycin (5µg/ml).

### 6.2.10 Statistics.

Analysis. Data obtained from all experiments were then uploaded in GraphPad Software to perform statistical analysis and generate plots. If not indicated, a two-sided and unpaired t-test was carried out. *indicated P-values >0.05, ** > 0.01, *** > 0.001 and **** > 0.0001

# Annex I

## Table 2: Differentially regulated genes between Fltp$^{+}$ and Fltp$^{\pm}$ β-cells

| Fltp$^{+}$ | |
|---|---|
| Nnat | Atp5b |
| Higd1a | Aldoa |
| Vapa | Rps2 |
| Smim10l1 | Ttr |
| Rpl13 | Gm42418 |
| Gpx3 | Ghrl |
| Cst3 | Tubb5 |
| Ube2d3 | |
| Gm8797 | |
| Selenow | |
| Eif3k | |
| Hnrnpa1 | |
| Mafb | |
| Igfbp7 | |
| Ffar4 | |
| Gnas | |
| Shisa5 | |
| Rpl3 | |
| Lmo1 | |
| Calm3 | |
| Gapdh | |
| U2af1 | |
| Cpe | |
| Psma3 | |
| Eif4a1 | |
| Sin3b | |
| Ly6e | |
| Xaf1 | |
| Sept7 | |
| Ctsz | |
| Snrpd3 | |
| Prdx1 | |
| Serping1 | |
| Rpl10a | |
| Eif3e | |
| Slc25a5 | |
| Hnrnph2 | |
| Cfl1 | |
| Anapc11 | |
| Cenps | |
| Naca | |
| Rbm3 | |
| Fabp5 | |
| Chgb | |
| Btf3 | |
| Srsf3 | |
| Epcam | |
| Rpl14 | |

vs

| Fltp± | | | |
|---|---|---|---|
| mt-Nd3 | Magt1 | Ptprf | Adgrl1 |
| Gm10073 | Foxp1 | Pkdcc | Srp19 |
| Wnt4 | Rrbp1 | Ago2 | Syt7 |
| Rpl9-ps6 | Plxnb2 | Tmem248 | Lman2 |
| Ftl1-ps1 | Ddit3 | Kdm2a | Ppp1r14b |
| Zbtb20 | Enpp2 | Pcsk2 | Glyr1 |
| Mrln | Nrd1 | mt-Atp6 | Pbxip1 |
| Cebpb | Rora | Phactr1 | Dsp |
| Rps28 | Ctnnb1 | Snap25 | Sh3pxd2a |
| Ankrd11 | Ubl3 | Lman1 | Hist1h4h |
| mt-Nd2 | mt-Nd4 | Trim44 | Wdr43 |
| Jund | Slc43a2 | Tmem256 | Agap1 |
| Cacna1a | S100a10 | Hyou1 | Smarca4 |
| Gm10076 | Bptf | Gm10320 | Ets2 |
| Tppp3 | Irak1 | Madd | Pabpn1 |
| mt-Co2 | Sez6l | Gng4 | Sptbn1 |
| Scd2 | H1fx | Cfap20 | Mical2 |
| Mast4 | Cnot6l | Rap1gap2 | Ctdspl |
| Sec61a1 | Arf3 | Hsp90b1 | March9 |
| Meg3 | Peg3 | Snrpb2 | Zmiz1 |
| Zdhhc2 | Igf1r | mt-Co3 | Usp22 |
| Neat1 | Gns | Unc80 | Ddx17 |
| Brd2 | Celf1 | Gfpt1 | Pum2 |
| Mlxipl | Ost4 | Wnk1 | Fndc3b |
| Ldlr | Nfic | Anapc13 | Tnrc6b |
| Nisch | Hmgcs1 | Golga4 | Stard4 |
| Rps29 | Shisal2b | Cmip | Adcy9 |
| Nktr | Prrc2b | Dpm3 | Ddx5 |
| Lpgat1 | Mcf2l | Larp4b | Rpia |
| Atf5 | Wdr89 | Marcks | |
| Gm10260 | Uhrf2 | Ica1 | |
| Rps21 | Srek1 | Jakmip1 | |
| Hmgcr | Akap13 | Grk3 | |
| Nectin3 | Ankrd40 | Rpl38 | |
| Gm11361 | Chd4 | Jak1 | |
| Ptp4a2 | Tox3 | Nfe2l1 | |
| Arid1a | Mxd4 | Ddx3x | |
| 2900097C17Rik | Disp2 | Rab37 | |
| Son | Tshz1 | Arhgef12 | |
| Ccnd1 | Rps27rt | Slc4a7 | |
| Rpl27-ps3 | Deptor | Dusp18 | |
| Sdk2 | Prlr | Bfar | |
| mt-Co1 | Foxn3 | Tnrc6c | |
| Tmem108 | Ppp2r5c | Sec63 | |
| Vegfa | Msmo1 | Cdc37l1 | |
| Rps12-ps3 | Cbx6 | Lamtor1 | |
| Ddx24 | Ash1l | Ndufa1 | |
| Golgb1 | Gm10036 | Gse1 | |

## Table 3: Differentially regulated genes between Fltp$^{+}$ and Fltp$^{-}$ β-cells

| **Fltp$^{+}$** | | | vs | **Fltp$^{-}$** | | | | | |
|---|---|---|---|---|---|---|---|---|---|
| Ninj1 | Galnt14 | H3f3b | | Ctrb1 | Gstp1 | Hnrnpa3 | Chd4 | Ppib | Smim4 |
| Dgcr6 | Ociad2 | Ing2 | | Clps | Dpm3 | Rnase1 | Naa38 | Pdcd4 | Rnf6 |
| Rab7 | Rnf130 | Uap1l1 | | Apoe | Wdr89 | Ndufb2 | Hist2h2ac | Ifitm2 | Chic1 |
| Abhd16a | Rpl3 | eGFP_plus | | Mgp | Cox7c | Sap18 | Nop10 | Snhg18 | |
| Clic1 | Eif3e | Lamp1 | | Gm10076 | Gm10320 | Nupr1 | Cox6a1 | Tnfrsf12a | |
| Abracl | Derl1 | Gde1 | | Reg1 | Rpl36al | Rps15a | Smim27 | Chga | |
| Map2k2 | Gcat | Hexa | | Prss2 | Cops9 | Ubb | Hist2h2aa1 | Cox16 | |
| Slc2a5 | Vapb | Tent5a | | Cela3b | 2210010C04Rik | Dbi | Rpl22 | Auts2 | |
| Oxct1 | mt-Co3 | Creg1 | | Ghrl | Atp5mpl | Gpx3 | Gm8186 | Rps20 | |
| Pmvk | Rpl4 | Hadh | | Ifitm3 | Rpl13a | Rps27l | 5330417C22Rik | Tmem167 | |
| Dap | Gpx1 | Lmo1 | | Uba52 | Rpl34 | Arpp19 | Hmgn2 | Lrrc58 | |
| Stk32a | Mir670hg | Plk3 | | Rpl35 | Ubl5 | Atpif1 | Prkca | Slc38a2 | |
| Atp2b1 | Selenow | Scg2 | | Try4 | Anapc13 | Junb | Dynll1 | Igf1r | |
| Ndufs7 | Atp2a2 | Gm42418 | | Cela2a | Pofut2 | Smim22 | Fxyd3 | Tomm6 | |
| Hsp90aa1 | Srsf3 | Actg1 | | Tmsb15b2 | Rpl31 | Mrps21 | Ndufb7 | Lsm6 | |
| Rpl7 | Emd | Jund | | Rpl10-ps3 | Snrpf | Cox7a2 | Rpl26 | Upf2 | |
| Mocs2 | Bex3 | Krt8 | | Pnliprp1 | Uqcr11 | Pin4 | Gng5 | Dynlt1a | |
| Pdgfa | Atp6v0b | Ftl1 | | Tmsb10 | Rpl27-ps3 | Uqcrq | Scd2 | Dynlt1f | |
| Eif3h | Vstm2l | Trpm5 | | Ccl5 | Son | Ndufa5 | Fam183b | Txnip | |
| Fam151a | Lrrc10b | Ucn3 | | Ccl2 | Elob | Hist3h2ba | Minos1 | Upp1 | |
| Emid1 | Psap | | | Gm10073 | Atp5j2 | Kpna2 | Skp1a | Meg3 | |
| Scaf11 | Sqstm1 | | | Rps28 | Ttr | Txn1 | Ndufaf8 | Rhoc | |
| Gnai2 | mt-Cytb | | | Rpl38 | Ndufa2 | Tmsb4x | Zfp787 | Gm5914 | |
| Slc25a4 | Cd63 | | | Rpl41 | Ctrl | Snrpe | Snhg6 | Psme2b | |
| Cebpb | Enho | | | Rps27 | Uqcr10 | Cycs | Rpl32 | Uchl1 | |
| Rps4x | Spc25 | | | Mrln | Ost4 | Lpl | Polr2k | Ttll7 | |
| Sec11c | Ero1lb | | | Rps29 | Rplp2 | Mlxipl | Anpep | Ndufa11 | |
| Ube2b | Cln6 | | | Rpl37 | Rpl35a | Rrbp1 | Cd200 | Lsm7 | |
| Dlk1 | 2010111I01Rik | | | Rpl9-ps6 | Cxcl10 | Rps15 | Mafb | Tmem108 | |
| Atp5c1 | Hist1h1c | | | Cela1 | Polr2l | Ndufa7 | AC126280.1 | Pcsk2 | |
| Phyh | Krt18 | | | Rpl39 | Rps27rt | Ndufb4 | Pet100 | Dusp1 | |
| Dnajc3 | Rnase4 | | | Td-Tomato-plus | Cpb1 | 1810022K09Rik | Slirp | Pla2g2f | |
| Pgls | Smap2 | | | Rps21 | Cox6c | Hist1h4h | Myl12b | Tm9sf2 | |
| D5Ertd579e | Cited2 | | | Ftl1-ps1 | Ndufv3 | Ier3ip1 | Serinc3 | Ier3 | |
| Ssrp1 | Ppp1r1a | | | Sec61g | Atp5l | mt-Nd4l | Slc6a6 | Hypk | |
| Zdhhc2 | Npc2 | | | Rpl37a | Usp50 | Ffar4 | Ndufb3 | Tspan8 | |
| Hist1h4i | Mpc1 | | | Tmem258 | Cd79a | Cox6b1 | Fndc3b | Chd3 | |
| Coro1c | Sf3b2 | | | Rbp4 | Rpl22l1 | Hmgb1 | Rplp1 | Gm6563 | |
| Fkbp1b | Pkm | | | Sparc | Tma7 | Rps25 | Sec61b | Ranbp1 | |
| Ptpn1 | Prlr | | | Ndufa1 | Grcc10 | Lsm5 | Rps23 | Mrpl23 | |
| Atp6v1e1 | Cnn3 | | | Rpl27 | Atox1 | Mrpl33 | Eif3j1 | mt-Atp8 | |
| Eef1b2 | Atp6ap2 | | | Usmg5 | Rps12-ps3 | Sec62 | Uqcc2 | Hsbp1 | |
| Bex1 | Defb1 | | | Rpl36 | Id3 | Cox8a | Gm16174 | Ldlr | |
| Camk2n1 | Atp6v1b2 | | | Gm11808 | Ndufa4 | Nptn | Fau | Rps12 | |
| Fam174b | Aga | | | Atp5e | Tmem256 | Rpl30 | Isg15 | Lrpprc | |
| Maff | Bex2 | | | Erh | Bola2 | Fmc1 | Tbca | Tox | |
| Suclg1 | Bace2 | | | Tomm7 | Rps17 | Cox5b | Msln | Tshz2 | |
| Rasgrf1 | Tnfaip8 | | | Cox17 | Mrpl52 | Srsf10 | Cltrn | Cox20 | |
| Rpsa | Dnajb9 | | | Rps26 | Ndufa6 | Serf2 | Ndufs5 | Alkbh1 | |
| Stx8 | Atp5b | | | Ndufa3 | Shisal2b | Rps18 | 1700023F06Rik | Smim26 | |
| Cirbp | Isg20 | | | Romo1 | Crip1 | Uqcrb | H2afj | Ucp2 | |
| Grina | Neat1 | | | Gm10260 | Rps10 | Pax6 | Uqcrh | Il1r1 | |
| Th | Napa | | | Atp5k | Gm10036 | Polr2i | Mrps36 | Luc7l3 | |
| Ywhah | Hsp90ab1 | | | mt-Nd3 | Gm11361 | Rps19 | Tnrc6a | Cd9 | |
| Tjp2 | Chchd10 | | | Cd81 | Ndufc1 | Slc43a2 | Tra2b | Eno1 | |
| Rtn4 | Cox7a2l | | | S100a11 | Mt2 | Vegfa | Neurod1 | Timm10b | |
| Tes | Ifit1 | | | Snrpg | Sem1 | Clu | Ccdc85b | Arpc4 | |
| Aes | Ccnd2 | | | Try5 | Gm2000 | Krtcap2 | Rpl27a | Sez6l2 | |
| Mtch1 | Cldn7 | | | Rpl36a | Gm9493 | Cox7b | Rpn1 | Pkib | |

## Table 4: Differentially regulated genes between Fltp$^{\pm}$ and Fltp$^{-}$ β-cells

| Fltp$^{\pm}$ | | | | | | vs | Fltp$^{-}$ | | | | |
|---|---|---|---|---|---|---|---|---|---|---|---|
| Trim44 | Maob | Sgpp1 | Glul | Pi4k2a | mt-Co2 | | Ctrb1 | Cox6c | Bola2 | Hnrnpk | Dbi |
| Aldh9a1 | Yipf2 | Prepl | G3bp2 | Larp1b | Hist1h1c | | Clps | Rps21 | Ndufb4 | Ost4 | Rpl21 |
| Dhx32 | Mien1 | Akap9 | Bsdc1 | Fam174b | Zdhhc2 | | Gpx3 | Mafb | Sycn | Pcsk1n | Cd24a |
| Usp22 | Wdr43 | Ube2m | Grk3 | Mpc1 | Krt8 | | Ghrl | Cops9 | Ranbp1 | Lsm7 | Eif3k |
| Ddx17 | Itga6 | Bag2 | Syt13 | Golgb1 | Ftl1 | | Apoe | Ctrl | Nupr1 | Ppib | Tomm6 |
| Arfip2 | Sfxn2 | Ncald | Hdgf | Maff | Neat1 | | Mgp | Uqcr11 | Serf2 | Rpl26 | Gm6563 |
| Hectd1 | Vdr | Arf3 | Cbx6 | Ninj1 | Cebpb | | Reg1 | Rpl31 | Fxyd3 | Rps27rt | Krt19 |
| Pts | Rims3 | Ifrd1 | March5 | Mtch1 | Wnt4 | | Prss2 | Grcc10 | Krtcap2 | Cd200 | 2410015M20Rik |
| Tnfaip8 | Irf2bp1 | Mxd4 | Uap1l1 | Magt1 | Trpm5 | | Cela3b | Atp5k | Fau | Ier3ip1 | H2-Q4 |
| Kdm5a | Cisd1 | Ankrd40 | Irak1 | Ero1lb | Ucn3 | | Ifitm3 | Rpl34 | Dynll1 | Marcksl1 | Rpl10a |
| Eid2 | Rpsa | Cnn3 | Rabl6 | Th | Jund | | Ttr | Cxcl10 | Ndufa5 | Ramp1 | Polr2j |
| Vegfb | Ubn2 | Gns | Ptpn1 | Odc1 | | | Rpl35 | Ndufa6 | Smim22 | Sept7 | Rtl8a |
| Pfkl | Ppp1r12a | Tmed9 | Hexa | Ppp1r37 | | | Tmsb10 | Hist3h2ba | Anapc13 | Hnrnpl | Nol12 |
| Sys1 | Marcks | D730003I15Rik | Sar1b | Atp2b1 | | | Try4 | Cpb1 | Prdx1 | Ndufs6 | Chga |
| 2900026A02Rik | Ppp1r14b | Atp6v1c1 | Sf3b1 | Sec61a1 | | | Tmsb15b2 | Ubb | Cox6a1 | Lpl | Hint1 |
| Socs2 | Rab24 | Frzb | Hist1h4i | Fam76a | | | Cela2a | Snrpf | Ly6e | Sarnp | Cox16 |
| Bex3 | Cdc37l1 | Aars | Slc7a14 | Foxn3 | | | Pnliprp1 | Atox1 | Rps23 | Pfn1 | Cstb |
| Rpl12 | Atp6v1g1 | Atp6v1d | Disp2 | Gng4 | | | Gm10076 | Rplp2 | Gm10073 | Lgals3bp | Syap1 |
| AI413582 | Ppm1a | Fermt2 | Dap | Ndrg1 | | | Ccl5 | Hmgn2 | mt-Nd4l | Ndufa7 | Rps2 |
| Tmc4 | Fam220a | Atp6v0b | Brd2 | Nktr | | | Rbp4 | Atp5l | Cltrn | Pet100 | Arpc4 |
| Sipa1l3 | Ppat | Tmem248 | Madd | Tent5a | | | Ccl2 | Gm8797 | Cd74 | Rpl27-ps3 | Tmem167 |
| Crls1 | Hagh | Oxct1 | Lrrfip2 | D5Ertd579e | | | Uba52 | Txn1 | Ndufb3 | Arpp19 | Polr2i |
| Alg2 | Siah2 | Bod1 | Tpt1 | Cacna1a | | | Rpl10-ps3 | Cox5b | Mrpl52 | Eno1 | Plp2 |
| Maob | Hspa5 | Calr | Lamp1 | Nisch | | | Cela1 | Uqcrb | Gpx2 | Rpl22 | Lsm5 |
| Yipf2 | Ets2 | Cdc34 | Rnase4 | Pdgfa | | | Rpl27 | Cox6b1 | Ubc | Prkca | Srsf10 |
| Mien1 | Emid1 | Fdft1 | Dnajc21 | Ate1 | | | Rpl41 | Sap18 | Tubb5 | Gm8186 | H2afj |
| Wdr43 | Chrac1 | Sqle | Mast4 | Hsp90ab1 | | | Td-Tomato | Ndufb2 | Smim10l1 | Gadd45b | Rpl30 |
| Itga6 | Eif4b | Nrd1 | Kif1a | Suclg1 | | | Cd81 | Rpl22l1 | Tbca | Minos1 | Snhg6 |
| Sfxn2 | Rab27a | Kcnmb2 | Herpud1 | AC078895.1 | | | Sparc | Rps18 | 1810022K09Rik | Tspan8 | Slc38a5 |
| Vdr | H2afy | Sytl4 | Atxn7l3b | Tes | | | Rpl37 | Igfbp7 | Rbm3 | Skp1a | Eif3j1 |
| Rims3 | Anapc5 | Cenpb | Fam151a | Dnajc3 | | | Usmg5 | Cd79a | Rpl32 | Son | Phpt1 |
| Irf2bp1 | Crb3 | Actg1 | Hsp90aa1 | Dnajb9 | | | Snrpg | Cycs | Vapa | Hsbp1 | Lsm6 |
| Cisd1 | Bccip | Rab7 | Camk2n1 | Ssrp1 | | | Rpl36 | Pofut2 | Isg15 | Trmt112 | Smim26 |
| Rpsa | Ppp1r2 | Ube2b | Sf3b2 | Cyfip2 | | | Rpl39 | Polr2l | Timm10b | Npm1 | Hnrnpr |
| Ubn2 | Shb | Dusp18 | H3f3b | Lrrc10b | | | S100a11 | Hnrnpa1 | Dbpht2 | Sfpq | Rps13 |
| Ppp1r12a | Srrm2 | Dnajc24 | Bcas2 | Ubl3 | | | Rps27 | Atpif1 | Pin4 | Sec61b | Impdh2 |
| Marcks | Rabac1 | H1f0 | Dynll2 | Ddx24 | | | Rpl37a | Mrln | Mrpl33 | Cfl1 | Hprt |
| Ppp1r14b | Cebpg | Txndc17 | Kras | Ddx3x | | | Tmem258 | Rnase1 | Nop10 | Rplp1 | Lrpprc |
| Rab24 | Pgls | Mgat2 | Phc2 | Tnrc6c | | | Rpl38 | Hmgb1 | Mrpl54 | Oasl1 | Cd9 |
| Cdc37l1 | Sar1a | mt-Nd1 | Stk32a | Lamtor1 | | | Gstp1 | Rps27l | Rps15 | Ndufb7 | Chmp4b |
| Atp6v1g1 | Desi2 | Zc3h13 | Chchd10 | Coro1c | | | Rpl13a | Uqcrq | Uqcc2 | Gm2000 | Ndufb6 |
| Ppm1a | Ubn1 | Mrps18b | Lmna | Zbtb20 | | | Erh | Dpm3 | Rpl9-ps6 | Srsf2 | Arpc3 |
| Fam220a | Gnai2 | Cabp7 | Mindy2 | Sqstm1 | | | Atp5mpl | Ndufv3 | Clu | Xaf1 | Atp5g1 |
| Ppat | Glrx5 | Srsf5 | Emd | Creg1 | | | Rpl36al | Snrpe | Ctsz | Txnip | Lrrc58 |
| Hagh | Clpx | Cuedc1 | Sdha | Tppp3 | | | Cox7c | Ndufc1 | Ftl1-ps1 | Eif6 | Tm9sf2 |
| Siah2 | Ubxn4 | Plxnb2 | Sec63 | Cox7a2l | | | Sec61g | Nnat | Pam | Hist2h2aa1 | Arf4 |
| Trim44 | Ociad2 | Myo6 | Kif5b | Enho | | | Atp5e | Ndufa2 | Rps25 | Idh1 | Cenps |
| Aldh9a1 | Ctnnd1 | Ppp1r1a | Eif5 | Atf5 | | | Try5 | Crip1 | Slirp | Ndufa11 | Hypk |
| Dhx32 | Wsb2 | Larp4b | Gcat | Syndig1l | | | Rps26 | Mrps21 | Nptn | Calm2 | Anxa5 |
| Usp22 | Mia3 | Zc3h7a | Rnf130 | Krt18 | | | Ndufa3 | Upp1 | Ndufs5 | Cnih1 | U2af1 |
| Ddx17 | Cdv3 | Lmo7 | Sdk2 | H1fx | | | Rpl36a | Cox7a2 | Cpe | Ssb | Rps27a |
| Arfip2 | Cmip | Atp6v1e1 | Mapk14 | Bace2 | | | Uqcr10 | Rps17 | Snrpd3 | Rpl23a | Fgb |
| Hectd1 | Rtn4 | Fhl2 | Bex1 | mt-Atp6 | | | Tomm7 | Serping1 | Ptges3 | Cryab | Rpl23 |
| Pts | Sfxn1 | Chd7 | Psap | mt-Cytb | | | Gm11808 | Gm10260 | Snrpd2 | Myl12a | Gm10036 |
| Tnfaip8 | Thyn1 | Npepl1 | Gmppb | Rasgrf1 | | | Elob | Ifitm2 | Junb | Rpl27a | Polr2k |
| Kdm5a | Lpgat1 | Rundc3a | Lman2 | Atp2a2 | | | 2210010C04Rik | Kpna2 | Cox7b | Pdia3 | Gsn |
| Eid2 | Uhrf2 | Tspan5 | Rora | Golga4 | | | Ubl5 | Cst3 | Fam183b | Arf5 | Smim27 |
| Vegfb | Lman1 | Fth1 | Akt1 | Msmo1 | | | Cox17 | Usp50 | Gm9493 | Fmc1 | Phgdh |
| Pfkl | Riok3 | Hdac5 | Fxyd6 | Ccnd2 | | | Ndufa1 | Gm10320 | Cdkn1a | Naa38 | Gm26917 |
| Sys1 | Bex2 | Cfap20 | Ing2 | mt-Nd2 | | | Ffar4 | Rps15a | Rps19 | Serpinh1 | Tspan3 |
| 2900026A02Rik | Abhd17a | Cyp51 | Ctnnb1 | Plk3 | | | Ndufa4 | Sem1 | Tmsb15b1 | Fam20c | |
| Socs2 | Nectin3 | Rpl5 | Rab37 | Hadh | | | Atp5j2 | Ccl7 | 1700023F06Rik | Uchl1 | |
| Bex3 | Luzp1 | Phactr1 | Ckb | Ankrd11 | | | Id3 | Wdr89 | Rcan2 | Ier3 | |
| Rpl12 | Derl2 | Syt7 | mt-Co1 | mt-Nd4 | | | Rps10 | Tma7 | Rpl28 | Dusp1 | |
| AI413582 | Ptprf | Chmp4c | Ptp4a2 | Ddit3 | | | Rps29 | Hnrnpa3 | Cox8a | Ier2 | |
| Tmc4 | Khk | Baiap2 | Npc2 | mt-Co3 | | | Romo1 | Myl12b | Ube2d3 | Ndufa12 | |
| Sipa1l3 | Podxl2 | Zbtb7a | S100a10 | Defb1 | | | Rpl35a | Eif4a1 | Rps16 | Fdps | |
| Crls1 | Papola | Enpp5 | Bri3 | Prlr | | | Higd1a | Cpa1 | Dpysl2 | Tmem256 | |
| Alg2 | Kmt2a | Abracl | Derl1 | Scg2 | | | Rps28 | Zg16 | AY036118 | Gng5 | |

## Table 1: Differentially regulated genes in postnatal CD81-grouped β-cells, as in Salinno et. al, 2021

| $CD81^{low/-}$ | | | | |
|---|---|---|---|---|
| Ucn3 | Ninj1 | Shc1 | Dlk1 | Atp8a1 |
| Trpm5 | Gde1 | Npc2 | Hsp90ab1 | Rpl22l1 |
| Prss53 | Glul | Emid1 | Fmo1 | Ankrd33b |
| Sytl4 | Tnfrsf9 | Gsdma | Scarb2 | Rhobtb1 |
| Mafa | Timm8b | Oxct1 | Gm26917 | Gm30551 |
| Gng12 | Gnai3 | Selenok | Ctnnbip1 | St8sia1 |
| Syndig1l | Bex3 | Tmem147 | Dph3 | Atp6v0b |
| Ero1lb | Dhrs4 | Ppp2r2d | Emb | Fkbp1a |
| Dnajc24 | Glrx5 | Gns | Cpeb1 | Sec61b |
| Cib2 | Crem | Hspe1 | Anapc13 | Ggact |
| Vstm2l | Rnase4 | Uqcrq | Nabp1 | Mns1 |
| Papss2 | Ndufc1 | Litaf | Slc25a4 | Mpp6 |
| Atp2a2 | Hist1h4h | AI413582 | Itgav | Sec61g |
| Fkbp1b | Vps35 | Rheb | Cln6 | Ripply3 |
| Nnat | Grin1 | Pdcd4 | Taf10 | Prkab2 |
| Plk3 | H3f3b | T2 | Vegfb | Fnip1 |
| G6pc2 | Pi4k2a | Trp53inp2 | Sar1a | Gabbr2 |
| Creg1 | St8sia5 | Glrx | Atp6v1g1 | Slc30a7 |
| Ppp1r1a | Dynll2 | Mif | Madd | Apobec1 |
| Vps8 | Tceal9 | Dhx32 | Slc16a10 | Ipmk |
| Slc2a2 | Cuta | Sec11c | Khk | Slc22a23 |
| Th | Ifrd1 | Npepl1 | Txnl1 | Adh1 |
| Tmem215 | Cib3 | Tnfrsf1a | Vamp4 | Fnip2 |
| Jund | Sqstm1 | Fam220a | Ift81 | Myl6 |
| Zc3h3 | Hist1h2bc | Fem1b | Spcs3 | Myo15b |
| Ttc28 | R3hdm2 | Akr1c12 | Lamp1 | Setd7 |
| Mpc1 | Ndufv3 | Atp6v1a | Plscr1 | Igsf11 |
| Spc25 | Car10 | Spock1 | Tollip | Fam107b |
| Hadh | Ndufb9 | Ywhaz | Mpp3 | Rhoq |
| Rasgrf1 | Camk2n1 | Mrps18b | Gm17767 | Sgpl1 |
| Park7 | Phf20l1 | Coa3 | Gsto1 | Sirpa |
| Bex2 | Pmvk | Atp6v1d | Bet1 | Npy |
| Zdhhc2 | Tacc2 | Lbh | Uck2 | Cntn1 |
| Cited2 | Lrrc10b | S100a10 | Ids | Spsb4 |
| Gm42418 | Dap | Mrps14 | Hsp90aa1 | Pfkp |
| Neat1 | Itpkb | Kdm2b | Pde5a | Mfng |
| Ftl1-ps1 | Ank2 | 2010111I01Rik | Psenen | Epb41l4a |
| Tmigd3 | Agpat3 | Lmo7 | Ndufab1 | Hpgds |
| Rtn4 | Peg3 | Ndufc2 | Fer1l6 | Adarb1 |
| Smim1 | Ddit3 | Golga4 | Psap | Flcn |
| Maob | Dapp1 | Ubr4 | Nup93 | Bhlha15 |
| Prlr | Rnf130 | Tifa | Gpr158 | Pde4b |
| Slc38a4 | Daam1 | Leprotl1 | Mtch1 | Rpl28 |
| Uap1l1 | St13 | Ppp1r2 | Fam83g | |
| Abracl | Prepl | Smim20 | Rnf128 | |
| mt-Nd3 | Rims3 | Guk1 | Hs3st6 | |
| Gad1 | Syt4 | Upf3b | Spcs1 | |
| Bace2 | Gm30648 | Tnr | Gabarap | |
| Ing2 | Dnajb9 | Ss18l2 | Svip | |
| Krt8 | Edem1 | Ddx3x | Rps2 | |
| Scg2 | Mir670hg | Tnfaip8 | Gapdh | |
| Selenow | Smap2 | Arl8b | Tes | |
| Fh1 | Derl2 | Bri3 | Usmg5 | |
| Maff | Aes | Ndufb8 | Dad1 | |
| Uqcc2 | Ddc | H2afj | Rufy3 | |
| Phactr1 | Pkm | Tcf25 | Lifr | |
| Ccnd2 | Nckap1 | Cct5 | Rragd | |
| Txndc17 | Mdh1 | Rpl39 | Tjp2 | |
| Hspa8 | Jak1 | Hexa | Sat1 | |
| Chchd10 | Clta | Eif5 | Cryzl2 | |
| Ap1s2 | Esd | Ate1 | Ndufa7 | |
| Ociad2 | Cox7a2l | Sqor | Coro2b | |
| Gng4 | Arhgap36 | Rab1a | Fam210b | |
| mt-Nd5 | Serp1 | Cttnbp2 | Rusc1 | |
| Atp6v1e1 | P2ry1 | Syn2 | Carmil3 | |
| Plut | Derl1 | Cox6a2 | Tmem229b | |
| Emd | Inpp5f | Ndufb2 | Cox7c | |
| Cd63 | Mrps12 | Ndufb4 | Dgkh | |
| Acot13 | 6330403K07Rik | Rgs4 | Cox8a | |
| Hist1h4i | Ntrk2 | Srp9 | Gm14085 | |
| Ufm1 | Gnai2 | Trappc2l | Gm30173 | |
| Tmem256 | Bpnt1 | Rcan3 | Cntnap2 | |

vs

| $CD81^{high}$ | | | | |
|---|---|---|---|---|
| Cd81 | Fam234a | Il1r1 | Bcl3 | Leprot |
| Rbp4 | Gstm1 | Ldlr | Higd1a | Ifih1 |
| Mafb | Hpcal1 | Slc6a6 | Wnk4 | Ankra2 |
| Shisal2b | Gadd45b | Ssr2 | P3h4 | St3gal6 |
| Cd79a | Ctso | Tmcc3 | Fnta | Gpd1 |
| Fxyd3 | Klc3 | Snrnp70 | 1810043G02Rik | Gm2a |
| Ramp1 | Cxxc5 | Fdft1 | Stard5 | Arhgef28 |
| Gpx3 | Dynll1 | Pdia3 | H3f3a | Dbn1 |
| Hist3h2ba | Foxp1 | Calb1 | Nenf | Rspo4 |
| Tspan8 | Alcam | Tmsb15b2 | Itpr1 | Soat1 |
| Cltrn | Ubc | Nfix | Lefty1 | Gchfr |
| Tshz2 | Lgals3bp | Fam213a | Oasl1 | Abhd17b |
| Igfbp7 | Cdkn1a | Kdelr3 | Tor2a | Slc35b3 |
| Ffar4 | H2-Q2 | Ank | Necab2 | Mslnl |
| Tnfrsf12a | Ankrd44 | Dusp26 | Impa1 | Nap1l5 |
| Kcnk16 | Cplx2 | Cmas | Thoc3 | Cd44 |
| Cd24a | Enpp2 | Ap1s1 | Rcn1 | Kcnk3 |
| Aplp1 | Irgm1 | Mycbp | Ube2e2 | Klhl22 |
| Mid1ip1 | Tmem184a | Arrdc4 | Hmgn1 | Nab2 |
| Lpl | Fxyd6 | Prelid3b | Anxa6 | Pdgfrl |
| Cldn3 | Wipi1 | App | Ube3c | Sesn2 |
| Txnip | Fabp5 | Mapre3 | Rpusd1 | Pcbp4 |
| Dbpht2 | Shisa5 | Klhdc8b | Scarb1 | Gclc |
| Serping1 | Gnb2 | Gm26699 | Ppp3ca | Zfp512 |
| Tmsb10 | Pgrmc1 | Tspan15 | Myo1b | Fez1 |
| Uchl1 | Elavl4 | Tmbim6 | Rhoc | Dhcr24 |
| Selenop | Ncam1 | Marcksl1 | Efhd2 | Tln2 |
| Pla2g16 | Chgb | C1qtnf4 | Slc37a1 | |
| Gnai1 | Fam20c | Rpn1 | Kcnk1 | |
| Pla2g2f | Upp1 | Arhgdig | Arf5 | |
| Ucp2 | Wnt4 | Samd9l | Chp1 | |
| Gstp1 | Fhad1 | Oaz2 | Tpst1 | |
| Anxa11 | Ndufa4 | Plp2 | Abcc3 | |
| Fos | Spint1 | Bst2 | Snhg20 | |
| Hmgn2 | Atp1a1 | Pink1 | Dhcr7 | |
| S100a11 | Aqp4 | Prdx4 | Isyna1 | |
| Mlxipl | Snhg18 | Cib1 | Lsm14a | |
| Rab3b | Scg3 | BC005561 | Runx1t1 | |
| Dnase2a | Nudt13 | Ctsd | Snx24 | |
| Ifit3 | Psmb8 | Gstm5 | Snhg11 | |
| Junb | Sox4 | Ocrl | Nsdhl | |
| Folr1 | Gata6 | Gm11837 | Ddhd2 | |
| Anpep | Xaf1 | Pnn | Mvd | |
| Limd2 | Isg15 | Tmed3 | Acat2 | |
| Ly6e | Prdx1 | Gpr180 | Sh2d5 | |
| Hap1 | Rnf138rt1 | Rgs11 | Gprasp2 | |
| Eci2 | Ifitm2 | 1500011B03Rik | Pla2g2d | |
| Cldn4 | Agpat4 | Rab34 | Tox | |
| Meg3 | Aacs | Calm2 | Hmgcl | |
| Pdzk1ip1 | 5330417C22Rik | Mpped2 | Rfx6 | |
| Ctsz | H2-D1 | Jup | Rorc | |
| Idh1 | Cnot6l | Dusp5 | Arl6 | |
| Apobec3 | Cd9 | Srsf3 | Pik3ip1 | |
| Zbtb20 | Trp53i13 | Pdcd6 | Klf10 | |
| Tssc4 | Ube2l6 | Tmem165 | Pacsin1 | |
| Cd200 | Pax6 | Tmed4 | Prss23 | |
| Crip1 | Ypel3 | Txn1 | Dhx58 | |
| Fgf12 | Trp53i11 | Por | Msi1 | |
| Bambi | Ambp | Slc29a1 | Spata7 | |
| Hmgcs1 | Itm2c | Mthfd2l | Scarf2 | |
| Pkib | Itm2b | Nell1 | Fut8 | |
| Pcp4 | Irf1 | Kdm1a | Cpt2 | |
| Bik | Sumo2 | Sult1d1 | Tmsb15l | |
| Maged2 | Hnrnpa1 | Sdf2 | St14 | |
| Tspan7 | Tomm22 | Psmd9 | Scn3a | |
| Lrpprc | Ier2 | Ppp1r14b | Jpt1 | |
| Rgs16 | Qsox1 | Eif2ak2 | AC149090.1 | |
| Ifit3b | Bsg | Cldn6 | Fam57b | |
| Epcam | Pon2 | Cd151 | Nebl | |
| Tspo | Vwa5b2 | Tmem132b | Tspan33 | |
| Btg2 | Tpm1 | Slc29a4 | Rtn4rl1 | |
| Ormdl3 | Card19 | Rbms1 | Synpr | |

# 7 List of publications

**CD81 marks immature and dedifferentiated pancreatic β-cells.**

**Salinno** C, Büttner M, Cota P, Tritschler S, Tarquis-Medina M, Bastidas-Ponce A, Scheibner K, Burtscher I, Böttcher A, Theis FJ, Bakhti M, Lickert H.Mol Metab. 2021 Feb 11;49:101188. doi: 10.1016/j.molmet.2021.101188. Online ahead of print.PMID: 33582383

**Generation of a Novel Nkx6-1 Venus Fusion Reporter Mouse Line**

Ingo Burtscher, Marta Tarquis-Medina, Ciro **Salinno**, Julia Beckenbauer, Mostafa Bakhti, Heiko Lickert. Int. J. Mol. Sci. 2021, 22(7), 3434; https://doi.org/10.3390/ijms22073434

**The glucose-dependent insulinotropic polypeptide (GIP) regulates body weight and food intake via CNS-GIPR signaling.**

Zhang Q, Delessa CT, Augustin R, Bakhti M, Colldén G, Drucker DJ, Feuchtinger A, Caceres CG, Grandl G, Harger A, Herzig S, Hofmann S, Holleman CL, Jastroch M, Keipert S, Kleinert M, Knerr PJ, Kulaj K, Legutko B, Lickert H, Liu X, Luippold G, Lutter D, Malogajski E, Medina MT, Mowery SA, Blutke A, Perez-Tilve D, **Salinno C**, Sehrer L, DiMarchi RD, Tschöp MH, Stemmer K, Finan B, Wolfrum C, Müller TD.Cell Metab. 2021 Feb 3:S1550-4131(21)00015-2. doi: 10.1016/j.cmet.2021.01.015. Online ahead of print.PMID: 33571454

**β-Cell Maturation and Identity in Health and Disease.**

**Salinno C**, Cota P, Bastidas-Ponce A, Tarquis-Medina M, Lickert H, Bakhti M.Int J Mol Sci. 2019 Oct 30;20(21):5417. doi: 10.3390/ijms20215417.PMID: 31671683. Review.

**Comprehensive single cell mRNA profiling reveals a detailed roadmap for pancreatic endocrinogenesis.**

Bastidas-Ponce A, Tritschler S, Dony L, Scheibner K, Tarquis-Medina M, **Salinno C**, Schirge S, Burtscher I, Böttcher A, Theis FJ, Lickert H, Bakhti M.Development. 2019 Jun 17;146(12):dev173849. doi: 10.1242/dev.173849.PMID: 31160421

**Conditional islet hypovascularisation does not preclude beta cell expansion during pregnancy in mice.**

Staels W, Heremans Y, Leuckx G, Van Gassen N, **Salinno C**, De Groef S, Cools M, Keshet E, Dor Y, Heimberg H, De Leu N.Diabetologia. 2017 Jun;60(6):1051-1056. doi: 10.1007/s00125-017-4243-1. Epub 2017 Mar 16.PMID: 28299380

# 8 Acknowledgments

I would like to thank Prof. Heiko Lickert for giving me the chance to work in such an incredible scientific environment and for allowing me to become an independent thinker.

Grateful to Dr. Mostafa Bakhti (Mos!) for being a friend, a mentor and a supervisor. He accepted me in his group and somehow that was the turning point of my PhD story. Above all, I thank him for believing in me when I didn´t do it enough myself.

Special thanks go to Dr. Ingo Burtscher and Donna Thompson, not only for their constant support in the everyday lab life but for creating with me a true bond that goes much further than work.

Next in line, Dr. Aimee Bastidas-Ponce (aka Mamacita), my (PhD) sister. From her I have learned a lot inside and outside the lab. She has a great heart, one of a kind. She was the one telling me the things I didn´t want to hear and, in a way, pushed me to overcome my limits. She has also been a constant source of food, alcohol and mental support in these long years. For all of these and more, I´ll be forever grateful to her.

Special thanks go to the group of girls that has been there for me throughout my PhD: Marta, Kathi and Perla! Not only they have been amazing colleagues, always ready to help and support, but also, they have become my Munich´s family. With them, I have always felt comfortable to be whoever I wanted to be and I have never felt misplaced around them. This incredible group of people provided a solid base on which to lean when I felt at my worst but also the best party gang to share my best moments.

So many other people have crossed my path during these years. Among them, I feel to mention Pallavi, Lisanne, Francesco (Dede), Anna, Joanne, Michi, Julia, Anika, Annalisa, Kerstin, Jessi, Noel, Christian, Sofia, Phivos, Hans, Ernesto, Sami and my long-distance friends Bubi, Roberta, Nicola and Emanuele! I feel extremely blessed for having met each and every one of them. They have enriched my life in many different ways.

Il ringraziamento più importante va alla mia **famiglia**, sempre al mio fianco, costante fonte di supporto. I buongiorno e buonanotte, le videochiamate la domenica, i 1000 km in treno, i pacchi terroni e i video del nipotino che cresce. Per avermi accettato nonostante le distanze, le differenze, i miei silenzi e cambi d'umore. I membri della mia famiglia sono come le radici di un albero che cresce. Lo tengono saldamente attaccato alla terra dalla quale è nato ma lasciano i suoi rami crescere a distanza. Grazie mamma, papà e Veronica!

# 9 Abbreviations

| | |
|---|---|
| 2D | Two Dimension |
| 3D | Three Dimension |
| ADP | Adenosine diphosphate |
| Aldh1a3 | Aldehyde dehydrogenase family 1 member A3 |
| Aldob | Fructose-bisphosphate aldolase B |
| AMPK | 5′ AMP-activated protein kinase |
| Apc | Adenomatous polyposis coli protein |
| Arx | Homeobox protein ARX |
| ATP | Adenosine triphosphate |
| Axin | Axin-1 |
| BP | Bipotent Progenitors |
| Ca2+ | Calcium ion |
| CamKII | Ca2+/calmodulin-dependent protein kinase II |
| Ccnd2 | G1/S-specific cyclin-D2 |
| CD31 | Platelet endothelial cell adhesion molecule |
| CD71 | Transferrin receptor protein 1 |
| CD81 | Target of the antiproliferative antibody 1 |
| Cdh1 | Cadherin-1 |
| Cfap126 | Cilia- and flagella-associated protein 126 |
| Chga | Chromogranin-A |
| Chgb | Chromogranin-B |
| Cpa1 | Carboxypeptidase A1 |
| C-pep | C-Peptide |
| Cpt2 | Carnitine Palmitoyltransferase 2 |
| Ctnnb1 | Catenin Beta 1 |
| DAPI | 4′,6-diamidino-2-phenylindole |
| DGEA | Differential gene expression analysis |
| DM | Diabetes mellitus |
| DNA | Deoxyribonucleic acid |
| Dvl2 | Segment polarity protein dishevelled homolog DVL-2 |
| ECM | Extracellular matrix |
| E-cad | E-cadherin |
| Eif4ebp1 | Eukaryotic translation initiation factor 4E-binding protein 1 |
| Epre | Endocrine precursor |
| Epro | Endocrine progenitor |
| ER | Endoplasmic reticulum |
| ERRγ | Estrogen-related receptor gamma |
| FACS | Fluorescence-activated cell sorting |
| FAK | Focal adhesion kinase |
| Fev | E26 transformation-specific transcriptional factor |
| Fltp | Flattop |
| Foxa2 | Forkhead Box A2 |
| Foxm1 | Forkhead box protein M1 |
| FVR | Fltp Venus Reporter |
| Fzd | Frizzled |
| G6P | Glucose 6-phosphate |
| Gapdh | Glyceraldehyde 3-phosphate dehydrogenase |
| Gcg | Glucagon |
| Gck | Glucokinase |
| GDM | Gestational diabetes mellitus |
| Ghrl | Ghrelin |
| GLP-1 | Glucagon-like peptide 1 |

| | |
|---|---|
| Glp1r | Glucagon-like peptide 1 receptor |
| Glu | Glucose |
| GM130 | Golgin subfamily A member 2 |
| GSIS | Glucose stimulated insulin secretion |
| Gsk3β | Glycogen synthase kinase-3 beta |
| hESC | Human embryonic stem cell |
| HNF1a | Hepatocyte nuclear factor 1-alpha |
| HNF1b | Hepatocyte nuclear factor 1-beta |
| HNF4a | Hepatocyte nuclear factor 4-alpha |
| Hsp90 | Heat shock protein 90 |
| Iapp | Islet amyloid polypeptide |
| iCre | Inducible Cre |
| IDF | International Diabetes Federation |
| IF | Immunofluorescence |
| Ins1 | Insulin 1 |
| iPSC | Induced pluripotent stem cell |
| Isl1 | Insulin gene enhancer protein isl-1 |
| Jnk | c-Jun N-terminal kinase |
| KO | Knock out |
| Lamp1 | Lysosomal-associated membrane protein 1 |
| Ldha | Lactate Dehydrogenase A |
| LED | Large extracellular loop |
| Lkb1 | Serine/threonine-protein kinase STK11 |
| LRP | Low-density lipoprotein receptor-related protein |
| Mafa | V-maf musculoaponeurotic fibrosarcoma oncogene homolog A |
| Mafb | V-maf musculoaponeurotic fibrosarcoma oncogene homolog B |
| MAPK | Mitogen-activated protein kinase |
| Mki67 | Marker Of Proliferation Ki-67 |
| MODY | Maturity Onset Diabetes of the Young |
| MPC | Multipotent progenitor cell |
| mTmG | Membrane tomato membrane GFP |
| mTOR | Mechanistic target of rapamycin |
| mTORC1 | mTOR Complex 1 |
| mTORC2 | mTOR Complex 2 |
| NeuroD1 | Neurogenic differentiation 1 |
| Ngn3 | Neurogenin-3 |
| Nkx2-2 | Homeobox protein Nkx-2.2 |
| Nkx6-1 | Homeobox protein Nkx-6.1 |
| Nkx6-1 | Homeobox protein Nkx-6.1 |
| NOD | Non-obese diabetic |
| NPY | Neuropeptide Y |
| PAGA | Partition-based Graph Abstraction |
| Pal | Palmitate |
| Pax4 | Paired box protein Pax-4 |
| Pc | Pyruvate Carboxylase) |
| PC | Protein Class |
| PCP | Planar Cell Polarity |
| Pcsk1 | Neuroendocrine convertase 1 |
| Pcx | Pyruvate carboxylase |
| Pdx1 | Pancreatic And Duodenal Homeobox 1 |
| PEG-Ins | PEG-Insulin |
| PEG-Ins/GLP-1-Oe | PEG-Insulin with GLP-1-Estrogen |
| Ppy | Pancreatic Polypeptide |
| Pro-Ins | Pro-Insulin |

| | |
|---|---|
| pS6 | Phosphor ribosomal protein S6 |
| PTEN | Phosphatase and tensin homolog |
| Ptf1a | Pancreas Associated Transcription Factor 1a |
| qPCR | Quantitative Polymerase Chain Reaction |
| Raptor | Regulatory-associated protein of mTOR |
| Rbp4 | Retinol-binding protein 4 |
| Rheb | GTP-binding protein Rheb |
| Rictor | Rapamycin-insensitive companion of mTOR |
| RNA | Ribonucleic acid |
| ROS | Reactive oxygen species |
| RT-qPCR | Real Time Quantitative Polymerase Chain Reaction |
| S6K | Ribosomal protein S6 kinase beta-1 |
| SASP | Senescence-associated secretory phenotype |
| scRNA-seq | Single cell RNA sequencing |
| SC-β-cells | Stem cell derived β-cells |
| SED | Small extracellular loop |
| SGLT2 | Sodium/glucose cotransporter 2 |
| Slc2a2 | Solute carrier family 2 |
| SNAP | Synaptosomal-Associated Protein |
| SNARE | SNAP REceptor |
| Sox9 | Transcription factor SOX-9 |
| Sst | Somatostatin |
| STZ | Streptozotocin |
| SYT | Synaptotagmin |
| Syt4 | Synaptotagmin-4 |
| Syt7 | Synaptotagmin-7 |
| T1D | Type 1 diabetes |
| T2D | Type 2 diabetes |
| TAZ | WW domain-containing transcription regulator protein 1 |
| TEAD | Transcriptional enhancer factor TEF |
| TF | Transcription factor |
| Tfr1 | Transferrin receptor protein 1 |
| Tsc2 | Tuberin |
| Tun | Tunicamycin |
| Ucn3 | Urocortin 3 |
| UMAP | Uniform Manifold Approximation and Projection |
| UPR | Unfolded protein response |
| VAMP | Vesicle-associated membrane protein |
| VDCC | Voltage-dependent calcium channel |
| VEGF-A | Vascular endothelial growth factor A |
| Wnt | Wingless-related integration site |
| WT | Wild type |
| YAP | Yes-associated protein 1 |
| α-cell | Alpha |
| β-cell | Beta cell |
| γ-cell | Gamma cell |
| δ-cell | Delta cell |
| ε-cell | Epsilon cell |

# 10 Bibliography


Abbott, C. (1996). Mouse Genetics: Concepts and Applications. By Lee Silver.Oxford University Press. 1995. 362 pages. Price £40.00 ISBN 0 195 07554 4. *Genetical Research*, *68*(2). https://doi.org/10.1017/s001667230003411x

Aguayo-Mazzucato, C., Andle, J., Lee, T. B., Midha, A., Talemal, L., Chipashvili, V., Hollister-Lock, J., van Deursen, J., Weir, G., & Bonner-Weir, S. (2019). Acceleration of β Cell Aging Determines Diabetes and Senolysis Improves Disease Outcomes. *Cell Metabolism*. https://doi.org/10.1016/j.cmet.2019.05.006

Ahlgren, U., Jonsson, J., & Edlund, H. (1996). The morphogenesis of the pancreatic mesenchyme is uncoupled from that of the pancreatic epithelium in IPF1/PDX1-deficient mice. *Development*, *122*(5), 1409–1416.

Ahrén, B. (2012). Islet nerves in focus-Defining their neurobiological and clinical role. In *Diabetologia*. https://doi.org/10.1007/s00125-012-2727-6

Ainscow, E. K., Zhao, C., & Rutter, G. A. (2000). Acute overexpression of lactate dehydrogenase-A perturbs β-cell mitochondrial metasbolism and insulin secretion. *Diabetes*. https://doi.org/10.2337/diabetes.49.7.1149

Akhmanova, M., Osidak, E., Domogatsky, S., Rodin, S., & Domogatskaya, A. (2015). Physical, Spatial, and Molecular Aspects of Extracellular Matrix of in Vivo Niches and Artificial Scaffolds Relevant to Stem Cells Research. *Stem Cells International*. https://doi.org/10.1155/2015/167025

Alcazar, O., & Buchwald, P. (2019). Concentration-Dependency and Time Profile of Insulin Secretion: Dynamic Perifusion Studies With Human and Murine Islets. *Frontiers in Endocrinology*, *10*. https://doi.org/10.3389/fendo.2019.00680

Alessandra, G., Algerta, M., Paola, M., Carsten, S., Cristina, L., Paolo, M., Elisa, M., Gabriella, T., & Carla, P. (2020). Shaping Pancreatic β-Cell Differentiation and Functioning: The Influence of Mechanotransduction. *Cells*. https://doi.org/10.3390/cells9020413

Alvarez-Dominguez, J. R., Donaghey, J., Rasouli, N., Kenty, J. H. R., Helman, A., Charlton, J., Straubhaar, J. R., Meissner, A., & Melton, D. A. (2020). Circadian Entrainment Triggers Maturation of Human In Vitro Islets. *Cell Stem Cell*. https://doi.org/10.1016/j.stem.2019.11.011

Alvarsson, A., Jimenez-Gonzalez, M., Li, R., Rosselot, C., Tzavaras, N., Wu, Z., Stewart, A. F., Garcia-Ocaña, A., & Stanley, S. A. (2020). A 3D atlas of the dynamic and regional variation of pancreatic innervation in diabetes. *Science Advances*. https://doi.org/10.1126/sciadv.aaz9124

Arda, H. E., Benitez, C. M., & Kim, S. K. (2013). Gene regulatory networks governing pancreas development. In *Developmental Cell* (Vol. 25, Issue 1, pp. 5–13). https://doi.org/10.1016/j.devcel.2013.03.016

Arous, C., & Wehrle-Haller, B. (2017). Role and impact of the extracellular matrix on integrin-mediated pancreatic β-cell functions. In *Biology of the Cell*. https://doi.org/10.1111/boc.201600076

Arrojo e Drigo, R., Lev-Ram, V., Tyagi, S., Ramachandra, R., Deerinck, T., Bushong, E., Phan, S., Orphan, V., Lechene, C., Ellisman, M. H., & Hetzer, M. W. (2019). Age Mosaicism across Multiple Scales in Adult Tissues. *Cell Metabolism*. https://doi.org/10.1016/j.cmet.2019.05.010

Artner, I., Blanchi, B., Raum, J. C., Guo, M., Kaneko, T., Cordes, S., Sieweke, M., & Stein, R. (2007). MafB is required for islet beta cell maturation. *Proceedings of the National Academy of Sciences*. https://doi.org/10.1073/pnas.0700013104

Artner, Isabella, Blanchi, B., Raum, J. C., Guo, M., Kaneko, T., Cordes, S., Sieweke, M., & Stein, R. (2007). MafB is required for islet β cell maturation. *Proceedings of the National Academy of Sciences of the United States of America*, *104*(10), 3853–3858. https://doi.org/10.1073/pnas.0700013104

Bader, E., Migliorini, A., Gegg, M., Moruzzi, N., Gerdes, J., Roscioni, S. S., Bakhti, M., Brandl, E., Irmler, M., Beckers, J., Aichler, M., Feuchtinger, A., Leitzinger, C., Zischka, H., Sattler, R. W., Jastroch, M., Tschöp, M., Machicao, F., Staiger, H., … Lickert, H. (2016). Identification of proliferative and mature β-cells in the islets of langerhans. *Nature*, *535*(7612), 430–434. https://doi.org/10.1038/nature18624

Baeyens, L., Hindi, S., Sorenson, R. L., & German, M. S. (2016). β-Cell adaptation in pregnancy. In *Diabetes, Obesity and Metabolism* (Vol. 18, pp. 63–70). https://doi.org/10.1111/dom.12716

Baron, M., Veres, A., Wolock, S. L., Faust, A. L., Gaujoux, R., Vetere, A., Ryu, J. H., Wagner, B. K., Shen-Orr, S. S., Klein, A. M., Melton, D. A., & Yanai, I. (2016). A Single-Cell Transcriptomic Map of the Human and Mouse Pancreas Reveals Inter- and Intra-cell Population Structure. *Cell Systems*, *3*(4), 346-360.e4. https://doi.org/10.1016/j.cels.2016.08.011

Bastidas-Ponce, Aimée, Roscioni, S. S., Burtscher, I., Bader, E., Sterr, M., Bakhti, M., & Lickert, H. (2017). Foxa2 and Pdx1 cooperatively regulate postnatal maturation of pancreatic β-cells. *Molecular Metabolism*, *6*(6), 524–534. https://doi.org/10.1016/j.molmet.2017.03.007

Bastidas-Ponce, Aimeé, Scheibner, K., Lickert, H., & Bakhti, M. (2017). Cellular and molecular mechanisms coordinating pancreas development. In *Development (Cambridge)* (Vol. 144, Issue 16, pp. 2873–2888). https://doi.org/10.1242/dev.140756

Bastidas-Ponce, Aimée, Tritschler, S., Dony, L., Scheibner, K., Tarquis-Medina, M., Salinno, C., Schirge, S., Burtscher, I., Böttcher, A., Theis, F. J., Lickert, H., & Bakhti, M. (2019). Comprehensive single cell mRNA profiling reveals a detailed roadmap for pancreatic endocrinogenesis. *Development (Cambridge)*. https://doi.org/10.1242/dev.173849

Baumgartner, B. K., Cash, G., Hansen, H., Ostler, S., & Murtaugh, L. C. (2014). Distinct requirements for beta-catenin in pancreatic epithelial growth and patterning. *Developmental Biology*. https://doi.org/10.1016/j.ydbio.2014.03.019

Beamish, C. A., Zhang, L., Szlapinski, S. K., Strutt, B. J., & Hill, D. J. (2017). An increase in immature β-cells lacking Glut2 precedes the expansion of β-cell mass in the pregnant mouse. *PLoS ONE*. https://doi.org/10.1371/journal.pone.0182256

Benjamin, D., & Hall, M. N. (2014). MTORC1: Turning off is just as important as turning on. In *Cell* (Vol. 156, Issue 4, pp. 627–628). https://doi.org/10.1016/j.cell.2014.01.057

Berthault, C., Staels, W., & Scharfmann, R. (2020). Purification of pancreatic endocrine subsets reveals increased iron metabolism in beta cells. *Molecular Metabolism*. https://doi.org/10.1016/j.molmet.2020.101060

Blum, B., Hrvatin, S., Schuetz, C., Bonal, C., Rezania, A., & Melton, D. a. (2012). Functional beta-cell maturation is marked by an increased glucose threshold and by expression of urocortin 3. *Nature Biotechnology*, *30*(3), 261–264. https://doi.org/10.1038/nbt.2141

Bonner-Weir, S. (2000a). Perspective: Postnatal pancreatic β cell growth. In *Endocrinology* (Vol. 141, Issue 6, pp. 1926–1929). https://doi.org/10.1210/endo.141.6.7567

Bonner-Weir, S. (2000b). Perspective: Postnatal pancreatic β cell growth. In *Endocrinology*. https://doi.org/10.1210/endo.141.6.7567

Bonner-Weir, S., Aguayo-Mazzucato, C., & Weir, G. C. (2016). Dynamic development of the pancreas from birth to adulthood. In *Upsala Journal of Medical Sciences* (Vol. 121, Issue 2, pp. 155–158). https://doi.org/10.3109/03009734.2016.1154906

Borden, P., Houtz, J., Leach, S. D., & Kuruvilla, R. (2013). Sympathetic innervation during development is necessary for pancreatic islet architecture and functional maturation. *Cell Reports*. https://doi.org/10.1016/j.celrep.2013.06.019

Bosco, D., Rouiller, D. G., & Halban, P. A. (2007). Differential expression of E-cadherin at the surface of rat β-cells as a marker of functional heterogeneity. *Journal of Endocrinology*. https://doi.org/10.1677/JOE-06-0169

Böttcher, A., Büttner, M., Tritschler, S., Sterr, M., Aliluev, A., Oppenländer, L., Burtscher, I., Sass, S., Irmler, M., Beckers, J., Ziegenhain, C., Enard, W., Schamberger, A. C., Verhamme, F. M., Eickelberg, O., Theis, F. J., & Lickert, H. (2021). Non-canonical Wnt/PCP signalling regulates intestinal stem cell lineage priming towards enteroendocrine and Paneth cell fates. *Nature Cell Biology*. https://doi.org/10.1038/s41556-020-00617-2

Bourgeois, S., Sawatani, T., Van Mulders, A., De Leu, N., Heremans, Y., Heimberg, H., Cnop, M., & Staels, W. (2021). Towards a Functional Cure for Diabetes Using Stem Cell-Derived Beta Cells: Are We There Yet? In *Cells* (Vol. 10, Issue 1, pp. 1–24). https://doi.org/10.3390/cells10010191

Brennand, K., & Melton, D. (2009). Slow and steady is the key to β-cell replication. In *Journal of Cellular and Molecular Medicine*. https://doi.org/10.1111/j.1582-4934.2008.00635.x

Brereton, M. F., Rohm, M., & Ashcroft, F. M. (2016). β-Cell dysfunction in diabetes: a crisis of identity? In *Diabetes, Obesity and Metabolism*. https://doi.org/10.1111/dom.12732

Brereton, Melissa F., Vergari, E., Zhang, Q., & Clark, A. (2015). Alpha-, Delta- and PP-cells: Are They the Architectural Cornerstones of Islet Structure and Co-ordination? *Journal of Histochemistry and Cytochemistry*, *63*(8), 575–591. https://doi.org/10.1369/0022155415583535

Brissova, M., Fowler, M. J., Nicholson, W. E., Chu, A., Hirshberg, B., Harlan, D. M., & Powers, A. C. (2005). Assessment of human pancreatic islet architecture and composition by laser scanning confocal microscopy. *Journal of Histochemistry and Cytochemistry*. https://doi.org/10.1369/jhc.5C6684.2005

Brouwers, B., Coppola, I., Vints, K., Dislich, B., Jouvet, N., Van Lommel, L., Segers, C., Gounko, N. V., Thorrez, L., Schuit, F., Lichtenthaler, S. F., Estall, J. L., Declercq, J., Ramos-Molina, B., & Creemers, J. W. M. (2021). Loss of Furin in β-Cells Induces an mTORC1-ATF4 Anabolic Pathway That Leads to β-Cell Dysfunction. *Diabetes*, *70*(2), 492–503. https://doi.org/10.2337/db20-0474

Burlison, J. S., Long, Q., Fujitani, Y., Wright, C. V. E., & Magnuson, M. A. (2008). Pdx-1 and Ptf1a concurrently determine fate specification of pancreatic multipotent progenitor cells. *Developmental Biology*. https://doi.org/10.1016/j.ydbio.2008.01.011

Burris, R. E., & Hebrok, M. (2007). Pancreatic innervation in mouse development and β-cell

regeneration. *Neuroscience*. https://doi.org/10.1016/j.neuroscience.2007.09.079

Burtscher, I., Tarquis-medina, M., Salinno, C., Beckenbauer, J., Bakhti, M., & Lickert, H. (2021). Generation of a novel Nkx6-1 Venus fusion reporter mouse line. *BioRxiv*, *22*, doi: https://doi.org/10.1101/2021.01.29.428800. https://www.mdpi.com/1422-0067/22/7/3434/htm

Byrnes, L. E., Wong, D. M., Subramaniam, M., Meyer, N. P., Gilchrist, C. L., Knox, S. M., Tward, A. D., Ye, C. J., & Sneddon, J. B. (2018). Lineage dynamics of murine pancreatic development at single-cell resolution. *Nature Communications*. https://doi.org/10.1038/s41467-018-06176-3

Cabrera, O., Berman, D. M., Kenyon, N. S., Ricordi, C., Berggren, P. O., & Caicedo, A. (2006). The unique cytoarchitecture of human pancreatic islets has implications for islet cell function. *Proceedings of the National Academy of Sciences of the United States of America*. https://doi.org/10.1073/pnas.0510790103

Cebola, I., Rodríguez-Seguí, S. A., Cho, C. H. H., Bessa, J., Rovira, M., Luengo, M., Chhatriwala, M., Berry, A., Ponsa-Cobas, J., Maestro, M. A., Jennings, R. E., Pasquali, L., Morán, I., Castro, N., Hanley, N. A., Gomez-Skarmeta, J. L., Vallier, L., & Ferrer, J. (2015). TEAD and YAP regulate the enhancer network of human embryonic pancreatic progenitors. *Nature Cell Biology*. https://doi.org/10.1038/ncb3160

Chien, H. J., Chiang, T. C., Peng, S. J., Chung, M. H., Chou, Y. H., Lee, C. Y., Jeng, Y. M., Tien, Y. W., & Tang, S. C. (2019). Human pancreatic afferent and efferent nerves: mapping and 3-D illustration of exocrine, endocrine, and adipose innervation. *American Journal of Physiology. Gastrointestinal and Liver Physiology*. https://doi.org/10.1152/ajpgi.00116.2019

Choo, A. Y., Roux, P. P., & Blenis, J. (2006). Mind the GAP: Wnt Steps onto the mTORC1 Train. In *Cell*. https://doi.org/10.1016/j.cell.2006.08.025

Cirulli, V., Beattie, G. M., Klier, G., Ellisman, M., Ricordi, C., Quaranta, V., Frasier, F., Ishii, J. K., Hayek, A., & Salomon, D. R. (2000). Expression and Function of αvβ3 and αvβ5 Integrins in the Developing Pancreas. *Journal of Cell Biology*. https://doi.org/10.1083/jcb.150.6.1445

Coffey, G. P., Rajapaksa, R., Liu, R., Sharpe, O., Kuo, C. C., Krauss, S. W., Sagi, Y., Davis, R. E., Staudt, L. M., Sharman, J. P., Robinson, W. H., & Levy, S. (2009). Engagement of CD81 induces ezrin tyrosine phosphorylation and its cellular redistribution with filamentous actin. *Journal of Cell Science*. https://doi.org/10.1242/jcs.045658

Collombat, P., Mansouri, A., Hecksher-sørensen, J., Serup, P., Krull, J., Gradwohl, G., & Gruss, P. (2003). *Opposing actions of Arx and Pax4 in endocrine pancreas development Opposing actions of Arx and Pax4 in endocrine pancreas development*. *4*, 2591–2603. https://doi.org/10.1101/gad.269003

Condon, K. J., & Sabatini, D. M. (2019). Nutrient regulation of mTORC1 at a glance. *Journal of Cell Science*. https://doi.org/10.1242/JCS.222570

Cortijo, C., Gouzi, M., Tissir, F., & Grapin-Botton, A. (2012). Planar Cell Polarity Controls Pancreatic Beta Cell Differentiation and Glucose Homeostasis. *Cell Reports*. https://doi.org/10.1016/j.celrep.2012.10.016

Cottle, L., Gan, W. J., Gilroy, I., Samra, J. S., Gill, A. J., Loudovaris, T., Thomas, H. E., Hawthorne, W. J., Kebede, M. A., & Thorn, P. (2021). Structural and functional polarisation of human pancreatic beta cells in islets from organ donors with and without type 2 diabetes. *Diabetologia*, *64*(3), 618–629. https://doi.org/10.1007/s00125-020-05345-8

Crotta, S., Ronconi, V., Ulivieri, C., Baldari, C. T., Valiente, N. M., Abrignani, S., & Wack, A. (2006). Cytoskeleton rearrangement induced by tetraspanin engagement modulates the activation of T and NK cells. *European Journal of Immunology*. https://doi.org/10.1002/eji.200535527

Da Silva Xavier, G. (2018). The Cells of the Islets of Langerhans. *Journal of Clinical Medicine*, *7*(3), 54. https://doi.org/10.3390/jcm7030054

Da Silva Xavier, G., & Rutter, G. A. (2020). Metabolic and Functional Heterogeneity in Pancreatic β Cells. In *Journal of Molecular Biology* (Vol. 432, Issue 5, pp. 1395–1406). https://doi.org/10.1016/j.jmb.2019.08.005

Dale, R. M., Sisson, B. E., & Topczewski, J. (2009). The emerging role of Wnt/PCP signaling in organ formation. *Zebrafish*. https://doi.org/10.1089/zeb.2008.0563

Davey, C. F., & Moens, C. B. (2017). Planar cell polarity in moving cells: Think globally, act locally. In *Development (Cambridge)*. https://doi.org/10.1242/dev.122804

de Klerk, E., & Hebrok, M. (2021). Stem Cell-Based Clinical Trials for Diabetes Mellitus. In *Frontiers in Endocrinology* (Vol. 12, Issue February). https://doi.org/10.3389/fendo.2021.631463

Dean, P. M., & Matthews, E. K. (1968). Electrical activity in pancreatic islet cells. In *Nature*. https://doi.org/10.1038/219389a0

DeFronzo, R. A., Ferrannini, E., Groop, L., Henry, R. R., Herman, W. H., Holst, J. J., Hu, F. B., Kahn, C. R., Raz, I., Shulman, G. I., Simonson, D. C., Testa, M. A., & Weiss, R. (2015). Type 2 diabetes mellitus. *Nature Reviews Disease Primers*. https://doi.org/10.1038/nrdp.2015.19

Diaferia, G. R., Jimenez-Caliani, A. J., Ranjitkar, P., Yang, W., Hardiman, G., Rhodes, C. J., Crisa, L., & Cirulli, V. (2013). β1 integrin is a crucial regulator of pancreatic β-cell expansion. *Development (Cambridge)*. https://doi.org/10.1242/dev.098533

Dolai, S., Xie, L., Zhu, D., Liang, T., Qin, T., Xie, H., Kang, Y., Chapman, E. R., & Gaisano, H. Y. (2016). Synaptotagmin-7 functions to replenish insulin granules for exocytosis in human islet β-cells. *Diabetes*. https://doi.org/10.2337/db15-1436

Dore, B. A., Grogan, W. M. L., Madge, G. E., & Webb, S. R. (1981). Biphasic development of the postnatal mouse pancreas. *Neonatology*, *40*(5–6), 209–217. https://doi.org/10.1159/000241494

Dorrell, C., Schug, J., Canaday, P. S., Russ, H. A., Tarlow, B. D., Grompe, M. T., Horton, T., Hebrok, M., Streeter, P. R., Kaestner, K. H., & Grompe, M. (2016a). Human islets contain four distinct subtypes of β cells. *Nature Communications*. https://doi.org/10.1038/ncomms11756

Dorrell, C., Schug, J., Canaday, P. S., Russ, H. A., Tarlow, B. D., Grompe, M. T., Horton, T., Hebrok, M., Streeter, P. R., Kaestner, K. H., & Grompe, M. (2016b). Human islets contain four distinct subtypes of β cells. *Nature Communications*, *7*. https://doi.org/10.1038/ncomms11756

Du, J., Zu, Y., Li, J., Du, S., Xu, Y., Zhang, L., Jiang, L., Wang, Z., Chien, S., & Yang, C. (2016). Extracellular matrix stiffness dictates Wnt expression through integrin pathway. *Scientific Reports*. https://doi.org/10.1038/srep20395

Ellis, H. (2007). Anatomy of the pancreas. In *Surgery*. https://doi.org/10.1016/j.mpsur.2006.12.005

Ewen-Campen, B., Comyn, T., Vogt, E., & Perrimon, N. (2020). No Evidence that Wnt Ligands Are Required for Planar Cell Polarity in Drosophila. *Cell Reports*.

https://doi.org/10.1016/j.celrep.2020.108121

Figeac, F., Uzan, B., Faro, M., Chelali, N., Portha, B., & Movassat, J. (2010). Neonatal growth and regeneration of β-cells are regulated by the Wnt/β-catenin signaling in normal and diabetic rats. *American Journal of Physiology - Endocrinology and Metabolism*. https://doi.org/10.1152/ajpendo.00538.2009

Formstone, C. J., & Little, P. F. R. (2001). The flamingo-related mouse Celsr family (Celsr1-3) genes exhibit distinct patterns of expression during embryonic development. *Mechanisms of Development*. https://doi.org/10.1016/S0925-4773(01)00515-9

Gan, Wan J., Zavortink, M., Ludick, C., Templin, R., Webb, R., Webb, R., Ma, W., Poronnik, P., Parton, R. G., Gaisano, H. Y., Shewan, A. M., & Thorn, P. (2017). Cell polarity defines three distinct domains in pancreatic β-cells. *Journal of Cell Science*, *130*(1), 143–151. https://doi.org/10.1242/jcs.185116

Gan, Wan Jun, Do, O. H., Cottle, L., Ma, W., Kosobrodova, E., Cooper-White, J., Bilek, M., & Thorn, P. (2018). Local Integrin Activation in Pancreatic β Cells Targets Insulin Secretion to the Vasculature. *Cell Reports*. https://doi.org/10.1016/j.celrep.2018.08.035

Gao, T., Zhou, D., Yang, C., Singh, T., Penzo-Méndez, A., Maddipati, R., Tzatsos, A., Bardeesy, N., Avruch, J., & Stanger, B. Z. (2013). Hippo signaling regulates differentiation and maintenance in the exocrine pancreas. *Gastroenterology*. https://doi.org/10.1053/j.gastro.2013.02.037

García-Delgado, N., Velasco, M., Sánchez-Soto, C., Díaz-García, C. M., & Hiriart, M. (2018). Calcium channels in postnatal development of rat pancreatic beta cells and their role in insulin secretion. *Frontiers in Endocrinology*. https://doi.org/10.3389/fendo.2018.00040

Garofano, A., Czernichow, P., & Bréant, B. (1998). Beta-cell mass and proliferation following late fetal and early postnatal malnutrition in the rat. *Diabetologia*, *41*(9), 1114–1120. https://doi.org/10.1007/s001250051038

Gegg, M., Böttcher, A., Burtscher, I., Hasenoeder, S., Van Campenhout, C., Aichler, M., Walch, A., Grant, S. G. N., & Lickert, H. (2014). Flattop regulates basal body docking and positioning in mono- and multiciliated cells. *ELife*, *3*. https://doi.org/10.7554/eLife.03842

George, N. M., Day, C. E., Boerner, B. P., Johnson, R. L., & Sarvetnick, N. E. (2012). Hippo Signaling Regulates Pancreas Development through Inactivation of Yap. *Molecular and Cellular Biology*. https://doi.org/10.1128/mcb.01034-12

George, Nicholas M., Boerner, B. P., Mir, S. U. R., Guinn, Z., & Sarvetnick, N. E. (2015). Exploiting expression of hippo effector, yap, for expansion of functional islet mass. *Molecular Endocrinology*. https://doi.org/10.1210/me.2014-1375

Georgia, S., & Bhushan, A. (2004a). β cell replication is the primary mechanism for maintaining postnatal β cell mass. *Journal of Clinical Investigation*. https://doi.org/10.1172/JCI22098

Georgia, S., & Bhushan, A. (2004b). β cell replication is the primary mechanism for maintaining postnatal β cell mass. *Journal of Clinical Investigation*, *114*(7), 963–968. https://doi.org/10.1172/JCI22098

Gerst, F., Jaghutriz, B. A., Staiger, H., Schulte, A. M., Lorza-Gil, E., Kaiser, G., Panse, M., Haug, S., Heni, M., Schütz, M., Stadion, M., Schürmann, A., Marzetta, F., Ibberson, M., Sipos, B., Fend, F., Fleming, T., Nawroth, P. P., Königsrainer, A., … Wagner, R. (2018). The expression of aldolase B in islets is negatively associated with insulin secretion in humans. *Journal of Clinical Endocrinology and*

*Metabolism*. https://doi.org/10.1210/jc.2018-00791

Ghazizadeh, Z., Kao, D. I., Amin, S., Cook, B., Rao, S., Zhou, T., Zhang, T., Xiang, Z., Kenyon, R., Kaymakcalan, O., Liu, C., Evans, T., & Chen, S. (2017). ROCKII inhibition promotes the maturation of human pancreatic beta-like cells. *Nature Communications*. https://doi.org/10.1038/s41467-017-00129-y

Gilbert, J. M., & Blum, B. (2018). Synaptotagmins Tweak Functional β Cell Maturation. In *Developmental Cell*. https://doi.org/10.1016/j.devcel.2018.04.018

Gray, R. S., Roszko, I., & Solnica-Krezel, L. (2011). Planar Cell Polarity: Coordinating Morphogenetic Cell Behaviors with Embryonic Polarity. *Developmental Cell*. https://doi.org/10.1016/j.devcel.2011.06.011

Guillam, M. T., Hümmler, E., Schaerer, E., Wu, J. Y., Birnbaum, M. J., Beermann, F., Schmidt, A., Dériaz, N., & Thorens, B. (1997). Early diabetes and abnormal postnatal pancreatic islet development in mice lacking Glut-2. *Nature Genetics*, *17*(3), 327–330. https://doi.org/10.1038/ng1197-327

Gunasekaran, U., Hudgens, C. W., Wright, B. T., Maulis, M. F., & Gannon, M. (2012). Differential regulation of embryonic and adult β cell replication. In *Cell Cycle*. https://doi.org/10.4161/cc.20545

Guo, J., & Fu, W. (2021). Immune regulation of islet homeostasis and adaptation. *Journal of Molecular Cell Biology*, *12*(10), 764–774. https://doi.org/10.1093/jmcb/mjaa009

Hang, Y., & Stein, R. (2011). MafA and MafB activity in pancreatic β cells. In *Trends in Endocrinology and Metabolism* (Vol. 22, Issue 9, pp. 364–373). https://doi.org/10.1016/j.tem.2011.05.003

Hantak, M. P., Qing, E., Earnest, J. T., & Gallagher, T. (2018). Tetraspanins: Architects of Viral Entry and Exit Platforms. *Journal of Virology*. https://doi.org/10.1128/jvi.01429-17

Hao, M., Li, X., Rizzo, M. A., Rocheleau, J. V., Dawant, B. M., & Piston, D. W. (2005). Regulation of two insulin granule populations within the reserve pool by distinct calcium sources. *Journal of Cell Science*. https://doi.org/10.1242/jcs.02684

Hauge-Evans, A. C., King, A. J., Carmignac, D., Richardson, C. C., Robinson, I. C. A. F., Low, M. J., Christie, M. R., Persaud, S. J., & Jones, P. M. (2009). Somatostatin secreted by islet δ-cells fulfills multipleRoles as a paracrine regulator of islet function. *Diabetes*, *58*(2), 403–411. https://doi.org/10.2337/db08-0792

HELLERSTROM, C., PETERSSON, B., & HELLMAN, B. (1960). Some properties of the B cells in the islet of Langerhans studied with regard to the position of the cells. *Acta Endocrinologica*, *34*, 449–456. https://doi.org/10.1530/acta.0.xxxiv0449

Helman, A., Cangelosi, A. L., Davis, J. C., Pham, Q., Rothman, A., Faust, A. L., Straubhaar, J. R., Sabatini, D. M., & Melton, D. A. (2020a). A Nutrient-Sensing Transition at Birth Triggers Glucose-Responsive Insulin Secretion. *Cell Metabolism*. https://doi.org/10.1016/j.cmet.2020.04.004

Helman, A., Cangelosi, A. L., Davis, J. C., Pham, Q., Rothman, A., Faust, A. L., Straubhaar, J. R., Sabatini, D. M., & Melton, D. A. (2020b). A Nutrient-Sensing Transition at Birth Triggers Glucose-Responsive Insulin Secretion. *Cell Metabolism*, *31*(5), 1004–1016. https://doi.org/10.1016/j.cmet.2020.04.004

Hemler, M. E. (2014). Tetraspanin proteins promote multiple cancer stages. In *Nature Reviews Cancer*. https://doi.org/10.1038/nrc3640

Henquin, J. C., Ishiyama, N., Nenquin, M., Ravier, M. A., & Jonas, J. C. (2002). Signals and pools underlying biphasic insulin secretion. *Diabetes*. https://doi.org/10.2337/diabetes.51.2007.s60

Herzig, S., & Shaw, R. J. (2018). AMPK: Guardian of metabolism and mitochondrial homeostasis. In *Nature Reviews Molecular Cell Biology*. https://doi.org/10.1038/nrm.2017.95

Hogrebe, N. J., Augsornworawat, P., Maxwell, K. G., Velazco-Cruz, L., & Millman, J. R. (2020a). Targeting the cytoskeleton to direct pancreatic differentiation of human pluripotent stem cells. *Nature Biotechnology*. https://doi.org/10.1038/s41587-020-0430-6

Hogrebe, N. J., Augsornworawat, P., Maxwell, K. G., Velazco-Cruz, L., & Millman, J. R. (2020b). Targeting the cytoskeleton to direct pancreatic differentiation of human pluripotent stem cells. *Nature Biotechnology*, *38*(4), 460–470. https://doi.org/10.1038/s41587-020-0430-6

Huang, C., Walker, E. M., Dadi, P. K., Hu, R., Xu, Y., Zhang, W., Sanavia, T., Mun, J., Liu, J., Nair, G. G., Tan, H. Y. A., Wang, S., Magnuson, M. A., Stoeckert, C. J., Hebrok, M., Gannon, M., Han, W., Stein, R., Jacobson, D. A., & Gu, G. (2018). Synaptotagmin 4 Regulates Pancreatic β Cell Maturation by Modulating the Ca2+ Sensitivity of Insulin Secretion Vesicles. *Developmental Cell*, *45*(3), 347-361.e5. https://doi.org/10.1016/j.devcel.2018.03.013

Huang, H. C., & Klein, P. S. (2004). The frizzled family: Receptor for multiple signal transduction pathways. In *Genome Biology*. https://doi.org/10.1186/gb-2004-5-7-234

Huang, J. L., Lee, S., Hoek, P., van der Meulen, T., Van, R., & Huising, M. O. (2020a). Genetic deletion of urocortin 3 does not prevent functional maturation of beta cells. *Journal of Endocrinology*, *246*(1), 69–78. https://doi.org/10.1530/JOE-19-0535

Huang, J. L., Lee, S., Hoek, P., van der Meulen, T., Van, R., & Huising, M. O. (2020b). Genetic deletion of urocortin 3 does not prevent functional maturation of beta cells. *Journal of Endocrinology*. https://doi.org/10.1530/JOE-19-0535

Hunter, C. S., & Stein, R. W. (2017). Evidence for loss in identity, de-differentiation, and trans-differentiation of islet β-cells in type 2 diabetes. In *Frontiers in Genetics*. https://doi.org/10.3389/fgene.2017.00035

In't Veld, P., & Lammert, E. (2015). The dark side of islet vasculature. In *Diabetologia*. https://doi.org/10.1007/s00125-014-3418-2

Inoki, K., Ouyang, H., Zhu, T., Lindvall, C., Wang, Y., Zhang, X., Yang, Q., Bennett, C., Harada, Y., Stankunas, K., Wang, C. yu, He, X., MacDougald, O. A., You, M., Williams, B. O., & Guan, K. L. (2006). TSC2 Integrates Wnt and Energy Signals via a Coordinated Phosphorylation by AMPK and GSK3 to Regulate Cell Growth. *Cell*. https://doi.org/10.1016/j.cell.2006.06.055

Ishibashi, A., Saga, K., Hisatomi, Y., Li, Y., Kaneda, Y., & Nimura, K. (2020). A simple method using CRISPR-Cas9 to knock-out genes in murine cancerous cell lines. *Scientific Reports*. https://doi.org/10.1038/s41598-020-79303-0

Islam, S. (2015). Islets of langerhans, second edition. In *Islets of Langerhans, Second Edition*. https://doi.org/10.1007/978-94-007-6686-0

Jaafar, R., Tran, S., Shah, A. N., Sun, G., Valdearcos, M., Marchetti, P., Masini, M., Swisa, A., Giacometti, S., Bernal-Mizrachi, E., Matveyenko, A., Hebrok, M., Dor, Y., Rutter, G. A., Koliwad, S. K., & Bhushan, A. (2019). MTORC1-to-AMPK switching underlies βcell metabolic plasticity during

maturation and diabetes. *Journal of Clinical Investigation*. https://doi.org/10.1172/JCI127021

Jacinto, E., Loewith, R., Schmidt, A., Lin, S., Rüegg, M. A., Hall, A., & Hall, M. N. (2004). Mammalian TOR complex 2 controls the actin cytoskeleton and is rapamycin insensitive. *Nature Cell Biology*. https://doi.org/10.1038/ncb1183

Jain, R., & Lammert, E. (2009). Cell-cell interactions in the endocrine pancreas. In *Diabetes, Obesity and Metabolism* (Vol. 11, Issue SUPPL. 4, pp. 159–167). https://doi.org/10.1111/j.1463-1326.2009.01102.x

Jennings, R. E., Berry, A. A., Gerrard, D. T., Wearne, S. J., Strutt, J., Withey, S., Chhatriwala, M., Piper Hanley, K., Vallier, L., Bobola, N., & Hanley, N. A. (2017a). Laser Capture and Deep Sequencing Reveals the Transcriptomic Programmes Regulating the Onset of Pancreas and Liver Differentiation in Human Embryos. *Stem Cell Reports*. https://doi.org/10.1016/j.stemcr.2017.09.018

Jennings, R. E., Berry, A. A., Gerrard, D. T., Wearne, S. J., Strutt, J., Withey, S., Chhatriwala, M., Piper Hanley, K., Vallier, L., Bobola, N., & Hanley, N. A. (2017b). Laser Capture and Deep Sequencing Reveals the Transcriptomic Programmes Regulating the Onset of Pancreas and Liver Differentiation in Human Embryos. *Stem Cell Reports*, *9*(5), 1387–1394. https://doi.org/10.1016/j.stemcr.2017.09.018

Jennings, R. E., Berry, A. A., Kirkwood-Wilson, R., Roberts, N. A., Hearn, T., Salisbury, R. J., Blaylock, J., Hanley, K. P., & Hanley, N. A. (2013). Development of the human pancreas from foregut to endocrine commitment. *Diabetes*, *62*(10), 3514–3522. https://doi.org/10.2337/db12-1479

Jensen, D. M., Hendricks, K. V., Mason, A. T., & Tessem, J. S. (2020). Good Cop, Bad Cop: The Opposing Effects of Macrophage Activation State on Maintaining or Damaging Functional β-Cell Mass. *Metabolites*. https://doi.org/10.3390/metabo10120485

Jermendy, A., Toschi, E., Aye, T., Koh, A., Aguayo-Mazzucato, C., Sharma, A., Weir, G. C., Sgroi, D., & Bonner-Weir, S. (2011). Rat neonatal beta cells lack the specialised metabolic phenotype of mature beta cells. *Diabetologia*, *54*(3), 594–604. https://doi.org/10.1007/s00125-010-2036-x

Jo, J., Moo, Y. C., & Koh, D. S. (2007). Size distribution of mouse Langerhans islets. *Biophysical Journal*. https://doi.org/10.1529/biophysj.107.104125

Johansson, K. A., Dursun, U., Jordan, N., Gu, G., Beermann, F., Gradwohl, G., & Grapin-Botton, A. (2007). Temporal Control of Neurogenin3 Activity in Pancreas Progenitors Reveals Competence Windows for the Generation of Different Endocrine Cell Types. *Developmental Cell*, *12*(3), 457–465. https://doi.org/10.1016/j.devcel.2007.02.010

Johnson, R., & Halder, G. (2014). The two faces of Hippo: Targeting the Hippo pathway for regenerative medicine and cancer treatment. In *Nature Reviews Drug Discovery*. https://doi.org/10.1038/nrd4161

Johnson, W. E., Li, C., & Rabinovic, A. (2007). Adjusting batch effects in microarray expression data using empirical Bayes methods. *Biostatistics*. https://doi.org/10.1093/biostatistics/kxj037

Jones, E. L., Demaria, M. C., & Wright, M. D. (2011). Tetraspanins in cellular immunity. In *Biochemical Society Transactions*. https://doi.org/10.1042/BST0390506

Jonsson, J., Carlsson, L., Edlund, T., & Edlund, H. (1994). Insulin-promoter-factor 1 is required for pancreas development in mice. *Nature*, *371*(6498), 606–609. https://doi.org/10.1038/371606a0

Jung, Y. S., & Park, J. Il. (2020). Wnt signaling in cancer: therapeutic targeting of Wnt signaling beyond β-catenin and the destruction complex. In *Experimental and Molecular Medicine*. https://doi.org/10.1038/s12276-020-0380-6

Kang, T., Jensen, P., Huang, H., Christensen, G. L., Billestrup, N., & Larsen, M. R. (2018). Characterization of the molecular mechanisms underlying glucose stimulated insulin secretion from isolated pancreatic β-cells using post-translational modification specific proteomics (PTMomics). *Molecular and Cellular Proteomics*, *17*(1), 95–110. https://doi.org/10.1074/mcp.RA117.000217

Karakose, E., Ackeifi, C., Wang, P., & Stewart, A. F. (2018). Advances in drug discovery for human beta cell regeneration. In *Diabetologia* (Vol. 61, Issue 8, pp. 1693–1699). https://doi.org/10.1007/s00125-018-4639-6

Katoh, M. (2002). Strabismus (STB)/Vang-like (VANGL) gene family (Review). In *International journal of molecular medicine*. https://doi.org/10.3892/ijmm.10.1.11

Katsarou, A., Gudbjörnsdottir, S., Rawshani, A., Dabelea, D., Bonifacio, E., Anderson, B. J., Jacobsen, L. M., Schatz, D. A., & Lernmark, A. (2017). Type 1 diabetes mellitus. *Nature Reviews Disease Primers*. https://doi.org/10.1038/nrdp.2017.16

Kim-Muller, J. Y., Fan, J., Kim, Y. J. R., Lee, S. A., Ishida, E., Blaner, W. S., & Accili, D. (2016). Aldehyde dehydrogenase 1a3 defines a subset of failing pancreatic β cells in diabetic mice. *Nature Communications*. https://doi.org/10.1038/ncomms12631

Kim, J., & Guan, K. L. (2019). mTOR as a central hub of nutrient signalling and cell growth. In *Nature Cell Biology* (Vol. 21, Issue 1, pp. 63–71). https://doi.org/10.1038/s41556-018-0205-1

Komatsu, M., Takei, M., Ishii, H., & Sato, Y. (2013). Glucose-stimulated insulin secretion: A newer perspective. In *Journal of Diabetes Investigation*. https://doi.org/10.1111/jdi.12094

Komiya, Y., & Habas, R. (2008). Wnt signal transduction pathways. In *Organogenesis*. https://doi.org/10.4161/org.4.2.5851

Kühl, M., Sheldahl, L. C., Park, M., Miller, J. R., & Moon, R. T. (2000). The Wnt/Ca2+ pathway A new vertebrate Wnt signaling pathway takes shape. In *Trends in Genetics*. https://doi.org/10.1016/S0168-9525(00)02028-X

Kulenović, A., & Sarač-Hadžihalilović, A. (2010). Blood vessels distribution in body and tail of pancreas - A comparative study of age related variation. *Bosnian Journal of Basic Medical Sciences*, *10*(2), 89–93. https://doi.org/10.17305/bjbms.2010.2700

Lange, A., Gegg, M., Burtscher, I., Bengel, D., Kremmer, E., & Lickert, H. (2012). Fltp T2AiCre: A new knock-in mouse line for conditional gene targeting in distinct mono- and multiciliated tissues. *Differentiation*, *83*(2). https://doi.org/10.1016/j.diff.2011.11.003

Laplante, M., & Sabatini, D. M. (2009). mTOR signaling at a glance. *Journal of Cell Science*. https://doi.org/10.1242/jcs.051011

Law, C. W., Chen, Y., Shi, W., & Smyth, G. K. (2014). Voom: Precision weights unlock linear model analysis tools for RNA-seq read counts. *Genome Biology*. https://doi.org/10.1186/gb-2014-15-2-r29

Lemaire, K., Thorrez, L., & Schuit, F. (2016). Disallowed and Allowed Gene Expression: Two Faces of

Mature Islet Beta Cells. In *Annual Review of Nutrition*. https://doi.org/10.1146/annurev-nutr-071715-050808

Liu, J. S. E., & Hebrok, M. (2017). All mixed up: Defining roles for β-cell subtypes in mature islets. In *Genes and Development* (Vol. 31, Issue 3, pp. 228–240). https://doi.org/10.1101/gad.294389.116

Llacua, L. A., Faas, M. M., & de Vos, P. (2018). Extracellular matrix molecules and their potential contribution to the function of transplanted pancreatic islets. In *Diabetologia*. https://doi.org/10.1007/s00125-017-4524-8

MacDonald, B. T., Tamai, K., & He, X. (2009). Wnt/β-Catenin Signaling: Components, Mechanisms, and Diseases. *Developmental Cell*. https://doi.org/10.1016/j.devcel.2009.06.016

Madadi, F., Jawad, R., Mousati, I., Plaeke, P., & Hubens, G. (2019). Remission of Type 2 Diabetes and Sleeve Gastrectomy in Morbid Obesity: a Comparative Systematic Review and Meta-analysis. In *Obesity Surgery* (Vol. 29, Issue 12, pp. 4066–4076). https://doi.org/10.1007/s11695-019-04199-3

Mak, B. C., Kenerson, H. L., Aicher, L. D., Barnes, E. A., & Yeung, R. S. (2005). Aberrant β-catenin signaling in tuberous sclerosis. *American Journal of Pathology*. https://doi.org/10.1016/S0002-9440(10)62958-6

Mamidi, A., Prawiro, C., Seymour, P. A., de Lichtenberg, K. H., Jackson, A., Serup, P., & Semb, H. (2018). Mechanosignalling via integrins directs fate decisions of pancreatic progenitors. *Nature*. https://doi.org/10.1038/s41586-018-0762-2

Martens, G. A., Motté, E., Kramer, G., Stangé, G., Gaarn, L. W., Hellemans, K., Nielsen, J. H., Aerts, J. M., Ling, Z., & Pipeleers, D. (2013). Functional characteristics of neonatal rat β cells with distinct markers. *Journal of Molecular Endocrinology*, *52*(1), 11–28. https://doi.org/10.1530/JME-13-0106

Martín, J., Hunt, S. L., Dubus, P., Sotillo, R., Néhmé-Pélluard, F., Magnuson, M. A., Parlow, A. F., Malumbres, M., Ortega, S., & Barbacid, M. (2003). Genetic rescue of Cdk4 null mice restores pancreatic β-cell proliferation but not homeostatic cell number. *Oncogene*. https://doi.org/10.1038/sj.onc.1206506

Marty-Santos, L., & Cleaver, O. (2015). Progenitor Epithelium: Sorting Out Pancreatic Lineages. *Journal of Histochemistry & Cytochemistry*, *63*(8), 559–574. https://doi.org/10.1369/0022155415586441

Mazier, W., & Cota, D. (2017). Islet endothelial cell: Friend and foe. In *Endocrinology*. https://doi.org/10.1210/en.2016-1925

McIntyre, H. D., Catalano, P., Zhang, C., Desoye, G., Mathiesen, E. R., & Damm, P. (2019). Gestational diabetes mellitus. In *Nature Reviews Disease Primers* (Vol. 5, Issue 1). https://doi.org/10.1038/s41572-019-0098-8

McLin, V. A., Rankin, S. A., & Zorn, A. M. (2007). Repression of Wnt/β-catenin signaling in the anterior endoderm is essential for liver and pancreas development. *Development*. https://doi.org/10.1242/dev.001230

Meda, P. (2013). Protein-Mediated Interactions of Pancreatic Islet Cells. *Scientifica*, *2013*, 1–22. https://doi.org/10.1155/2013/621249

Mège, R. M., & Ishiyama, N. (2017). Integration of cadherin adhesion and cytoskeleton at adherens junctions. In *Cold Spring Harbor Perspectives in Biology* (Vol. 9, Issue 5).

https://doi.org/10.1101/cshperspect.a028738

Migliorini, A., & Lickert, H. (2015). Beyond association: A functional role for Tcf7l2 in β-cell development. In *Molecular Metabolism*. https://doi.org/10.1016/j.molmet.2015.03.002

Mikels, A. J., & Nusse, R. (2006). Wnts as ligands: Processing, secretion and reception. In *Oncogene* (Vol. 25, Issue 57, pp. 7461–7468). https://doi.org/10.1038/sj.onc.1210053

Mlodzik, M. (2016). The Dishevelled Protein Family: Still Rather a Mystery After Over 20 Years of Molecular Studies. In *Current Topics in Developmental Biology*. https://doi.org/10.1016/bs.ctdb.2015.11.027

Moullé, V. S., Ghislain, J., & Poitout, V. (2017). Nutrient regulation of pancreatic β-cell proliferation. In *Biochimie*. https://doi.org/10.1016/j.biochi.2017.09.017

Moullé, V. S., Tremblay, C., Castell, A. L., Vivot, K., Ethier, M., Fergusson, G., Alquier, T., Ghislain, J., & Poitout, V. (2019). The autonomic nervous system regulates pancreatic ß-cell proliferation in adult male rats. *American Journal of Physiology - Endocrinology and Metabolism*. https://doi.org/10.1152/ajpendo.00385.2018

Muratore, M., Santos, C., & Rorsman, P. (2021). The vascular architecture of the pancreatic islets: A homage to August Krogh. In *Comparative Biochemistry and Physiology -Part A : Molecular and Integrative Physiology*. https://doi.org/10.1016/j.cbpa.2020.110846

Muzumdar, M. D., Tasic, B., Miyamichi, K., Li, N., & Luo, L. (2007). A global double-fluorescent cre reporter mouse. *Genesis*. https://doi.org/10.1002/dvg.20335

Nam Han Cho. (2019). IDF Diabetes Atlas, 9th edn. Brussels, Belgium: 2019. In *International Diabetes Federation. Available at: http://www.diabetesatlas.org*.

Narayanan, S., Loganathan, G., Dhanasekaran, M., Tucker, W., Patel, A., Subhashree, V., Mokshagundam, S., Hughes, M. G., Williams, S. K., & Balamurugan, A. N. (2017). Intra-islet endothelial cell and β-cell crosstalk: Implication for islet cell transplantation. *World Journal of Transplantation*. https://doi.org/10.5500/wjt.v7.i2.117

Nasteska, D., Fine, N. H. F., Ashford, F. B., Cuozzo, F., Viloria, K., Smith, G., Dahir, A., Dawson, P. W. J., Lai, Y. C., Bastidas-Ponce, A., Bakhti, M., Rutter, G. A., Fiancette, R., Nano, R., Piemonti, L., Lickert, H., Zhou, Q., Akerman, I., & Hodson, D. J. (2021). PDX1LOW MAFALOW β-cells contribute to islet function and insulin release. *Nature Communications*, *12*(1). https://doi.org/10.1038/s41467-020-20632-z

Nishimura, W., Takahashi, S., & Yasuda, K. (2015). MafA is critical for maintenance of the mature beta cell phenotype in mice. *Diabetologia*, *58*(3), 566–574. https://doi.org/10.1007/s00125-014-3464-9

Oakie, A., & Nostro, M. C. (2021). Harnessing Proliferation for the Expansion of Stem Cell-Derived Pancreatic Cells: Advantages and Limitations. In *Frontiers in Endocrinology* (Vol. 12, Issue February, pp. 1–7). https://doi.org/10.3389/fendo.2021.636182

Offield, M. F., Jetton, T. L., Labosky, P. A., Ray, M., Stein, R. W., Magnuson, M. A., Hogan, B. L. M., & Wright, C. V. E. (1996). PDX-1 is required for pancreatic outgrowth and differentiation of the rostral duodenum Martin. *Development*. https://doi.org/10.1016/0076-6879(93)25031-v

Oguri, Y., Shinoda, K., Kim, H., Alba, D. L., Bolus, W. R., Wang, Q., Brown, Z., Pradhan, R. N., Tajima, K.,

Yoneshiro, T., Ikeda, K., Chen, Y., Cheang, R. T., Tsujino, K., Kim, C. R., Greiner, V. J., Datta, R., Yang, C. D., Atabai, K., … Kajimura, S. (2020). CD81 Controls Beige Fat Progenitor Cell Growth and Energy Balance via FAK Signaling. *Cell*, *182*(3), 563-577.e20. https://doi.org/10.1016/j.cell.2020.06.021

Pan, F. C., & Wright, C. (2011). Pancreas organogenesis: From bud to plexus to gland. In *Developmental Dynamics*. https://doi.org/10.1002/dvdy.22584

Puri, S., Roy, N., Russ, H. A., Leonhardt, L., French, E. K., Roy, R., Bengtsson, H., Scott, D. K., Stewart, A. F., & Hebrok, M. (2018). Replication confers β cell immaturity. *Nature Communications*, *9*(1). https://doi.org/10.1038/s41467-018-02939-0

Rathwa, N., Patel, R., Palit, S. P., Parmar, N., Rana, S., Ansari, M. I., Ramachandran, A. V., & Begum, R. (2020). β-cell replenishment: Possible curative approaches for diabetes mellitus. In *Nutrition, Metabolism and Cardiovascular Diseases*. https://doi.org/10.1016/j.numecd.2020.08.006

Redondo, M. J., Hagopian, W. A., Oram, R., Steck, A. K., Vehik, K., Weedon, M., Balasubramanyam, A., & Dabelea, D. (2020). The clinical consequences of heterogeneity within and between different diabetes types. In *Diabetologia* (Vol. 63, Issue 10, pp. 2040–2048). https://doi.org/10.1007/s00125-020-05211-7

Richards, D. M., Walker, J. J., & Tabak, J. (2020). Ion channel noise shapes the electrical activity of endocrine cells. *PLoS Computational Biology*, *16*(4). https://doi.org/10.1371/journal.pcbi.1007769

Rodnoi, P., Rajkumar, M., Moin, A. S. M., Georgia, S. K., Butler, A. E., & Dhawan, S. (2017). Neuropeptide Y expression marks partially differentiated β cells in mice and humans. *JCI Insight*. https://doi.org/10.1172/jci.insight.94005

Rodriguez-Calvo, T., Suwandi, J. S., Amirian, N., Zapardiel-Gonzalo, J., Anquetil, F., Sabouri, S., & von Herrath, M. G. (2015). Heterogeneity and Lobularity of Pancreatic Pathology in Type 1 Diabetes during the Prediabetic Phase. *Journal of Histochemistry and Cytochemistry*, *63*(8), 626–636. https://doi.org/10.1369/0022155415576543

Rodríguez-Seguel, E., Mah, N., Naumann, H., Pongrac, I. M., Cerdá-Esteban, N., Fontaine, J. F., Wang, Y., Chen, W., Andrade-Navarro, M. A., & Spagnoli, F. M. (2013). Mutually exclusive signaling signatures define the hepatic and pancreatic progenitor cell lineage divergence. *Genes and Development*. https://doi.org/10.1101/gad.220244.113

Rogala, K. B., Gu, X., Kedir, J. F., Abu-Remaileh, M., Bianchi1, L. F., Bottino1, A. M. S., Dueholm1, R., Niehaus1, A., Overwijn1, D., Priso Fils1, A. C., Zhou1, S. X., Leary, D., Laqtom1, N. N., Brignole, E. J., & Sabatini, D. M. (2019). Structural basis for the docking of mTORC1 on the lysosomal surface. *Science*. https://doi.org/10.1126/science.aay0166

Rorsman, P., & Renström, E. (2003). Insulin granule dynamics in pancreatic beta cells. In *Diabetologia*. https://doi.org/10.1007/s00125-003-1153-1

Rorsman, Patrik, & Ashcroft, F. M. (2018). Pancreatic β-cell electrical activity and insulin secretion: Of mice and men. *Physiological Reviews*. https://doi.org/10.1152/physrev.00008.2017

Rorsman, Patrik, Eliasson, L., Renström, E., Gromada, J., Barg, S., & Göpel, S. (2000). The cell physiology of biphasic insulin secretion. *News in Physiological Sciences*. https://doi.org/10.1152/physiologyonline.2000.15.2.72

Roscioni, S. S., Migliorini, A., Gegg, M., & Lickert, H. (2016). Impact of islet architecture on β-cell

heterogeneity, plasticity and function. In *Nature Reviews Endocrinology* (Vol. 12, Issue 12, pp. 695–709). https://doi.org/10.1038/nrendo.2016.147

Rourke, J. L., Hu, Q., & Screaton, R. A. (2018). AMPK and Friends: Central Regulators of β Cell Biology. In *Trends in Endocrinology and Metabolism*. https://doi.org/10.1016/j.tem.2017.11.007

Rui, J., Deng, S., Arazi, A., Perdigoto, A. L., Liu, Z., & Herold, K. C. (2017). β Cells that Resist Immunological Attack Develop during Progression of Autoimmune Diabetes in NOD Mice. *Cell Metabolism*. https://doi.org/10.1016/j.cmet.2017.01.005

Rulifson, I. C., Karnik, S. K., Heiser, P. W., Ten Berge, D., Chen, H., Gu, X., Taketo, M. M., Nusse, R., Hebrok, M., & Kim, S. K. (2007). Wnt signaling regulates pancreatic β cell proliferation. *Proceedings of the National Academy of Sciences of the United States of America*. https://doi.org/10.1073/pnas.0701509104

Sachs, S., Bastidas-Ponce, A., Tritschler, S., Bakhti, M., Böttcher, A., Sánchez-Garrido, M. A., Tarquis-Medina, M., Kleinert, M., Fischer, K., Jall, S., Harger, A., Bader, E., Roscioni, S., Ussar, S., Feuchtinger, A., Yesildag, B., Neelakandhan, A., Jensen, C. B., Cornu, M., … Lickert, H. (2020). Targeted pharmacological therapy restores β-cell function for diabetes remission. *Nature Metabolism*. https://doi.org/10.1038/s42255-020-0171-3

Salinno, C., Büttner, M., Cota, P., Tritschler, S., Tarquis-Medina, M., Bastidas-Ponce, A., Scheibner, K., Burtscher, I., Böttcher, A., Theis, F. J., Bakhti, M., & Lickert, H. (2021). CD81 marks immature and dedifferentiated pancreatic β-cells. *Molecular Metabolism*. https://doi.org/10.1016/j.molmet.2021.101188

Salinno, C., Cota, P., Bastidas-Ponce, A., Tarquis-Medina, M., Lickert, H., & Bakhti, M. (2019). β-Cell Maturation and Identity in Health and Disease. *International Journal of Molecular Sciences*, *20*(21). https://doi.org/10.3390/ijms20215417

Saricaoglu, Ö. C., Teller, S., Wang, X., Wang, S., Stupakov, P., Heinrich, T., Istvanffy, R., Friess, H., Ceyhan, G. O., & Demir, I. E. (2020). Localisation analysis of nerves in the mouse pancreas reveals the sites of highest nerve density and nociceptive innervation. *Neurogastroenterology and Motility*. https://doi.org/10.1111/nmo.13880

Saunders, D. C., Aamodt, K. I., Richardson, T. M., Hopkirk, A., Khan, Z., Aramandla, R., Poffenberger, G., Jenkins, R., Flaherty, D. K., Prasad, N., Levy, S. E., Powers, A. C., & Brissova, M. (2020). Coordinated interactions between endothelial cells and macrophages in the islet microenvironment promote β cell regeneration. *BioRxiv*, *615*, 2020.08.28.265728. https://doi.org/10.1101/2020.08.28.265728

Scaglia, L., Cahill, C. J., Finegood, D. T., & Bonner-Weir, S. (1997). Apoptosis participates in the remodeling of the endocrine pancreas in the neonatal rat. *Endocrinology*, *138*(4), 1736–1741. https://doi.org/10.1210/endo.138.4.5069

Scheibner, K., Bakhti, M., Bastidas-Ponce, A., & Lickert, H. (2019). Wnt signaling: implications in endoderm development and pancreas organogenesis. In *Current Opinion in Cell Biology*. https://doi.org/10.1016/j.ceb.2019.07.002

Schlessinger, K., Hall, A., & Tolwinski, N. (2009). Wnt signaling pathways meet Rho GTPases. In *Genes and Development*. https://doi.org/10.1101/gad.1760809

Segerstolpe, Å., Palasantza, A., Eliasson, P., Andersson, E. M., Andréasson, A. C., Sun, X., Picelli, S., Sabirsh, A., Clausen, M., Bjursell, M. K., Smith, D. M., Kasper, M., Ämmälä, C., & Sandberg, R.

(2016). Single-Cell Transcriptome Profiling of Human Pancreatic Islets in Health and Type 2 Diabetes. *Cell Metabolism*, *24*(4). https://doi.org/10.1016/j.cmet.2016.08.020

Shapiro, A. M. J., Pokrywczynska, M., & Ricordi, C. (2017). Clinical pancreatic islet transplantation. In *Nature Reviews Endocrinology* (Vol. 13, Issue 5, pp. 268–277). https://doi.org/10.1038/nrendo.2016.178

Shirakawa, J., & Kulkarni, R. N. (2016). Novel factors modulating human β-cell proliferation. In *Diabetes, Obesity and Metabolism*. https://doi.org/10.1111/dom.12731

Sinagoga, K. L., Stone, W. J., Schiesser, J. V., Schweitzer, J. I., Sampson, L., Zheng, Y., & Wells, J. M. (2017). Distinct roles for the mTOR pathway in postnatal morphogenesis, maturation and function of pancreatic islets. *Development (Cambridge)*. https://doi.org/10.1242/dev.146316

Solar, M., Cardalda, C., Houbracken, I., Martín, M., Maestro, M. A., De Medts, N., Xu, X., Grau, V., Heimberg, H., Bouwens, L., & Ferrer, J. (2009). Pancreatic Exocrine Duct Cells Give Rise to Insulin-Producing β Cells during Embryogenesis but Not after Birth. *Developmental Cell*. https://doi.org/10.1016/j.devcel.2009.11.003

Staels, W., Heremans, Y., Heimberg, H., & De Leu, N. (2019). VEGF-A and blood vessels: a beta cell perspective. In *Diabetologia*. https://doi.org/10.1007/s00125-019-4969-z

Stefan, Y., Meda, P., Neufeld, M., & Orci, L. (1987). Stimulation of insulin secretion reveals heterogeneity of pancreatic B cells in vivo. *Journal of Clinical Investigation*, *80*(1), 175–183. https://doi.org/10.1172/JCI113045

Steiner, D. J., Kim, A., Miller, K., & Hara, M. (2010). Pancreatic islet plasticity: Interspecies comparison of islet architecture and composition. In *Islets* (Vol. 2, Issue 3). https://doi.org/10.4161/isl.2.3.11815

Steinhart, Z., & Angers, S. (2018). Wnt signaling in development and tissue homeostasis. *Development (Cambridge, England)*. https://doi.org/10.1242/dev.146589

Stoffers, D. a, Ferrer, J., Clarke, W. L., & Habener, J. F. (1997). Early-onset type-II diabetes mellitus (MODY4) linked to IPF1. *Nature Genetics*, *17*(2), 138–139. https://doi.org/10.1038/ng1097-138

Stolovich-Rain, M., Enk, J., Vikesa, J., Nielsen, F. C., Saada, A., Glaser, B., & Dor, Y. (2015). Weaning Triggers a Maturation Step of Pancreatic β Cells. *Developmental Cell*, *32*(5), 535–545. https://doi.org/10.1016/j.devcel.2015.01.002

Szkudelski, T., & Szkudelska, K. (2019). The relevance of AMP-activated protein kinase in insulin-secreting β cells: a potential target for improving β cell function? In *Journal of Physiology and Biochemistry*. https://doi.org/10.1007/s13105-019-00706-3

Szot, G. L., Koudria, P., & Bluestone, J. A. (2007). Murine pancreatic islet isolation. *Journal of Visualized Experiments*, *7*. https://doi.org/10.3791/255

Talchai, C., Xuan, S., Lin, H. V., Sussel, L., & Accili, D. (2012). Pancreatic β cell dedifferentiation as a mechanism of diabetic β cell failure. *Cell*, *150*(6), 1223–1234. https://doi.org/10.1016/j.cell.2012.07.029

Tamai, K., Semenov, M., Kato, Y., Spokony, R., Liu, C., Katsuyama, Y., Hess, F., Saint-Jeannet, J. P., & He, X. (2000). LDL-receptor-related proteins in Wnt signal transduction. *Nature*. https://doi.org/10.1038/35035117

Tan, S. Y., Mei Wong, J. L., Sim, Y. J., Wong, S. S., Mohamed Elhassan, S. A., Tan, S. H., Ling Lim, G. P., Rong Tay, N. W., Annan, N. C., Bhattamisra, S. K., & Candasamy, M. (2019). Type 1 and 2 diabetes mellitus: A review on current treatment approach and gene therapy as potential intervention. In *Diabetes and Metabolic Syndrome: Clinical Research and Reviews*. https://doi.org/10.1016/j.dsx.2018.10.008

Termini, C. M., & Gillette, J. M. (2017). Tetraspanins function as regulators of cellular signaling. In *Frontiers in Cell and Developmental Biology*. https://doi.org/10.3389/fcell.2017.00034

Teta, M., Long, S. Y., Wartschow, L. M., Rankin, M. M., & Kushner, J. A. (2005). Very slow turnover of β-cells in aged adult mice. *Diabetes*. https://doi.org/10.2337/diabetes.54.9.2557

Thompson, P. J., Shah, A., Ntranos, V., Van Gool, F., Atkinson, M., & Bhushan, A. (2019). Targeted Elimination of Senescent Beta Cells Prevents Type 1 Diabetes. *Cell Metabolism*, *29*(5), 1045-1060.e10. https://doi.org/10.1016/j.cmet.2019.01.021

Thorens, B. (2015). GLUT2, glucose sensing and glucose homeostasis. In *Diabetologia* (Vol. 58, Issue 2, pp. 221–232). https://doi.org/10.1007/s00125-014-3451-1

Thurmond, D. C. (2007). Regulation of insulin action and insulin secretion by SNARE-mediated vesicle exocytosis. In *Mechanisms of Insulin Action: Medical Intelligence Unit*. https://doi.org/10.1007/978-0-387-72204-7_3

Townsend, S. E., & Gannon, M. (2019a). Extracellular Matrix-Associated Factors Play Critical Roles in Regulating Pancreatic β-Cell Proliferation and Survival. In *Endocrinology*. https://doi.org/10.1210/en.2019-00206

Townsend, S. E., & Gannon, M. (2019b). Extracellular Matrix-Associated Factors Play Critical Roles in Regulating Pancreatic β-Cell Proliferation and Survival. In *Endocrinology* (Vol. 160, Issue 8, pp. 1885–1894). https://doi.org/10.1210/en.2019-00206

Urakami, T. (2019). Maturity-onset diabetes of the young (MODY): Current perspectives on diagnosis and treatment. In *Diabetes, Metabolic Syndrome and Obesity: Targets and Therapy* (Vol. 12, pp. 1047–1056). https://doi.org/10.2147/DMSO.S179793

van Amerongen, R., & Berns, A. (2006). Knockout mouse models to study Wnt signal transduction. In *Trends in Genetics*. https://doi.org/10.1016/j.tig.2006.10.001

Van Der Meulen, T., Donaldson, C. J., Cáceres, E., Hunter, A. E., Cowing-Zitron, C., Pound, L. D., Adams, M. W., Zembrzycki, A., Grove, K. L., & Huising, M. O. (2015). Urocortin3 mediates somatostatin-dependent negative feedback control of insulin secretion. *Nature Medicine*. https://doi.org/10.1038/nm.3872

van der Meulen, T., Mawla, A. M., DiGruccio, M. R., Adams, M. W., Nies, V., Dólleman, S., Liu, S., Ackermann, A. M., Cáceres, E., Hunter, A. E., Kaestner, K. H., Donaldson, C. J., & Huising, M. O. (2017). Virgin Beta Cells Persist throughout Life at a Neogenic Niche within Pancreatic Islets. *Cell Metabolism*, *25*(4), 911-926.e6. https://doi.org/10.1016/j.cmet.2017.03.017

VanderVorst, K., Hatakeyama, J., Berg, A., Lee, H., & Carraway, K. L. (2018). Cellular and molecular mechanisms underlying planar cell polarity pathway contributions to cancer malignancy. In *Seminars in Cell and Developmental Biology*. https://doi.org/10.1016/j.semcdb.2017.09.026

Veres, A., Faust, A. L., Bushnell, H. L., Engquist, E. N., Kenty, J. H. R., Harb, G., Poh, Y. C., Sintov, E.,

Gürtler, M., Pagliuca, F. W., Peterson, Q. P., & Melton, D. A. (2019). Charting cellular identity during human in vitro β-cell differentiation. *Nature*, *569*(7756), 368–373. https://doi.org/10.1038/s41586-019-1168-5

Villalba, A., Rodriguez-Fernandez, S., Perna-Barrull, D., Ampudia, R. M., Gomez-Muñoz, L., Pujol-Autonell, I., Aguilera, E., Coma, M., Cano-Sarabia, M., Vázquez, F., Verdaguer, J., & Vives-Pi, M. (2020). Repurposed Analog of GLP-1 Ameliorates Hyperglycemia in Type 1 Diabetic Mice Through Pancreatic Cell Reprogramming. *Frontiers in Endocrinology*. https://doi.org/10.3389/fendo.2020.00258

Villasenor, A., Chong, D. C., Henkemeyer, M., & Cleaver, O. (2010). Epithelial dynamics of pancreatic branching morphogenesis. *Development (Cambridge, England)*, *137*(24), 4295–4305. https://doi.org/10.1242/dev.052993

Wang, J., Yang, X., & Zhang, J. (2016). Bridges between mitochondrial oxidative stress, ER stress and mTOR signaling in pancreatic β cells. In *Cellular Signalling*. https://doi.org/10.1016/j.cellsig.2016.05.007

Wang, X., Misawa, R., Zielinski, M. C., Cowen, P., Jo, J., Periwal, V., Ricordi, C., Khan, A., Szust, J., Shen, J., Millis, J. M., Witkowski, P., & Hara, M. (2013). Regional Differences in Islet Distribution in the Human Pancreas - Preferential Beta-Cell Loss in the Head Region in Patients with Type 2 Diabetes. *PLoS ONE*, *8*(6). https://doi.org/10.1371/journal.pone.0067454

Welters, H. J., & Kulkarni, R. N. (2008). Wnt signaling: relevance to β-cell biology and diabetes. In *Trends in Endocrinology and Metabolism* (Vol. 19, Issue 10, pp. 349–355). https://doi.org/10.1016/j.tem.2008.08.004

Wesolowska-Andersen, A., Jensen, R. R., Alcántara, M. P., Beer, N. L., Duff, C., Nylander, V., Gosden, M., Witty, L., Bowden, R., McCarthy, M. I., Hansson, M., Gloyn, A. L., & Honore, C. (2020). Analysis of Differentiation Protocols Defines a Common Pancreatic Progenitor Molecular Signature and Guides Refinement of Endocrine Differentiation. *Stem Cell Reports*. https://doi.org/10.1016/j.stemcr.2019.11.010

Wilcox, C. L., Terry, N. A., Walp, E. R., Lee, R. A., & May, C. L. (2013). Pancreatic α-Cell Specific Deletion of Mouse Arx Leads to α-Cell Identity Loss. *PLoS ONE*, *8*(6). https://doi.org/10.1371/journal.pone.0066214

Wilkinson, M. B., Dias, C., Magida, J., Mazei-Robison, M., Lobo, M., Kennedy, P., Dietz, D., Covington, H., Russo, S., Neve, R., Ghose, S., Tamminga, C., & Nestler, E. J. (2011). A novel role of the WNT-dishevelled-GSK3β signaling cascade in the mouse nucleus accumbens in a social defeat model of depression. *Journal of Neuroscience*. https://doi.org/10.1523/JNEUROSCI.0039-11.2011

Willert, K., & Nusse, R. (2012). Wnt proteins. *Cold Spring Harbor Perspectives in Biology*, *4*(9). https://doi.org/10.1101/cshperspect.a007864

Wolf, F. A., Angerer, P., & Theis, F. J. (2018). SCANPY: Large-scale single-cell gene expression data analysis. *Genome Biology*, *19*(1). https://doi.org/10.1186/s13059-017-1382-0

Wu, K. L., Gannon, M., Peshavaria, M., Offield, M. F., Henderson, E., Ray, M., Marks, A., Gamer, L. W., Wright, C. V, & Stein, R. (1997). Hepatocyte nuclear factor 3beta is involved in pancreatic beta-cell-specific transcription of the pdx-1 gene. *Molecular and Cellular Biology*.

Xin, Y., Gutierrez, G. D., Okamoto, H., Kim, J., Lee, A. H., Adler, C., Ni, M., Yancopoulos, G. D., Murphy, A.

J., & Gromada, J. (2018). Pseudotime ordering of single human B-cells reveals states of insulin production and unfolded protein response. *Diabetes*, *67*(9), 1783–1794. https://doi.org/10.2337/db18-0365

Xue, Y., Bhushan, B., Mars, W. M., Bowen, W., Tao, J., Orr, A., Stoops, J., Yu, Y., Luo, J., Duncan, A. W., & Michalopoulos, G. K. (2020). Phosphorylated Ezrin (Thr567) Regulates Hippo Pathway and Yes-Associated Protein (Yap) in Liver. *American Journal of Pathology*. https://doi.org/10.1016/j.ajpath.2020.03.014

Yang, L., Zhu, Y., Yu, H., Cheng, X., Chen, S., Chu, Y., Huang, H., Zhang, J., & Li, W. (2020). ScMAGeCK links genotypes with multiple phenotypes in single-cell CRISPR screens. *Genome Biology*. https://doi.org/10.1186/s13059-020-1928-4

Yang, Y., & Mlodzik, M. (2015). Wnt-Frizzled/Planar Cell Polarity Signaling: Cellular Orientation by Facing the Wind (Wnt). *Annual Review of Cell and Developmental Biology*. https://doi.org/10.1146/annurev-cellbio-100814-125315

Ying, W., Lee, Y. S., Dong, Y., Seidman, J. S., Yang, M., Isaac, R., Seo, J. B., Yang, B. H., Wollam, J., Riopel, M., McNelis, J., Glass, C. K., Olefsky, J. M., & Fu, W. (2019). Expansion of Islet-Resident Macrophages Leads to Inflammation Affecting β Cell Proliferation and Function in Obesity. *Cell Metabolism*. https://doi.org/10.1016/j.cmet.2018.12.003

Yoshihara, E., O'Connor, C., Gasser, E., Wei, Z., Oh, T. G., Tseng, T. W., Wang, D., Cayabyab, F., Dai, Y., Yu, R. T., Liddle, C., Atkins, A. R., Downes, M., & Evans, R. M. (2020). Immune-evasive human islet-like organoids ameliorate diabetes. *Nature*. https://doi.org/10.1038/s41586-020-2631-z

Yoshihara, E., Wei, Z., Lin, C. S., Fang, S., Ahmadian, M., Kida, Y., Tseng, T., Dai, Y., Yu, R. T., Liddle, C., Atkins, A. R., Downes, M., & Evans, R. M. (2016). ERRγ Is Required for the Metabolic Maturation of Therapeutically Functional Glucose-Responsive β Cells. *Cell Metabolism*. https://doi.org/10.1016/j.cmet.2016.03.005

Zaret, K. S. (2006). Pancreatic β cells: Responding to the matrix. In *Cell Metabolism*. https://doi.org/10.1016/j.cmet.2006.02.006

Zhang, C., Moriguchi, T., Kajihara, M., Esaki, R., Harada, A., Shimohata, H., Oishi, H., Hamada, M., Morito, N., Hasegawa, K., Kudo, T., Engel, J. D., Yamamoto, M., & Takahashi, S. (2005). MafA Is a Key Regulator of Glucose-Stimulated Insulin Secretion. *Molecular and Cellular Biology*. https://doi.org/10.1007/s12237-012-9569-9

Zhang, H., Ackermann, A. M., Gusarova, G. A., Lowe, D., Feng, X., Kopsombut, U. G., Costa, R. H., & Gannon, M. (2006). The FoxM1 transcription factor is required to maintain pancreatic β-cell mass. *Molecular Endocrinology*. https://doi.org/10.1210/me.2006-0056

Zhao, B., Li, L., & Guan, K. L. (2010). Hippo signaling at a glance. In *Journal of Cell Science*. https://doi.org/10.1242/jcs.069070

Zhou, Q., Brown, J., Kanarek, A., Rajagopal, J., & Melton, D. A. (2008). In vivo reprogramming of adult pancreatic exocrine cells to β-cells. *Nature*. https://doi.org/10.1038/nature07314

Zhu, H., Sewell, A. K., & Han, M. (2015). Intestinal apical polarity mediates regulation of TORC1 by glucosylceramide in C. elegans. *Genes and Development*, *29*(12), 1218–1223. https://doi.org/10.1101/gad.263483.115